

**PREPARATION, CHARACTERISATION AND
OPTIMISATION OF LIQUID CRYSTALLINE POLYMER AND
THERMOPLASTIC BLENDS**

*Thesis submitted to the University of Minho as partial requirement of the award of the degree
of Doctor of Philosophy in Materials Science*

Susana Andrea Lopes Filipe

December 2004

“The most beautiful thing we can experience is the mysterious. It is the source of all true art and science.”

Albert Einstein

“O degrau de uma escada não serve simplesmente para que alguém permaneça em cima dele, destina-se a sustentar o pé de um homem pelo tempo suficiente para que ele coloque o outro pé um pouco mais alto.”

Thomas Huxley

To my parents

Aos meus pais

ACKNOWLEDGMENTS

I would like to start by thanking in general all the persons who might have somehow contributed, whether scientifically or personally during the period in which this work took place.

First of all, I would like to thank my father, José Filipe and my mother, Jesus Filipe for always providing me with their tender patience and understanding. Without their constant support and motivation, it would have been impossible for me to get this far. To my dear sister, Silvia Filipe, for her optimistic outlook, for her advices and all her love and friendship given to me on all the short occasions we've been together these last years. To my nephews for their smiles, their tantrums and the innocence with which they accepted my absence. To my grandfather, for the calm and tranquility he transmitted to me all the times we were together. To my grandmother, who taught me to be persistent and to fight for my goals. To my boyfriend José Leitão, for his love and companionship. His ability to listen to what I had to say, always with attention and patience, was a pivotal aid in overcoming the barriers and celebrating the breakthroughs

To my supervisors Doctor Teresa Cidade and Doctor João Maia for their unconditional support during all stages of this work, and for making me grow richer scientifically and personally, showing me the realistic and the optimistic side of every situation, in the moments when I was less sure of myself.

To Doctor Manfred Wilhelm, for his enlightening discussions and his total support (personal and professional) with which he greeted me into his Rheology group, for the duration of a year in the Max Planck Institut für Polymerforschung.

I am also thankful to all the elements of the Rheology and NMR group of MPIP, especially to Christopher Klein, who accompanied me, always cheerful, in the final stage of writing the thesis.

To the Extrusion group and their permanent elements, Professor Doctor J. A. Covas, Doctor Olga Carneiro, Doctor Miguel Nóbrega, Doctor Fernando Duarte, Doctor Ana Vera Machado, Doctor Gaspar Cunha, for their ideas and help given throughout the course of my PhD.

To my dear friend Vitor Barroso, for his words of support, especially during the stage of writing this thesis, for his friendship, for the scientific discussions and others, related with the production and consumption of German beer and Chilean wine. To my great friend Cristina

Silva, who helped me with her words, to overcome the most difficult moments and with whom I learned the true meaning of the word “generosity”.

An acknowledgement is also due to my friends and colleagues Rachele Musampa, Sandra Ribeiro, Maurício Malheiro, Rita Campos, Pedro Costa and also Marcos Sampaio, Carla Leer, Jorge Silva, Natália Domingues, Eva Barroso and Bruno Machado for their companionship and friendship. Their words and actions turned out to be fundamental throughout this period and they turned out to be the best part of this “harvest”.

To the technicians of the Processing Laboratory, Mr. João Paulo Peixoto and Mr. Sampaio for their support during the extrusion and injection.

An acknowledgement is due to Doctor A. V. Machado, for supplying compatibilisers D and E, to Professor Doctor J.C. Bordado and A. Duarte for the synthesis of compatibilisers A, B and C. and finally to Doctor Catarina Leal for the SEM measurements.

Finally I would like to acknowledge for the financial support given by Fundação de Ciência e Tecnologia (project POCTI/CTM/32658/99) and Marie Curie Training site (HPMT-CT-2000-00015).

Thank you to everyone who experienced this stage with me and to all those who helped me grow. I’ll remember you all with care, in every future step.

Susana Filipe

AGRADECIMENTOS

Gostaria de começar por agradecer a todas as pessoas, em geral, que possam de algum modo ter contribuído, quer a nível científico, quer a nível pessoal, durante o período em que decorreu este trabalho.

Em primeiro lugar gostava de agradecer ao meu pai, José Filipe e à minha mãe, Jesus Filipe, pela paciência que tiveram durante este tempo e pelo carinho, compreensão, que sempre demonstraram. Sem o seu apoio e motivação constantes, teria sido impossível chegar a este ponto. À minha querida irmã, Sílvia Filipe, pela sua visão optimista, pelos seus conselhos e pelo amor e amizade demonstrados nas poucas vezes que estivemos juntas durante estes anos. Aos meus sobrinhos pelos seus sorrisos, pelas suas birras e pela santa ingenuidade com que aceitaram a minha ausência. Ao meu avô, pela tranquilidade e calma que me transmitiu em todos os nossos encontros. À minha avó, que me ensinou a ser persistente e a lutar pelos meus objectivos. Ao meu namorado, José Leitão, pelo seu amor e companheirismo. A sua capacidade de ouvir o que eu tinha para dizer, sempre com paciência e atenção, constituiu uma ajuda imprescindível para ultrapassar as barreiras e celebrar as conquistas.

Aos meus orientadores Professora Doutora Teresa Cidade e Professor Doutor João Maia pelo seu apoio incondicional, durante todas as fases do trabalho, pelo modo como me enriqueceram a nível científico e pessoal, mostrando-me o lado realista e optimista das situações, naqueles momentos em que eu dispunha de menor capacidade de discernimento.

Ao Professor Doutor Manfred Wilhelm, pelas discussões enriquecedoras e pelo apoio total (pessoal e profissional) com que me recebeu no seu grupo de reologia, durante o total de um ano que passei em Mainz, no Max Planck Institut für Polymerforschung.

Agradeço igualmente a todos os elementos do grupo de reologia e de RMN do MPIP, especialmente ao Christopher Klein, que me acompanhou, sempre com boa disposição, na fase final da escrita da tese.

Ao grupo de extrusão e seus elementos permanentes, Professor Doutor J. A. Covas, Professora Doutora Olga Carneiro, Doutor Miguel Nóbrega, Doutor Fernando Duarte, Professora Doutora Ana Vera Machado, Professor Doutor Gaspar Cunha, pelas ideias e pela ajuda demonstrados no decurso deste doutoramento.

Ao meu querido amigo Vitor Barroso pelas suas palavras de apoio, especialmente durante a escrita desta tese, pela sua amizade, pelas discussões científicas e outras, relacionadas com a produção e consumo de cerveja alemã e vinho chileno. À minha grande

amiga Cristina Silva que com as suas palavras me ajudou a superar os momentos mais difíceis e com quem aprendi o verdadeiro significado da palavra generosidade.

Um agradecimento é devido aos meus amigos e colegas, Rachelle Musampa, Sandra Ribeiro, Maurício Malheiro, Rita Campos, Pedro Costa, Marcos Sampaio, Carla Leer, Jorge Silva, Natália Domingues, Eva Barroso e Bruno Machado pelo companheirismo e amizade demonstrados. As suas palavras e acções revelaram-se fundamentais durante este período e a sua amizade foi um dos maiores, senão o maior fruto desta “colheita”.

Aos técnicos do Laboratório de Processamento, Sr. João Paulo Peixoto e Sr. Sampaio pelo apoio durante a extrusão e injeção.

Um agradecimento é devido à Professora Doutora A. V. Machado, pelo fornecimento do compatibilizantes D e E, ao Professor Doutor J. C. Bordado e Dr. Ana Duarte, pela síntese dos compatibilizantes A, B e C e à Professora Doutora Catarina Leal pelos ensaios SEM.

Finalmente gostaria de agradecer o suporte financeiro fornecido pela Fundação de Ciência e Tecnologia (projecto POCTI/CTM/32658/99) e pelo Marie Curie Training site (HPMT-CT-2000-00015).

Obrigada a todos os que viveram esta fase comigo e a todos aqueles que me ajudaram a crescer. Lembrar-vos-ei sempre com carinho, em todos os passos que se seguirem.

Susana Filipe

ABSTRACT

Liquid Crystalline Polymers (LCP) are often added to thermoplastics (TP) in order to improve their mechanical performance. This improvement arises from the formation of fibrillar structures of the LCP (due to the fact that both components are immiscible), which are oriented along the thermoplastic and which lead to the formation of *in-situ* composites. In this work LCP/TP blends were studied not only in terms of their final morphological, rheological and mechanical properties, as in the great majority of the work already performed with these kind of blends, but also with respect to the evolution of their morphological and rheological properties at different stages of the extrusion process. The later study was performed by resorting to a special home-built collecting device system, developed and built at University of Minho [Covas 2001] and was carried out for compatibilised and non-compatibilised systems, based on Rodrun LC3000 and Polypropylene.

This work was firstly devoted to non-compatibilised systems and included the study of the influence of different liquid crystalline polymer contents. Due to the fact that compatibilisation is often needed for these systems, different compatibilisers were added in order to choose the best compatibiliser(s). After choosing two different compatibilisers their contents, as well as the contents of the LCP were varied in order to establish the best compatibiliser and LCP contents, *i.e.*, those that lead to the achievement of the best ratio mechanical performance/cost. The blends obtained with the optimum LCP/compatibiliser contents were used for the optimisation of the processing conditions, which consisted on the variation of the screw speed, output and temperature and which constituted the last part of the work.

During all this steps, correlations were established between the morphological and rheological evolution along the extruder length and the final mechanical performance of compatibilised and non-compatibilised LCP/TP systems.

Apart the unusual collecting device system used for the analysis of the kinetic of mixture, several techniques were used in addition to the ordinary rheological measurements under steady shear and oscillatory shear (in the linear regime), namely transient shear and Fourier Transform Rheology (FTR), which allowed for a more insightful description of the deformation and break-up processes of the LCP structures dispersed in the thermoplastic matrix, along the extruder length. Additionally, the analysis performed in terms of the influence of the application of different screw speeds, outputs and temperatures was very important for a more detailed description of the extrusion of this kind of systems and was essential for the optimisation process.

[Covas 2001] J. A. Covas, O. S. Carneiro and J. M. Maia, *Intern. J. Polym. Mat.* **50** (3-4), 445 (2001)

RESUMO

Polímeros Líquido Cristalinos (PLC) são usualmente adicionados a termoplásticos de modo a melhorar a sua performance mecânica. Esta melhoria tem origem na formação de estruturas fibrilares de PLC (devido à imiscibilidade entre os dois polímeros), que se orientam ao longo da matriz termoplástica e que levam à formação de compósitos *in-situ*.

Neste trabalho estudaram-se misturas de Polímeros Líquido Cristalinos e Termoplásticos (PLC/TP), não só em termos das propriedades morfológicas, reológicas e mecânicas finais, como tem acontecido na grande maioria dos trabalhos já realizados com este tipo de misturas, mas também no que respeita à evolução das suas propriedades morfológicas e reológicas, nas diversas etapas do processo de extrusão. O estudo referido anteriormente foi efectuado recorrendo a um sistema especial de recolha de amostras, desenvolvido e construído na Universidade do Minho [Covas 2001] e foi levado a cabo para misturas compatibilizadas e não-compatibilizadas, de Rodrun LC3000 e Polipropileno.

Este trabalho foi inicialmente dedicado ao estudo de sistemas não-compatibilizados e incluiu o estudo da influência de diferentes conteúdos de polímero líquido cristalino. Devido ao facto de que neste tipo de sistemas a compatibilização é usualmente necessária, foram adicionados diferentes compatibilizantes com a finalidade de encontrar o melhor ou melhores compatibilizantes. Depois de escolher dois compatibilizantes, variaram-se as percentagens de PLC e de compatibilizante, de modo a escolher a melhor percentagem de PLC/compatibilizante, *i.e.*, aqueles que levam à obtenção da melhor razão performance mecânica/custo. As misturas obtidas com a percentagem óptima de PLC e compatibilizante foram posteriormente utilizadas no processo de optimização das condições de processamento, que consistiu na variação destas, nomeadamente velocidade de rotação, caudal e temperatura, e que constituiu a última parte do trabalho.

Durante todas estas etapas foram estabelecidas correlações entre a evolução morfológica e reológica ao longo da extrusora e a performance mecânica final de misturas compatibilizadas e não-compatibilizadas.

Para além do invulgar sistema de recolha usado na análise da cinética de mistura, foram usadas diversas técnicas, nomeadamente, corte em regime transiente e FTR (Fourier Transform Rheology), para além de outras normalmente usadas para a caracterização deste tipo de sistemas, tais como, corte em regime estacionário e oscilatório em regime linear. Através destas foi possível descrever com maior detalhe os processos de deformação e quebra das estruturas dispersas de PLC na matriz termoplástica, ao longo do comprimento da extrusora. Adicionalmente, a análise levada a cabo em termos da influência da aplicação de diferentes velocidades de rotação, caudais e temperaturas foi muito importante para a descrição do processo de extrusão deste tipo de sistemas e essencial para o processo de optimização.

[Covas 2001]

J. A. Covas, O. S. Carneiro and J. M. Maia, *Intern. J. Polym. Mat.* **50 (3-4)**, 445 (2001)

LIST OF SYMBOLS AND ABBREVIATIONS

ABS	Acrylonitrile-butadiene acrylate
a_n	Amplitude
AP	Aminophenol
Comp.	Compatibiliser
Ca	Capillary number
D_m	Average droplet diameter
E_f	Young's modulus of the composite
E_f	Young's modulus of the dispersed phase
E_m	Young's modulus of the matrix
EPDM	Ethylene Propylene Diene Monomer
EP-g-MA	Anhydride Maleic grafted Ethylene Propylene copolymer
ϕ_n	Phase
FTR	Fourier Transform Rheology
G'	Storage modulus
G''	Loss modulus
GPC	Gel Permeation Chromatography
γ_0	Strain amplitude
γ -PBLG	Poly(γ -benzyl-L-glutamate)
$\dot{\gamma}$	Strain rate
Γ	Interfacial tension
η_0	Zero shear viscosity
η^*	Complex viscosity
η	Shear viscosity

η_E^+	Transient uniaxial extensional viscosity
η_m	Matrix viscosity
η_D	Dispersed phase viscosity
HBA	p-hydroxybenzoic acid
HDPE	High Density Polyethylene
HIPS	High Impact Polystyrene
HPC	Hydroxypropylcellulose
HQ	Hydroquinone
$I(3\omega_1) / I(\omega_1)$	Non-Linear Character Intensity (Intensity of the third harmonic over the fundamental)
LAOS	Large Amplitude Oscillatory Shear
L/D	Length to diameter ratio
LC(s)	Liquid Crystal(s)
LCP(s)	Liquid Crystalline Polymer(s)
LVE	Linear Viscoelastic Regime
MA-g-EPDM	Maleic Anhydride grafted Ethylene Propylene Diene Monomer
MA-g-PP	Maleic Anhydride grafted Polypropylene
MA-g-SEBS	Maleic Anhydride grafted Styrene-Ethylene-Butylene-Styrene
MFI	Melt Flow Index
\overline{M}_w	Weight-average molecular weight
$N1^+$	Transient first normal stress difference
NBR	Acrylonitrile Rubber
PA	Polyamide
PBA	Polybenzamide
PBO	Polybenzoxazole

PBT	Poly(butylene therephthalate)
PBZT	Poly(p-phenylene benzobisthiazole)
PC	Polycarbonate
PE	Polyethylene
PET	Poly(ethylene therephthalate)
PP	Polypropylene
PPO	Polyphenylene Oxide
PPS	Polyphenylene Sulphide
PPTA	Poly(1,4-phenylene terephthalamide)
PS	Polystyrene
PVC	Polyvinylchloride
σ_f	Volume fraction of the dispersed phase
σ^+	Transient shear stress
r	radius of LCP droplets
SEBS	Styrene (Ethylene-Butylene) Styrene
SEM	Scanning Electron Microscopy
t	Time
T	Temperature
TA	Therephthalic acid
TLCP(s)	Thermotropic Liquid Crystalline Polymer(s)
TMV	Tobacco Mosaic Virus solutions
TOFA	Tall Oil Fatty Acid
TP	Thermoplastic
V_i	Valve i
ω	Angular frequency

$\omega_1 / 2 \pi$	Fundamental frequency
wt %	Weight percentage
$\zeta = 2 l/d$	Length to diameter ratio of LCP fibrils
$\tan \delta$	Loss tangent
x	Parameter that measures the degree of adhesion between the dispersed and the continuous phases

GENERAL INDEX

Acknowledgments	I
Agradecimientos	III
Abstract	V
Resumo	VII
List of symbols and abreviations	IX
General Index	XIII
1 Introduction	1
2 Liquid crystalline polymers and composites: an overview	5
3 Materials and methods.....	33
4 Non-compatible liquid crystalline polymer and thermoplastic blends	47
4.1 Study of the influence of the LCP content on the evolution along the extruder length	47
4.2 Study of the influence of the LCP content on the final morphological, rheological and mechanical properties	69
4.3 Study of the influence of the use of different screw configuration on the final morphological and mechanical properties.....	96
5 Compatible liquid crystalline polymer and thermoplastic blends	105
5.1 Study of the influence of different compatibilisers on the evolution along the extruder length.....	105
5.2 Study of the influence of different compatibilisers on the final morphological, rheological and mechanical properties	129
6 Optimisation of LCP and compatibiliser contents on compatible liquid crystalline polymer and thermoplastic blends	151
7 Optimisation of processing conditions for compatible LCP/TP blends	181
8 General conclusions.....	221
9 Future work	227
Appendix I- Synthesis of compatibilisers A to C	229
Appendix II- Fourier Transform Rheology	235
Appendix III-Distribution of the LCP diameters for different processing conditions	240

1 INTRODUCTION

Polymer blending is an important process to obtain new reinforced materials, in which improved processability and properties are achieved by combining the individual properties of each pure component. Liquid crystalline polymers (LCP) and thermoplastic (TP) blends were subject of several studies, which is basically due to the exceptional mechanical properties and easier processability of LCP, comparing with those of other reinforced materials, namely, glass and carbon fibre composites [Baird 1996, Isayev 1996, Meng 1998]. However, because the cost associated to the synthesis of LCP is still very high and their use for the mechanical reinforcement of thermoplastics often requires the addition of compatibilisers [Bualek 1999, Brostow 1996, Datta 1995, Magagnini 1993, Magagnini 1998, Lee 2003, Lee 2003a], the industrial application of LCP on the reinforcement of engineering thermoplastics has been somewhat limited. These drawbacks can only be overcome, by studying and developing compatibilisers which will improve even more the mechanical properties of LCP/TP blends, not only in terms of the tensile strength, but also in terms of their impact resistance. Previous studies on compatibilised LCP/TP blends, showed that there is an improvement of strength, usually accompanied by a decrease of toughness [Tjong 1996, Tjong 2003]. The interest on LCP/TP blends for industrial applications will certainly increase if both strength and toughness will be obtained, this being one of the purposes of this work. Additionally, the emphasis of previous studies has been on the evaluation of the properties of the blends under stationary conditions and not under non-stationary ones which are, in fact, those most relevant to processing sequences [Liang 2002, Tjong 2003, Bualek-Limcharoen 1999, Brostow 1996, Magagnini 1998]. This is an additional task of this work. Another important issue is to attain a better understanding and improved knowledge on the process of formation of these *in-situ* composites during the different stages of the extrusion process, by resorting to different methods and techniques. This knowledge can be used to

monitor, control and optimise liquid crystalline polymer and thermoplastic blends and the techniques here employed may actually be used on the optimisation of other systems.

This thesis basically leads with the preparation, characterisation and optimisation of liquid crystalline polymer and thermoplastic blends, and is based on several papers (published and submitted) to several journals of the field [Filipe 2004a-h]. The thesis is divided in 9 chapters, which will be described below. This chapter, chapter 1, describes the structure of this thesis as well as its main objectives. In chapter 2, an introduction to liquid crystalline polymers structure and applications, as well as an historical overview about composites (particularly, LCP/TP blends) will be carried out. Chapter 3 comprise a description of the materials used and methods employed. In chapters 4, 5, 6 and 7 a description of the most important results will be carried out. In chapter 4, the discussion will be devoted to non-compatible LCP/TP blends. The study will be performed in terms of the evolution of the morphological and rheological properties during the extrusion process (chapter 4, sub-chapter 4.1) and on the influence of different LCP contents on the final mechanical, morphological and rheological properties (chapter 4, sub-chapter 4.2). This analysis was done resorting to techniques that were for the first time used to characterise the influence of different LCP contents on the properties developed along the extruder and/or at the end of the process, namely, Fourier Transform Rheology (FTR), Transient Uniaxial Extensional Measurements and Rheo-Optics. The last part of chapter 4, sub-chapter 4.3, was devoted to the study of the influence of different screw configurations on the way how the morphology evolves along the extruder length and on its influence on the final mechanical and morphological properties. In chapter 5, the main task was to enlarge the study of chapter 4 to compatible systems. Sub-chapter 5.1 was devoted to the study of the influence of different compatibilisers on the kinetic of mixture at the different stages of the extrusion process. The techniques used in chapter 5 were the same of chapter 4, but in this case the objective was to evaluate the influence of the

use of compatibilisers with distinct chemical natures, on the final morphological, rheological and mechanical properties (chapter 5, sub-chapter 5.2). Chapter 6 was devoted to the optimisation of the LCP and compatibiliser contents for the system LCP/TP under study (Rodrun LC3000/PP). The main objective was to find the optimum compatibiliser and LCP contents, having in mind the optimisation of the ratio performance/cost. Finally, in chapter 7 focused on the analysis of the influence of different processing conditions on the properties of the blends, which resulted from the optimisation performed previously and described in chapter 6. The most essential conclusions and achievements of the present work are summarized in chapter 8, whereas the future work is presented in chapter 9.

References

- [Baird 1996] J. P. de Souza Robertson, D. G. Baird, *Liquid Crystalline Polymer Systems: Technological Advances* (Chap. 6), ed. A. I. Isayev, T. Kyu and S. Z. D. Cheng, ACS Books, Washington DL 1996
- [Brostow 1996] W. Brostow, T. Sterzynski and S. Triouleyre *Polym.* **37**, 1561 (1996)
- [Bualek-Limcharoen 1999] S. Bualek-Limcharoen, J. Samran, T. Amornsakchai and W. Meesiri *Polym. Eng. Sci.* **39**, 312 (1999)
- [Datta 1995] A. Datta and D. G. Baird *Polym.* **36**, 505 (1995)
- [Filipe 2004a] S. Filipe, M. T. Cidade, M. Wilhelm and J. M. Maia, *Polym.* **45**, 2367 (2004)
- [Filipe 2004b] S. Filipe, J. M. Maia and M. T. Cidade *Adv. Mat. Forum* **456**, 476 (2004)
- [Filipe 2004c] S. Filipe, J. M. Maia, C. R. Leal and M. T. Cidade, *J. Polym. Eng.*, *accepted*
- [Filipe 2004d] S. Filipe, J. M. Maia, A. Duarte, C. R. Leal and M. T. Cidade, *J. Appl. Polym. Sci.*, *submitted* (June 2004).
- [Filipe 2004e] S. Filipe, M. T. Cidade, M. Wilhelm and J. M. Maia, *J. Appl. Polym. Sci.*, *submitted* (August 2004)
- [Filipe 2004f] S. Filipe, J. M. Maia, C. R. Leal, A. R. R. Menon, A. Duarte and M. T. Cidade, *J. Appl. Polym. Sci.*, *submitted* (November 2004)

- [Filipe 2004g] S. Filipe, J. M. Maia, C. R. Leal and M. T. Cidade, *J. Polym. Eng. Sci.*, *submitted* (December 2004).
- [Filipe 2004h] S. Filipe, M. T. Cidade and J. M. Maia, *Rheol. Acta*, *submitted* (December 2004)
- [Isayev 1996] A. I. Isayev, T. Kyu, S. Z. D. Cheng, *Self-reinforced composites involving liquid crystalline polymers: Overview and Applications* (ed) Liquid-Crystalline Polymer Systems. Technological Advances, America Chemical Society, Washington, p. 1 (1996)
- [Lee 2003] M. W. Lee, X. Hu, C. Y. Yue, L. Li and K. C. Tam *Comp. Sci. Tech.* **63**, 339 (2003)
- [Lee 2003a] M. W. Lee, X. Hu, L. Lin, C. Y. Yue, K. C. Tam and L. Y. Cheong *Comp. Sci. Tech.* **63**, 1921 (2003)
- [Magagnini 1993] P. Magagnini *Thermotropic Liquid Crystalline Blends* (Chap. 1), Technomic Publ. Co. Lancaster PA (1993)
- [Magagnini 1998] P. L. Magagnini, M. Pracella, L. I. Minkova, T. S. Miteva, D. Sek, J. Grobelny, F. P. La Mantia and R. Scaffaro *J. Appl. Polym. Sci.* **69**, 391 (1998)
- [Meng 1998] Y. Z. Meng, S. C. Tjong and A. S. Hay, *Polym.* **39**, 1845 (1998)
- [Tjong 1996] S. C. Tjong, S. L. Liu and R. K. Y. Li *J. Mater. Sci.* **31**, 479 (1996)
- [Tjong 2003] S. C. Tjong *Mat. Sci. Eng.* **R41**, 1 (2003)

2 LIQUID CRYSTALLINE POLYMERS AND COMPOSITES: AN OVERVIEW

The purpose of this chapter is to introduce the reader to the structure, properties and applicability of liquid crystalline polymers and to provide an overview on the importance and meaning of the appearance of blends and composites, as well on the work performed during the last few years on these systems. An historical overview will be additionally presented for a special kind of composites (*in-situ composites*), most precisely liquid crystalline polymer and thermoplastic blends.

LIQUID CRYSTALLINE POLYMERS

BRIEF HISTORICAL REVIEW

Liquid Crystalline Polymers (LCP) are materials that possess a phase of matter (partial ordered state) which is somewhere between the isotropic liquid and the solid crystal state and that is usually referred as mesomorphic phase or mesophase [Friedel 1922]. The definition of liquid crystalline polymer character described above (by Friedel in 1922) does not constitute, however, the start of liquid crystalline polymer history. The discovery of this intermediate state of matter in 1888, is commonly attributed to the Austrian botanist Friedrich Reinitzer [Reinitzer 1888], who observed a double melting behaviour for cholesteryl benzoate, between which the liquid showed some birefringence as well as iridescent colours. After this discovery further investigations were carried out by the German physicist O. Lehman, who observed and confirmed the F. Reinitzer findings, using a polarizing microscope with a hot stage, which was developed by himself some years before, for the study of crystal transitions [Lehman 1890]. They started to work together and in 1889, Lehman described the materials with this behaviour as “flowing crystals” and one year later as “crystalline liquids”. In the next years O. Lehman, G. Friedel and Vorlander, among others, worked in this field and concluded on the existence of different types of liquid crystallinity. In 1922, the French scientist Friedel

publishes a paper in which he clarified the concept of liquid crystallinity [Friedel 1922]. Friedel was also responsible for the first classification of liquid crystals (LC), which consisted in three types, nematic, smectic and cholesteric (chiral nematic), according to the different types of mesogens and the level of order of the molecules in the bulk material [Friedel 1922]. In 1923, Vorlander started to investigate the influence on the liquid crystalline character of liquid crystalline molecules with different lengths. This was the first pursuit of the concept of liquid crystalline polymers [Vorlander 1923]. For this purpose he devoted his work to the synthesis of rods with several benzene rings, linked via ester groups and he found an increase of the transition temperatures, with the increase of the benzene rings. Some years later Badwen and Pirie found out two liquid phases in the stiff rod-like molecules of tobacco mosaic virus solutions (TMV), one of which presented birefringence [Badwen 1937].

In 1956, Robinson published a work, concerning polymers showing liquid crystalline character in solution, which was focused on their structure and phase equilibria [Robinson 1956]. Two years later Ballard produced fibres from the lyotropic phase of poly(γ -benzyl-L-glutamate (γ -PLBG)) [Ballard 1958]. However, the first commercial liquid crystalline polymer, an aromatic amide fibre with the trade name Kevlar, was developed by DuPont, in the 1960's [Kwolek 1971].

In the 1970's the research of Jackson and co-workers led to the appearance of random copolymers and aromatic copolyesters [Jackson 1976]. By this method they reduced significantly the melting point (in comparison with that observed for the liquid crystalline polymer developed previously by Vorlander), minimizing the degradation problems during processing. From there on, the interest on liquid crystalline polymers enlarged significantly and several both lyotropic and thermotropic liquid crystalline polymers were industrially produced and applied.

STRUCTURE

Liquid crystalline polymers can be either thermotropic or lyotropic, depending on the conditions that induce the liquid crystallinity. The liquid crystalline character of thermotropic LCP occurs in the temperature range between the molten and the solid states, while in the case of lyotropic LCP the formation of liquid crystals occurs by dissolution in appropriate solvents. In the later case the liquid crystalline polymer character is controlled by the solvent, by the temperature of the solution and by the amount of polymer in solution.

The structure of thermotropic liquid crystalline polymer molecules usually consists of a central rigid core, which is often aromatic, and a flexible moiety, generally constituted by aliphatic groups. According to this structure thermotropic liquid crystalline polymers can be divided in two classes, calamitic and discotic liquid crystals.

Calamitic LCs (also defined as rod-like LCs) are mesomorphic compounds that possess an elongated shape. The anisotropy arises from the significant differences in terms of molecular length and molecular width (the later is usually, much shorter), as depicted in figure 2.1.

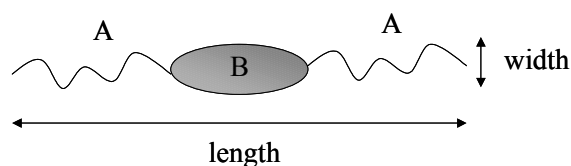


Figure 2.1 - Schematic structure of calamitic liquid crystals.

Calamitic liquid crystals can, in turn be divided in two types of mesophases, nematic and smectic. The nematic state is the least ordered mesophase, *i.e.*, the closest to the isotropic liquid state. In nematic mesophase only one order of orientation is present (orientational order).

In this case the polymer chains are lying more or less parallel one to another, along one axis. The medium direction of this orientation is defined as nematic director axis.

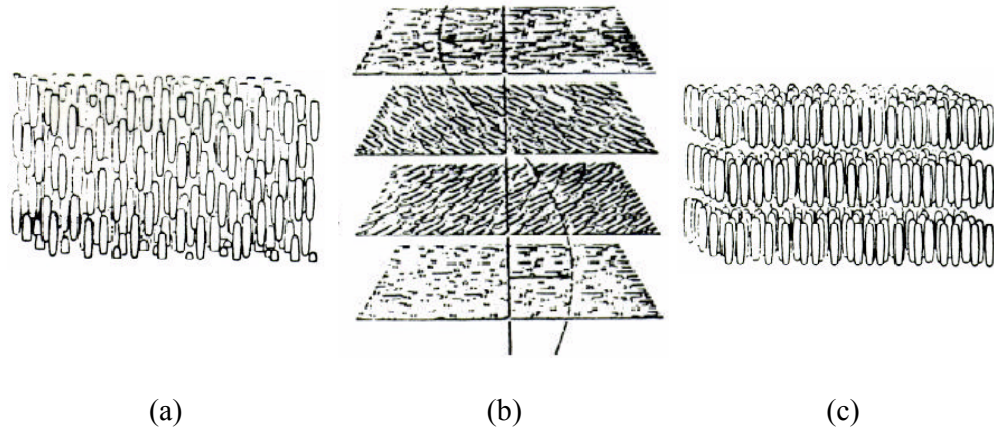


Figure 2.2 - Schematic Structure of nematic (a) chiral nematic (b) and smectic (c) mesophases (Calamitic LC) [Chung 1986].

It should be pointed out that the cholesteric mesophase (figure 2.2 (b)) is actually defined as a subset of the nematic, usually known as chiral nematic mesophase. In the cholesteric mesophase each plan of polymer chains has a nematic director, but has the additional feature that the directors show a cumulative twist, as each plane is examined in sequence (figure 2.2 b). This twist is generated by asymmetrical intermolecular forces between the nematic layers, which are created by the chiral centers in the mesogens. Therefore, a periodic helical structure is created which characterise cholesteric mesophase.

In the smectic mesophase two degrees of ordering exists, orientational and positional order (figure 2.2 (c)). Orientational order means that the chains are both lying more or less in parallel directions, one to another, while positional order implies that the molecules organise in layered structures. There are several different kinds of smectic phases: they can be divided into orthogonal and tilted phases, and can possess either short range order or long range order, as depicted in Figure 2.3. smectic A, C, C_{alterned} and hexatic B are examples of short range order, while crystal B, crystal K and crystal H are examples of long range order.






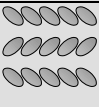

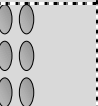
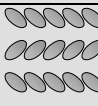
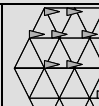
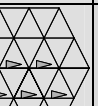
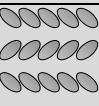
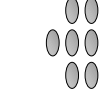
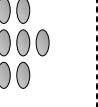
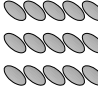
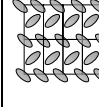
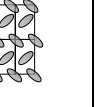
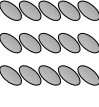
Orthogonal phases		Tilted phases				
						short range order
Smectic A	Smectic C		Smectic C _{alterned}			
						long range order
Hexatic B	Smectic I		Smectic F			
						
Crystal B	Crystal K		Crystal H			

Figure 2.3 - Some types of smectic phases.

For example, in smectic phase A, the layers are perpendicular to the director, while in smectic C the director is tilted at an angle other than 0° , to the normal layers (see figure 2.3).

Discotic liquid crystals, are a second kind of mesogenic structure which possess a general structure comprising a planar rigid core, usually aromatic, that is surrounded by a flexible periphery (usually pendant chains), as seen schematically in figure 2.4. In this case, the anisotropy arises from the fact that the molecular diameter is much greater than the disk thickness (see figure 2.4).

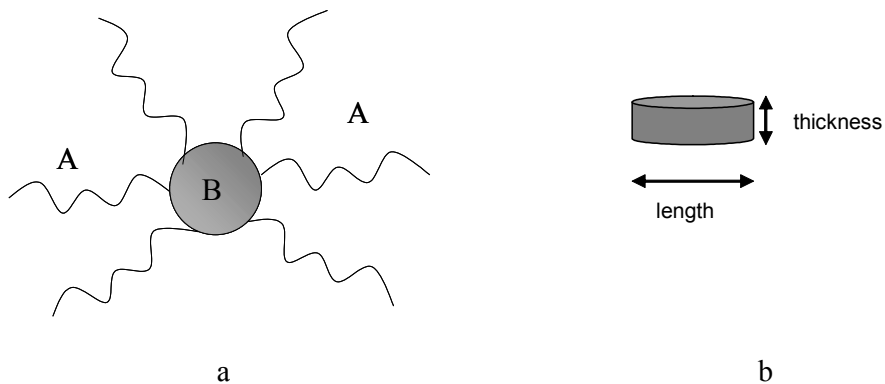


Figure 2.4 - Schematic structure of some of the discotic liquid crystals.

Discotic LCs can be either nematic discotic or columnar (see figure 2.5). In nematic discotic the molecules have only orientational order (no positional order exists), being usually aligned on average with the director. In columnar phases the disc-shaped cores have a tendency to stack one on the top of another, forming columns. Two different arrangements are possible, namely columnar rectangular and columnar hexagonal.

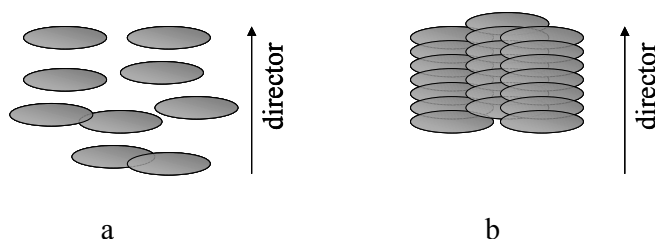


Figure 2.5 - Schematic structure of some nematic and hexagonal discotic liquid crystals.

A new class of liquid crystals defined as Polycatenar can be defined as an hybrid class of thermotropic liquid crystals. The molecular arrangement is intermediate between rod-like and disc-like mesogens. The central core of this kind of liquid crystals comprises a calamitic region, with half discs on the extremities. This structure allows both calamitic and columnar phases to be generated, depending on the structure of the components.

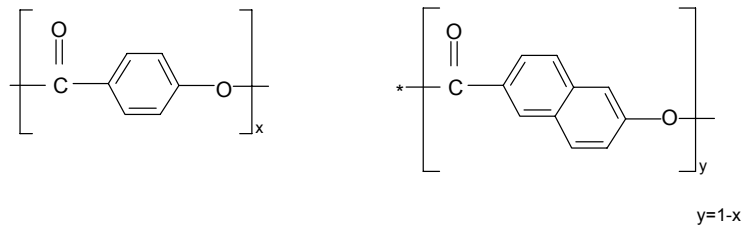
Liquid crystalline polymers are a specific type of polymer that possesses properties typical of liquid crystals. As already stated, the first reference to a polymer possessing liquid crystalline character was done in 1937, by Badwen and Pirie, who observed birefringence on tobacco mosaic virus solutions (TMV), above a critical concentration [Badwen 1937]. Some years later, most precisely in 1956, Robinson reported on polymers showing liquid crystalline character in solution [Robinson 1956]. From there on scientists discovered the possibility of adding low molecular mass mesogens in polymer chains, retaining the liquid crystalline character. Several work was done on the synthesis of liquid crystalline polymers, by incorporating the mesogenic groups into either a side chain or the main chain. The first thermotropic liquid crystalline polymers were reported in the seventies by Roviello and Jackson [Roviello 1975, Jackson 1976]. The main chain of liquid crystalline polymers can be either fully aromatic or can possess an aromatic part and an aliphatic part, *i.e.*, rigid mesogens and flexible spacers [Donald 1992]. Mesogens are usually based on stiff, aromatic units with bridging groups linking the individual aromatic units. They can be constituted, for example, by hydroxibenzoic acid (HBA), hydroquinone (HQ), terephthalic acid (TA), among others [Magagnini 1993].

The majority of commercial available LCP are copolyesters, copolyamides or polyester amides. According to their chemical structure, they might be fully aromatic or partially aliphatic and so a wide range of melting points can be found for LCP. Due to the high presence of aromatic compounds in their chemical structure, they often exhibit very high melting points, which might be an important drawback. Some examples of TLCP are Vectra A900 and Vectra A950, from Hoechst-Celanese (which chemical constitution is based on hydroxybenzoic acid (HBA) and hydroxynaphthoic acid (HNA)), Vectra B900 and Vectra B950, also from Hoechst-Celanese (chemically constituted by hydroxybenzoic acid (HBA), hydroxynaphthoic acid (HNA) and Aminophenol (AP)), and HX1000 and HX4000 from

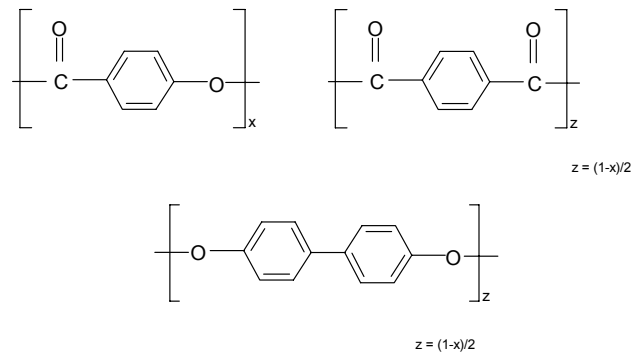
DuPont (based on hydroquinone (HQ) and terephthalic acid (TA)). More details about the chemical structure of TLCP are given in figure 2.6 (a). Fortunately, a new range of LCP has been discovered, which possess an aliphatic part in its structure, resulting in a lower melting temperature, and thus in an easier processability, from which Rodrun, from Unitika, is an example. In this case the chemical constitution is based on polyethylene terephthalate (PET) and hydroxybenzoic acid (HBA). Another important drawback of LCP is related with their low solubility in common organic solvents [Donald 1992]. In the case of aromatic liquid crystalline polymers and due to their chemical nature, some compatibility problems towards other materials with a chemical structure essentially aliphatic may occur.

The chemical structure of LCP is different depending if one talks about thermotropic or lyotropic LCP. The chemical structure of thermotropic LCP usually consists in alternating sequences of flexible and rigid units, along the main backbone of the polymer, coupled together via ester bonds. In the case of lyotropic LCP the common solvents in which the liquid crystalline character is developed are water, meta-cresol, acetic anhydride, among others. Some examples of lyotropic liquid crystalline polymers are hydroxypropylcellulose (HPC), which presents liquid crystalline behaviour in the presence of water and m-cresol, for instance, γ -PBLG (polybenzil-L-glutamate) which presents LC behaviour in solutions of m-cresol, benzyl-alcohol, chloroform and methylene chloride, and PPTA (Poly(1,4-phenylene terephthalamide)), which possess LC character in sulfuric acid, among others (see figure 2.6 (b)).

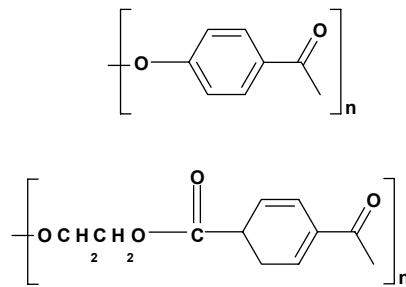
a



Vectra A



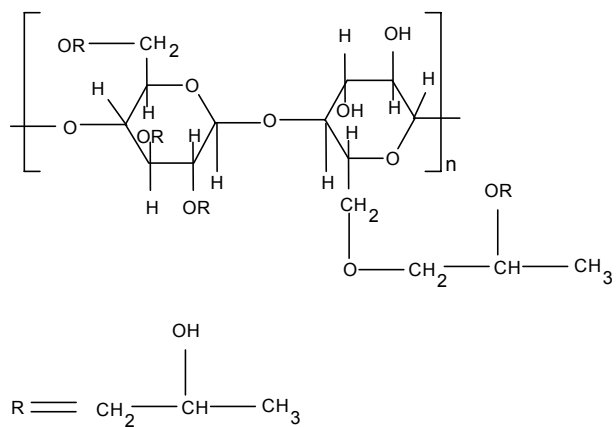
Xydar



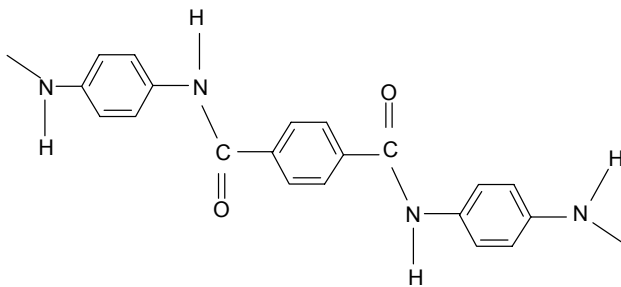
Rodrun

Figure 2.6 (a) - Some thermotropic liquid crystalline polymers commercially available.

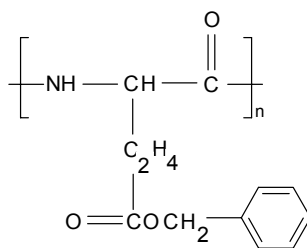
b



HPC



PPTA (Kevlar)



γ -PBLG

Figure 2.6 (b) - Some lyotropic liquid crystalline polymers commercially available.

PROPERTIES AND APPLICATIONS

Thermotropic Liquid Crystalline Polymers (TLCP) are widely recognized by their exceptional properties. The most important characteristics are a high mechanical strength, stiffness and toughness [Muramatsu 1987, Sarlin 1993, Yoon 1990] (which are associated with the ability to orient themselves along the flow direction), good barrier properties, good surface features, great dielectric properties [Brown 1993, Plummer 1993], high dimensional stability and easy moldability, high chemical and thermal resistance [Yoon 1992, Plummer 1993], low coefficient of thermal expansion [Cox 1987, Yoon 1992, Plummer 1993, Roggero 1993, Williams 1991], low flammability and permeability [Brown 1993, Cox 1987].

The exceptional properties of liquid crystalline polymers described above are behind the wide range of applications of these materials. Some examples are: high temperature connectors, encapsulation hybrid and micro circuitry in the electric and electronic industry, pumps, tower packing, connectors, couplers, fibre optics applications, valves for the chemical industry, bullet-proof jackets, components for aeroplanes, among several other applications [Kessler 1992, Donald 1992, Plummer 1993].

Nevertheless, the cost that is associated to the production of TLCP is still very high, and thus blending of these materials to other engineering thermoplastics, and consequent production of reinforced composites (where the engineering thermoplastics acts as the matrix) is usually performed.

REINFORCED MATERIALS

BLENDS: HISTORICAL PERSPECTIVE

The initial idea of obtain high performance materials by blending different polymers was developed by Thomas Hancock, who developed a blend which contained natural rubber and gutta percha [Hancock 1846]. From there on, several other attempts were made in order to

obtain materials with new and advantageous properties, combining those of both pure components. In 1934, Konrad developed an acrylonitrile rubber [Konrad 1934], which some years later was used to produce the one that is considered as the first thermoplastic blend and in 1942 appeared the first patent in thermoplastic polymer blends, an acrylonitrile rubber/polyvinylchloride (NBR/PVC) [Badum 1942]. Meanwhile several other products were produced by blending different materials, like for example, ethylene-propylene rubbers (EPR) [Greshman 1960], ethylene-propylene-diene rubbers (EPDM) [Irving 1962], blends of polypropylene/ ethylene propylene diene monomer (PP/EPDM) (which started to be used as impact modifiers) [Coran 1969], poly(ethylene terephthalate)/poly(butylene terephthalate) (PET/PBT) blends (which were developed by General Electric) [Vaccarl 1975], polycarbonate/ acrylonitrile-butadiene acrylate (PC/ABS) blends for automobile applications (developed by Dow chemical) [Dow 1986], among many others.

Composites

The appearance of composites arises from the need of obtain materials with high strength and stiffness, that will combine the properties of both pure components. Composites usually are the result of the combination of two materials one of them, called the reinforcing phase, is in the form of fibres or particles, and is usually embedded and dispersed in the matrix phase. The reinforcing and the matrix phases can be either metal, ceramic, or polymer [Mallick 1988]. Typically, reinforcing materials are strong with low densities while the matrix is usually a ductile, or tough, material. If design and fabrication is done properly, the final material combines the strength of the reinforcement with the toughness of the matrix. A combination of the properties of the pure components can be achieved, and additionally some new properties may result from this combination, which are not available in any single conventional material [Kessler 1992]. The drawback is that such composites are often more expensive than conventional materials.

The strength of the composite depends primarily on the amount, arrangement and type of fibres (or particles) in the matrix. Typically, the higher the reinforcement content, the greater the strength. In some cases, glass fibres are combined with other fibres, such as carbon or aramid (Kevlar), to create a hybrid composite that combines the properties of more than one reinforcing material [Tjong 2002, Tjong 2003a, Tjong 2003b]. In addition, the composite is often formulated with fillers and additives that change processing or performance parameters.

As already described, there are essentially two types of composites: particle-reinforced and fibre-reinforced composites [Mathews 1999]. In particle-reinforced composites the particles used include ceramics and glasses, small mineral particles, metal particles such as aluminium, and amorphous materials, including polymers and carbon black. By the addition of these particles one expects an increase of the modulus and a decrease of both permeability and ductility of the matrix. In the case of fibre-reinforced composites, the addition of fibres is usually reflected by an increase of the modulus relatively to that of the matrix. The strong covalent bonds along the fibres length gives them a very high modulus in this direction because to break or extend the fibres implies that the bonds must also be broken or moved. Fibres are usually difficult to process into composites, which makes fibre-reinforced composites relatively expensive. The arrangement and relative orientation of the fibres, the fibre content, and their distribution, have a significant influence on the strength and other properties of the composites [Mathews 1999]. Applications involving totally multidirectional applied stresses normally use discontinuous fibres, which are randomly oriented in the matrix material [Mathews 1999].

In order to increase the strength and stiffness of thermoplastics several attempts were made by adding fibres. The mechanical reinforcement is usually achieved by the use of glass fibres, carbon fibres, graphite or aromatic polyamides. The use of glass fibres is the most common which is essentially due to their low cost, compared with other reinforcing agents

[Shibley 1982]. However the use of glass fibres usually has some drawbacks, namely their high density, which makes them unfeasible, for example, for use in industry applications. Another drawback is related with the recycling of glass fibre composites. The reprocessing of such materials is usually limited, considerable fibre breakage occurs during the recycling process. But these are not the only drawbacks of the addition of glass-fibre to thermoplastics. Some other disadvantages are the increase of the matrix viscosity, which will result in the increase of the machinery abrasion and the difficulties in injection moulding processes in more complex moulds.

The use of liquid crystalline polymers (in the form of fibres) might be an interesting option if one considers that they can surmount some of these drawbacks. Baird and co-workers compared the mechanical properties of neat thermotropic liquid crystalline polymers (TLCP) and glass fibres and they found out that they are quite similar; the tensile moduli of the TLCP ranges from 50-100 GPa, while in the case of glass fibres it ranges from 69 to 83 GPa. With respect to the strength of neat TLCP they found out that it is ranging from 1 to 2 GPa, depending if its a spun or annealed, against 1.72 to 2.07 GPa for neat glass fibres [Baird 1996]. If one considers that the density of TLCP is much lower than that of glass fibres (1.4 g/cm^3 against 2.5 g/cm^3), and having into account that the mechanical properties of TLCP fibers are clearly near those of glass fibres, than it can be considered that the substitution of glass fibres by TLCP fibres may be a good option. Another important advantage of liquid crystalline polymers is that they can be recycled from LCP/TP blends, whereas both glass fibers and carbon fibers cannot [Bastida 1995, Xu 2000, Collier 1998].

In conclusion, it looks like TLCP possess an interesting combination of high mechanical properties and low density which suggests that they could be competitive with glass fibres, as reinforcing agents.

LIQUID CRYSTALLINE AND THERMOPLASTIC BLENDS

MONITORING OF KINETIC OF MIXTURE ALONG THE EXTRUDER LENGTH

The first studies on thermotropic liquid crystalline polymer blends go back to the early eighties and since then considerable interest has been focused on this kind of blends [Gabellini 1996, Qin 1993, Wanno 2000, Choi 1996]. Several different points were subject of reflection, namely the influence of the LCP content [Choi 1996, Viswanathan 1995], the importance of the chemical character of both LCP and thermoplastic on the final properties [Wano 2000, Choi 1996b, Qin 1993] and the influence of the processing conditions on the mechanical, rheological and morphological properties of the blends [Heino 1994, Filipe 2004b]. These works were essentially focused on the final properties and only a few researchers devoted their attention to the evolution of the morphology during the extrusion itself, one example being, the work of Boersma and Van Turnout [Boersma 1999]. The study of the evolution of polymer blend morphology during processing received an extreme attention, but for other kind of blends, different techniques being used [Shi 1992, Tyagi 2002, Potente 2000, Potente 2001, Scott 1995, Bordereau 1992]. In what concerns liquid crystalline polymer and blends (LCP/TP), however, there are still many unanswered questions, and a more in deep study must be carried out.

There are many factors to be considered on the study of the kinetic of mixture for LCP/TP blends. During compounding several factors influence the final morphology, including shear, elongational and hydrodynamic forces involved during compounding and also the rheological properties of the components of the blend. The deformation of the LCP droplets into fibrillar structures or the coalescence of the LCP structures depends on the ratio between the viscous and the interfacial forces. This ratio is frequently described by the Capillary number, Ca , which is defined by:

$$Ca = \frac{\eta_m \cdot \dot{\gamma} \cdot r}{\Gamma} \quad 2.1$$

where, η_m is the viscosity of the matrix, $\dot{\gamma}$ is the shear rate, r is the radius of the LCP droplets and Γ is the interfacial tension between the two pure components. The influence of the capillary number on the stability of the LCP structures has already been studied in liquid crystalline polymer and thermoplastic blends [Lazkano 2002]. Postema and Fennis, Chan and co-workers, Kernick and Wagner studied the influence of both viscous and interfacial forces in the final morphology, confirming the importance of the capillary number [Postema 1997, Chan 1997, Kernick 1999].

The morphology obtained during extrusion of immiscible blends varies along the different regions within the extruder. At the beginning of the compounding process the pure components are added at room temperature in the form of pellets or powder, after which they are heated and melted, giving rise to a heterogeneous blend containing a dispersed and a continuous phase (due to the immiscibility of both components). At the beginning of the extruder, specifically in the feed zone, the shear forces are the dominant ones in the process [Qin 1993]. Furthermore, at this stage the blend is not completely melted and the dispersed phase is usually constituted by spherical or ribbon-like structures, which will start to be stretched afterwards, as a result of the combination of shear and elongational forces. This deformation processes usually starts upon melting, where the formation of droplets and/or elongated structures is expected [Qin 1993]. Nevertheless, break-up processes or coalescence processes will also start and the ratio between the interfacial forces (that tend to keep the drop spherical) and the viscous forces (that tend to elongate the droplets) will define which of these will dominate [Qin 1993, Qin 1993a, Filipe 2003, Sepålla 1992]. In the mixing zones of the extruder, the shear forces are increased relatively to the previous stages, and therefore the breaking processes of the elongated structures will be dominant. At this region of the extruder,

spherical structures, with a decreased domain size and a narrower distribution, than those observed at the beginning of the process are observed [Qin 1993]. The final dimensions of these structures depend on the mechanical history and also on the ratio between the viscosity of the two components of the blend [Wano 2000, Filipe 2004a]. Finally, due to the high shear rates and extensional forces developed in the extruder die, a fibrillar morphology will be produced, as a result of the elongation suffered by the spherical LCP structures formed previously, at the metering zone.

Some theoretical derivations were also made regarding the evolution of the morphology for blends during compounding in a twin-screw extruder [Shi 1992, Huneault 1995]. In these studies different mechanisms were used to explain droplet's break-up and dispersion. They considered two different mechanisms for the break-up: one where the stable filaments are formed and that describes the behaviour of the large droplets and another, where break-up occurs during flow and is responsible for the generation of relatively small droplets. They stated that, according to the capillary number involved, one of these break-up mechanisms would occur. Relatively to the influence of the processing conditions, they noticed that the morphology is very sensitive to the screw configuration used during extrusion.

The study of the kinetic of mixture at the different stages of the extrusion process is essential, because the final morphology depends largely on the morphological evolution during polymer blending. This issue must then be addressed, since the morphology obtained at the end of the process is directly related to the ultimate mechanical properties. The processing conditions employed, like temperature profile, screw speed, throughput and also the configuration of the screw, control the several stages of the extrusion process. Therefore they will define the morphology obtained during and at the end of the compounding process. For example, the use of kneading blocks in the screw configuration will promote mixing and will lead to the reduction of the droplet's diameters. This effect is more pronounced for high screw

speeds and also for high throughputs. In the work of Boersma and Van Turnhout, for example, (in which they resorted to dielectric spectroscopy for on-line monitoring the morphological evolution of liquid crystalline and thermoplastic blends), they stated that the fibrillar structures are achieved in the mixing elements and that the mean particle size decreases with increasing shear rate [Boersma 1999]. Finally, Potente *et al.* investigated the morphology development in polypropylene and polyamide blends during processing in a co-rotating twin-screw extruder. They stated that only a small change of the number average diameter of the dispersed phase was observed along the extruder length. They concluded on the existence of an inverse correlation between the viscosity of the matrix, and the average diameter observed for the dispersed phase [Potente 2001].

In conclusion, the deliberate optimisation of the material properties, by means of monitoring the physico-chemical phenomena developed along the extruder axis is needed, since these processes are directly related with the final characteristics of the material and therefore with its ultimate mechanical performance [Potente 2000, Bordereau 1992, Boersma 1999, Chin 1979, Serpe 1990]. Several studies were performed in order to quantify the degree of break-up, coalescence and deformation of dispersed phase particles at the different stages of the extrusion process [Potente 2000, Bordereau 1992, Boersma 1992, Sundaraj 1995]. This work was in its majority performed for non-compatibilised and compatibilised systems, but only a few authors focused their attention on liquid crystalline and thermoplastic blends [Boersma 1999]. In this work attention will be focused on non-compatibilised and compatibilised LCP/TP blends, the main task being to address some important issues like the influence of different LCP and compatibiliser contents, the importance of the use of compatibilisers with different chemical natures, as well as the processing conditions, on the deformation, break-up and coalescence processes at the different stages of the extrusion process. Since the above-mentioned phenomena are essentially dynamic

processes, which change progressively according to the region of the extruder, it is of primary interest to study their evolution along the extruder length. Thus, there is a need to understand the applicability of the knowledge described above on the prediction and control of the morphology development during compounding in a twin-screw extruder, having in mind the optimisation of the mechanical performance.

CORRELATION OF THE FINAL EXTRUDATE PROPERTIES WITH TYPE OF LCP, MATRIX, COMPATIBILISERS AND PROCESSING CONDITIONS

As already pointed out, the interest in studying liquid crystalline polymer and thermoplastic blends has increased significantly in the last few years and can be attributed to the mechanical and processability improvement potential of these blends. These advantages arise respectively from the high level of macroscopic molecular orientation developed in these blends and from the decrease of viscosity, comparing with that of other reinforced materials like, for example, those with glass fibers [Heino 1994, Wanno 2000, Chan 1997]. The formation of high aspect ratio LCP fibrils inside the thermoplastic matrix, after crossing the die, leads to the creation of reinforced *in-situ* composites.

The great majority of the work devoted to liquid crystalline polymer and thermoplastic blends was done in order to study their ultimate morphological, mechanical, thermal and rheological properties. Amongst other parameters, the authors devoted their attention to the influence of the LCP content on the final morphology [Viswanathan 1995, Yoshikai 1996]. In these works they stated that the increase of the LCP content leads to the increase of the fibrils and that the formation of fibrils is easier for the blends with the highest LCP contents. Additionally, they found out that the fibrils are thicker, longer and with a better packing for the blends with the higher LCP content, which can explain the mechanical improvement obtained in these cases. Other researchers studied the influence of other important parameters on the final morphology, like for example the effect of the thermoplastic

viscosity on the LCP structure formed in blends of polypropylene and Rodrun LC3000 [Wano 2000]. They found that the high aspect ratio LCP fibers are achieved only for blends in which the matrix has the higher viscosity.

As a consequence of the morphology being largely retained after processing, a mechanical enhancement in the extrusion direction is obtained, *i.e.*, an improvement of both tensile modulus and tensile strength are achieved through the addition of LCP to thermoplastics ([Yoshikai 1996, Datta 1995], among others). The elongation at break, however, is usually drastically reduced. Another problem is that, owing to their high aromatic content, LCP typically exhibit high interfacial tension towards aliphatic polymers. Accordingly, a decrease of the impact strength is also usually obtained for LCP/TP blends [Tjong 2003, Tjong 1996]. Therefore, the industrial application of these in-situ reinforced materials is still limited.

The latter problem can be partially overcome through the addition of compatibilisers that promote a decrease of the interfacial tension between the two components and a better dispersion of the LCP in the matrix, as previously observed by a number of researchers [Bualek 1999, Brostow 1996, Datta 1995, Isa 2001, Magagnini 1998, Miller 1995, Miller 1997, O'Donnel 1995, Lee 2003]. The compatibilisation is usually achieved by physical or chemical interactions between the components of the blend and the compatibiliser. Therefore, functionalized graft or block copolymers are often used for the compatibilisation of LCP/TP blends [Datta 1995, Magagnini 1998, Miller 1995, Miller 1997, O'Donnel 1995]. Both graft and block compatibilisers should contain segments identical with those of the blend components, allowing them to migrate to the interface and reduce the tension between the matrix and the dispersed phase. As previously described, an extensive number of studies were performed with compatibilised LCP/TP blends. This literature review, will be, however, essentially focused in systems containing Rodrun LC3000 [Wano 1998, Bualek 1999, Datta

1995, O'Donnell 1995], since this is the liquid crystalline polymer that is present in the LCP/TP systems in study.

Datta and Baird used maleic anhydride-grafted-PP (MA-g-PP) as a compatibiliser for Rodrun/PP blends and found that the addition of this compatibiliser leads to an increase of the Young's modulus for values higher than those predicted by the rule of mixtures. This increase was observed for blends with 20, 50 and 80 wt % LCP. Additionally, an increase of both tensile strength and toughness was observed. In this sense, the addition of MA-g-PP revealed to be quite effective in terms of improvement of the tensile properties. Nevertheless, no information exists about the influence of the addition of MA-g-PP on the impact properties of the blends [Datta 1995].

The addition of a compatibiliser to an LCP/TP blend may be detrimental for the formation of the typical fibrillar structure that is known to be responsible for the mechanical enhancement in the flow direction. O'Donnell and Baird found that the addition of a considerable amount of compatibiliser gives rise to LCP droplets with small dimensions that difficult the formation of fibrillar structures [O'Donnell 1995]. Thus, it is fundamental to analyse properly the best chemical structure and also the correct amount of compatibiliser, in order to improve the adhesion between the two components of the blend, without compromising the typical fibrillar morphology.

The influence of the compatibiliser on the morphological properties of polypropylene and Rodrun LC3000 was studied [Wanno 1998]. For this purpose, they used three compatibilisers: a tri-block copolymer of styrene (ethylene-butylene) styrene (SEBS), an ethylene-propylene diene monomer (EPDM) and an anhydride maleic grafted EPDM (MA-g-EPDM). They reported that the composites containing compatibilisers have a better dispersion of the LCP and that the LCP fibrils are thinner comparing with those in the non-compatibilised blends. The compatibiliser that showed the best results was SEBS, which was attributed to its

chemical structure (constituted by groups chemically compatible with both the dispersed and the continuous phase). With respect to the rheology, they observed an increase of the viscosity with the addition of compatibilisers, especially for the blends where SEBS was used. This behaviour was only observed for the lower shear rates and was attributed to an enhancement of the molecular entanglements at the interface. This study was only focused on the morphological and rheological properties, with no information about the mechanical behaviour of the compatibilised blends being provided.

The effect of the addition of compatibilisers on the tensile and impact properties of films of Rodrun LC3000/PP blends was studied. The compatibilisation was, in this case, performed by the use of three compatibilisers, a triblock thermoplastic elastomer of styrene-ethylene-butylene-styrene (SEBS), a maleic anhydride grafted SEBS (MA-SEBS) and a maleic anhydride grafted polypropylene (MA-g-PP) containing 1.8 wt % and 0.1 wt % of maleic anhydride, respectively. Their aim was to study the influence of the addition of compatibilisers with elastomeric and thermoplastic natures (by comparing the properties of blends compatibilised with SEBS and MA-g-PP) and the influence of the presence or absence of anhydride maleic in compatibilisers with an elastomeric nature (by comparing the blends with SEBS and SEBS-g-MA). The main conclusions were: a) elastomeric compatibilisers, SEBS and SEBS-g-MA are more effective than MA-PP, since they lead to the increase of the viscosity and thus to the formation of thinner fibrils and to an improvement of the impact strength and b) the effectiveness of compatibilisers with elastomeric nature is reduced by the addition of maleic anhydride. A shortcoming of this study was the fact that it was carried out for films and not for injection moulded samples and the applicability of LCP/TP compatibilised systems in industrial purposes requires an analysis in terms of injection moulded specimens, since the thermo-mechanical history imparted on the material in the latter is very different from that of the former.

From the rheological point of view, the emphasis of the previous studies on compatibilised liquid crystalline polymer and thermoplastic blends has been on the evaluation of their fundamental properties under stationary conditions ([Liang 2002, Tjong 2003, Bualek-Limcharoen 1999, Brostow 1996, Magagnini 1998], among others) and not under transient ones which are, in fact, those most important during processing. One of the few exceptions is the work of Lazkano *et al.*, where the authors studied the transient response [Lazkano 2002]. The preparation of these blends was carried out in a different way, thus leading to two blends, differing in terms of the diameters of the LCP structures. In their work, some relationships were established between the evolution of both stress and first normal stress difference as a function of the strain and the diameters of the LCP structures. The transient results obtained for the LCP/TP blend revealed a shear stress overshoot for very low deformations, followed by a shallow undershoot at higher deformations and a normal stress overshoot located at approximately the same strain. They considered that this behaviour is due to the orientation and deformation of the LCP structures [Lazkano 2002].

Taking into account the potential industrial interest of these materials, it should be considered, however, that there is still a lack of knowledge on specific properties, which are essential to understand and, eventually, control the processing. For example, during processing the behaviour of the materials is not fully developed since the properties are essentially in a transient state. However, as shown previously, the data in this area is very scarce in the literature, with the work of Lazkano *et al.* (in which the authors studied the transient response of polypropylene, Rodrun LC5000 and blends containing 30 wt % LCP) being the exception [Lazkano 2002]. Thus, it is quite clear that an improved knowledge of the rheological response of these materials under non-stationary and non-linear conditions is needed, particularly in which concerns the influence of the LCP and compatibiliser content, as well as the type of compatibiliser used.

References

- [Badum 1942] E. Badum, U. S. Pat. No. 2.297.194 (1942)
- [Badwen 1937] F. C. Badwen and N. W. Pirie, *Proc. Roy. Soc. London, Ser. B*, **123**, 274
- [Baird 1996] J. P. de Souza Robertson, D. G. Baird, *Liquid Crystalline Polymer Systems: Technological Advances* (Chap. 6), ed. A. I. Isayev, T. Kyu and S. Z. D. Cheng, ACS Books, Washington DL 1996
- [Ballard 1958] D. G. H. Ballard, *Cortaulds Ltd*, U.K. Patent BP 864 (1958)
- [Bastida 1995] S. Bastida, J. I. Eguiazábal and J. Nazábal, *J. Appl. Polym. Sci.* **56**, 1487(1995)
- [Boersma 1999] A. Boersma and J. Van Turnhout *Polym.* **40**, 5023(1999)
- [Bordereau 1992] V. Bordereau, Z. H. Shi, L.A. Utracki, P. Sammut and M. Carrega *Polym. Eng. Sci.* **32**, 1846 (1992)
- [Brostow 1996] W. Brostow, T. Sterzynski and S. Triouleyre *Polym.* **37**, 1561 (1996)
- [Brown 1993] C. S. Brown, P.T. Alder *Polymer Blends and Alloys*, ed. M. J. Folkes and P. S. Hope, Chapman and Hall, London (1993)
- [Bualek-Limcharoen 1999] S. Bualek-Limcharoen, J. Samran, T. Amornsakchai and W. Meesiri *Polym. Eng. Sci.* **39**, 312 (1999)
- [Chan 1997] C. K. Chan, C. Whitehouse, P. Gao and C. K. Chai *Polym.* **42**, 7847 (1997)
- [Chin 1979] H. B. Chin and C. D. Han *J. Rheol.* **29**, 557 (1979)
- [Choi 1996] G. D. Choi, S. H. Kim and W. H. Jo *Polym. J.* **28**, 527 (1996)
- [Choi 1996a] G. D. Choi, W. H. Jo and H. G. Kim *J. Appl. Polym. Sci.* **59**, 443 (1996a)
- [Chung 1986] T. S. Chung, *Polym. Eng. Sci.* **26(13)**, 901 (1986)
- [Collier 1998] M. C. Collier, *Reclamation and Reprocessing of a Thermotropic Liquid Crystalline Polymer from Composites of Polypropylene Reinforced with Liquid Crystalline Polymer*, Masters of Science, Virginia (1998)
- [Coran 1969] A. Y. Coran and R. Patel, *Rubber Chem. Technol.* **53**, 1063 (1969)
- [Cox 1987] M. K. Cox *Mol. Cryst. Liq. Cryst.* **153**, 415 (1987)

- [Datta 1995] A. Datta and D. G. Baird *Polym.* **36**, 505 (1995)
- [Donald 1992] A. M. Donald, A. H. Windle, *Liquid Crystalline Polymers*, Cambridge University Press, Cambridge (1992)
- [Dow 1986] *Plast. Technolog.*, **44**, 103 (1986)
- [Farasoglou 2000] P. Farasoglou, E. Kontou, G. Spathis, J. L. Gomez Ribelles and G. Gallego Ferrer *Polym. Composite* **21**, 84 (2000)
- [Filipe 2004a] S. Filipe, M. T. Cidade, M. Wilhelm and J. M. Maia *Polym.* **45**, 2367 (2004)
- [Filipe 2004b] S. Filipe, J. M. Maia and M. T. Cidade *Adv. Mat. Forum* **456**, 476 (2004)
- [Friedel 1922] G. Friedel *Ann. Phys.* **18**, 273 (1922)
- [Gabellini 1996] G. Gabellini and R. E. S. Bretas *J. Appl. Polym. Sci.* **61**, 1803 (1996)
- [Gotsis 2000] A. D. Gotsis and M. A. Odriozola *J. Rheol.* **44**, 1205 (2000)
- [Greshman 1960] W. F. Greshman and M. Hunt, U.S. Pat. No. 2 933 480, Apr. 10, 1960
- [Hancock 1846] T. Hancock, Engl. Pat. No. 11, 147 (1846)
- [Heino 1994] M. T. Heino, P. T. Hietaoja, T. P. Vainio and J. V. Seppälä *J. Appl. Polym. Sci.* **51**, 259 (1994)
- [Huneault 1995] M. A. Huneault, Z. H. Shi and L. A. Utracki *Polym. Eng. Sci.* **35**, 115 (1995)
- [Irving 1962] H. H. Irving, U.S. Pat. No. 3.010.936 (1961)
- [Jackson 1976] W. J. Jackson and H. F. Kuhfuss, *J. Poly. Chem.* **14**, 2043 (1976)
- [Kessler 1992] S. Kessler, *Plastics Additives and Modifiers Handbook* (Chap. 48), Ed. J. Edenbaum, Van Nostrand Reinhold, New York (1992)
- [Kernick 1999] W. A. Kernick III and N. J. Wagner *J. Rheol.* **43**, 521 (1999)
- [Konrad 1934] E. Konrad and E. Tschunkur, U. S. Patent No. 1. 973. 000 (1934)
- [Kwolek 1971] S. L. Kwolek, DuPont, U.S. Pat. No. 3 600 350 (1971)
- [Lazkano 2002] J. M. Lazkano, J. J. Peña, M. E. Muñoz and A. Santamaría *J. Rheol.* **46**, 959 (2002)
- [Lee 2003] M. W. Lee, X. Hu, C. Y. Yue, L. Li and K. C. Tam *Comp. Sci. Tech.* **63**, 339 (2003)

- [Lee 2003a] M. W. Lee, X. Hu, L. Lin, C. Y. Yue, K. C. Tam and L. Y. Cheong *Comp. Sci. Tech.* **63**, 1921 (2003)
- [Lee 1994] S. Lee, S. Man Hong, Y. Seo, T. Suk Park, S. Sang Hwang, K. Ung Kim and J. Wook Lee *Polym.* **35**, 519 (1994)
- [Lehman 1890] O. Lehman, *Phys. Chem.* **5**, 427 (1890)
- [Liang 2002] Y. C. Liang and A. I. Isayev *Polym. Eng. Sci.* **42**, 994 (2002)
- [Magagnini 1993] P. Magagnini, *Thermotropic Liquid Crystalline Blends* (Chap. 1), Technomic Publ. Co. Lancaster PA (1993)
- [Magagnini 1998] P. L. Magagnini, M. Pracella, L. I. Minkova, T. S. Miteva, D. Sek, J. Grobelny, F. P. La Mantia and R. Scaffaro *J. Appl. Polym. Sci.* **69**, 391 (1998)
- [Mallick 1988] P. K. Mallick, *Fiber-Reinforced Composites*, Marcel Dekker, New York (1988)
- [Mathews 1999] F. L. Matthews and R. D. Rawlings, *Composite Materials: Engineering and Science*, Chapman and Hall, New York (1999)
- [Miller 1997] M. M. Miller, J. M. G. Cowie, D. L. Brydon and R. R. Mather *Polym.* **38**, 1565 (1997)
- [Miller 1995] M. M. Miller, J. M. G. Cowie, J. G. Tait, D. L. Brydon and R. R. Mather *Polym.* **36**, 3107 (1995)
- [Muramatsu 1987] J. Muramatsu and W. R. Krigbaum *J. Polym. Sci.: Part B: Polym. Phys.* **25**, 2303 (1987)
- [Ober 1984] C. K. Ober, J. I. Jin and R. W. Lenz, *Adv. Polym. Sci.* **59**, 103 (1984)
- [O'Donnell 1995] H. G. O'Donnell and D. G. Baird *Polym.* **36**, 3113 (1995)
- [Plummer 1993] Ch. J. G. Plummer, *Advanced Thermoplastic Composites: Characterization and Processing* (Chap. 8), Hanser Publishers, New York (1993)
- [Postema 1997] A. R. Postema and P. J. Fennis *Polym.* **38**, 5557 (1997)
- [Potente 2000] H. Potente, M. Bastian, A. Gehring, M. Stephan and P. Potschke *J. Appl. Polym. Sci.* **76**, 708 (2000)
- [Potente 2001] H. Potente, M. Bastian, K. Bergemann, M. Senge, G. Scheel and Th. Winkelmann *Polym. Eng. Sci.* **41**, 222 (2001)
- [Qin 1993] Y. Qin, D. L. Brydon, R. R. Mather and R. H. Wardman *Polym.* **34**, 1197 (1993)

- [Qin 1993a] Y. Qin, D. L. Brydon, R. R. Mather and R. H. Wardman *Polym.* **34**, 3597 (1993)
- [Reinitzer 1888] F. Reinitzer *Monatsch* **9**, 421 (1888)
- [Robinson 1956] C. Robinson *Trans.Faraday Soc.* **52**, 571 (1956)
- [Roggero 1993] A. Roggero, *Thermotropic Liquid Crystal Polymer Blends*, ed. F. P. La Mantia, Technomic, Lancaster (PA) (1993)
- [Roviello 1975] A. Roviello and A. Sirugi *J. Polym. Sci.: Polym. Lett.* **13**, 455 (1975)
- [Sarlin 1993] J. Sarlin and P. Tormala *J. Appl. Polym. Sci.* **50**, 1225 (1993)
- [Seppalla 1992] J. V. Seppalla, M. T. Heino and C. Kapanen *J. Appl. Polym. Sci.* **44**, 1051 (1992)
- [Serpe 1990] G. Serpe, J. Jarrin and F. Dawnas *Polym. Eng. Sci.* **30**, 553 (1990)
- [Scaffaro 1999] R. Scaffaro, F. P. La Mantia, I. T. Pentchev and G. H. Hu *Mol. Cryst. Liq. Cryst.* **336**, 169 (1999)
- [Scott 1995] C. E. Scott and C. W. Macosko *Polym.* **36**, 461 (1995)
- [Shibley 1982] A. M. Shibley, *Handbook of Composites* (Chap. 7), ed. G. Lubin, Van Nostrand Reinhold, New York (1982)
- [Shi 1992a] Z. H. Shi and L. A. Utracki *Polym. Eng. Sci.* **32**, 1824 (1992)
- [Shi 1992] Z. H. Shi and L. A. Utracki *Polym. Eng. Sci.* **32**, 1834 (1992)
- [Sundaraj 1995] U. Sundaraj and C. W. Macosko *Macromolecules* **28**, 2647 (1995)
- [Tjong 1996] S. C. Tjong, S. L. Liu and R. K. Y. Li *J. Mater. Sci.* **31**, 479 (1996)
- [Tjong 2002] S. J. Tjong, S. A. Xu and Y. W. Mai *Polym. Comp.* **24**, 437 (2003)
- [Tjong 2003] S. C. Tjong *Mat. Sci. Eng.* **R41**, 1 (2003)
- [Tjong 2003a] S. J. Tjong, S. A. Xu and Y. W. Mai *J. Appl. Polym. Sci.* **88**, 1384 (2003)
- [Tjong 2003b] S. J. Tjong, S. A. Xu and R. K. Y. Li *Comp. Sci. Technol.*, **62**, 2017 (2002)
- [Tyagi 2002] S. Tyagi S and A. K. Ghosh *Polym. Eng. Sci.* **42**, 1309 (2002)
- [Yoon 1990] H. N. Yoon *Coll. Polym. Sci.* **268**, 230 (1990)
- [Yoon 1992] H. N. Yoon, L. C. Charbonneau and G. W. Calundann *Adv. Mat.* **4**, 206 (1992)

- [Yoshikai 1996] K. Yoshikai, K. Nakayama and M. Kyotani *J. Appl. Polym. Sci.* **62**, 1331 (1996)
- [Vaccarl 1976] J. A. Vaccarl, *Prod. Eng.* **39**, 212, (1976)
- [Viswanathan 1995] R. Viswanathan and A. I. Isayev *J. Appl. Polym. Sci.* **55**, 1117 (1995)
- [Wanno 1998] B. Wanno, J. Samran and S. Bualek-Limcharoen *Rheol. Acta* **37**, 399 (1998)
- [Wanno 2000] B. Wanno, J. Samran and S. Bualek-Limcharoen *Rheol. Acta* **39**, 311 (2000)
- [Williams 1991] D. J. Williams *Adv. Polym. Tech.* **10**, 173 (1991)
- [Wilson 1992] T. S. Wilson and D. G. Baird *J. Non-Newt. Fluid. Mech.* **44**, 85 (1992)
- [Xu 2000] Q. W. Xu and H. C. Mau, *Polym.* **41**, 7391 (2000)

3 MATERIALS AND METHODS

MATERIALS

The pure materials used to produce the blends studied in this thesis were polypropylene (Stamylan P 12E62 from DSM) and a liquid crystalline polymer (Rodrun LC3000 from Unitika, which chemical structure is depicted in figure 3.1). The thermoplastic used for the preparation of the blends is an isotactic polymer with a weight-average molecular weight (\overline{M}_w) of 1,200,000 g/mol (obtained by GPC) and a melt flow index of 0.8 g/10 min (at 230 °C and for 21.6 N). The liquid crystalline polymer is an aleatory copolyester of 60 % mol of *p*-hydroxybenzoic acid (HBA) and 40 % mol of polyethylene terephthalate (PET). The molecular weight for the LCP was not obtainable, since no solvent was found to dissolve Rodrun LC3000 [Filipe 2004a].

In order to improve the compatibility between the liquid crystalline polymer and the thermoplastic, five different compatibilisers were used. Of these, three (compatibilisers A, B and C) were prepared in the framework of the present work. Since the composites that are being tested are based on blends of LCP (a co-polyester) with polypropylene (thermoplastic), the compatibilisers synthesised present an oligomeric aliphatic and linear structure as schematised in figure 3.2 [Duarte 2004]. The reactants used in the synthesis of compatibiliser A were dodecanol, a dimeric acid and one oligomeric polyester, with the commercial name TerolTM. The dodecanol and the dimeric acid, due to their chain length, present higher compatibility with polypropylene while the oligomeric acid presents more compatibility with Rodrun LC3000. In the second compatibiliser, B, TerolTM has been substituted by PET, thus increasing the compatibility with the LCP and, finally, compatibiliser C is based on Tall Oil Fatty Acid (TOFA), and PET, which allowed for a decrease in the aliphatic chain length. The fourth compatibiliser, D is a commercial material constituted by maleic anhydride-grafted polypropylene (0.3 wt %) with the commercial name

Epolene G-3003 Wax) and was supplied by Eastman. Compatibiliser E, the fifth compatibiliser, is an ethylene-propylene copolymer grafted with maleic anhydride (0.3 % by weight), with the commercial name Exxelor VA 18020 and was supplied by Exxon Mobil Chemical. The chemical structure of the different compatibilisers is presented in figure 3.3. More details about the synthesis of compatibilisers A, B and C (prepared by A.P Duarte under the supervision of J.C. Bordado) are available in Appendix I.

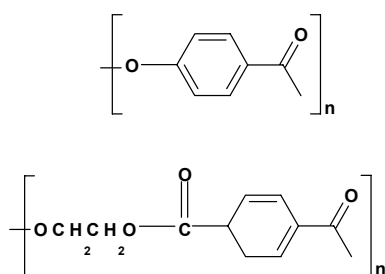


Figure 3.1 - Chemical structure of Rodrun LC3000.

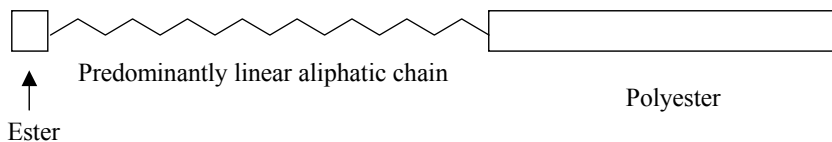
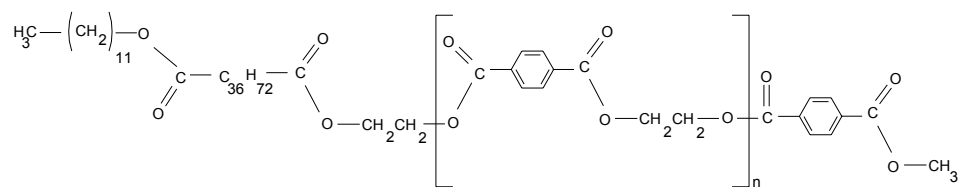
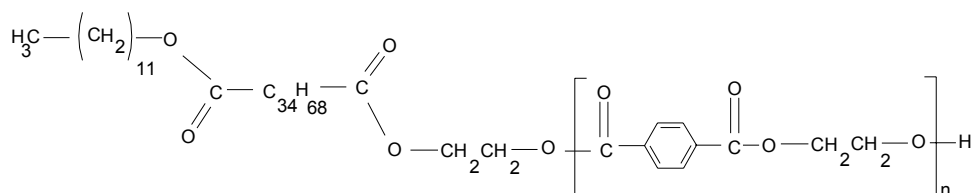


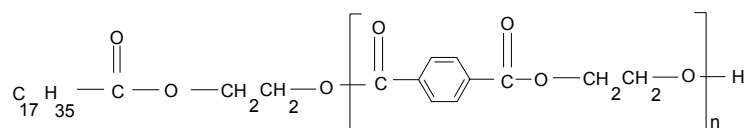
Figure 3.2 - Schematic representation of compatibiliser's chemical structure



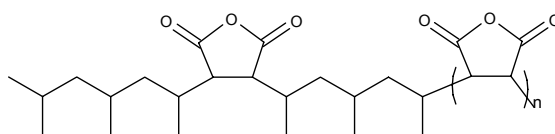
compatibiliser A



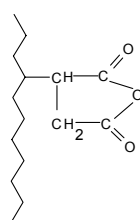
compatibiliser B



compatibiliser C



compatibiliser D



compatibiliser E

Figure 3.3 - Chemical structure of the compatibilisers.

METHODS

PROCESSING

Extrusion

Pellets of the pure components (PP and Rodrun LC3000) were mixed in the weight percentage desired, by tumbling them together for 30 minutes. In the case of compatibilised blends (which will be discussed in chapters 5 and 6), the compatibiliser was also added to the LCP and PP at this point. After this procedure all the materials were dried in an oven at 90 °C for 24 hours, before extrusion.

The extrusion was performed resorting to a Leistritz LSM 30.34 co-rotating intermeshing twin-screw extruder with a screw diameter of 33.7 mm and a length to diameter ratio (L/D) of 29. Two different cylinders and screw configurations were used for the preparation of the LCP/TP blends, which are presented in figure 3.4 and 3.5 (from now on, they will be described as configuration 1 and configuration 2, respectively).

In both configurations, configuration 1 and 2 (figures 3.4 and 3.5) the screw is comprised by a series of transport elements (conveying regions) which are separated by mixing zones, constituted by staggering kneading blocks and left-handed elements (reverse-conveying elements). The screw used in configuration 1 is constituted by a conveying elements region, followed by a reverse-conveying element (displayed in red, in figure 3.4), which is located near valve 5. After this, the screw is constituted by a conveying region, which is followed by eleven staggering kneading blocks (with a staggering angle of -60 °) and by another group of conveying elements.

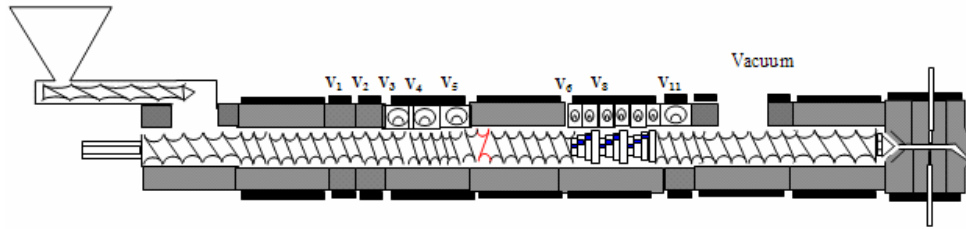


Figure 3.4 - Schematic representation of the screw and cylinder profiles used in the preparation of Rodrun LC3000/PP blends. Configuration 1.

In the case of configuration 2, a higher number of kneading-blocks is present, which are distributed along the screw length. The screw configuration is constituted by three mixing regions. The first comprises a group of eight staggering kneading blocks offset -60° , which is followed by a left-handed element (represented in red, at figure 3.5). The second mixing zone is located near valve 4 and it contains a group of five kneading blocks (with a staggering angle of 90°). Between valves 4 and 5 a conveying region exists and at valve 5 one can find the third mixing zone, which comprises a group of 6 kneading blocks with a staggering angle of 90° . After valve 5 a new conveying region exists and at valve 6 there is a reverse-conveying element, followed by a new conveying region.

The cylinder and screw configurations were defined in such a way that the zones of the screw in which the highest positive pressures exists (left-handed elements and kneading blocks) coincide with the zones where the valves are placed. In such a way it is possible to collect samples in those locations where the highest morphological changes are expected to occur. In the particular case of configuration 1 (see figure 3.4) a group of six small valves was placed near the region where the kneading blocks exists. This procedure was made in order to evaluate the way how the morphology develops, before, during and after the kneading blocks region.

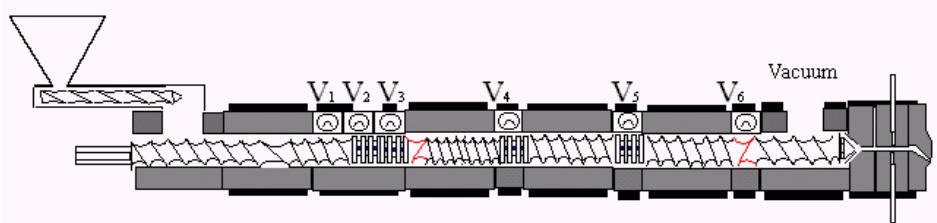


Figure 3.5 - Schematic representation of the screw and cylinder profiles used in the preparation of Rodrun LC3000/PP blends. Configuration 2.

In the first part of the work that deals with the preparation and characterisation of LCP/TP systems (chapter 4 to 6), the screw speed was set at 150 rpm, the output rate used was 4 kg/h and the processing temperatures, set constant along the extruder profile, were 220 °C [Filipe 2004a-f]. In the second part of the work, in which the optimisation was carried out (chapter 7), different screw speeds, temperatures and throughputs were used, which are depicted in table 3.1 [Filipe 2004g]. The screw and cylinder configuration used in chapter 4 to 7, was the one defined as configuration 1, which is depicted in figure 3.4. In sub-chapter 4.3, a different screw configuration was used, configuration 2, which is depicted in figure 3.5.

Table 3.1- Processing conditions employed in the optimisation process.

Processing conditions	Cond. 1	Cond. 2	Cond. 3	Cond. 4	Cond. 5	Cond. 6
Temperature (°C)	220	240	220	220	220	220
Screw Speed (rpm)	150	150	100	200	150	150
Output (kg/h)	4	4	4	4	2	8

After processing, the blends were immediately quenched in a water bath and subsequently pelletized. During processing samples were removed in different locations along the extruder length, using the home built collecting device system depicted in figures 3.4 and 3.5 (DEP-University of Minho [Machado 1999, Covas 2001]). The working principle of the collecting device system is represented in figure 3.6 and is described in more detail elsewhere [Machado 1999]. The remotion of samples is possible due to the presence of a circular orifice

that is located at the barrel wall (depicted in figure 3.6 as 1). A valve system comprising two cavities (represented by 3 and 4 in figure 3.6) is used to move the material from the inside of the extruder to the outside, where it will be immediately quenched in liquid nitrogen, for further analysis. Such a process can be accomplished by rotation of this valve in such a way that cavity number 4 moves to position 1. With this system, 1-3 g samples can be collected in less than 3 seconds and without disturbing the flow. Thus, the original morphology developed inside the extruder was almost completely retained. This system was previously used to study the morphological evolution in different kinds of blends (see, for example, [Covas 2001, Machado 1999, Van Duin 2001]). By the use of this collecting device it was possible to monitor the evolution of both morphology and rheology along the extruder length, which is in fact essential to control the final morphology and thus, the final mechanical performance. Additionally, it was possible to monitor the temperature at the different stages of the extrusion process, resorting to a fast thermocouple.

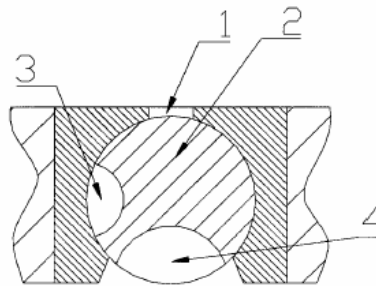


Figure 3.6 - Schematic representation of the sampling device system [Machado 1999].

Injection moulding

Before injection moulding all the blends previously obtained by extrusion were dried in an oven at 90 °C for 24 hours. Tensile specimens (dogbone-shaped) with 60x4x2 mm (length x width x thickness), impact specimens with 55 mm by 40 mm by 2 mm (length by width by

thickness), and flexural specimens with 40x12x2 mm (length x width x thickness) were produced by injection moulding using an injection moulding machine ENGEL model ES200/45 HL-V [Filipe 2004b-f].

The temperature profiles used for the preparation of the impact, flexural and tensile specimens were the presented in table 3.2. The different zones of the injection moulding machine are depicted in figure 3.6.

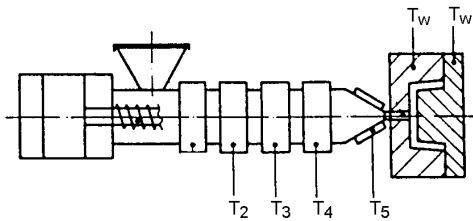


Figure 3.6- Scheme of injection moulding temperature profile.

Table 3.2- Processing temperatures for the injection moulding of tensile, flexural and impact specimens

T ₂ (°C)	T ₃ (°C)	T ₄ (°C)	T ₅ (°C)	T _w (°C)
170	190	200	210	30

MORPHOLOGICAL CHARACTERISATION

The evolution of the morphology along the extruder length was studied by means of Scanning Electron Microscopy (SEM). This characterisation was performed for samples collected at different locations along the extruder, for all the blends with and without compatibiliser [Filipe 2004a-g]. In addition, longitudinal as well as transversal cryogenically fractures of samples of the final extrudates were examined by this technique, the main objective being to observe both the degree of fibrillation and the adhesion between the two phases. The equipment used for this purpose was a Scanning Electron Microscope (SEM) ZEISS DSM with samples coated with gold using a POLARON SC502 and then examined at an accelerating voltage of 10 kV.

The morphology of the samples (in the form of compression moulded discs) used in the rheological measurements (both in the linear and non-linear regime) was also characterised by light microscopy, using a Linkam shearing system CSS 450. This procedure was used in addition to scanning electron microscopy because the shear cell allows the observation of the morphology before, during and after shearing, which is not possible to be done using solely SEM. This procedure allowed the morphology of the dispersed phase structures during and after shear to be checked at the same conditions used for the rheological measurements.

RHEOLOGICAL CHARACTERISATION

The samples collected along the extruder as well as the final extrudates were compression moulded in discs of 8 and 25 mm diameter (1 mm thick) and then characterised rheologically. The discs with the lower diameters were used for the oscillatory measurements, while the others were used for the measurements under steady and transient shear. Although this compression induces an extra thermal cycle on the samples, this has been found before [Filipe 2004a] to alter the morphology only slightly (and in the same way for all samples), since shear is virtually absent and compression moulding is carried out at relatively low temperatures. Thus, any differences in the original morphology between the different samples will, by and large, be retained after compression moulding.

The rheological measurements were carried out under oscillatory shear, both in the linear and non-linear regimes (LAOS) in order to establish differences between the different samples removed at different locations in the extruder and also to evaluate the influence of different LCP and compatibiliser contents, as well as distinct compatibilisers on the rheological behaviour of the final extrudates.

The rheometer used for the oscillatory measurements as well for both steady and transient shear measurements was an ARES rotational rheometer from Rheometrics. In order to

analyse the rheological behaviour of the materials for higher shear rates, a Rosand RH8-2 capillary rheometer was used.

The dynamic experiments in the linear regime were performed in oscillatory regime, applying a strain amplitude of $\gamma_0 = 0.1$. These measurements were carried out at different temperatures, ranging from 170 to 240 °C. According to the material in study, the frequency range varied, the minimum frequency being 0.26 rad.s⁻¹ and the maximum 300 rad.s⁻¹ (see chapters 4 to 7).

For the Large Amplitude Oscillatory Shear (LAOS), time sweep measurements were carried out for several strain amplitudes, ranging from $\gamma_0 = 0.1$ to $\gamma_0 = 7$. The sinusoidal strain was applied, for a constant temperature (170 °C) and frequency (6.28 rad.s⁻¹). A plate-plate geometry (diameter = 8 mm) and a gap of 0.25 mm were used. The time data was Fourier transformed, generating a Fourier spectra, consisting of several peaks, located at $3\omega_1$, $5\omega_1$, $7\omega_1$, etc., and also at the fundamental frequency (ω_1). Each one of these peaks is described by means of an amplitude (a_n) and a phase (ϕ_n). The non-linear character was obtained from the relative intensity between the third harmonic ($3\omega_1$) and the fundamental frequency (ω_1) and is represented by the normalized quantity $I(3\omega_1)/I(\omega_1)$ [Filipe 2004a, Filipe 2004c-f]. This technique was already used to characterise the non-linear character of other materials [Wilhelm 1999, Wilhelm 2000, Neidhöfer 2003]. The fundamentals of Fourier Transform Rheology are described in more detail in Appendix II.

In addition to the typical steady shear flow (by both rotational and capillary rheometry) measurements performed for LCP/TP blends, transient shear measurements were also carried out, in order to establish the rheological behaviour under non-steady conditions, which are actually, those that are known to be most important during processing. The latter measurements are usually very sensitive to the phenomena developed at the interface, and its use is thus essential to evaluate the compatibilisation processes [Filipe 2004c-d].

The steady shear (capillary and rotational) and the transient measurements were performed at temperatures between 200 and 240 °C. For the steady shear measurements a plate-plate geometry (diameter = 25 mm) was used and the gap was set at 1 mm. For the transient shear measurements a cone-plate (diameter = 25 mm, cone angle = 0.02 rad) was used. A pre-shear rate of 0.3 s^{-1} was applied during 600 s to the samples before measurements in transient shear were performed, in order to have the same initial condition for all the samples. For the transient shear measurement itself, a shear rate of 1 s^{-1} was applied during 600 s.

Considering the importance of extensional flow in industrial processes (namely extrusion and injection moulding) one should be aware of the rheological behaviour under elongation. For this reason, the pure materials and the blends (with and without compatibiliser) were also studied with respect to their elongational flow behaviour [Filipe 2004h]. This study was, until now only performed for pure liquid crystalline polymers, and no information is available concerning the influence of the LCP content, neither the importance of the use of different compatibilisers on the extensional flow behaviour. For these measurements a modified rotational rheometer (Weissenberg rheogoniometer, from Carrimed) was used [Maia 1999]. Different strain rates, ranging from 0.07 and 0.48 s^{-1} were applied at a temperature of 240 °C. The testing temperature used was the maximum temperature for which one could simultaneously have reliable data and minimize the residual crystallinity. Due to experimental constraints related with difficulties during the loading of the pure LCP samples (and consequent very low reproducibility) at the testing temperature (240 °C), no results will be shown for the pure liquid crystalline polymer. The real strain rates were obtained by measuring the evolution of the diameters (image analysis). A digital camera was used for this purpose. The strands used in the uniaxial extensional flow measurements were prepared in a capillary rheometer Rosand RH8-2, by extruding the material through a die with 2 mm diameter, at a

constant and low velocity. In order to avoid residual stresses in the samples, special care was taken before each measurement, by keeping each strand for some minutes at the test temperature, after loading. The samples were then stretched back into the measuring position, were allowed to relax further and the experiment only started when the torque measurement on the instrument was zero [Barroso 2003].

Some considerations must be taken with respect to the rheological measurements. The first consideration concerns the possibility of polypropylene degrading at the measuring temperatures (between 200 and 240 °C). In order to check it, shear was applied during 30 minutes at both 220 °C and 240 °C. Both viscosity and storage modulus remained constant, which indicates no degradation of the material. Additionally, Postema and Fennis [Postema 1997] have found that below 260 °C no thermal degradation occurs for a polypropylene with MFI ranging from 0.7 to 20 g/10 min, whereas the MFI of the PP used in this work is 0.8 g/10 min. Considering that the processing temperatures were 220 °C and 240 °C and that the material was always below 260 °C (as can be observed in the temperature profiles measured in both cases), no degradation was expected to occur.

Additionally it should be stated that the temperature used for the LAOS measurements (170 °C), was the highest temperature for which reproducible results were obtained. It should be kept in mind, however, that at this temperature the liquid crystalline polymer phase might possess some residual crystallinity, which therefore, may induce higher non-linearities than those expected in the absence of crystallinity.

MECHANICAL CHARACTERISATION

Tensile, flexural and impact measurements were carried out for injection moulded specimens [Filipe 2004b-d, Filipe 2004f-g].

The equipment used for the impact measurements was a Rosand Instrumented Falling Weight Impact Tester, Type 5. The impact mass used was 25 kg and the impact velocity was

set at 2 m/s. A set of 5 measurements was done and the final results from the peak force were obtained by the mean value of the different measurements. The tensile properties were tested using an Instron Universal Tester Machine model 1.16 at room temperature. A cross-head speed of 5 mm/min and a load cell of 50 kN were used. An extensometer (model Instron 2630-100) was used for these measurements. The mean and the standard deviation for the different tensile properties were calculated from 5 specimens.

The flexural properties were measured using an Instron Universal Tester Machine model 1.16 at room temperature. The cross-head speed was set at 2 mm/min. These measurements were carried out for specimens produced in the direction of the flow and in the direction perpendicular to the flow and the results were obtained from the average of a set of 5 measurements.

References

- [Barroso 2003] V. C. Barroso, Ph. D. Thesis, *Viscoelasticity of polymer melts in uniaxial extension flows* (2003)
- [Covas 2001] J. A. Covas, O. S. Carneiro and J. M. Maia, *Intern. J. Polym. Mat.* **50** (3-4), 445 (2001)
- [Duarte 2004] A. Duarte, M. T. Cidade, S. Filipe, C. B. Correia and J. Clarke, J. C. M. Bordado, *to be published*
- [Filipe 2004a] S. Filipe, M. T. Cidade, M. Wilhelm and J. M. Maia, *Polym.* **45**, 2367 (2004)
- [Filipe 2004b] S. Filipe, J. M. Maia and M. T. Cidade *Adv. Mat. Forum* **456**, 476 (2004)
- [Filipe 2004c] S. Filipe, J. M. Maia, C. R. Leal and M. T. Cidade, *J. Polym. Eng.*, *accepted*
- [Filipe 2004d] S. Filipe, J. M. Maia, A. Duarte, C. R. Leal and M. T. Cidade, *J. Appl. Polym. Sci.*, *submitted* (June 2004)
- [Filipe 2004e] S. Filipe, M. T. Cidade, M. Wilhelm and J. M. Maia, *J. Appl. Polym. Sci.*, *submitted* (August 2004)
- [Filipe 2004f] S. Filipe, J. M. Maia, C. R. Leal, A. R. Menon, A. Duarte and M. T. Cidade, *J. Appl. Polym. Sci.*, *submitted* (November 2004)
- [Filipe 2004g] S. Filipe, J. M. Maia, C. R. Leal and M. T. Cidade, *J. Polym. Eng. Sci.*, *submitted* (December 2004)

- [Filipe 2004h] S. Filipe, M. T. Cidade and J. M. Maia, *Rheol. Acta*, submitted (December 2004)
- [Machado 1999] A. V. Machado, J. A. Covas and M. Van Duin, *J. Appl. Polym. Sci.* **71**, 135 (1999)
- [Maia 1999] J. M. Maia, J. A. Covas, J. M. Nóbrega, T. F. Dias and F. E. Alves *J. Non-New. Fluid. Mech.* **80**, 183 (1999)
- [Neidhöfer 2003] T. Neidhöfer and M. Wilhelm *J. Rheol.* **47**, 1351 (2003)
- [Postema 1997] A. R. Postema, P. J. Fennis *Polym.* **38**, 5557 (1997)
- [Van Duin 2001] M. Van Duin, A. V. Machado and J. A. Covas *Macromol. Symp.* **170**, 29 (2001)
- [Wilhelm 1999] M. Wilhelm, P. Reinheimer and M. Ortseifer, *Rheol. Acta* **38**, 349 (1999)
- [Wilhelm 2002] M. Wilhelm *Macromol. Mater. Eng.* **287**, 83 (2002)

4 NON-COMPATIBILISED LIQUID CRYSTALLINE POLYMER AND THERMOPLASTIC BLENDS

4.1 STUDY OF THE INFLUENCE OF THE LCP CONTENT ON THE EVOLUTION ALONG THE EXTRUDER LENGTH*

INTRODUCTION

As referred in the introduction, several studies were conducted in order to understand how the morphological evolution occurs during the compounding of immiscible blends. However, the rheological evolution along the extruder length, and the relation between the morphology and the rheology developed during the compounding of liquid crystalline polymer and thermoplastic blends was not studied yet. In this work, a rheological study was carried out, both in the linear and in the non-linear regime, in order to attain an improved knowledge on this subject.

RESULTS AND DISCUSSION

MORPHOLOGY

During extrusion the developed morphology depends on several different parameters such as processing temperature, screw speed, throughput and screw elements. Taking these facts into account, different morphologies are to be found at different locations along the extruder length, according to the specific conditions in each zone. Even in the current case, where the same temperature was set for the different heating zones along the extruder, thermal differences were observed along the cylinder length, as can be seen in table 4.1. For example, the temperature at the conveying elements was lower than the observed at the kneading elements, which is essentially due to the lower shear rates and pressures in the former.

* adapted from S. Filipe, M. T. Cidade, M. Wilhelm, J. M. Maia, *Morphological and Rheological Evolution Along the Extruder Length for Rodrun LC3000 and PP*, Polymer, 45, 2367-2380 (2004)

Table 4.1 - Temperature profiles measured along the extruder length for the blends with 10, 20 and 40 wt % LCP, processed at 220 °C and 240 °C.

Processing Temperature (°C)	LCP content (wt %)	Temperature (°C)							
		valve 4	valve 5	valve 6	valve 7	valve 8	valve 9	valve 10	extrudate
220	10	226.2	228.4	227.9	229.4	229.6	231.7	232.2	236.1
	20	225.6	224.7	225.3	228.4	229.2	230.9	231.8	233.7
	40	222.6	224.3	224.7	225.2	227.3	228.9	231.0	231.5
240	10	242.5	243.2	243.4	244.8	244.1	244.9	245.2	245.4
	20	241.6	243.1	243.1	244.4	244.2	244.3	244.8	245.1
	40	241.2	242.7	241.7	241.2	243.3	243.9	241.0	243.9

The morphological measurements carried out for the blends with 10, 20 and 40 wt % LCP (see figures 4.1, 4.2 and 4.3, for blends processed at 220 °C and figures 4.5, 4.6 and 4.7, for blends processed at 240 °C) show that, at the beginning of the extruder, the LCP structures are essentially droplets distributed along the thermoplastic matrix. These LCP structures are progressively elongated along the extruder length, giving rise to fibrillar structures at the exit of the die. During processing, the material is subjected to shear and elongational forces that are responsible for the deformation and eventual break-up of the LCP structures.

Looking at the SEM images (figure 4.1) obtained for the blend with 10 wt % LCP (processed at 220 °C) it can be concluded that the LCP structures in the samples collected at valve 5 are less elongated than the samples removed at valve 6. This was expected, since the first sample was collected near a reverse-conveying element (located near valve 5), while the second sample was removed at valve 6, situated at the beginning of the mixing elements. The larger dimensions observed for the samples collected at the reverse-conveying zone can be explained as a consequence of the increase in the residence time that occurs in this region of the screw. On the other hand, at the mixing zones, *i.e.*, the kneading blocks, the shear rate is increased and as a consequence the shear stress is high enough to guarantee the elongation of the LCP droplets, as can be observed for the samples collected at valve 8. Finally, the material crosses the die, where it experiences the highest shear rates and elongations. Consequently, a

maximum deformation will occur, giving rise to a morphology where the LCP structures have the form of fibrils with the highest aspect ratio.

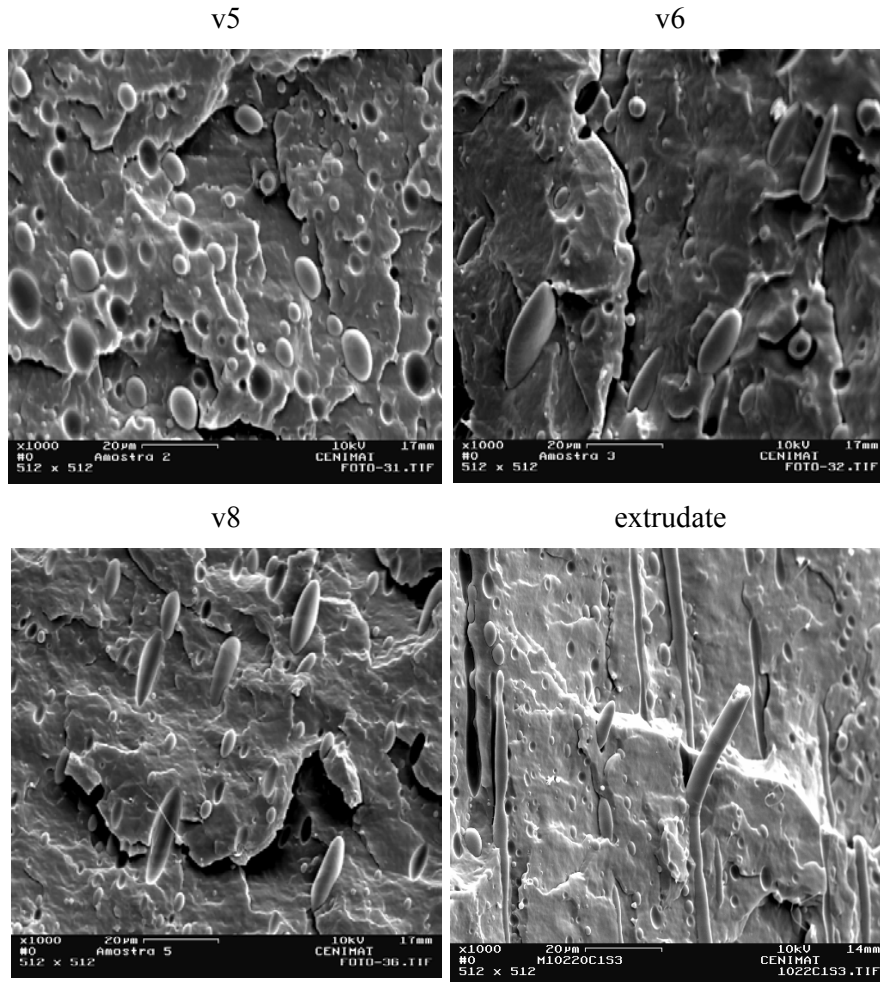


Figure 4.1 - Morphological evolution along the extruder length for the blend with 10 wt % LCP processed at 220 °C (SEM) - magnification of x1000 for all figures.

It is important to point out that in figures 4.1 to 4.3 and 4.5 to 4.7, the microphotography presented for the extrudate was obtained with samples cryogenically fractured in the longitudinal direction, instead of the usual transverse direction, since this allowed for a better definition of the fibrils.

When comparing the SEM images obtained for the blends with different LCP contents, processed at the same temperature (220 °C), it is possible to extract some conclusions about the influence of the LCP content on the morphology along the extruder length.

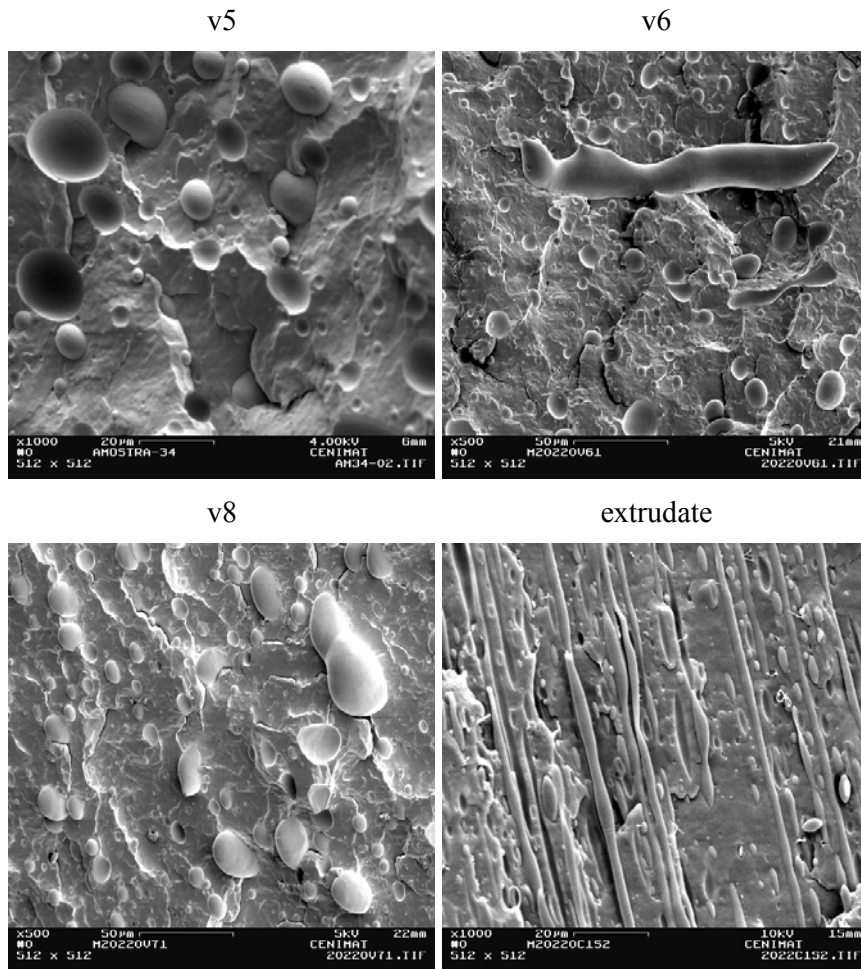


Figure 4.2 - Morphological evolution along the extruder length for the blend with 20 wt % LCP processed at 220 °C (SEM) - magnification of x500 for valves v6 and v8 and x1000 for v5 and extrudate.

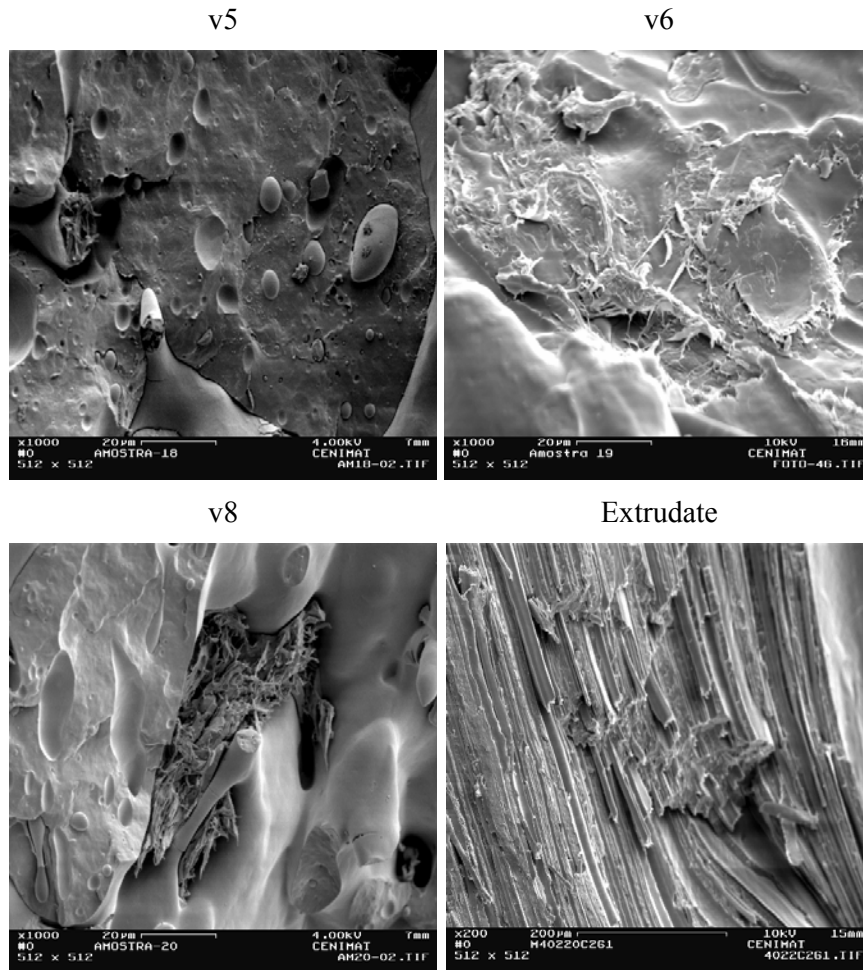


Figure 4.3 - Morphological evolution along the extruder length for the blend with 40 wt % LCP processed at 220 °C (SEM) - magnification of x1000 for all figures except extrudate (x200).

Comparing figures 4.1, 4.2 and 4.3 it can be concluded that an increase of the dispersed phase content leads to an increase of the mean particle size at a given location along the extruder, as expected (figure 4.4). This increase was not observed for the final extrudates, in which no significant differences were observed between the different blends, except that the density of the LCP fibrils increases clearly with the LCP concentration.

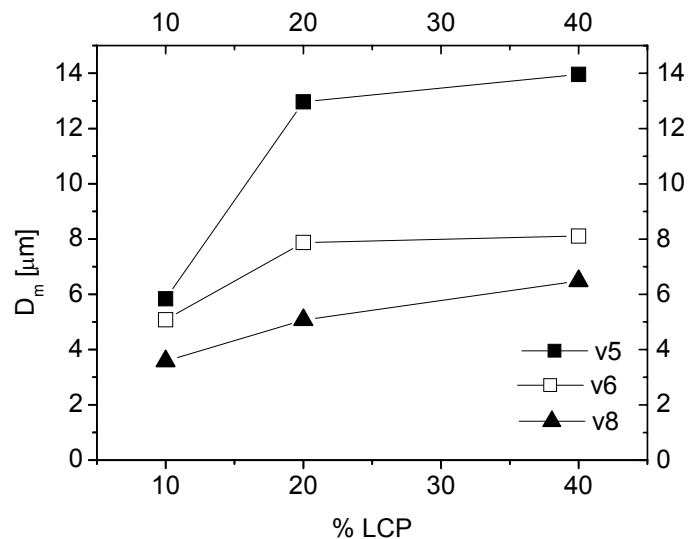


Figure 4.4 - Average droplet diameters for samples collected along the extruder of blends with 10, 20 and 40 wt % processed at 220 °C (lines are guides to the eyes).

In order to make a preliminary assessment of the influence of the temperature on the morphology, two different processing temperatures were used, 220 °C and 240 °C (see figures 4.5 to 4.7).

The first consideration, and the most important one, is that high processing temperatures lead to a lower viscosity of both components, which promotes the coalescence of the dispersed phase.

Moreover, the relative viscosity ratio between the two components was higher at 220 °C comparing with the one observed at 240 °C (see figure 4.8). As is known [Shi 1992] the formation of fibrillar structures is easier for a viscosity ratio close to one. Furthermore, the viscosity ratio slightly increases as a function of the shear rate, since at high shear rates, the polypropylene matrix shows more pronounced shear-thinning than the LCP.

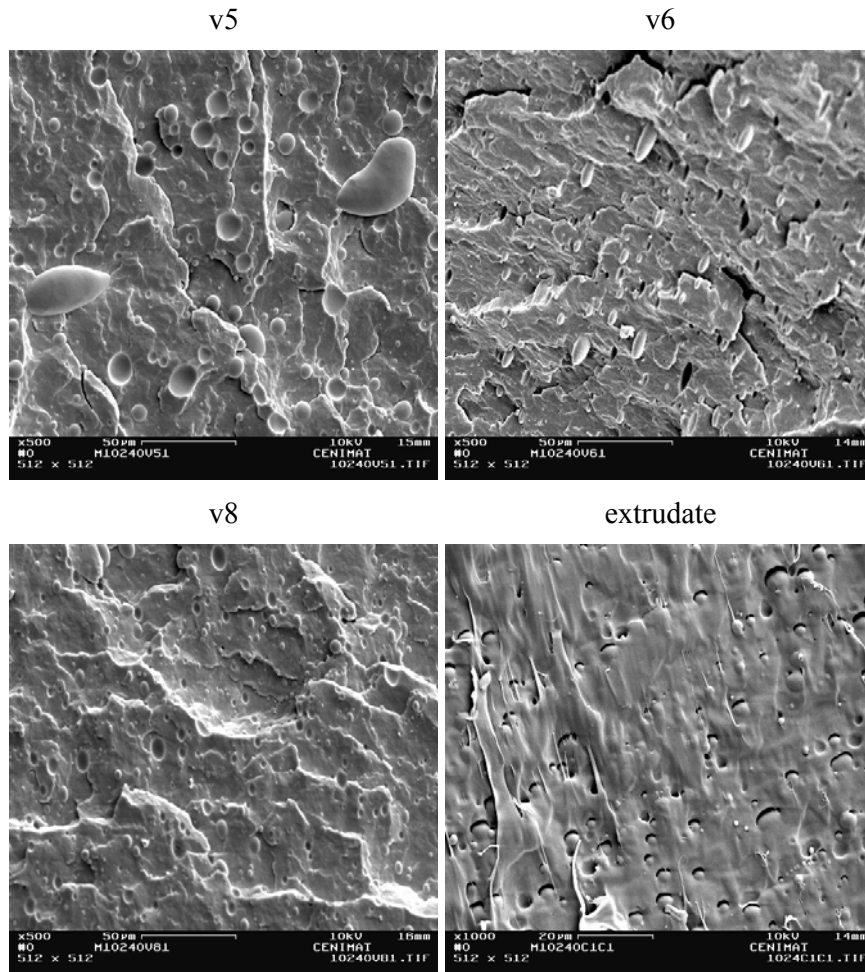


Figure 4.5 - Morphological evolution along the extruder length for the blend with 10 wt % LCP processed at 240 °C (SEM) - magnification of x500 for all valves except final extrudate (x1000).

Therefore, the formation of fibrillar structures was significantly improved for the blends with 10 and 20 wt % LCP processed at 220 °C, (figure 4.1, 4.2), whereas for the 40 % wt LCP blend, the incorporation content of the latter is so high that no significant differences can be seen, long fibrils being present in large numbers for both processing temperatures.

For a lower processing temperature the higher viscosity of the matrix hinders the flow of the dispersed phase inside the continuous phase. Due to the higher viscosity of the matrix, the stress to which the LCP structures are subjected is significantly higher than the stress observed at higher processing temperatures, leading to an easier deformation and thus to a more homogeneous morphology.

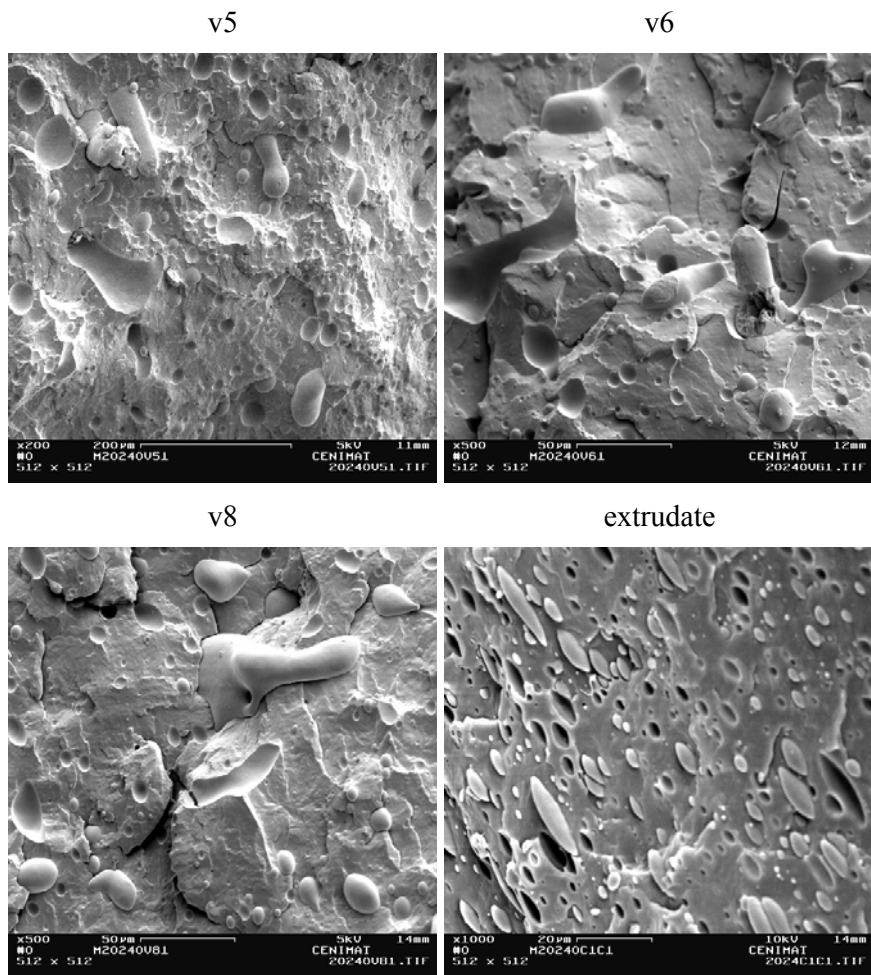


Figure 4.6 - Morphological evolution along the extruder length for the blend with 20 wt % LCP processed at 240 °C (SEM) - magnification of x200 for valve 5, x500 for valves 6 and 8 and x1000 for extrudate.

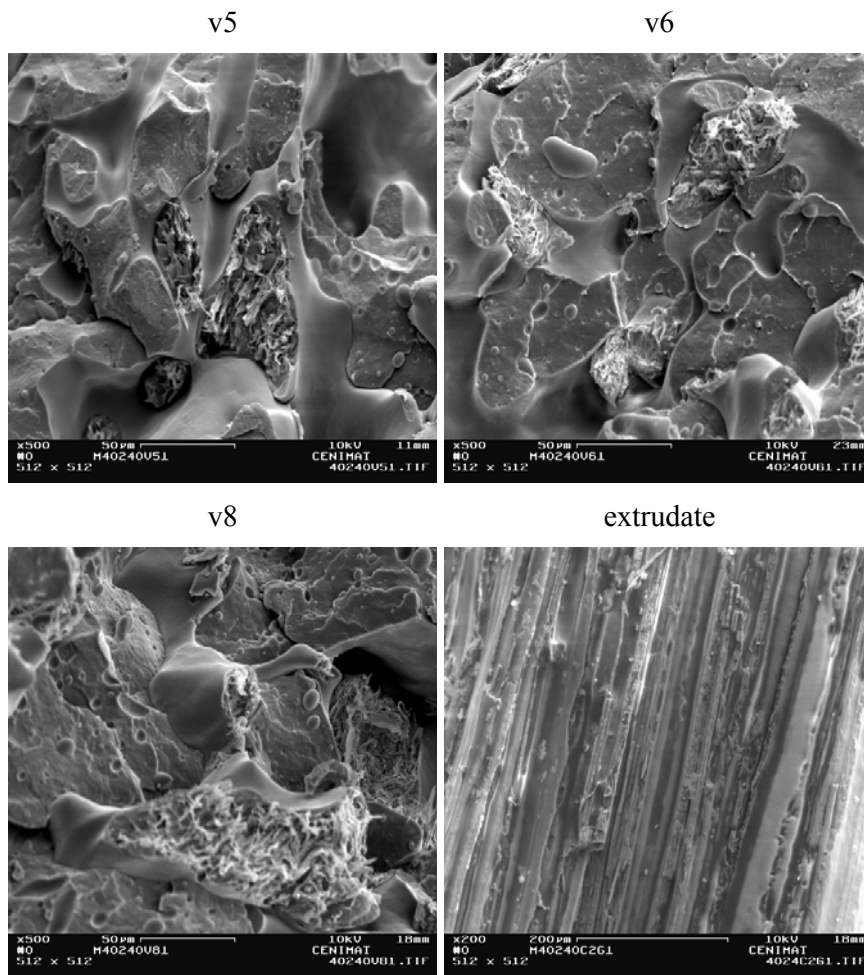


Figure 4.7 - Morphological evolution along the extruder length for the blend with 40 wt % LCP processed at 240 °C (SEM) - magnification of x500 for the valves and x200 for the extrudate.

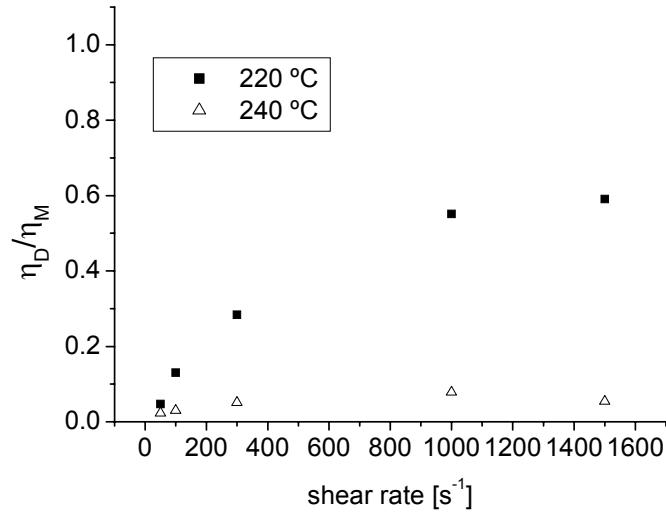


Figure 4.8 - Viscosity ratio between the dispersed phase and the matrix (η_D/η_M) as a function of shear rate at 220 °C and 240 °C.

As already described, moulded discs were produced from the samples collected along the extruder and in the extrudate, in order to study the evolution of the rheological properties along its length. In order to confirm the morphological changes observed by SEM inside the extruder, optical measurements under shear were also performed for samples collected along its length, at 170 °C, using a Linkam Shearing System CSS450 coupled with an optical microscope.

v5



v6



v8

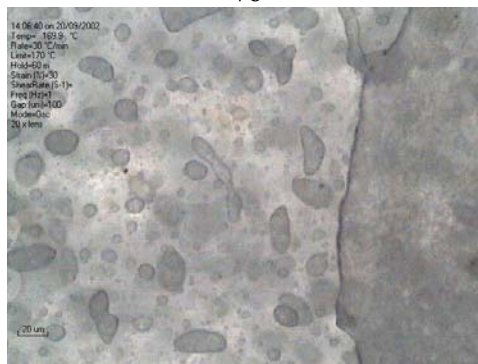


Figure 4.9 - Morphological evolution along the extruder length for the blend with 10 wt % LCP, at $T=170\text{ }^{\circ}\text{C}$, $\gamma_0 = 0.3$ (conducted using the Linkam optical shear system).

v5



v6



v8

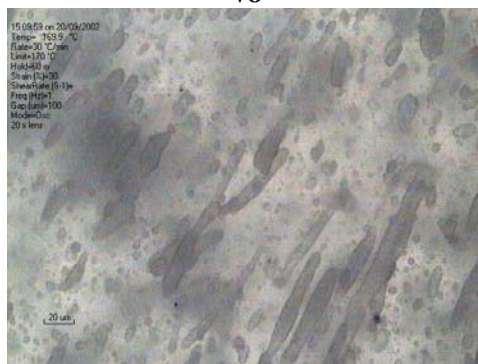


Figure 4.10 - Morphological evolution along the extruder length for the blend with 20 wt % LCP, at $T=170\text{ }^{\circ}\text{C}$, $\gamma_0 = 0.3$ (conducted using the Linkam optical shear system).

The images obtained for the discs corresponding to 10 wt % LCP (processed at $220\text{ }^{\circ}\text{C}$) allow several conclusions to be drawn: the moulded discs that correspond to the samples collected at valve 5 show LCP structures with droplet shapes, while for the moulded discs corresponding to the samples removed at valves 6 and 8, elongated LCP structures were observed. These observations are in agreement with the morphological results obtained for the samples directly collected from the extruder valves (figure 4.1). Similar conclusions can be

drawn for the blend with 20 wt % LCP (figure 4.10). It was not possible to use the Linkam System for the morphological analysis of the blend with 40 wt % LCP, due to the opacity of this material.

LINEAR OSCILLATORY RHEOLOGY

The study of the linear rheological properties of the pure components and blends is essential to understand the morphology developed for LCP/TP blends. As already discussed, a fibrillar morphology or a dispersed droplet morphology will develop depending on the viscosity ratio and on the capillary number. For a viscosity ratio lower than one, a finer and a more uniform distribution of the LCP phase is obtained, while for viscosity ratios higher than one, the LCP structures became larger and the dispersion will be less uniform. The formation of fibrillar structures is easier for viscosity ratios near unity [Heino 1994, Choi 1996]. Deformation of the LCP particles is to be anticipated provide enough shear is applied in order to be possible to the viscous forces to overwhelm the interfacial forces. Since break-up processes are also possible for this viscosity ratio, it is expected that the blends with the higher LCP content will be those with the larger LCP structures, since the probability of coalescence will increase.

An increase of the deformation of the LCP structures is expected along the extruder, with the consequent decrease of the mean diameter, because the shear rate increases from the beginning to the end of the extruder. In principle, smaller average particle diameters, together with the fact that non-spherical particles yield higher apparent volume fractions than spherical particle, should yield an increase in interfacial area and a consequent increase in viscosity. However, in the case on non-compatibilised blends such as the ones studied in this chapter, lack of adhesion at the interface and the orientation of the dispersed phase may become the dominant factor [Mustafa 2003] and may actually decrease the viscosity.

In what regards elasticity in the case of non-compatibilised blends and due to the poor load transfer ability of the material through the interface, in principle the amount of energy stored by the material (G') should be higher for the samples with spherical structures and with lower aspect ratios, since this is the situation that minimises interfacial area.

The evolution of both the storage and the loss modulus as a function of frequency was evaluated for the samples collected from valve 4 to valve 10 and for the final extrudates of the blends with 10, 20 and 40 wt % LCP content.

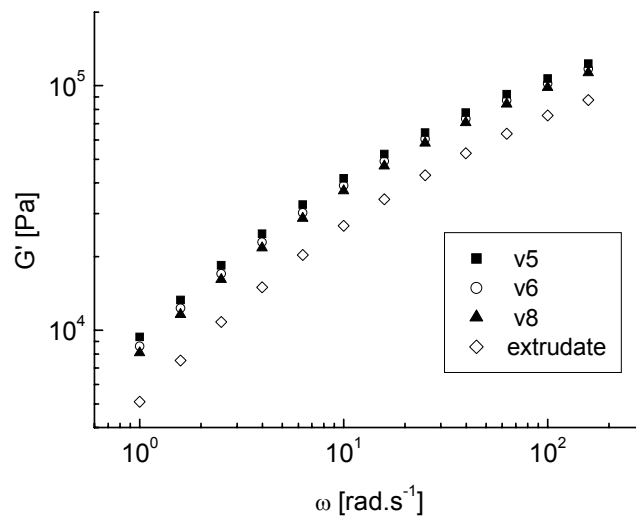


Figure 4.11 - Evolution of the storage modulus along the extruder length for the blend with 10 wt % LCP, at $T=170$ °C, $\gamma_0 = 0.1$.

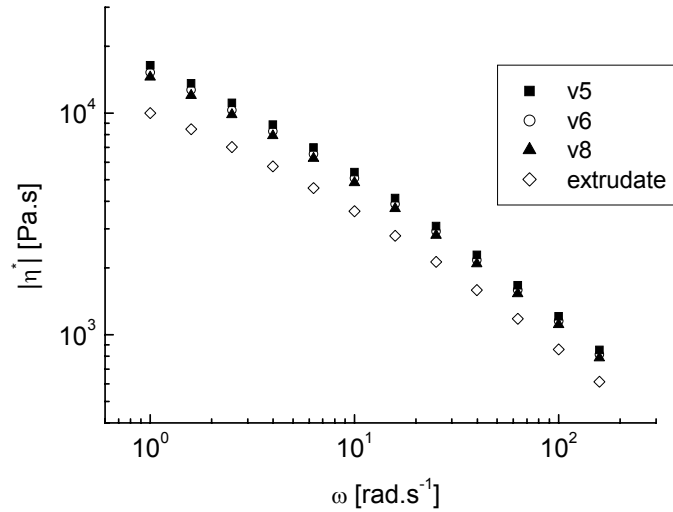


Figure 4.12- Evolution of the complex viscosity along the extruder length for the blend with 10 wt % LCP, at T=170 °C, $\gamma_0 = 0.1$.

The analysis performed for the blend with 10 wt % LCP (figures 4.11 and 4.12) showed that, within experimental error, both the elastic modulus and the viscosity (η^*) remain approximately constant (or, at most, decrease slightly) as the material progresses along the extruder length. The storage modulus and the complex viscosity decrease, however, for the extrudates, which means that the differences are only noticeable when comparing the viscosity of samples with droplets and fibrils as the dispersed phase.

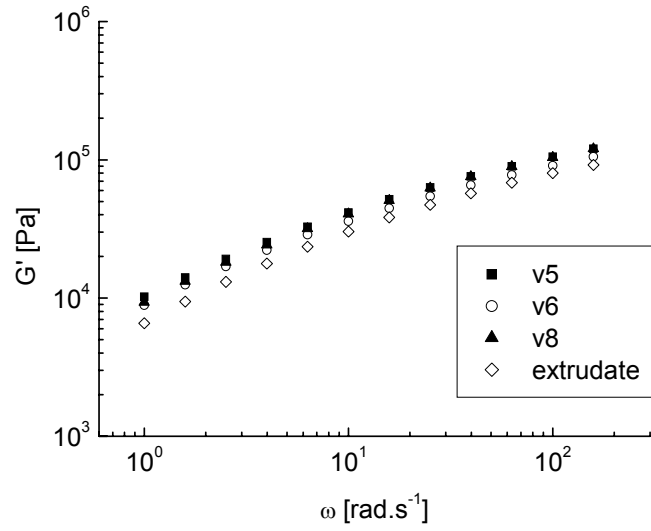


Figure 4.13 - Evolution of the storage modulus along the extruder length for the blend with 20 wt % LCP, at $T=170\text{ }^{\circ}\text{C}$, $\gamma_0 = 0.1$.

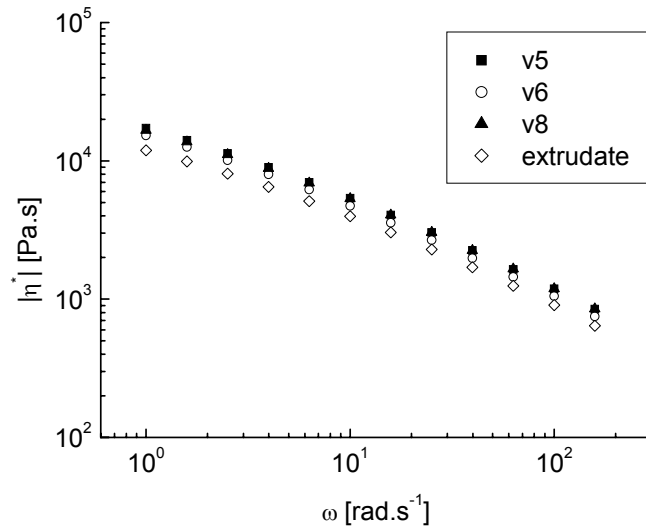


Figure 4.14 - Evolution of the dynamic viscosity along the extruder length for the blend with 20 wt % LCP, at $T=170\text{ }^{\circ}\text{C}$, $\gamma_0 = 0.1$.

The blend with 20 wt % LCP shows qualitatively similar results to the 10 wt % LCP one, *i.e.*, there is a negligible (if at all) decrease in both the storage modulus (G') and the

dynamic viscosity (η^*) along the extruder. However, once again, a decrease of both G' and η^* was observed for the final extrudates (figures 4.13 and 4.14).

For the blend with 40 wt % LCP, there are larger differences in modulus and complex viscosity along the extruder, especially for the lower frequencies, which is a normal phenomenon (see figures 4.15 and 4.16). This can be explained by the morphology present (figure 4.3), namely by the combination of larger average particle size due to the increased LCP content and orientation.

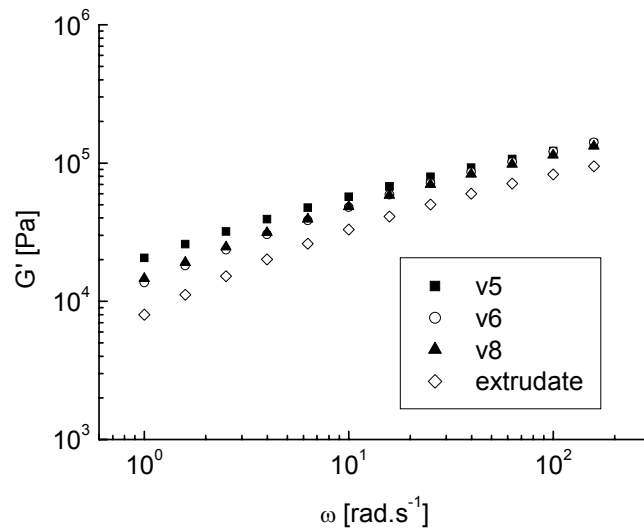


Figure 4.15 - Evolution of the storage modulus along the extruder length for the blend with 40 wt % LCP, at $T=170$ °C, $\gamma_0 = 0.1$.

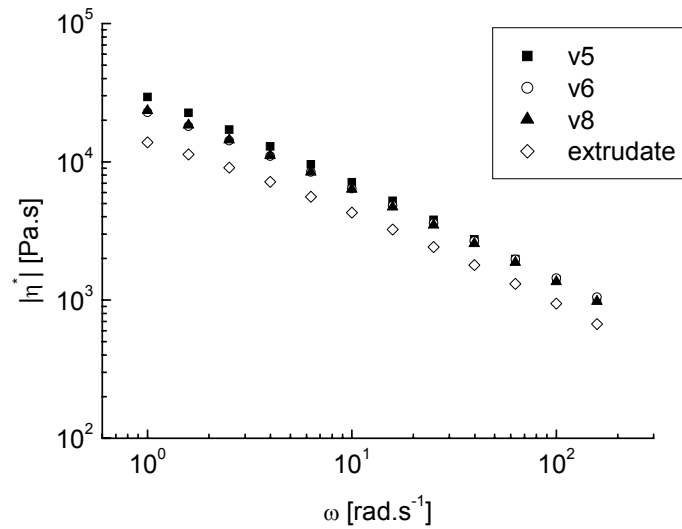


Figure 4.16 - Evolution of the dynamic viscosity along the extruder length for the blend with 40 wt % LCP, at T=170 °C, $\gamma_0 = 0.1$.

NON-LINEAR OSCILLATORY RHEOLOGY

Large Amplitude Oscillatory Shear (LAOS) was applied to the different samples collected at different locations along the extruder in order to generate a non-linear response. The non-linear character was obtained from the relative intensity between the third harmonic ($3\omega_1/2\pi$) and the fundamental frequency ($\omega_1/2\pi$) and is represented by the normalized quantity $I(3\omega_1/2\pi)/I(\omega_1/2\pi)$; the higher this relative intensity, the more non-linear is the response.

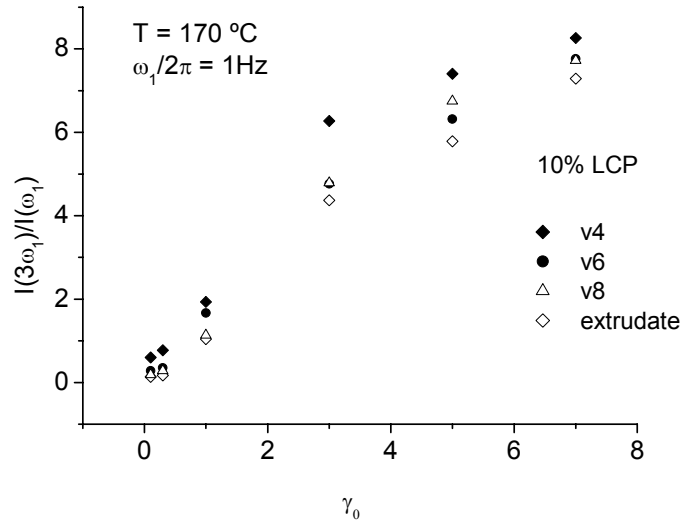


Figure 4.17 - Increase of $I(3\omega_1)/I(\omega_1)$ with the applied strain amplitude for the different samples collected along the extruder length (blend with 10 wt % LCP, at $T=170\text{ }^\circ\text{C}$).

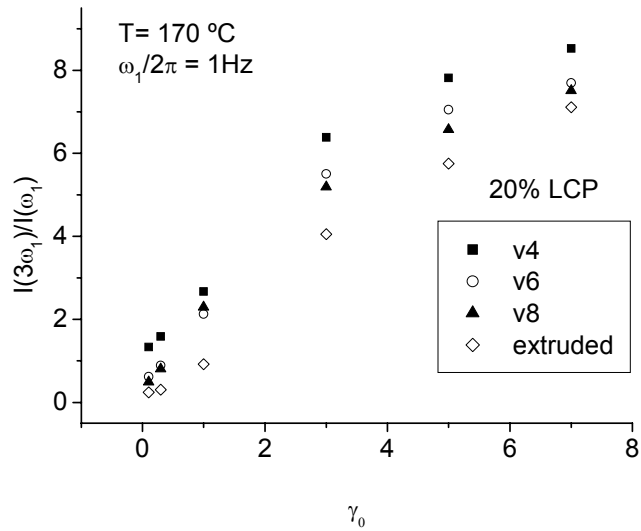


Figure 4.18 - Increase of $I(3\omega_1)/I(\omega_1)$ with the applied strain amplitude for the different samples collected along the extruder length (blend with 20 wt % LCP, at $T=170\text{ }^\circ\text{C}$).

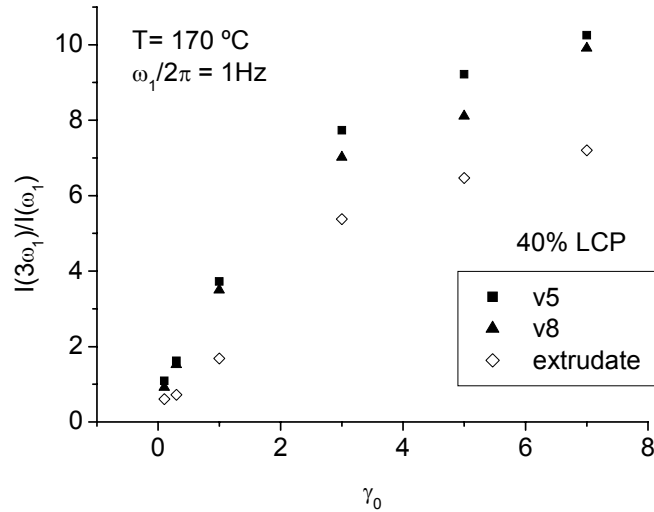


Figure 4.19 - Increase of $I(3\omega_1)/I(\omega_1)$ with the applied strain for the different samples collected along the extruder length (blend with 40 wt % LCP, at $T=170\text{ }^\circ\text{C}$).

The evolution of the relative intensity of the third harmonic over the fundamental frequency with the applied strain amplitude was obtained for all the samples, from valve 4 to the final extrudate. As expected, this type of experiments proved to be very sensitive to the LCP content (clearly more so than linear oscillatory rheology), with large differences being observed for the evolution of the 20 and, especially, the 40 wt % LCP blends along the extruder. Comparing the evolution of the $I(3\omega_1)/I(\omega_1)$ as a function of the applied strain amplitude (γ_0) for the samples collected at different locations along the extruder, shown in figures 4.17 to 4.19, significant differences were observed for intermediate and high strain amplitudes only ($\gamma_0 > 1.0$). In what regards the degree of non-linearity, it decreases markedly along the extruder, especially for the samples with higher LCP content. For example, when comparing samples collected at valve 4 and at the die it can be noticed that valve 4 displays higher non-linearity.

At this point of the compounding, the extruder element is a reverse-conveying one, which is responsible for an increase of the residence time of the material. Since the time

available for the contact between the LCP structures is increased in this region, an increased coalescence of the LCP structures, which would lead to an increase of the mean diameter size and to the appearance of LCP structures with spherical shapes is expected, as can be observed in figure 4.1. Therefore, the compression moulded discs obtained from these samples possess LCP structures with higher mean diameters than those observed, for example, for those prepared from the final extrudates (see figure 4.9). According to the capillary number definition (equation 2.1, chapter 2) the higher the radius of the LCP structures, the higher will be the capillary number. Therefore, the deformation will be easier for the samples collected at the beginning of the extruder, since these are the ones with the highest mean diameter. So, these were the samples for which one expected the highest degree of non-linearity. When the material crosses the region of the screw containing a set of kneading blocks, the deformation level is intermediate between that observed at the reverse-conveying elements and the one at the die. In this region, deformation of the LCP structures at the kneading blocks is higher than the observed at the conveying and reverse-conveying elements, leading to a decrease of the mean LCP dimensions. Therefore, the non-linearity for the samples collected at valve 8, for instance, is lower than that observed for the samples collected at valve 5. Nevertheless, the lowest non-linearity was obtained for the samples collected at the end of the extruder. This is the condition for which higher deformations were achieved and, as a consequence, the samples collected at this point possess a dispersed phase, consisting of droplets with similar volume, but higher aspect ratio than that observed for the samples removed at the beginning and at the middle of the compounding process.

CONCLUSIONS

The increase of the LCP content gives rise to extrudates with different morphologies, but the morphological evolution along the extruder length seems to occur similarly for all the different blends, always leading to an extrudate in which the dispersed phase appears as

fibrillar structures dispersed in the polypropylene matrix and oriented along the flow direction. During extrusion the LCP structures can be described as spherical shapes, elongated shapes or fibrillar structures depending on the extruder position and thus on the shear rate applied. A special home-built collecting device system was used that allowed the collection of samples at different locations along the extruder length [Covas 2001]).

The rheological behaviour in the linear-regime allowed samples collected at different locations in the extruder to be studied. The linear viscoelastic differences along the extruder are clearly related to the different morphologies obtained, as studied by optical and electron microscopy. These results were confirmed through rheological measurements in both the linear and non-linear regimes. In the linear regime, the storage modulus and the complex viscosity decrease very slightly along the extruder, although it presents a significant decrease in the case of the extrudates. Furthermore, the mechanical non-linearity (for constant frequency and strain amplitudes) decreases from the beginning to the end of the extrusion process, which is again related to the morphological evolution observed. The rheological measurements performed in the linear and especially in the non-linear regime (Fourier Transform Rheology) are important tools to quantify the morphological evolution during compounding and are essential to a better understanding of the mixing processes and to predict and control the final properties of the blend as generated by an extruder.

4.2 STUDY OF THE INFLUENCE OF THE LCP CONTENT ON THE FINAL MORPHOLOGICAL, RHEOLOGICAL AND MECHANICAL PROPERTIES*

INTRODUCTION

The first part of this chapter will be devoted to the influence of the LCP content on the morphological, rheological and mechanical properties of non-compatibilised blends, while in the second part of the study the attention will be focused on exemplifying the sensitivity of the different techniques to relatively small changes in the processing conditions, in this case processing temperature.

Considering the importance of extensional flow on the majority of industrial processes and its relevance on the formation of highly oriented fibrillar structures in LCP/TP blends, it is of primary interest to study the elongational flow behaviour on LCP/TP blends, evaluating the influence of the LCP content, which will also be reported in this chapter.

RESULTS AND DISCUSSION

INFLUENCE OF THE LCP CONTENT

In this part of the work, the influence of the LCP content on the final morphological, rheological and mechanical properties for the extrudates of LCP/TP blends processed at 220 °C will be addressed.

MORPHOLOGICAL PROPERTIES

Regarding the morphological properties of the final extruded blends processed at 220 °C, some observations can be made: the addition of the LCP to the thermoplastic matrix leads to a biphasic structure where the LCP phase is distributed inside the thermoplastic matrix,

* adapted from S. Filipe, J. M. Maia, M. T. Cidade, *PP/LCP blends: influence of the LCP content on the mechanical, rheological and morphological properties*, Materials Science Forum, Vol. 455-456, 2004, 476-479, from S. Filipe, J. M. Maia, M. T. Cidade, *Transient uniaxial extensional flow for LCP/TP blends*, submitted to Reologica Acta and from S. Filipe, C. R. Leal, J. M. Maia, M. T. Cidade, *A study of LCP/TP blends under different stationary and non-stationary shear conditions: the influence of LCP content and processing temperature*, accepted for publication in J. Polym. Eng.

with the form of fibrillar structures, mostly oriented along the flow direction. These observations are not new, and were already reported in similar LCP/thermoplastic blends [Qin 1993, Viswanathan 1995]. This analysis, however, is needed in order to establish correlations between the rheological behaviour (under both, steady and transient conditions) and the morphology presented.

Not surprisingly, several holes were observed along the matrix for the transversal cuts, meaning that pullout of the LCP fibrils occurred during the cryogenic fracture, which is basically due to the poor adhesion between the liquid crystalline polymer and the thermoplastic phases (see figure 4.20).

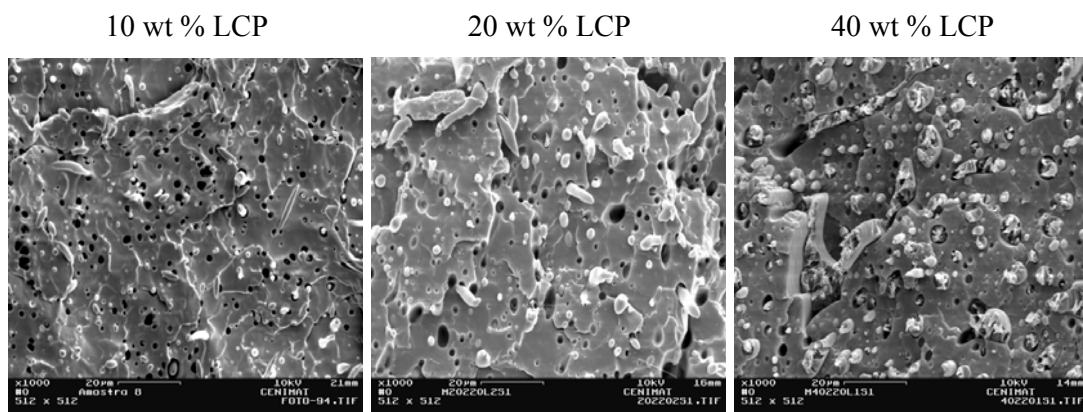


Figure 4.20 - Transversal cuts of the final extrudates for the blends processed at 220 °C with 10, 20 and 40 wt % LCP (SEM) (magnification of x1000).

In order to better clarify the morphology developed in these systems, longitudinal cuts were performed to the final extrudates in addition to the traditional transversal cuts, since the latter only allow the observation of the dispersed phase distribution and the presence or absence of fibril pullout.

The longitudinal cuts done to the final extrudates showed very clearly that the formation of LCP fibrils occurred in the flow direction, as it was already expected (see figure 4.21). The higher the LCP content, the more fibrils/volume it is possible to find. It seems

that the formation of fibrillar structures is enhanced for the higher LCP contents. In fact, the higher the diameters of the LCP droplets formed during extrusion, the easier will the deformation of these droplets be (according to the capillary number); thus, the formation of LCP fibrils will be more efficient for the blends with a higher LCP content.

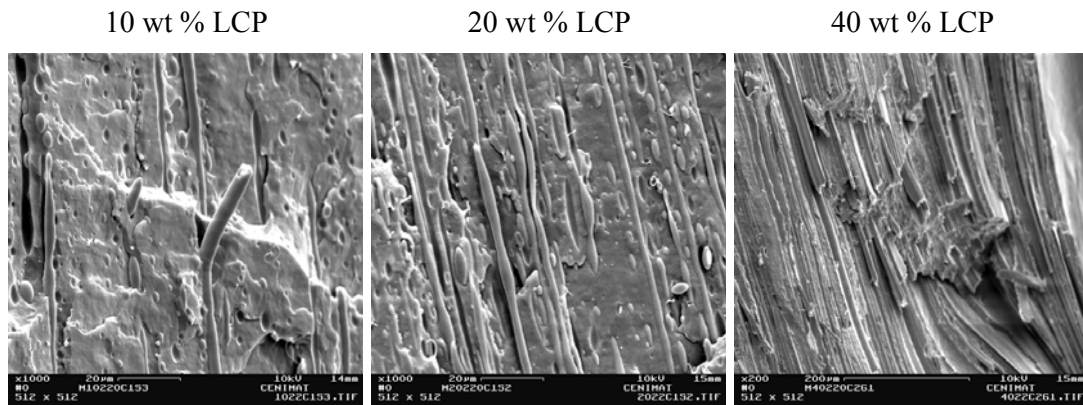


Figure 4.21 - Longitudinal cuts of the final extrudates for the blends processed at 220 °C with 10, 20 and 40 wt % LCP (SEM) (magnification of x1000 for blend with 10 and 20 wt % LCP and magnification of x200 for blend with 40 wt % LCP).

RHEOLOGICAL PROPERTIES

The rheological behaviour of LCP/TP blends has also been widely studied and generally there is an agreement about the influence of the LCP addition on the viscosity and storage modulus of the blends [Saenguan 2003]; the addition of liquid crystalline polymer to thermoplastic leads to a decrease of both viscosity and storage modulus.

The flow curve ($T = 220\text{ °C}$) obtained for blends processed at 220 °C (see figure 4.22) shows that the LCP possesses a shear-thinning behaviour all over the shear rate range studied, while the thermoplastic shows a Newtonian plateau for low shear rates followed by a shear-thinning behaviour, as expected.

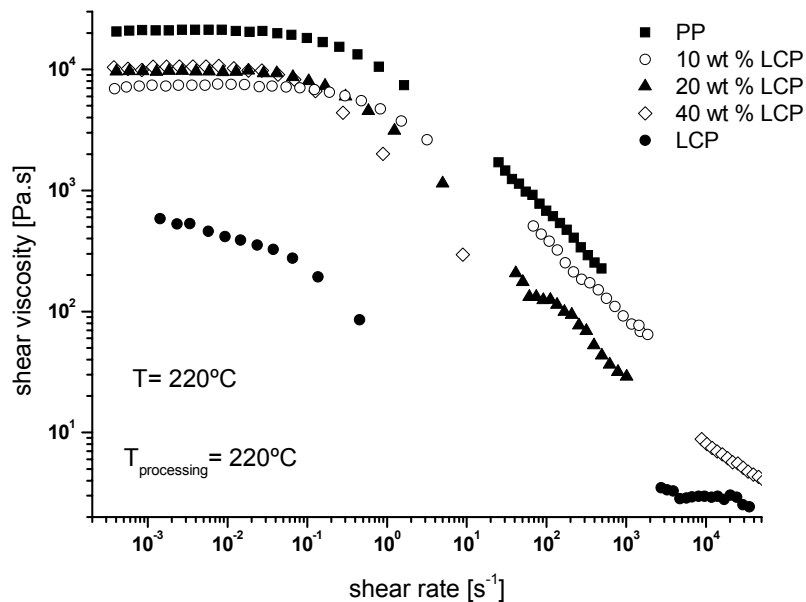


Figure 4.22 - Flow curves for blends processed at 220 °C with 10, 20 and 40 wt % LCP and for pure components, at T= 220 °C.

The transition between the Newtonian and the shear-thinning behaviour for the thermoplastic occurs for a shear rate range of approximately 0.15 s^{-1} . Regardless of the LCP content, the rheological behaviour of the blends was always similar to the one observed for the pure thermoplastic, *i.e.*, a Newtonian behaviour at low shear rates followed by a shear-thinning behaviour. However, the shear rate at which the transition from Newtonian to shear-thinning behaviour occurs decreases with increasing LCP content. Additionally, although the viscosity of the blends falls between the viscosity of the pure components, in the Newtonian plateau the increase of LCP content leads to an increase of the viscosity (which can be explained by the internal friction that occurs for this range of shear rate) and the shear-thinning behaviour becomes more pronounced as the LCP content increases (which is due to the orientation of the LCP domains inside the matrix) giving rise to a crossover of the viscosity of the different curves for shear rates above 1 s^{-1} , approximately. This means that above this critical shear rate the increase of the LCP leads to a decrease of the viscosity of the blends. This transition was

already reported for similar blends; at low shear rates, the LCP structure is specially constituted by pillared polydomains and as the shear rate increases, these polydomains tend to orient themselves, giving rise to a co-continuous monodomain [Choi 1996a].

The measurements performed in the transient regime showed a different behaviour for the evolution of the transient stress (σ^+) with the strain. The pure LCP does not present any overshoot, contrary to what happens with the PP, which presents a small overshoot for the transient shear stress. This overshoot is always present for the blends, its magnitude increasing with the increase of LCP content, as can be seen on figure 4.23.

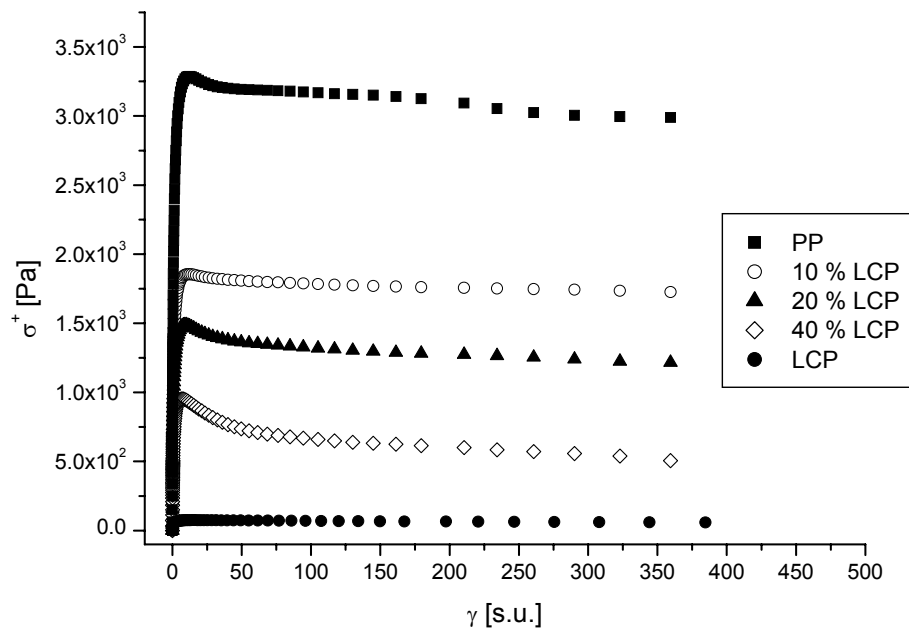


Figure 4.23 - Transient stress (σ^+) for the blends with 10, 20 and 40 wt % LCP and for the pure components (start-up at 1 s^{-1} , $T = 200 \text{ }^\circ\text{C}$).

This phenomenon was already observed for blends of polypropylene and Rodrun LC5000 (with 30 wt % LCP) being associated with interfacial effects that occurred in the system, namely the deformation of the LCP structures [Lazkano 2002]. It is known that the

higher the diameters of the LCP structures, the easier their deformation, which explains the highest overshoot of the transient stress for the blend with the higher LCP content (40 wt % LCP).

From the measurements done in oscillatory shear (in the linear regime) at 220 °C it was observed that the pure thermoplastic is the more elastic material (figure 4.24).

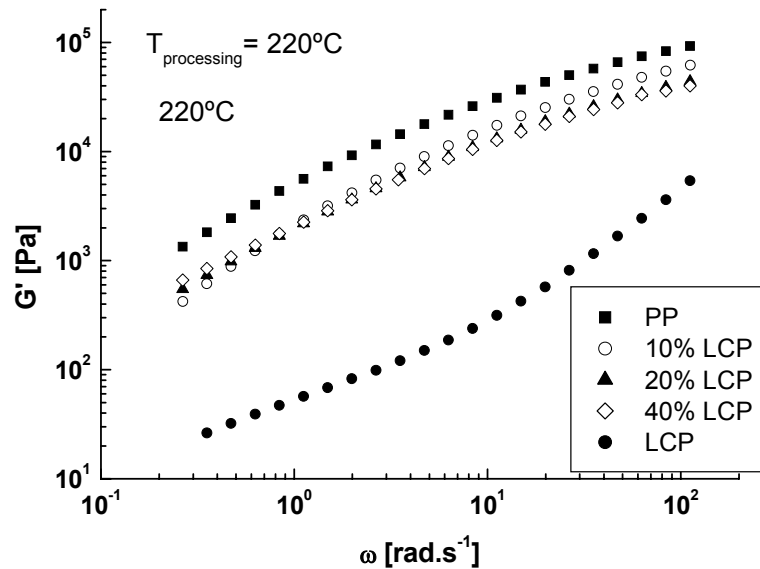


Figure 4.24 - Evolution of the storage modulus (G') with frequency for blends processed at 220 °C with 10, 20 and 40 wt % LCP and for pure components, at $T=220\text{ °C}$, $\gamma_0 = 0.1$.

In all the frequency range studied, the LCP is the material that presents the lower G' , the values for the blends lying between those of the pure components. Similarly to the steady state results, a change in behaviour was also observed from the lower to the higher frequencies; for frequencies below 1 rad.s^{-1} the higher the LCP content, the higher the elasticity, while for frequencies above 1 rad.s^{-1} the opposite behaviour was observed. The thermoplastic is the material that presents the higher complex viscosity, and the addition of the LCP leads to the

decrease of the viscosity, as observed in figure 4.25, although in the very low frequency range the trend, again, seems to be of an inversion in behaviour.

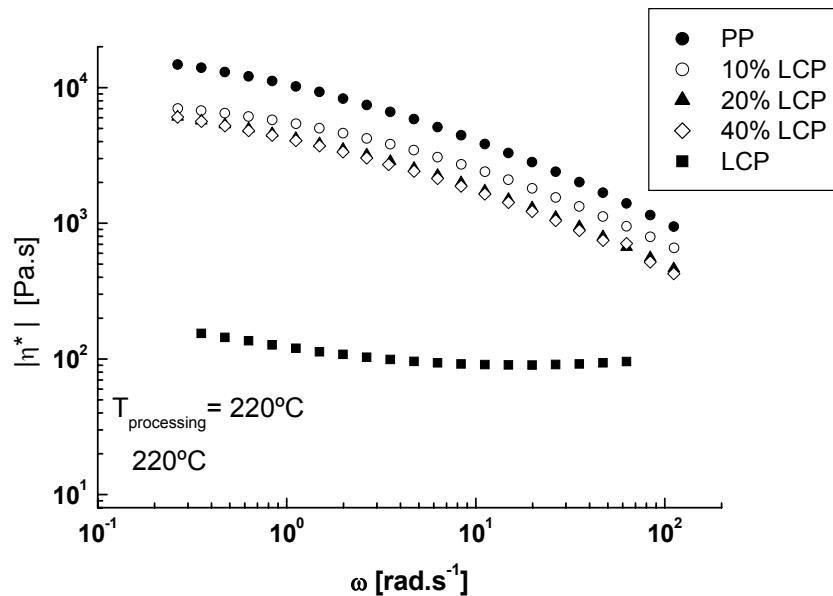


Figure 4.25 - Evolution of the complex viscosity with frequency for blends processed at 220 °C with 10, 20 and 40 wt % LCP and for pure components, at $T = 220\text{ °C}$, $\gamma_0 = 0.1$.

This behaviour was not observed for other Rodrun/Polypropylene blends [Saenguwan 2003], but only in systems with other dispersed phases in thermoplastics, like for example PPS/PPO and Vectra B950, which were previously studied [Choi 1996a].

The measurements performed in oscillatory regime at non-linear conditions allow some conclusions about the influence of the LCP content on the evolution of $I(3\omega_1)/I(\omega_1)$ with the applied strain amplitude. The results show that the non-linearity increases with the addition of the LCP content (figure 4.26), with the maximum value being obtained for the pure liquid crystalline polymer (although this maximum value may be influenced by the biphasic nature of the LCP, present at the measuring temperature).

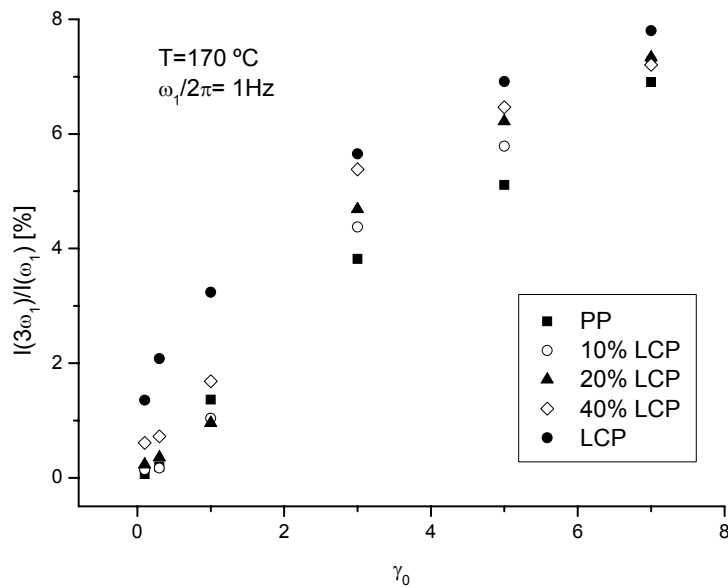


Figure 4.26 - Evolution of $I(3\omega_1)/I(\omega_1)$ with the applied strain for blends processed at 220 °C with 10, 20 and 40 wt % LCP and for pure components, at $T= 170$ °C.

For the lower strain amplitudes, the blends with lower LCP content behave similarly to the thermoplastic. However, for strain amplitudes between $\gamma_0 = 1$ and $\gamma_0 = 5$ it is possible to distinguish between the blends, the larger differences being observed for a strain amplitude (γ_0) equal to 3. For the higher strain amplitudes ($\gamma_0 = 7$) all the blends present approximately the same non-linearity and their values lie in between those of the pure components. This behaviour has already been reported [Filipe 2004a] and is due to the fact that, for the higher strain amplitudes, the deformation reaches a limit value above which no more morphological changes are induced and the samples behave alike, independently of their LCP content.

Until now not so many studies were performed in order to understand the influence of the liquid crystalline polymer content on the elongational flow behaviour of liquid crystalline polymer/thermoplastic blends, neither on other blends [Silva 2004, Mechbal 2004]. This knowledge is crucial, due to the importance of the extensional flow behaviour in industrial processes, namely extrusion and injection moulding. Having by basis this lack of knowledge,

transient uniaxial extensional viscosity measurements were performed for blends with 10, 20 and 40 wt % LCP and for polypropylene. The transient uniaxial extensional viscosity for PP and the blends described above are depicted in figures 4.27 to 4.30, for two different strain rates.

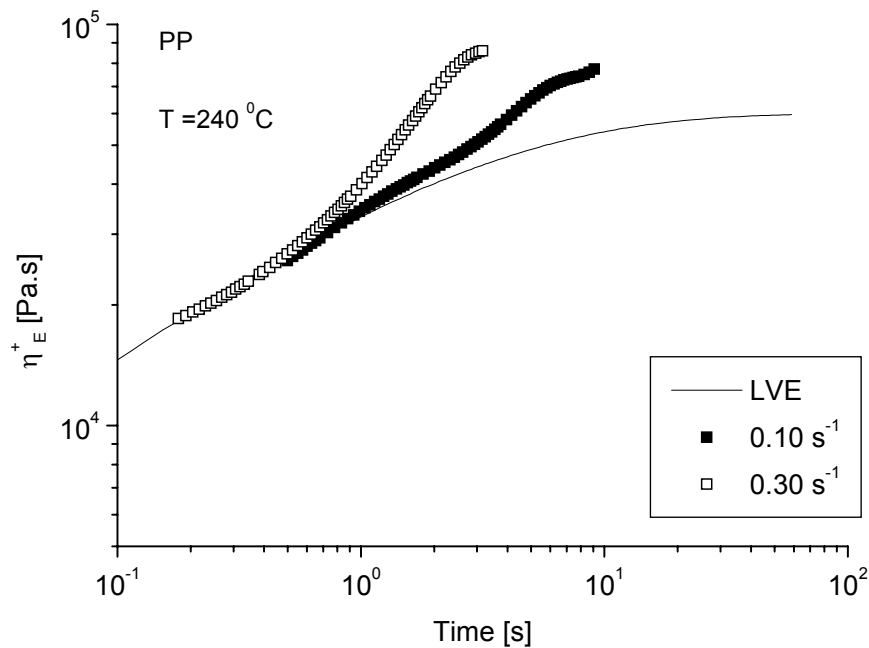


Figure 4.27 - Transient uniaxial extensional viscosity at 240 °C for polypropylene.

In what regards the polypropylene, although it is a linear material, it shows a small degree of strain-hardening, which can be due, for example, to the presence of a small tail of high molecular weight material. In fact, this PP is a commercial material (and, thus, of possible complex composition) and the presence of even small amounts of a high molecular weight component is known to produce a strong effect on the strain-hardening of linear polymers [Sugimoto 2001].

As far as the blends are concerned, for short times all the materials follow the linear viscoelastic regime, LVE, while for longer ones a low to moderate strain hardening behaviour that depends on the LCP content was observed. This behaviour is more clearly seen if one

analyses the Trouton ratio as a function of the time for the different materials (figures 4.31 and 4.32).

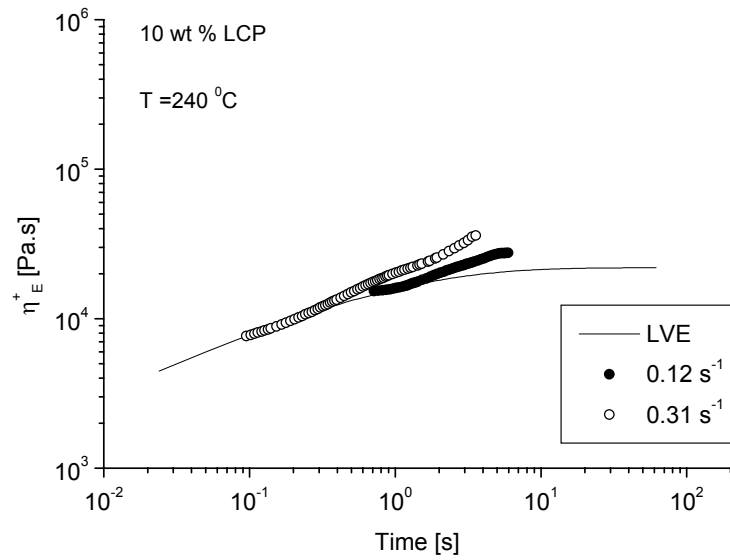


Figure 4.28 - Transient uniaxial extensional viscosity at 240 °C for the blend with 10 wt % LCP.

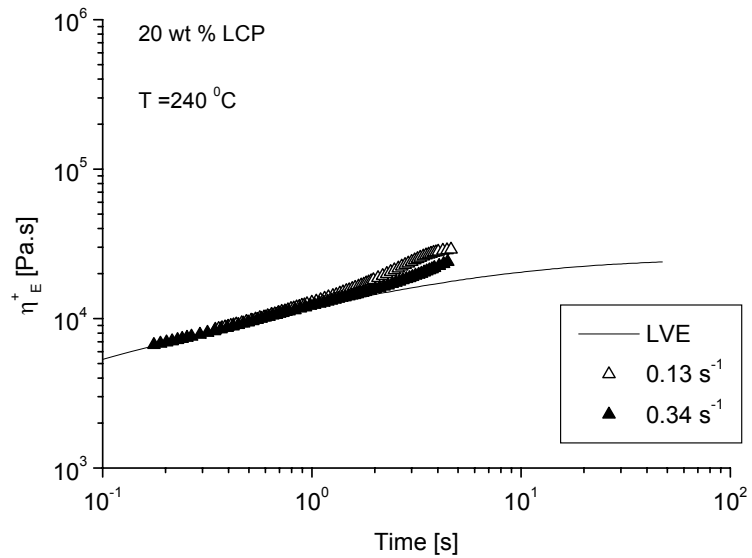


Figure 4.29 - Transient uniaxial extensional viscosity at 240 °C for the blend with 20 wt % LCP.

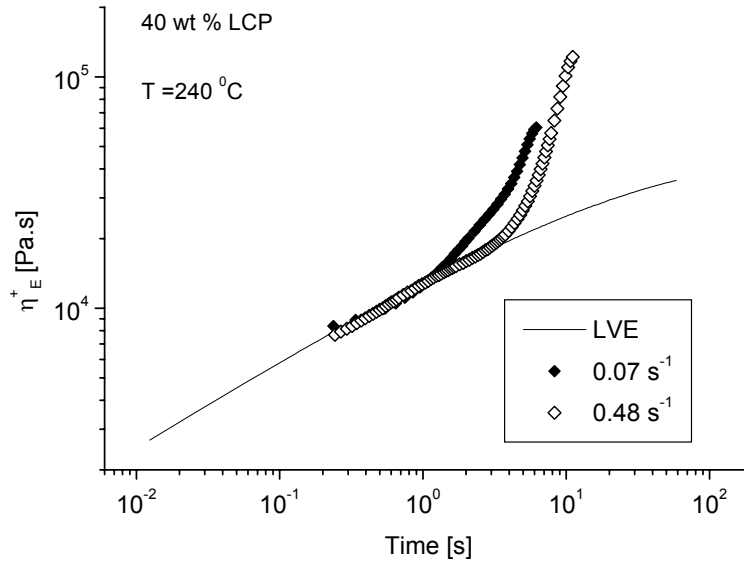


Figure 4.30 - Transient uniaxial extensional viscosity at 240 °C for the blend with 40 wt % LCP.

Analysing figure 4.31, for the lower range of strain rates (between 0.07 and 0.13 s⁻¹) it is possible to observe that steady state can be achieved for PP and the blends with 10 and 20 wt % LCP. Also, it can be stated that no clear distinction can be made between the pure matrix and the blend with 10 wt % LCP in terms of the deviation from the linear viscoelastic regime and that the magnitude of the strain hardening increases only slightly (around 10 %) with the increase of the LCP content from 10 to 20 wt %. On the other hand, when the LCP content is increased to 40 wt %, the rheological behaviour changes dramatically, with a much higher durability and degree of strain hardening being apparent. Also, steady state is not achieved, even with the increased testing times.

The reasons for this behaviour are unclear but are probably related with the fact that for pure liquid crystalline polymers, the strain hardening behaviour is usually related with the presence of some residual crystallinity, especially in those cases where the measuring temperature is only slightly higher than the temperature that guarantees total absence of crystallinity (isotropic temperature) [Wilson 1992]. At the temperature used for the uniaxial

extensional flow measurements, 240 °C, the presence of a residual crystallinity for the LCP is expected to be low, if not negligible. However, and considering the above results, it may be possible that some residual crystallinity is still present, especially in the 40 wt % sample, where the morphology is nearly co-continuous.

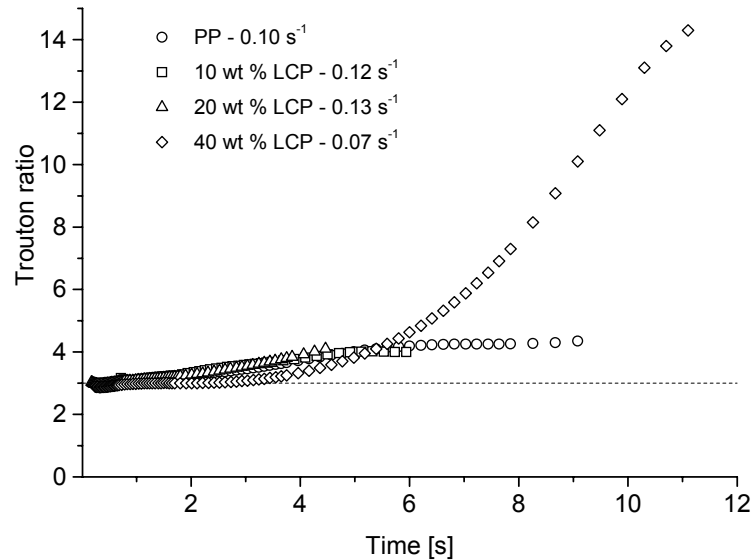


Figure 4.31 - Influence of the LCP content on the Trouton ratio of PP and blends with 10, 20 and 40 wt % LCP, at 240 °C (strain rates around 0.07-0.14 s⁻¹).

When higher shear rates are applied (ranging from 0.31 to 0.48 s⁻¹), the behaviour is changed, with the increase in LCP content yielding a decrease of the strain hardening behaviour, up to LCP contents of 20 wt %, as seen in figure 4.32. This is in accordance with the results obtained under steady shear (see figure 4.22), for which one observed an increase of the viscosity with the increase of the LCP content, for the lower shear rates and the opposite behaviour for the higher strain rates. Again, when the LCP content is increased from 20 to 40 wt % LCP, there is the same high increase in terms of strain-hardening and durability that existed for low strain rates.

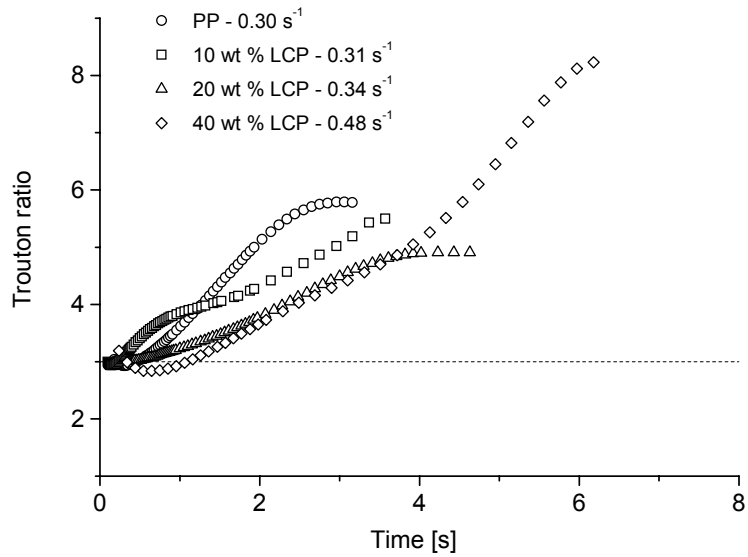


Figure 4.32 - Influence of the LCP content on the Trouton ratio of PP and blends with 10, 20 and 40 wt % LCP, at 240 °C (strain rates around 0.30-0.46 s⁻¹).

MECHANICAL PROPERTIES

The tensile properties of the pure components and blends have been determined on injection moulded specimens. The evolution of both Young's modulus and elongation at break with the LCP content are presented in figures 4.33 and 4.34, respectively. The ductility decreases with the increase of the LCP content, while the Young's modulus increases as the LCP content increases.

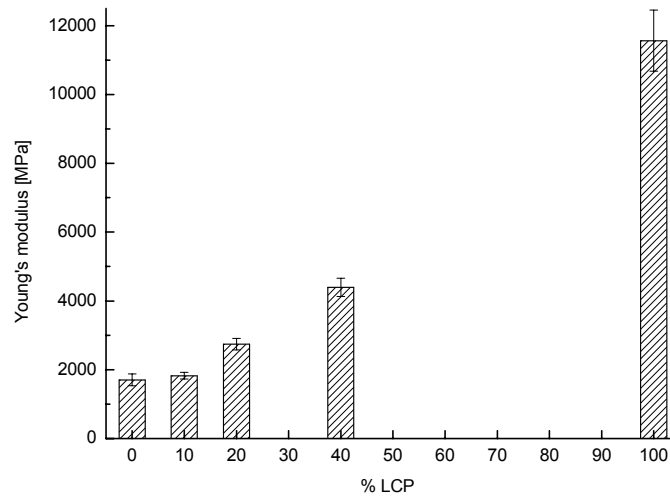


Figure 4.33 - Influence of the LCP content on the Young's modulus, for blends processed at 220 °C with 10, 20 and 40 wt % LCP and for pure components.

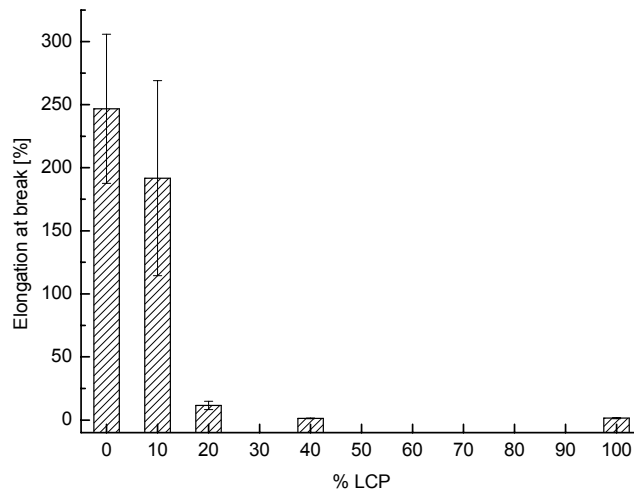


Figure 4.34 - Influence of the LCP content on the elongation at break, for blends processed at 220 °C with 10, 20 and 40 wt % LCP and for pure components.

The behaviour observed for the pure thermoplastic and for the blend with 10 wt % in LCP during the tensile measurements was essentially ductile, while for the other blends and for the pure LCP was brittle. Similar results were reported by Guerrica-Echevarría *et al.*, for

blends of polypropylene and Rodrun LC5000 and by Mi *et al.*, for PEK-C/LCP blends [Guerrica-Echevarria 2000, Mi 1998].

Several models were developed over the years to predict the Young's modulus of reinforced composites [Voigt 1928, Reuss 1929, Hirsch 1962, Halpin 1976, among many others]. These models were specially developed for fibres, and therefore can be used in the present work, since at the final extrudates the dispersed phase has the form of fibrils.

One of the simplest is the Voigt model, for which isostrain conditions ($\varepsilon_m = \varepsilon_f$) and perfect adhesion between the two phases are assumed [Voigt 1928, Ward 1996]. According to this model, which was specially developed for fibres, E_c is defined by:

$$E_c = E_f \cdot \vartheta_f + E_m \cdot (1 - \vartheta_f) \dots \dots \dots 4.1$$

$E_f \equiv$ Young's modulus of the dispersed phase

$E_m \equiv$ Young's modulus of the matrix

$\vartheta_f \equiv$ volume fraction of the dispersed phase (LCP)

The Reuss model, on the other hand, assumes no adhesion between the matrix and the dispersed phase and an isotress condition ($\sigma_m = \sigma_f$) [Reuss 1929]. The Young's modulus of the composite, E_c is in this case defined as:

$$E_c = \frac{E_m \cdot E_f}{E_m \cdot \vartheta_f + E_f \cdot \vartheta_m} \dots \dots \dots 4.2$$

Besides fitting the data to these models, the results were also fitted to the Hirsch model, in which the Young's modulus of the composite can be expressed by:

$$E_c = x \cdot (E_f \cdot \vartheta_f + E_m \cdot (1 - \vartheta_f)) + (1 - x) \cdot \frac{E_m \cdot E_f}{E_f \cdot (1 - \vartheta_f) + E_m \cdot \vartheta_f} \quad 4.3$$

where x is a parameter that gives an idea about the degree of adhesion between the dispersed and the continuous phases. For $x = 0$, there is no adhesion between the fibers and the matrix (thus reducing itself to the Reuss model), while for $x = 1$ the adhesion between phases is perfect (thus reducing itself to the Voigt model) [Hirsch 1962].

Figure 4.35 shows a comparison between the predictions of the three models and the experimental data. As expected, the best fit to the data is given by Hirsch model, in this case for $x = 0.9$. This means that the models predict the existence of long fibrils, perfectly oriented along the flow direction which was to be expected but, and quite unexpectedly, also shows good adhesion between the matrix and the LCP.

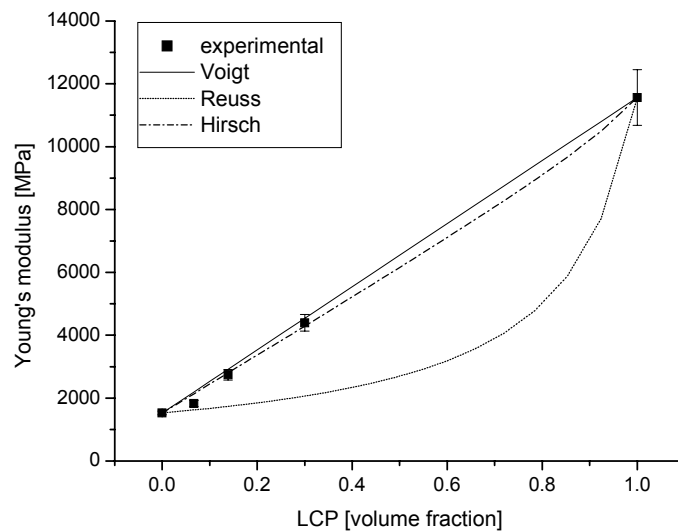


Figure 4.35 - Young's modulus of blends with 10, 20 and 40 wt % LCP (processed at 220 °C), predicted by Voigt, Reuss and Hirsch (for $x = 0.9$) models (lines) and experimental results (points).

This is in clear contradiction with the results from the morphological analysis (see figure 4.21), the reasons for this discrepancy not being immediately apparent. One possible reason is that the deformation levels involved in the tensile measurements are relatively low when compared to those applied during cryogenic fracture.

The length to diameter ratio of the blends can be predicted using the Halpin-Tsai model [Halpin 1976]. In this, the Young's modulus of the composite (E_c) is expressed as a function of the Young's modulus of the matrix (E_m) and of the Young's modulus of the LCP (E_f) by the following equation:

$$E_c = E_m \cdot \frac{1 + \xi \cdot B \cdot \vartheta_f}{1 - B \cdot \vartheta_f} \quad 4.4$$

and,

$$B = \frac{\frac{E_f}{E_m} - 1}{\frac{E_f}{E_m} + \xi} \quad 4.5$$

where, ϑ_f is the volume fraction of the dispersed phase (LCP) and ξ is defined by:

$$\xi = \frac{2 \cdot l}{d} \quad 4.6$$

The results are depicted in table 4.2 and it is apparent that the length to diameter ratio increases with the increase of the LCP content, as expected and in accordance to the morphological analysis.

Table 4.2 Parameter ξ for blends with 10, 20 and 40 wt % LCP processed at 220 °C obtained from Tsai-Halpin model.

	% LCP	ξ (obtained from the Halpin-Tsai model)
10 % LCP	10	3.2
20 % LCP	20	31.6
40 % LCP	40	72.1

INFLUENCE OF THE PROCESSING TEMPERATURE: A SENSITIVITY TEST

In the second part of the work, the sensitivity of experiments in stationary vs. non-stationary conditions to a relatively small change in processing temperature will be accessed. The reason for this choice of processing parameter has to do with the fact that, due to several factors like shear heating, melt temperature is one of the parameters that is more difficult to control during processing.

As will be seen later, the use of FT-Rheology is essential to estimate the rheological behaviour under non-linear conditions and is of great importance on the evaluation of differences arising from the application of different processing temperatures. By the use of this technique it will be shown that, under these conditions, the effect of the processing temperature is highly pronounced. Considering that the processing occurs under non-stationary conditions, the high sensitivity of FT-Rheology should be employed in order to evaluate changes in morphology and rheology, and provide further insight into the phenomena that occur under conditions similar to those present during processing.

MORPHOLOGICAL AND MECHANICAL PROPERTIES

In terms of the observed morphology, there were differences between the blends processed at 220 °C and 240 °C. The formation of fibrillar structures of LCP seems to be easier for the lower processing temperatures, as shown by the morphological analysis done to the blends processed at 220 and 240 °C, figures 4.21 and 4.36.

The improvement of the fibrillar formation that occurred for the blends processed at a lower processing temperature can be explained considering that at 220 °C the LCP structures are subjected to higher stresses due to the higher viscosity of the matrix. Additionally, at 220 °C the coalescence processes of the LCP droplets are reduced and the elongation of the LCP structures is the dominant process, thus leading to a higher fibrillar formation. This behaviour is obviously related to the viscosity ratio between the two pure components, that is higher for 220 °C than for 240 °C [Filipe 2004a].

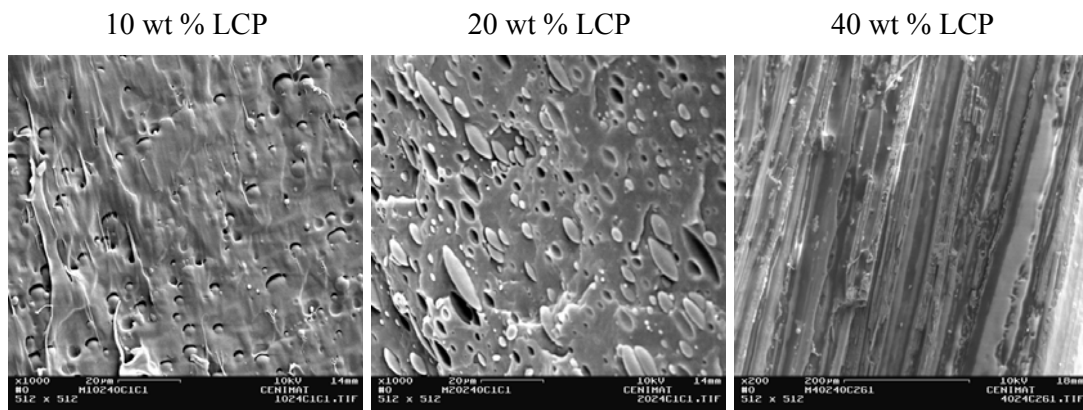


Figure 4.36 - Longitudinal cuts of the final extrudates for the blends processed at 240 °C with 10, 20 and 40 wt % LCP (SEM) (magnification of x1000 for blend with 10 and 20 wt % LCP and magnification of x500 for blend with 40 wt % LCP).

With respect to the influence of the processing temperature on the tensile properties it can be stated that a lower processing temperature leads to a slightly higher Young's modulus (figure 4.37) and to a slightly lower elongation at break (figure 4.38) when compared with the mechanical properties of the blends processed at 240 °C, which, again, is due to the fact that, at higher temperatures, the formation of the LCP fibrils is less effective.

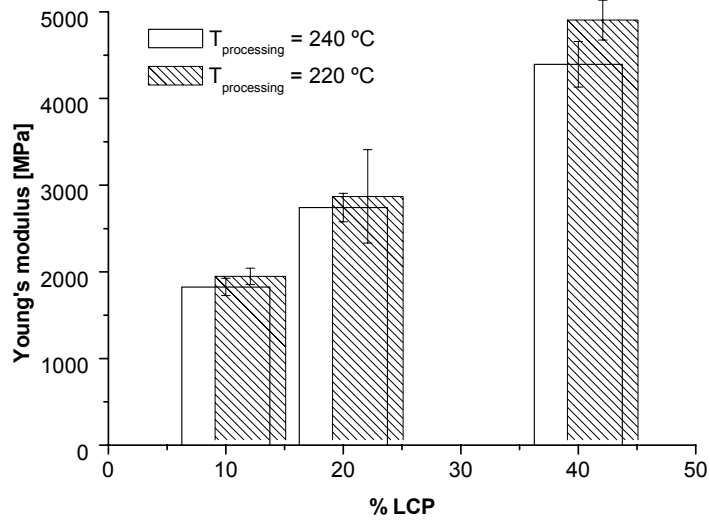


Figure 4.37 - Influence of the LCP content on the Young's modulus (blends with 10, 20 and 40 wt % LCP, processed at 220 and 240 °C).

In the analysis above, however, one should bear in mind that the testing was done on injection moulded samples and, thus, possible post-extrusion differences will have been severely reduced.

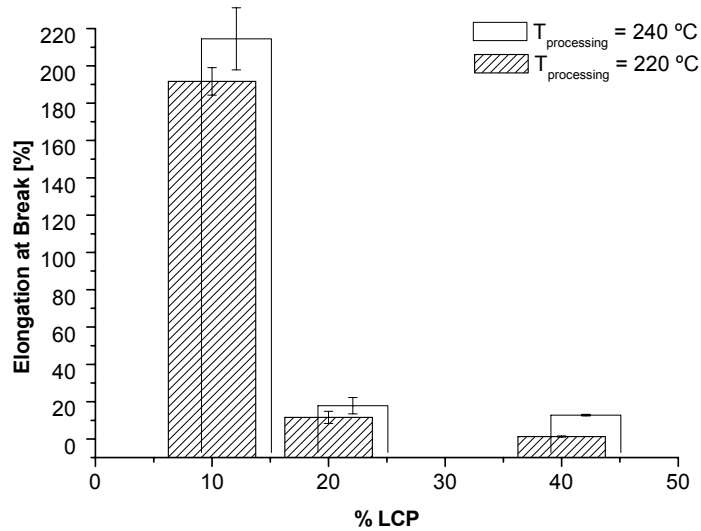


Figure 4.38 - Influence of the LCP content on the elongation at break (blends with 10, 20 and 40 wt % LCP, processed at 220 °C and 240 °C).

RHEOLOGICAL PROPERTIES

Some differences in the rheological behaviour were observed for the blends processed at 220 °C and 240 °C for the measurements performed in steady shear flow, as can be seen in figures 4.39, 4.40 and 4.41, where the shear viscosity as a function of the shear rate is presented for the blends with 10, 20 and 40 wt % LCP, respectively.

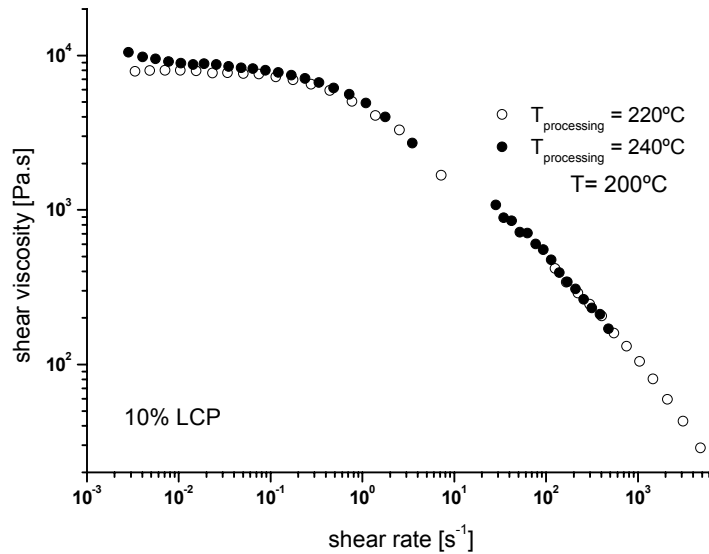


Figure 4.39 - Influence of processing temperature on the flow curves of blends with 10 wt % LCP, at T= 220 °C.

From these figures, it can be noticed that the most visible differences are in the Newtonian plateau, which shows an increase in η_0 , while the shear thinning region remains virtually unchanged. This difference in η_0 increases with the increase of the LCP content.

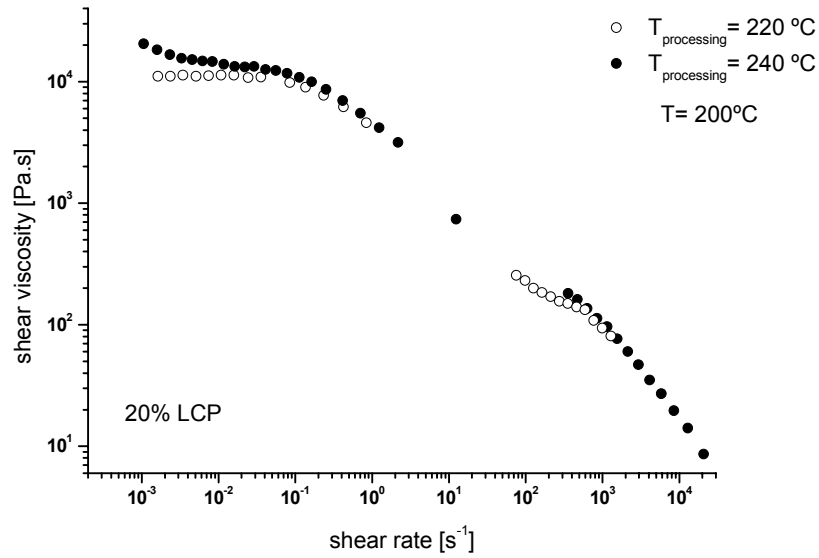


Figure 4.40 - Influence of processing temperature on the flow curves of blends with 20 wt % LCP, at $T = 220\text{ }^\circ\text{C}$.

These differences are probably related with the different morphologies observed for the different processing temperatures: due to the poor adhesion characteristics of the blends, the higher fibrillar formation observed for the blends processed at $220\text{ }^\circ\text{C}$ leads to a decrease of the viscosity when compared with the blends processed at $240\text{ }^\circ\text{C}$. For shear rates in the region of shear-thinning behaviour, *i.e.*, higher than typically 0.1 s^{-1} , the differences between blends processed at both temperatures are drastically reduced due to the orientation of the LCP structures that all blends undergo.

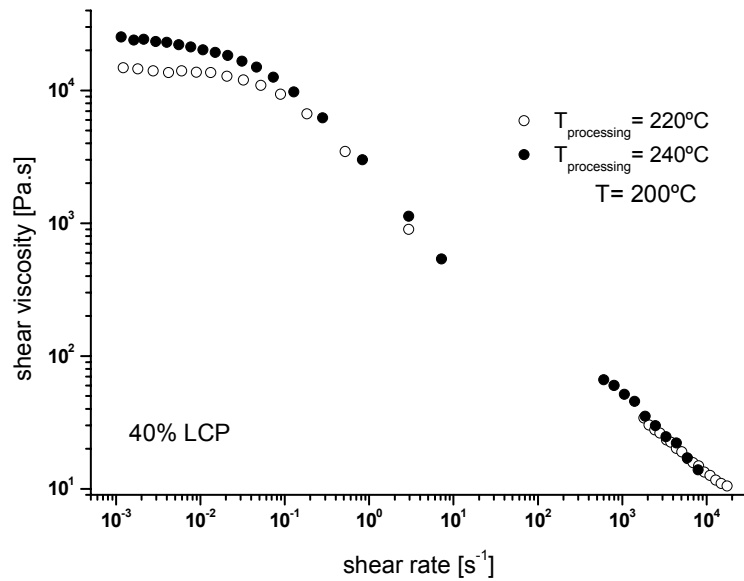


Figure 4.41 - Influence of processing temperature on the flow curves of blends with 40 wt % LCP, at $T = 220\text{ }^{\circ}\text{C}$.

The rheological measurements performed in oscillatory shear under non-linear conditions, on the other hand, showed a much higher degree of sensitivity to differences in processing temperature than shear experiments.

In fact, it was possible to observe that: a) increasing the processing temperature by $20\text{ }^{\circ}\text{C}$ results in a much stronger non-linearity in the response (see figures 4.42, 4.43 and 4.44, for the 10, 20 and 40 wt % LCP blends, respectively) and b) these differences are more pronounced for the blends with higher LCP contents (similarly to what was observed for the steady shear state measurements, albeit in the latter case the differences were much less evident).

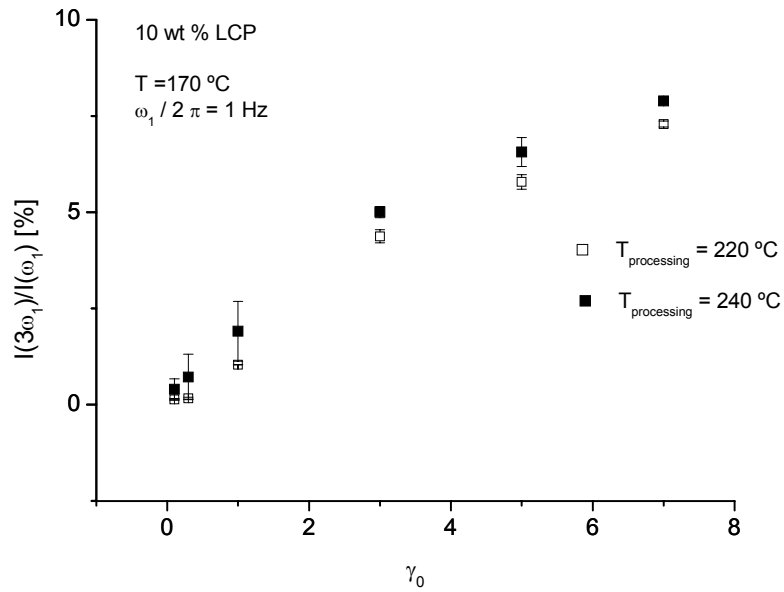


Figure 4.42 - Influence of processing temperature on the evolution of $I(3\omega_1)/I(\omega_1)$ as a function of applied strain, of blends with 10 wt % LCP, at $T = 170$ °C.

This is consistent with the fact that the LCP droplets presented higher diameters for the blends that were processed at 240 °C.

In view of the results above, it can be clearly stated that rheological experiments performed under non-stationary conditions, such as LAOS, are much more sensitive to the changes in morphology that occur when the processing temperature is changed than rheological experiments under stationary conditions, such as steady-shear.

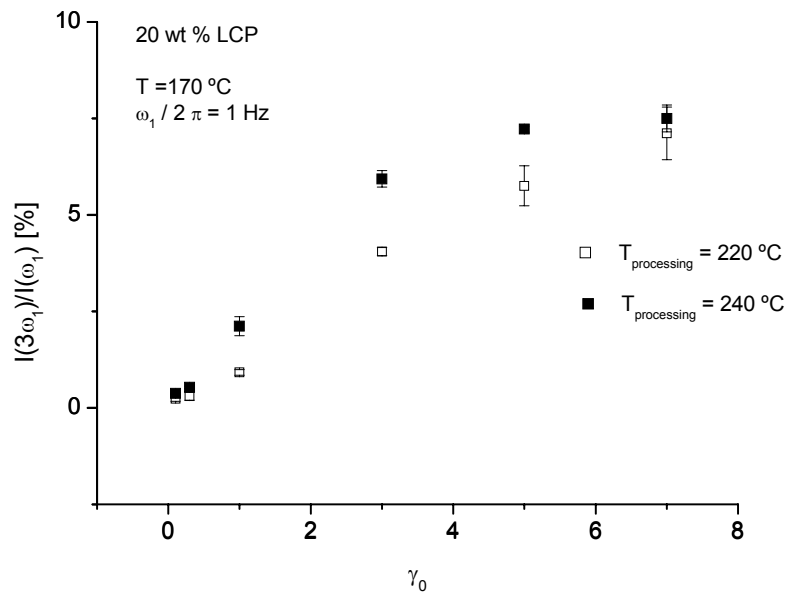


Figure 4.43 - Influence of processing temperature on the evolution of $I(3\omega_1)/I(\omega_1)$ as a function of applied strain, of blends with 20 wt % LCP, at $T = 170$ °C.

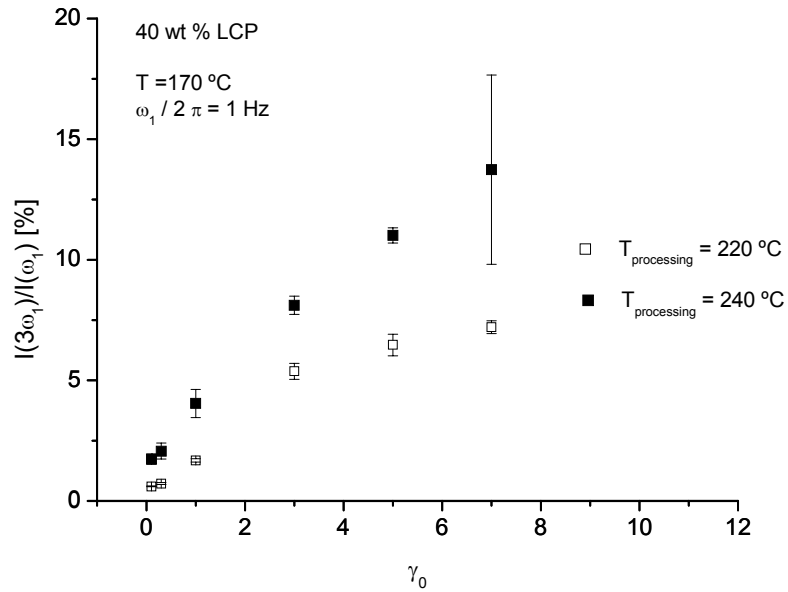


Figure 4.44 - Influence of processing temperature on the evolution of $I(3\omega_1)/I(\omega_1)$ as a function of applied strain, of blends with 40 wt % LCP, at $T = 170$ °C.

CONCLUSIONS

Reinforced polypropylene is obtained by the addition of small amounts of liquid crystalline polymer. The formation of LCP fibrils inside the thermoplastic leads to the mechanical enhancement in terms of the Young's modulus and to a decrease of the elongation at break, as a result of the addition of a component with a brittle nature (LCP). From the morphological point of view, significant differences are observed by changing the amount of LCP, *i.e.*, the increase of LCP leads to the increase of LCP fibrils/volume, and their formation seems to be easier for the blends with higher LCP contents. With respect to the rheological properties it can be pointed out that the behaviour of the blends is dominated by the matrix. It can be also stated that the addition of LCP leads to a decrease of the viscosity, for high shear rates, the ones employed during processing (essentially due to the fibrillar formation that increases with the increase of the LCP content, as verified in the morphological characterisation). This part of the work was essentially dedicated to the study of the behaviour of LCP/TP systems under non-stationary conditions, which has not been suitably studied before, and assess the relevance of such experiments to changes in the processing conditions, when compared to experiments under stationary conditions. The transient shear measurements revealed an overshoot of the transient stress, the intensity of which is dependent on the LCP content. This was verified for the all the blends and the maximum was obtained for the blend with the higher LCP content (40 wt % LCP). Since no overshoot was observed for the pure liquid crystalline polymer (which may be due to the low shear rate employed in these measurements) it is possible to attribute it, to the orientation and deformation of the LCP structures. This hypothesis was confirmed in a LAOS analysis, in which the blends with 20 and 40 wt % LCP were those for which the highest non-linear character, $I(3\omega_1)/I(\omega_1)$, that is associated to highest deformation and shear thinning, were observed. The behaviour of the LCP/TP blends depends on the applied strain rate: for the lower strain rates the increase of the

LCP content leads to an increase of the deviation from the LVE (until 20 wt % LCP), while for the higher strain rates the opposite occurs. In both cases, for the lower and for the higher strain rates, the behaviour of the blend with 40 wt % LCP is extremely different from the one observed for the blends with lower LCP contents, an extremely high strain hardening behaviour being observed, possibly attributed to the presence of some residual crystallinity.

Considerable differences in morphology were observed for the blends processed at 220 and 240 °C, confirming the importance of the processing temperature on the preparation of these blends. The use of FT rheology was again essential to understand and estimate the influence of the processing temperature on the rheological behaviour of the blends under non-stationary conditions, which, as already pointed out, may reflect their behaviour during processing. A lower processing temperature improves the formation of the LCP fibrils, leading to a decrease of viscosity and to an increase of the Young's modulus. The main conclusions obtained from the FT measurements were that rheological experiments performed under non-stationary conditions are much more sensitive to the changes in morphology that occur when the processing temperature is changed than rheological experiments under stationary conditions.

4.3 STUDY OF THE INFLUENCE OF THE USE OF DIFFERENT SCREW CONFIGURATION ON THE FINAL MORPHOLOGICAL AND MECHANICAL PROPERTIES

INTRODUCTION

The main aim of the present chapter is to perform a brief evaluation of the degree of which the application of different screw and cylinder configurations affects the final morphological properties, and thus the mechanical performance of non-compatibilised LCP/TP blends. Work was done with respect to the final properties, in particular on the effects of different processing conditions on both morphological and mechanical properties [Blizard 1987, Subrananiam 1991, Heino 1992, Heino 1994]. In these studies the attention was focused on the influence of the use of different blending equipments, as well as different processing conditions, namely screw speed and output. However, these works were only devoted to the study of the final extrudates and were not focused on the morphological evolution along the extruder length.

RESULTS AND DISCUSSION

MORPHOLOGICAL PROPERTIES

In sub-chapter 4.1 the evolution of the morphology along the extruder length for blends processed using configuration 1 (figure 3.4, Chapter 3) was studied and correlations were established between the morphological properties and the mechanical properties, for blends containing 10, 20 and 40 wt % LCP (sub-chapter 4.2). From this analysis it was possible to conclude that for the blend with the lowest LCP content (10 wt % LCP), a progressive elongation of the dispersed phase structures occurs (figure 4.1 (a)). Increasing the LCP content led to the increase of the number of fibrils *per* volume (figure 4.1), as expected, all blends

presenting fibrillar structures oriented along the flow direction and distributed along the thermoplastic matrix.

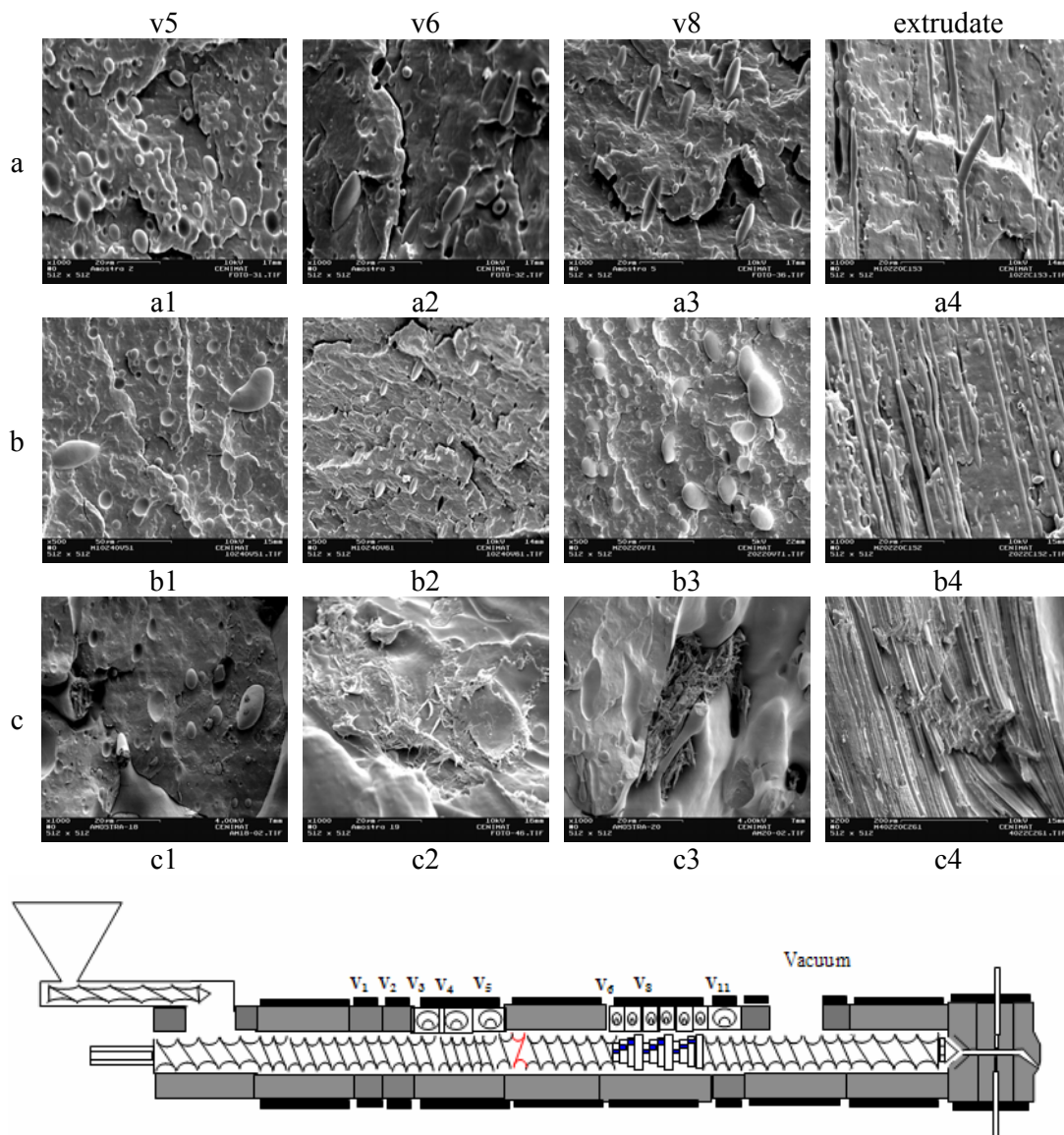


Figure 4.45 - Morphological evolution along the extruder length for blends with 10 (a), 20 (b) and 40 (c) wt % LCP, processed with configuration 1 (SEM images with magnification of x1000 for a, b4, c1-c3, x500 for b1-b3 and x200 for c4).

Before starting the analysis of the morphological evolution along the extruder length for the blends processed using configuration 2, some considerations must be made. Firstly, it should be pointed out that in configuration 2 the number of kneading blocks is much higher than the one present in configuration 1 (see chapter 3). In configuration 1, the kneading blocks

are concentrated in a specific part of the metering zone (figure 4.45), while in configuration 2 (figure 4.46), they are distributed along the extruder length.

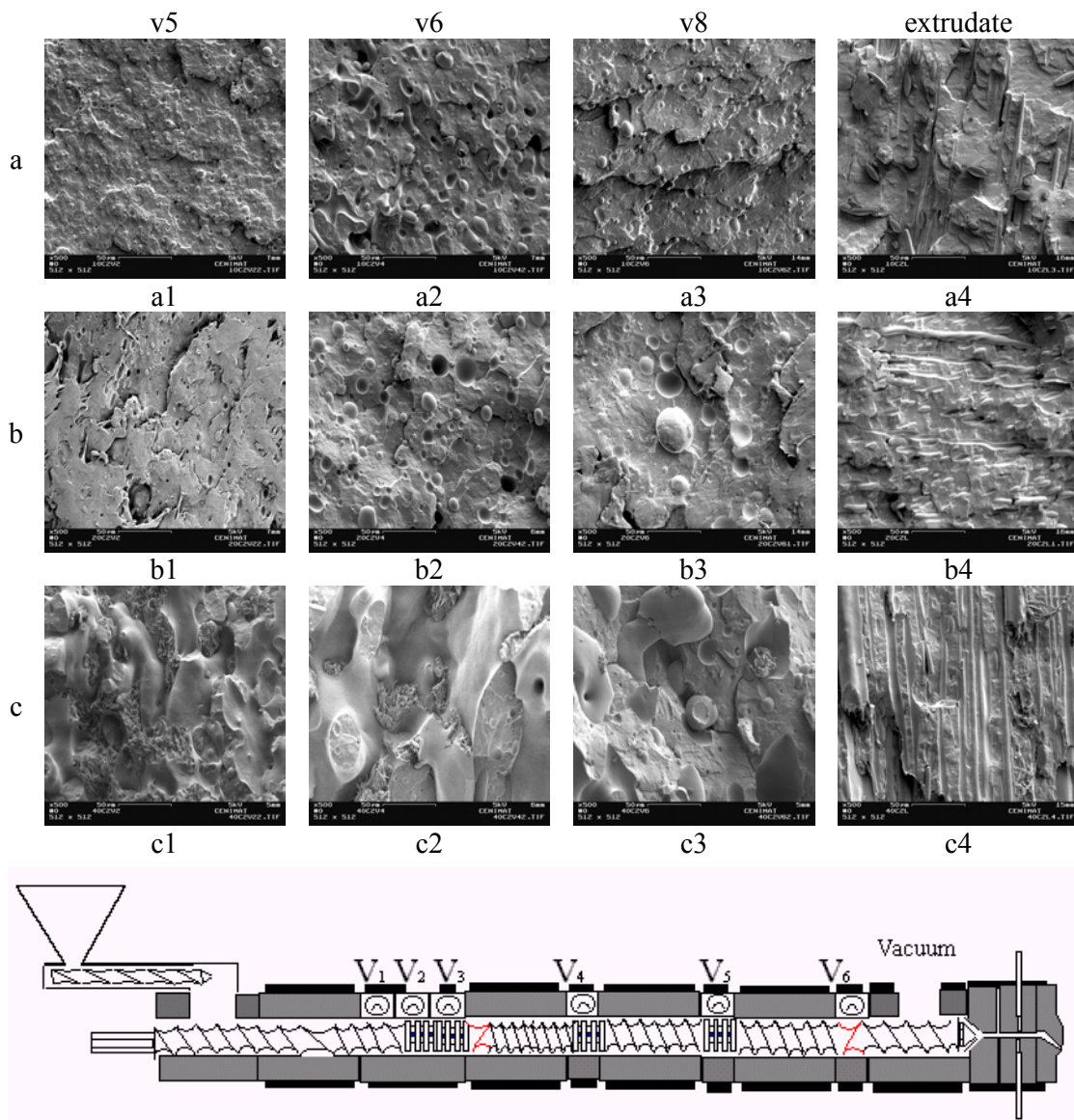


Figure 4.46 - Morphological evolution along the extruder length for blends with 10 (a), 20 (b) and 40 (c) wt % LCP, processed with configuration 2 (SEM images with magnification of x500).

Due to the fact that a higher number of kneading blocks are present in configuration 2 (which are distributed along the screw), an improvement of the degree of mixing (both dispersive and distributive) by the use of this configuration, relatively to that of the blends processed with configuration 1 is to be expected.

In fact, upon analysis of the morphology obtained for the blend with 10 wt % LCP along the extruder length, it is possible to state that the dispersed phase structures possess in average much lower diameters, than the ones, for the blend processed by using configuration 1, for the same LCP content.

From the analysis of figure 4.46 (a) it is apparent that the LCP structures evolve along the extruder length differently from what was seen for the blend processed by using configuration 1 (figure 4.45 (a)). In the later case, and as already stated, a progressive elongation occurs as proceeding downstream in the extruder. When configuration 2 is used, on the other hand, the LCP droplets are broken almost at the beginning of the process, the average diameters at valve 2 being already very small. However, some relaxation seems to occur from valve 2 to valve 4, which is probably due to the fact that no compatibiliser exists to help to prevent the coalescence processes, resulting in an increase of the average diameters at valve 4 (relatively to those obtained at valve 2) since a conveying region exists. If a compatibiliser was added the coalescence at the conveying elements would be prevented, keeping the morphology developed at the first kneading blocks region relatively unchanged (this phenomena will be explained in more detail in chapter 5).

At valve 6 a new decrease of average diameters occurs relatively to valve 4, which is associated to the previous passage of the material through two kneading-blocks regions (located at valve 4 and valve 5, as shown in figure 4.46).

Despite the fact that the use of configuration 2 leads to a dispersed phase with much lower average diameters at the valves, this is not the screw and cylinder configuration for which one observed a higher fibrillation. This is relatively unexpected, but is probably due to the fact that (according to the capillary number definition) the deformation and break-up of the dispersed phase structures is much more difficult or even impossible, after a given critical diameter is reached [Majumdar 1997].

For the blends containing 20 wt % LCP, the differences in terms of configuration are not as clear as those observed for a lower LCP content. However, it seems, again, that the use of configuration 2 leads to an increase of the average diameters (at the several locations along the extruder length) in comparison with configuration 1. For configuration 1 there is a decrease of the average diameters from valve 5 to valve 6, followed by an increase from valve 6 to valve 8. On the other hand, the use of configuration 2 leads to a progressive increase of the average diameters, as seen in figure 4.46. In both cases (configuration 1 and 2) the coalescence seems to be more pronounced for the blends with 20 wt % LCP than for the blends with a lower LCP content (10 wt %), which was expected since, increasing the LCP content, increases the probability of the contact between LCP droplets. At the end of the process, the main conclusions are that the fibrillar formation was enhanced by the use of configuration 1, as seen in figures 4.45 and 4.46. Similar conclusion can be made with respect to the blends containing 40 wt % LCP.

MECHANICAL PROPERTIES

The mechanical measurements confirmed the results obtained by SEM. The use of configuration 2 is detrimental for the formation of fibrillar structures and therefore, there is a decrease of the tensile strength and increase of elongation at break with respect to the blends processed by using configuration 1. The increase of the LCP content leads to the increase of the Young's modulus and a decrease of the elongation at break, independently of the configuration used, as seen in figures 4.47 and 4.48.

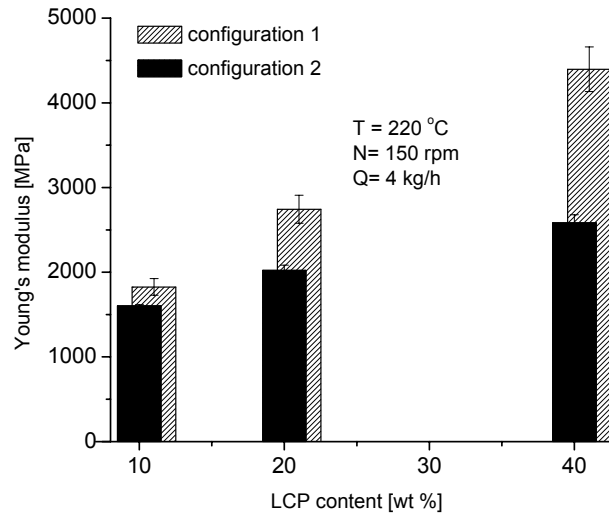


Figure 4.47- Influence of screw and cylinder configuration on the Young's modulus of non-compatible blends with 10, 20 and 40 wt % LCP.

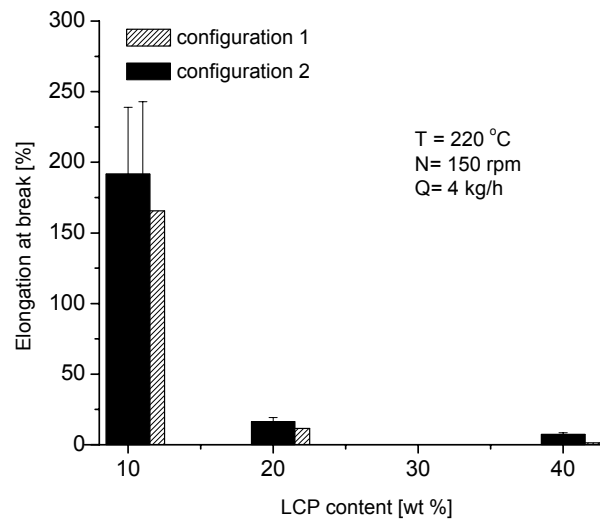


Figure 4.48 - Influence of screw and cylinder configuration on the elongation at break of non-compatible blends with 10, 20 and 40 wt % LCP.

In what concerns the influence of the screw and cylinder configuration on the impact properties it can be stated that the use of configuration 1, as expected, results in a higher impact strength, than the use of configuration 2, as can be see in figure 4.49.

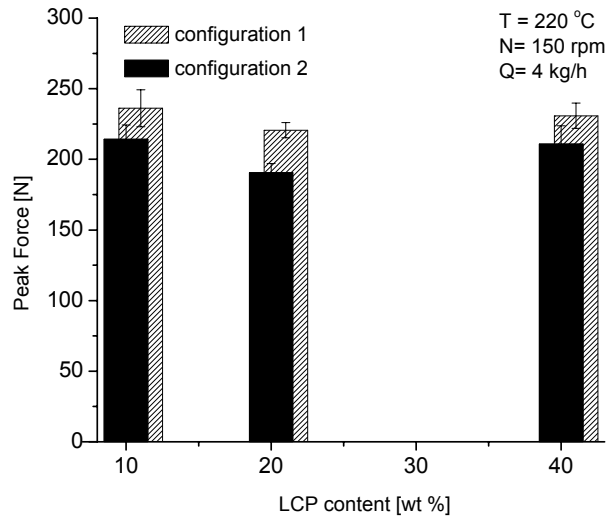


Figure 4.49 - Influence of screw and cylinder configuration on the peak force of non-compatibilised blends with 10, 20 and 40 wt % LCP.

CONCLUSIONS

The morphological and mechanical properties of LCP/TP systems might be dramatically changed by the use of different screw and cylinder configurations. The use of mixing elements (kneading blocks), which is usually responsible by the improvement of both dispersive and distributive mixing in immiscible blends, must be analysed in detail for LCP/TP systems. In what concerns non-compatibilised LCP/TP systems, such as those in this study, it looks like the best fibrillar formation takes place when the break-up of the dispersed phase structures occurs in a more progressive way (like the observed for the blends with 10 wt % LCP, prepared with configuration 1). The use of an excessive number of intensive mixing elements (configuration 2) may result in the decrease of the average diameters at an early stage in the extrusion process (for example, for the blend with 10 wt % LCP processed with configuration 2, the LCP average diameters are already very small at the beginning of the process). After the minimum particle size is reached and due to the absence of compatibiliser (which, if present, would lead to the stabilisation of the morphology formed at the beginning of

the extrusion process), the average diameters obtained at the end, before the die, are much higher than those obtained for screw configurations with a lower number of kneading blocks (like those in configuration 1). Accordingly, the fibrils formed will possess higher aspect ratios for those blends processed with configuration 1, and thus, the mechanical enhancement will be higher for these screw and cylinder configurations.

References

- [Blizard 1987] K. G. Blizard, D. G. Baird, *Polym. Eng. Sci.* **27**, 653 (1987)
- [Choi 1996] G. D. Choi, S. H. Kim and W. H. Jo *Polym. J.* **28**, 527 (1996)
- [Choi 1996a] G. D. Choi, W. H. Jo and H. G. Kim *J. Appl. Polym. Sci.* **59**, 443 (1996)
- [Covas 2000] J. A. Covas, A. V. Machado and M. Van Duin *Adv. Polym. Tech.* **19**, 260 (2000)
- [Filipe 2004a] S. Filipe, M. T. Cidade, M. Wilhelm and J M. Maia *Polym.* **45**, 367 (2004)
- [Guerrica-Echevarria 2000] G. Guerrica-Echevarria, J. I. Eguiazabal and J. Nazabal *Polym. Comp.* **21**, 864 (2000)
- [Halpin 1976] J. C. Halpin and J. L. Kardos *Polym. Eng. Sci.* **16**, 344 (1976)
- [Heino 1992] M. T. Heino, and J. V. Seppälä *J. Appl. Polym. Sci.* **44**, 2185 (1992)
- [Heino 1994] M. T. Heino, P. T. Hietaoja, T. P. Vainio and J. V. Seppälä *J. Appl. Polym. Sci.* **51**, 259 (1994)
- [Hirsh 1962] T. J. Hirsch *J. Amer. Conc. Inst.* **59**:427 (1962)
- [Lazkano 2002] J. M. Lazkano, J. J. Peña, M. E. Muñoz and A. Santamaría *J. Rheol.* **46**, 959 (2002)
- [Majumdar 1997] B. Majumdar, D. R. Paul and A. J. Oshinski, *Polym* **38**, 1787-1808 (1997)
- [Mechbal 2004] N. Meschbal and M. Bousmina *Rheol. Acta* **43 (2)**, 119 (2004)
- [Mi 1998] Y. Mi, C. M. Chan and S. Zheng, *J. Appl. Polym. Sci.* **69**, 1923 (1998)
- [Mustafa 2003] H. U. Mustafa, M. Ishizuki, I. Shige and H. Suzuki *Korea-Aust. Rheol. J.* **15**, 19 (2003)
- [Postema 1997] A. R. Postema and P. J. Fennis *Polym.* **38**, 5557 (1997)

- [Qin 1993] Y. Qin, D. L. Brydon, R. R. Mather and R. H. Wardman *Polym.* **34**, 1197 (1993)
- [Reuss 1929] A. Reuss, *Zeitschrift fur Angewandte Mathematik und Mechanik* **9**, 49 (1929)
- [Saenguan 2003] S. Saenguan, S. Bualek-Limcharoen, G. R. Mitchell and R. H. Olley *Polym.* **44**, 3407 (2003)
- [Shi 1992] Z. H. Shi and L. A. Utracki *Polym. Eng. Sci.* **32**, 1824 (1992)
- [Silva 2004] L.B. Silva, M. M. Ueki, V. C. Barroso, J. M. Maia and R. E. S. Bretas, *Rheol. Acta*, submitted
- [Subramanian 1991] P. R. Subramanian and A. I. Isayev, *Polym.* **32**, 1961 (1991)
- [Sugimoto 2001] M. Sugimoto, Y. Masubuchi, J. Takimoto and K. Koyama *Macromol.* **34**(17), 6056 (2001)
- [Viswanathan 1995] R. Viswanathan and A. Isayev *J. Appl. Pol. Sci.* **55**, 1117 (1995)
- [Voigt 1928] Voigt W, *Lehrbuch der Krystallphysic*, B. G. Teubner, Leipzig, Germany (1928)
- [Ward 1996] I. M. Ward, D. W. Hadley, *An introduction to the mechanical properties of solid polymers*, Chichester, England (1996)

5 COMPATIBILISED LIQUID CRYSTALLINE POLYMER AND THERMOPLASTIC BLENDS

5.1 STUDY OF THE INFLUENCE OF DIFFERENT COMPATIBILISERS ON THE EVOLUTION ALONG THE EXTRUDER LENGTH*

INTRODUCTION

In sub-chapter 4.1 the attention was devoted to the evolution of both morphological and rheological properties along the extruder length for non-compatibilised blends of Rodrun LC3000 and polypropylene. In the present chapter, this study will be extended to compatibilised Rodrun LC3000/PP blends, containing 10 wt % LCP and different compatibilisers, in order to be able to extract the influence of the addition of a compatibiliser during processing, and consequently on the final properties, of such systems.

Liquid crystalline polymer (LCP) and olefinic thermoplastic (TP) blends were investigated during the last years as promising systems, due to their improved mechanical properties, easier processability and cost efficiency. The main problem in blending LCP is that due to their chemical structure, with frequently high aromatic content, they often exhibit low adhesion towards the thermoplastic polymer. This problem can be overcome through the addition of compatibilisers, the use of which will improve even more the mechanical properties of these blends. Several attempts were carried out in order to achieve high mechanical improvements by the addition of compatibilisers [Datta 1995, Wanno 2000, Bualek-Limcharoen 1999, Miller 1995]. All these studies concluded that the addition of compatibilisers to LCP/PP blends leads to an improvement of the dispersion of the LCP fibrils in the polypropylene matrix and to the formation of thinner LCP fibrils than those observed for non-compatibilised blends.

* adapted from S. Filipe, M. T. Cidade, M. Wilhelm, J. M. Maia, *Evolution of Morphological and Rheological Properties of Compatibilised Rodrun LC3000/PP blends*, submitted to J. Appl. Polym. Sci. (August 2004)

None of the above studies was focused on the evolution of the morphological and rheological properties of liquid crystalline polymer and thermoplastic blends during the processing itself. Quite a few studies were done on this subject for other kind of non-compatible immiscible blends, like for example the works of Potente *et al.* and Bordereau *et al.*, that studied blends of PP/PA and PS/HDPE, respectively [Potente 2000, Bordereau 1992]. Boersma and Van Turnhout used dielectric spectroscopy to study the evolution of the morphology during extrusion, for LCP/TP blends [Boersma 1999].

In sub-chapter 4.1 the main conclusions regarding the morphological and rheological evolution along the extruder length for non-compatible Rodrun LC3000/PP blends, were that a decrease of the viscosity was verified along the length of the extruder. This first conclusion was associated to the progressive elongation and break-up of the LCP structures during the extrusion process. At the beginning of the extruder the LCP structures present a droplet-like structure, while at the die exit they have the form of fibrils, oriented along the flow direction (with the consequent reduction of the viscosity).

The main aim of this study is to extend the work already performed with non-compatible Rodrun LC3000/PP blends [Filipe 2004a], to blends in which compatibilisation was carried out. Considering that the final properties of immiscible blends are strongly dependent on the morphology developed during extrusion, the study of the evolution of both morphology and rheology for compatibilised blends is essential to control and optimise the performance of LCP/TP blends. This study will be carried out along several stages of the extrusion process, by measuring morphological and rheologically samples collected along the extruder length. The use of LAOS will be essential to determine the rheological behaviour under non-stationary conditions and as it will be shown later, will be essential to distinguish between different morphologies.

RESULTS AND DISCUSSION

MORPHOLOGICAL PROPERTIES

Since the aim of this part of the work is to evaluate the influence of the presence of different compatibilisers on the rheological and morphological evolution during extrusion, a comparison will be continuously carried out between the different compatibilised blends and the non-compatibilised blend at similar stages during the extrusion process. For this part of the work blends with 10 wt % LCP and 2 wt % compatibiliser were used. Due to the high cost of liquid crystalline polymers, a blend containing a low amount of LCP was used, since, in principle, this will be the most interesting and less expensive option, for industrial applications. The choice of the amount of compatibiliser was based on previous studies carried out for similar systems [Miller 1995, Miller 1997, Tjong 2003].

The processing parameters such as screw and cylinder profiles, temperature, screw speed and throughput were the same for all the blends, with and without compatibiliser. The study of the morphology and temperature profiles developed during extrusion, were carried out by the use of the collecting device system mentioned before (Chapter 3). It should be once more pointed out that with this system it is possible to collect samples in less than three seconds, which are immediately quenched in liquid nitrogen, thus retaining the original morphology. Additionally, the use of this collecting device system allowed the evolution of the true melt temperature to be measured with a quick response thermocouple. The analysis of the temperature profiles revealed that an increase of the temperature occurs along the extruder and that the addition of different compatibilisers leads to different temperature profiles, as seen in table 5.1

Table 5.1 Temperature profiles measured along the extruder length and pressure at die for the blends with and without compatibiliser.

Materials	Temperature (°C)				Pressure at die (bar)
	valve 4	valve 6	valve 8	extrudate	
non-comp.	226.2	227.6	229.6	236.1	30
comp. A	225.1	226.1	228.4	231.1	34
comp. B	226.8	228.5	230.2	237.0	38
comp. C	227.1	228.9	231.9	237.4	36
comp. D	227.2	230.1	231.4	237.1	39
comp. E	228.2	231.4	233.2	238.2	46

The temperatures at the reverse-conveying element (valve 4 and 5) are always lower than those presented at the region of kneading-blocks (valve 6 to valve 10), which is mainly due to the higher shear rates and pressures that are present in the later.

The first blend to be analysed and taken as the reference is the one without compatibiliser, which was already studied in chapter 4. In the beginning of the extrusion process the morphology can be essentially described by large dispersed drops of liquid crystalline polymer, which will progressively deform and elongate by action of increasing shear stress (valve 6 and valve 8). At the die (the photos presented for the extrudates are the ones obtained with samples cryogenically fractured in the longitudinal direction), the droplets are subjected to the highest deformations, leading to the formation of some fibrils (figure 5.1) which are jointly present with the droplets.

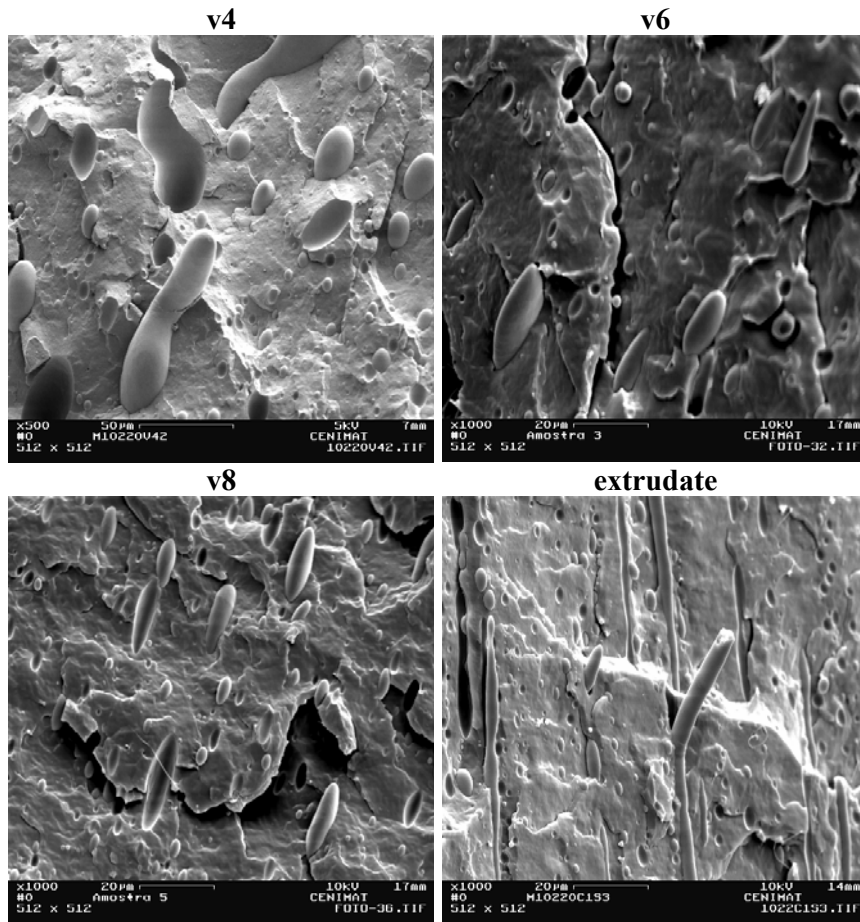


Figure 5.1 - Morphological evolution along the extruder length for the non-compatible blend (SEM) - (images with magnification of x500 for valve 4 and x1000 for valves 6, 8 and extrudate).

The addition of compatibiliser A does not have a significant effect in the morphology at the beginning of the process (compare valve 4, figures 5.1 and 5.2), meaning that the LCP droplets present diameters similar to those verified at the same position, for the non-compatible blend (figure 5.2). Distributive mixing is dominant at this stage since the capillary numbers present at this point are higher than the critical capillary number. Therefore, the interfacial stress is overruled by the shear stress, and the deformation mechanisms are the dominant process. It seems that from valve 4 to valve 6 an improvement of the dispersion of the LCP structures along the matrix is verified. At this stage, a decrease of the diameters of the LCP structures is seen and a more homogenous distribution of these droplets along the matrix is obtained. Nevertheless, elongated structures are still present at valve 6, but in lower numbers

and with lower aspect ratios than those present at valve 4. There are no significant differences between the samples collected at valve 6 and valve 8 for the blend containing compatibiliser A. Finally, the material is subjected to the highest elongational forces, the maximum deformation is achieved when it crosses the die and the final morphology shows the presence of elongated structures, similar in aspect but thicker than the fibrils present in the non-compatible blend.

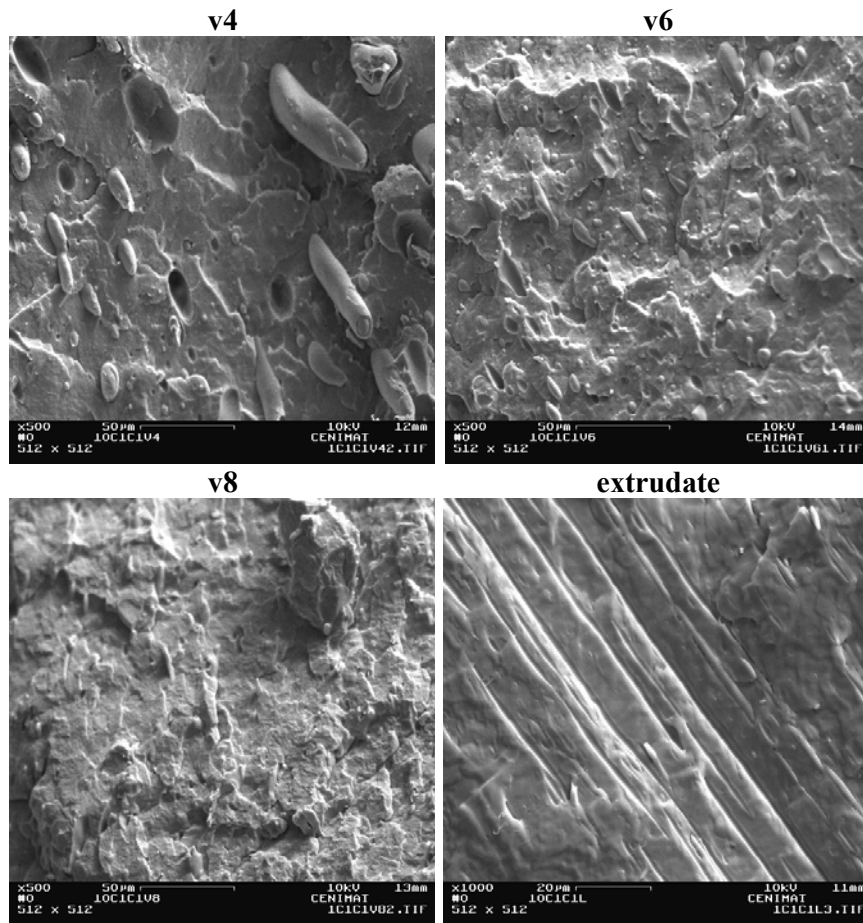


Figure 5.2 - Morphological evolution along the extruder length for the blend with compatibiliser A (SEM) - (images with magnification of x500 for all valves and x1000 for the extrudate).

The different chemical structure presented by compatibiliser B, prefigures a different morphological evolution along the extruder. In this case, the part of the chemical structure that is supposed to be compatible with the liquid crystalline polymer is constituted by the PET, instead of the oligomeric polyester (TerolTM) present in the chemical structure of

compatibiliser A. This new arrangement is supposed to be more compatible with the liquid crystalline polymer, that also contains PET, and thus to lead to a more efficient compatibilisation via similar Van der Waals and π - π interactions [Boersma 1999]. The morphological analysis at valve 4 revealed a slight decrease of LCP droplet diameters, when compared with those of the non-compatibilised blend and of the blend with compatibiliser A, at the same point (figure 5.3).

It is known that the presence of this compatibiliser B leads to an increase of the overall pressure at the die, when comparing with those of both the non-compatibilised blend and the blend with compatibiliser A (see table 5.1). This might be the reason why the addition of compatibiliser B is more effective in terms of distributive mixing than compatibiliser A. The higher pressures might be derived from an increase of the viscosity, relatively to that of the blends with compatibiliser A and without compatibiliser, that will later be shown to exist. An increase of the viscosity will originate an increase of the capillary number, leading to a more efficient and faster elongation and break-up of the LCP structures. As the local length scale decreases, the interfacial stress will become of the same order of magnitude as the shear stress and the dispersive mixing will be dominant. The LCP structures previously elongated will then start to break into droplets with smaller diameters and the distribution of these structures along the matrix will occur in a more efficient way. In the case of the blend with compatibiliser B, this process seems to occur quite quickly, since no significant differences were observed between the samples collected at valve 6 and valve 8 (figure 5.3).

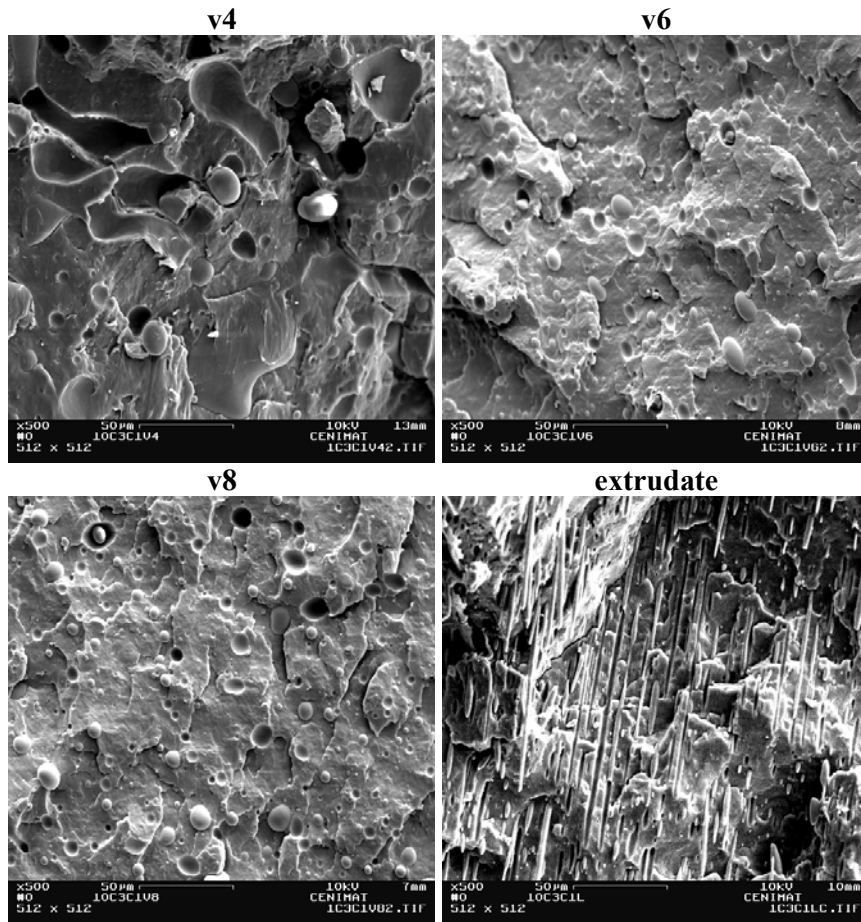


Figure 5.3 - Morphological evolution along the extruder length for the blend with compatibiliser B (SEM) - (images with magnification of x500).

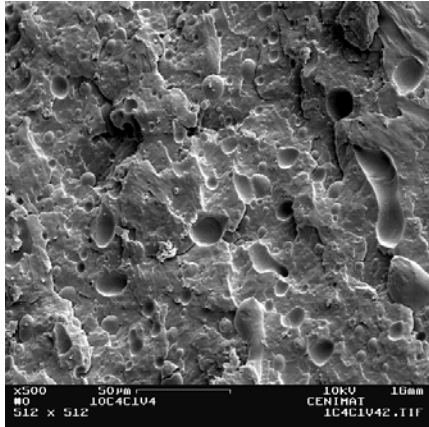
It should be mentioned again that valve 6 is at the beginning of a kneading blocks region, while valve 8 is at the end of this region (see screw configuration at chapter 3, figure 3.4). Also, the dispersion of the LCP structures is almost completely accomplished at valve 6. This means that the shear stress provided before the kneading blocks is already enough for the break-up of the LCP structures into droplets with smaller diameters. The formation of LCP fibrils, when crossing the die, with high aspect ratios was clearly seen, confirming the previous comments, which reported to the higher effectiveness of compatibiliser B, when comparing with compatibiliser A (figure 5.2 and 5.3, respectively).

The addition of compatibiliser C seems to generate a blend in which a further reduction of the LCP diameters occurs, especially when compared with compatibiliser A. The

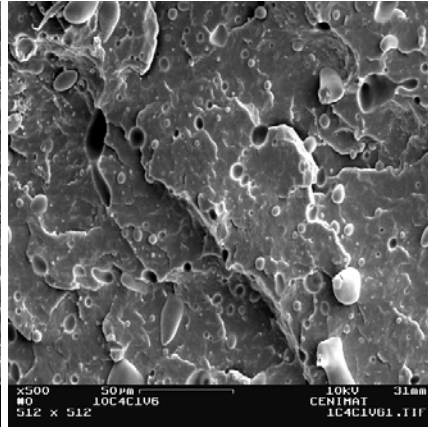
chemical structure of this compatibiliser is expected to be more compatible with both the liquid crystalline polymer and the thermoplastic, since the part of the backbone that is supposed to be compatible with the LCP is constituted by PET. Additionally, the backbone part that is compatible with the thermoplastic possess a smaller length, which reduces the plasticizing effect observed in the case of compatibiliser A.

The morphologies presented at valve 4 and valve 6 are visibly indistinguishable, as it will be confirmed later by linear rheology (figure 5.10). A better dispersion of the LCP along the matrix seems to occur between valves 6 and 8; however, the diameters seem to be almost unchanged from what was seen at valve 4 (figure 5.4). The morphology presented by the final extrudate is, as expected, constituted by fibrils with high aspect ratios. The morphological similarity between the final extrudates of the blends with compatibiliser C and compatibiliser B is evident. The mechanical analysis previously performed, however, showed marked differences between the two compatibilised blends (the blend with compatibiliser C possess a higher tensile strength). Again, only slight differences between valve 4 and valve 8 are present in the blend with compatibiliser D, as shown in figure 5.5.

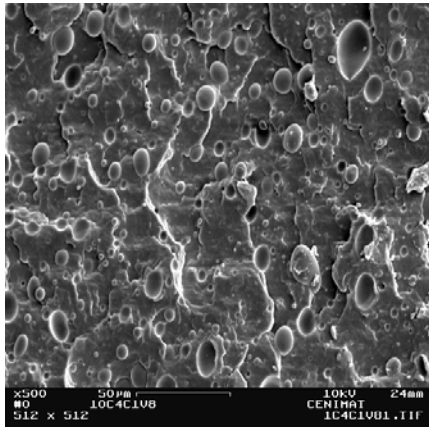
v4



v6



v8



extrudate

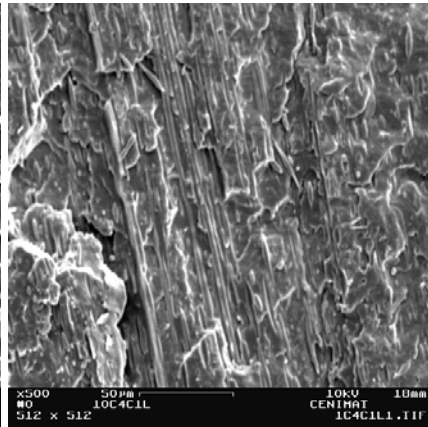


Figure 5.4 - Morphological evolution along the extruder length for the blend with compatibiliser C (SEM) - (images with magnification of x500).

The degree of dispersion is improved for all compatibilisers along the extruder length. However, the resulting fibrils for the blend with compatibiliser D have lower aspect ratios when compared with those observed for the blends with compatibiliser B and C.

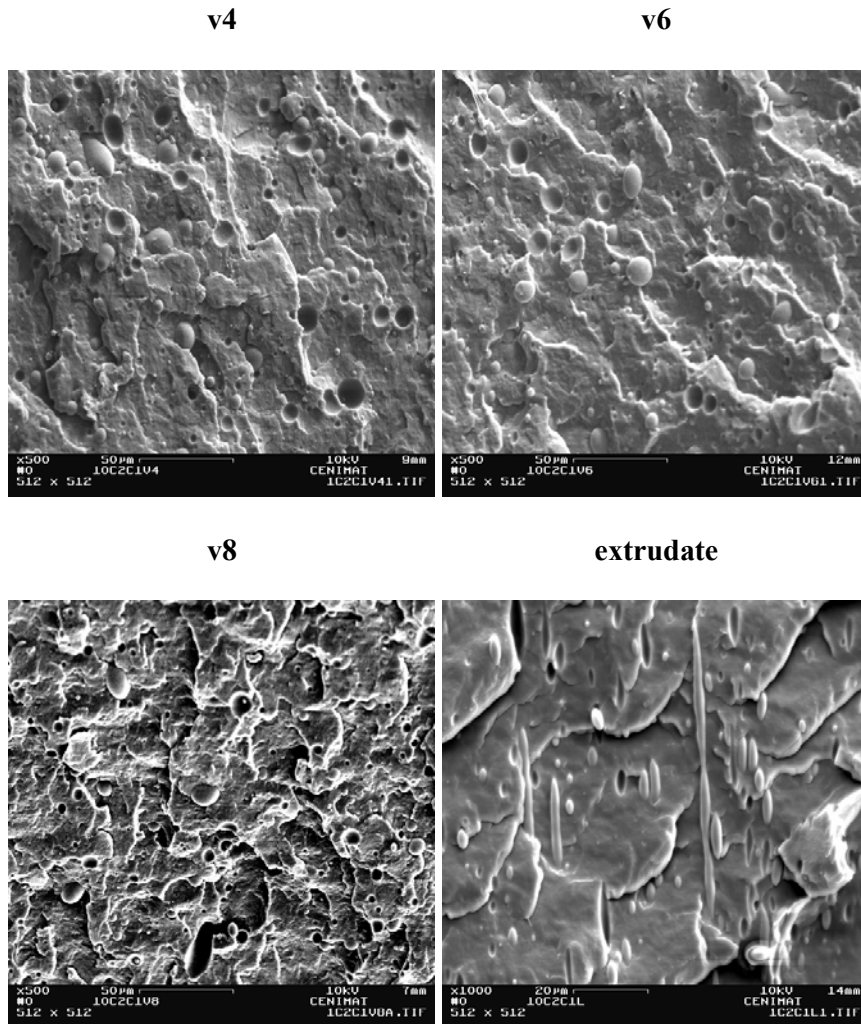


Figure 5.5 - Morphological evolution along the extruder length for the blend with compatibiliser D (SEM) - (images with magnification of x500 for all valves and x1000 for the extrudate).

The morphology shown for the blend in which compatibiliser E was used is significantly different, as depicted in figure 5.6. Firstly, the addition of this compatibiliser did not lead to a significant decrease of the diameters of the LCP structures at valve 4, as occurred for the blends with compatibiliser B, C and D. The shape of the LCP structures is clearly different from what was previously seen for other compatibilised blends (figures 5.2 to 5.5). A high degree of elongation is, however, observed, meaning that at this point the distributive mixing is still the dominant process, contrary to what occurred for the blends containing compatibiliser B, C and D (figure 5.3, 5.4 and 5.5, respectively). A clear decrease of the

diameters of the LCP structures occurred between valves 4 and 6, contrary to what occurred for the other compatibilised blends.

The break-up processes for the blends with compatibilisers B, C and D seem to occur faster, than for the blend with compatibiliser E. By the action of the shear stress developed inside the extruder, these structures will then break, giving rise to the formation of LCP droplets with considerable lower diameters, at valve 6. From valve 6 to valve 8, the observed improvement is not in terms of the decrease of the diameters (which seems to be already accomplished at valve 6), but in terms of distribution. Finally, after the die, the liquid crystalline polymer structures attain the maximum elongation, and a fibrillar formation occurs.

The break-up of the LCP structures seems to occur in a larger extent in this blend, this being the reason why the LCP fibrils present lower aspect ratios than those observed for the blends in which compatibilisers C and B were used (figure 5.6).

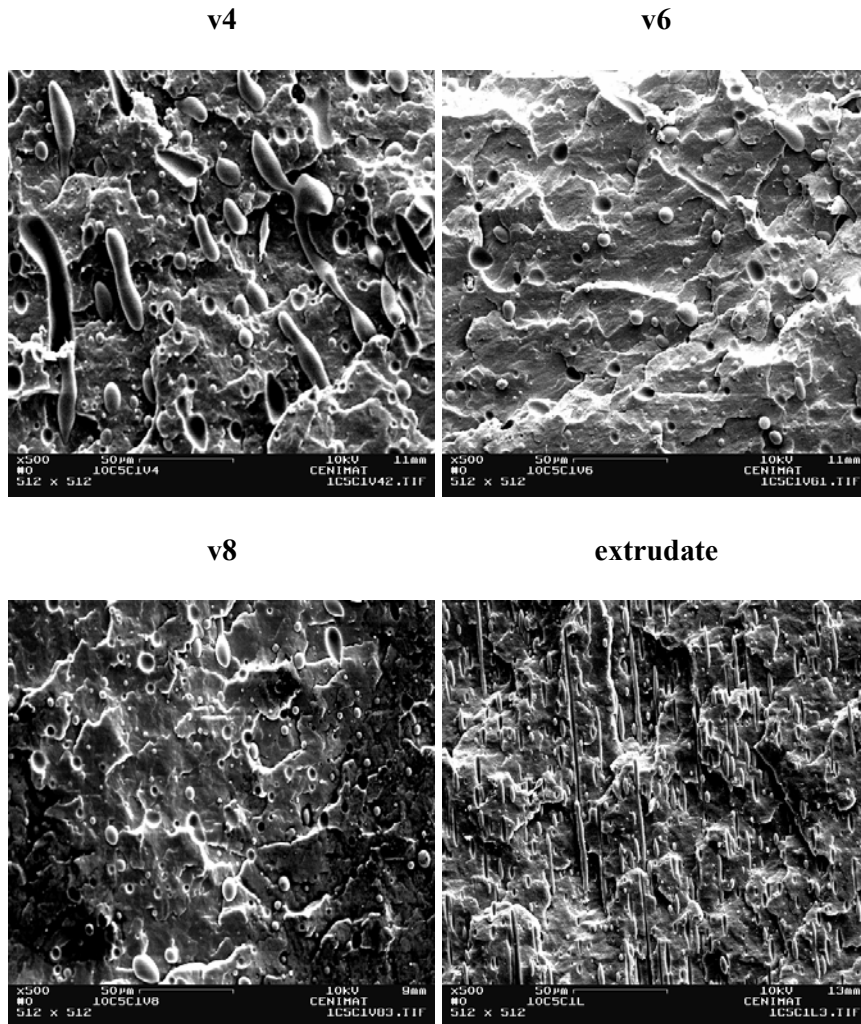


Figure 5.6 - Morphological evolution along the extruder length for the blend with compatibiliser E (SEM) - (images with magnification of x500).

RHEOLOGICAL PROPERTIES

As described above, the study of the evolution along the extruder length was carried out by the use of oscillatory shear, within the linear and the non-linear regimes. The first part of this analysis will be devoted to the evolution of the storage modulus and complex viscosity along the extruder (figures 5.7 to 5.12). In the second part, a quantification of the non-linear character will be done, in order to estimate how the progression of the non-linearity occurs during processing (figures 5.13 to 5.18).

Due to the improved efficiency in terms of dispersive and distributive mixing that occur when compatibilisers are added to the blend, smaller differences between samples collected at different locations along the extruder are expected than those of the blend without compatibiliser.

Considering the results in linear oscillatory shear, for all the blends (figures 5.7 to 5.12) it is apparent that both the storage modulus and the complex viscosity remain relatively constant along the extruder and that only at the die can significant changes be observed. In this case a decrease of both viscosity and storage modulus was observed between samples collected before and after the die, which might be associated to the different morphologies presented (inside the extruder the LCP has the form of droplets, while for the extrudates it presents a fibrillar morphology).

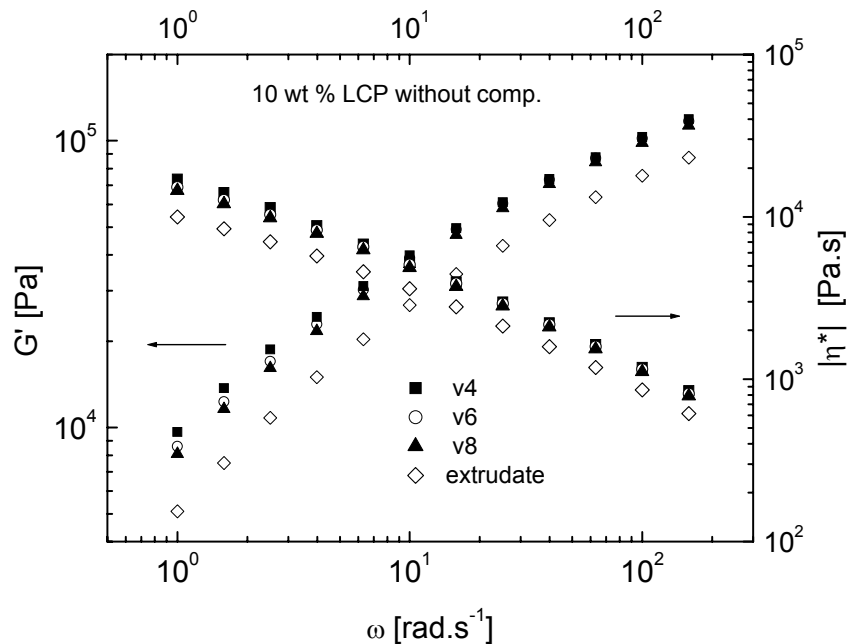


Figure 5.7 - Evolution of the storage modulus and complex viscosity along the extruder length for the non-compatibilised blend, at $T=170$ °C, $\gamma_0 = 0.1$.

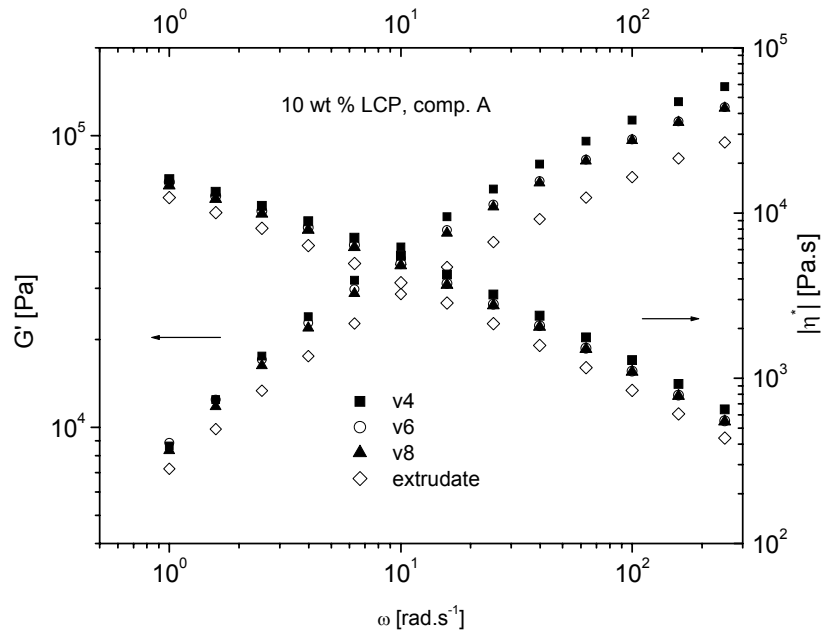


Figure 5.8 - Evolution of the storage modulus and complex viscosity along the extruder length for the blend with compatibiliser A, at $T=170$ °C, $\gamma_0 = 0.1$.

This effect is particularly relevant for the non-compatibilised blend and the blend with compatibiliser A. In principle, non-spherical particles will yield higher apparent volume fractions than spherical particles, and thus, an increase in viscosity was expected for the final extrudates. However, in cases where no compatibilisation is carried out or ineffective compatibilisation occurred, lack of adhesion at the interface occurs and the orientation of the LCP structures may become the dominant factor, thus leading to a decrease of the viscosity for the final extrudates (figures 5.7 and 5.8).

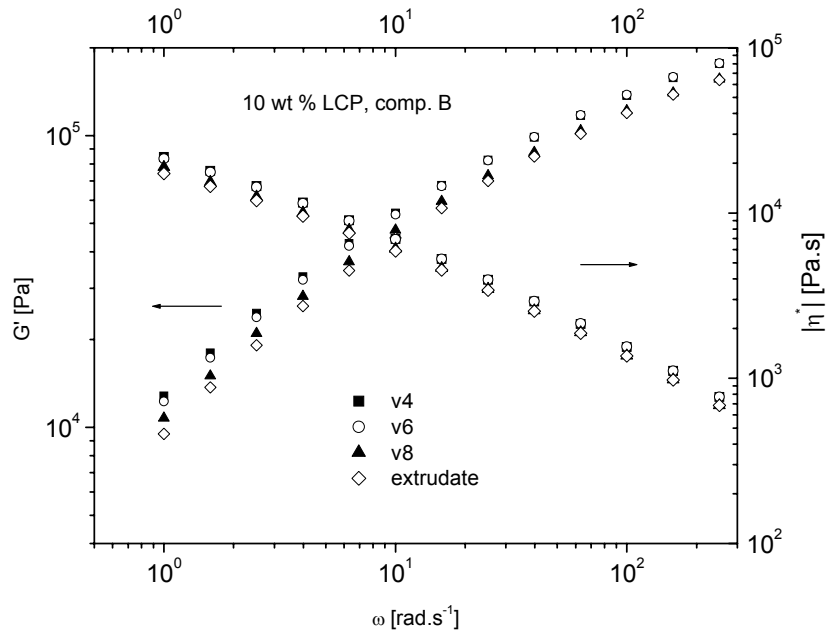


Figure 5.9 Evolution of the storage modulus and complex viscosity along the extruder length for the blend with compatibiliser B, at T=170 °C, $\gamma_0 = 0.1$.

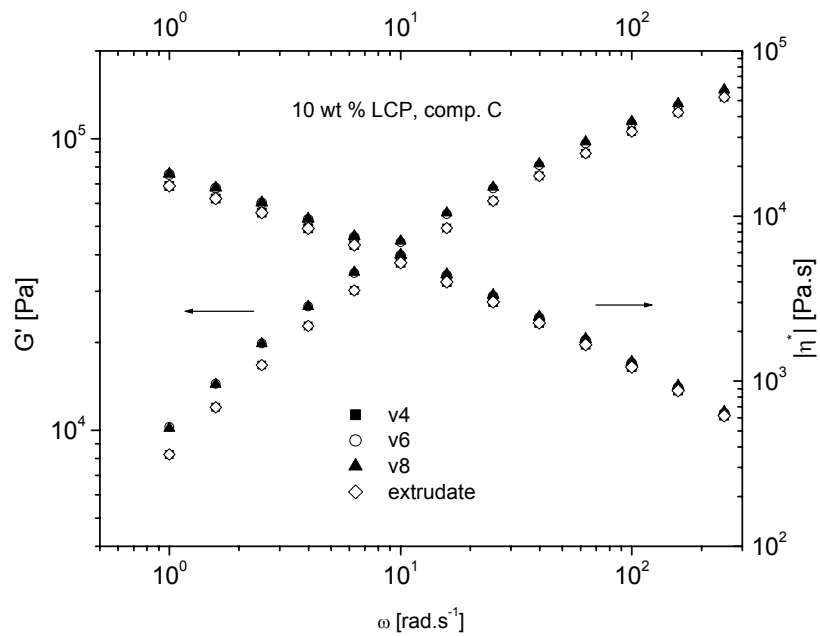


Figure 5.10 - Evolution of the storage modulus and complex viscosity along the extruder length for the blend with compatibiliser C, at T=170 °C, $\gamma_0 = 0.1$.

When the compatibilisation is carried out with compatibilisers B to E, changes in the rheological behaviour of the LCP/PP system along and at the exit of the extruder still occur (figures 5.9 to 5.12), but with a much lower order of magnitude. In fact, the viscosities between samples collected before (valves 4, 6 and 8) and after the die are now almost indistinguishable and although a slight decrease of both viscosity and storage modulus was observed at the die exit, the effect is much smaller than previously.

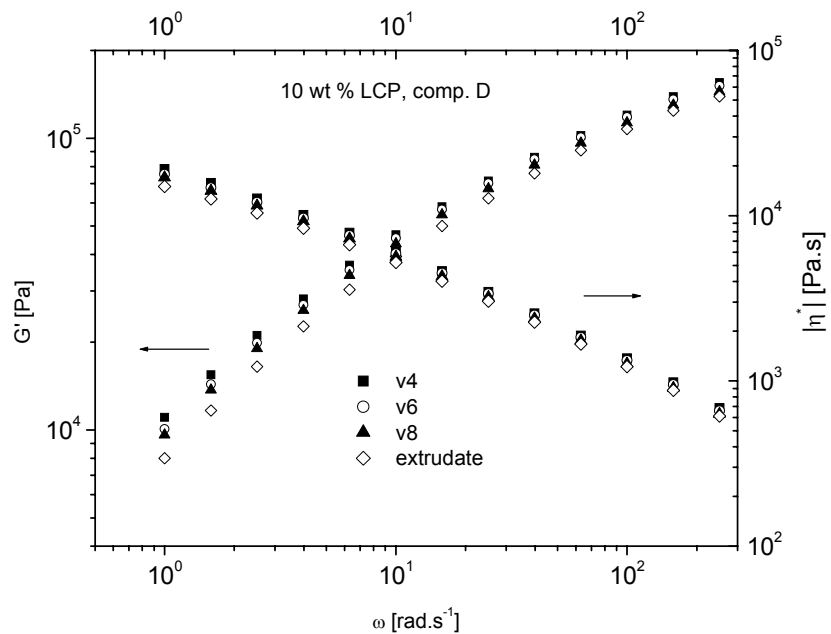


Figure 5.11 - Evolution of the storage modulus and complex viscosity along the extruder length for the blend with compatibiliser D, at $T=170$ °C, $\gamma_0 = 0.1$.

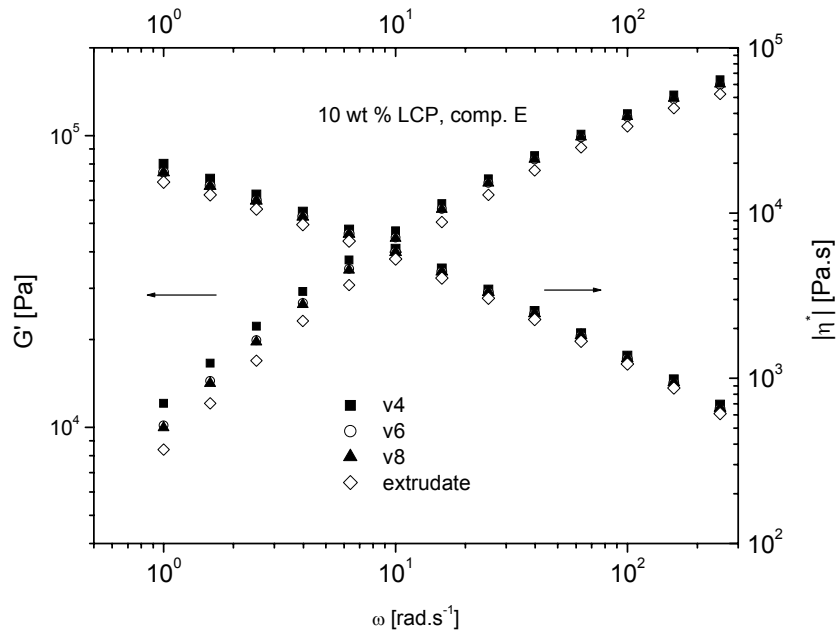


Figure 5.12 - Evolution of the storage modulus and complex viscosity along the extruder length for the blend with compatibiliser E, at $T=170\text{ }^{\circ}\text{C}$, $\gamma_0 = 0.1$.

In conclusion, for these materials, linear oscillatory shear was able to distinguish between the type of structures present, but was not sensitive enough to detect finer differences between droplet dimensions as the material progresses inside the extruder. In addition to this drawback, the majority of industrial processes occur in a non-linear regime and, therefore, it is of great interest to study the rheological behaviour under these conditions and not under linear ones.

A prime candidate for this study, due to its ease of use and large potential for this type of systems [Wilhelm 2002] is Large Amplitude Oscillatory Shear (LAOS). In this case, we have followed the method outlined for non-compatibilised blends containing different LCP contents [Filipe 2004a], whereby a sinusoidal strain excitation was applied for a constant frequency and temperature and the resultant torque response was Fourier transformed. The evaluation of the non-linear character will be obtained from $I(3\omega_1/2\pi)/I(\omega_1/2\pi)$, which represents the relative intensity between the third harmonic ($3\omega_1/2\pi$) and the fundamental

excitation frequency ($\omega_1/2\pi$). The evolution of $I(3\omega_1/2\pi)/I(\omega_1/2\pi)$ with the applied strain was studied for all the samples collected along the extruder length (from valve 4 to the final extrudate).

Considering the rheological response under non-linear conditions and in contrast to the linear data, a clear distinction between samples collected at different locations along the extruder can be made. The non-linear character, expressed by means of the evolution of $I(3\omega_1)/I(\omega_1)$ as a function of the strain amplitude differs according to the location in the extruder. As verified previously for non-compatibilised systems (see sub-chapter 4.1), the degree of non-linearity decreases progressively, and in a very clear way, along the extruder for all the blends (figures 5.13 to 5.18), which can be directly related with the progressive decrease of the dispersed phase diameters.

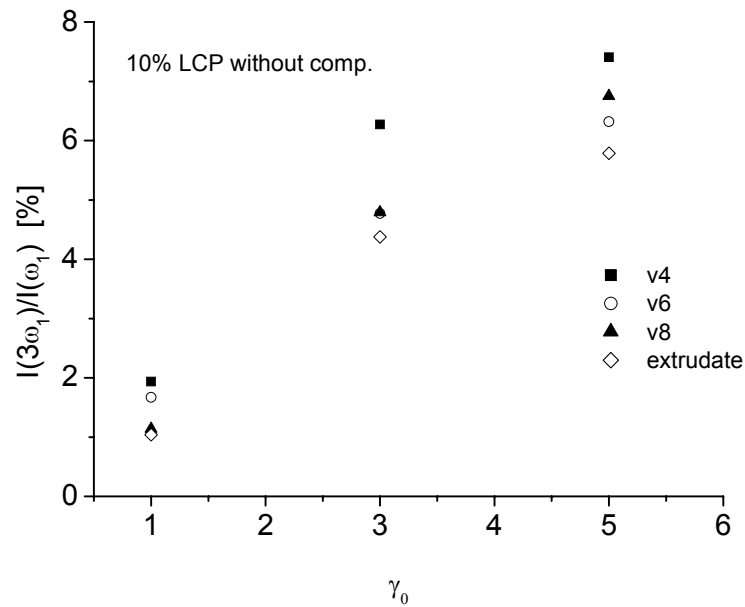


Figure 5.13 - Increase of $I(3\omega_1)/I(\omega_1)$ with the applied strain amplitude for the different samples collected along the extruder length (blend without compatibiliser, at $T=170^\circ\text{C}$, $\omega_1/2\pi = 1\text{ Hz}$).

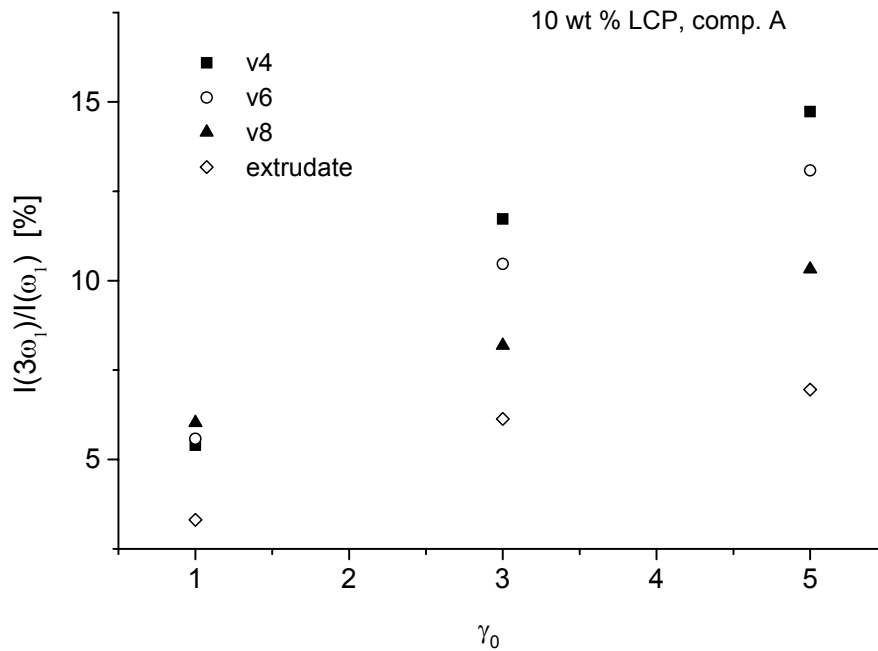


Figure 5.14 Increase of $I(3\omega_1)/I(\omega_1)$ with the applied strain amplitude for the different samples collected along the extruder length (blend with compatibiliser A, at $T=170$ °C, $\omega_1/2\pi = 1$ Hz).

The differences in terms of non-linear character are especially pronounced for the blend with compatibiliser A, as seen in figure 5.14. This is in agreement with the morphological analysis, which shows that this is the blend for which the LCP droplets present the highest dimensions (figure 5.2). It should be considered, however, that at valve 4 the morphology presented for the blend with compatibiliser A is quite similar to the one observed for the non-compatibilised blend (figures 5.1 and 5.2). Thus, the non-linear character must not depend exclusively on the diameters of the dispersed phase; the action of the compatibiliser at the interface must have an additional and important contribution.

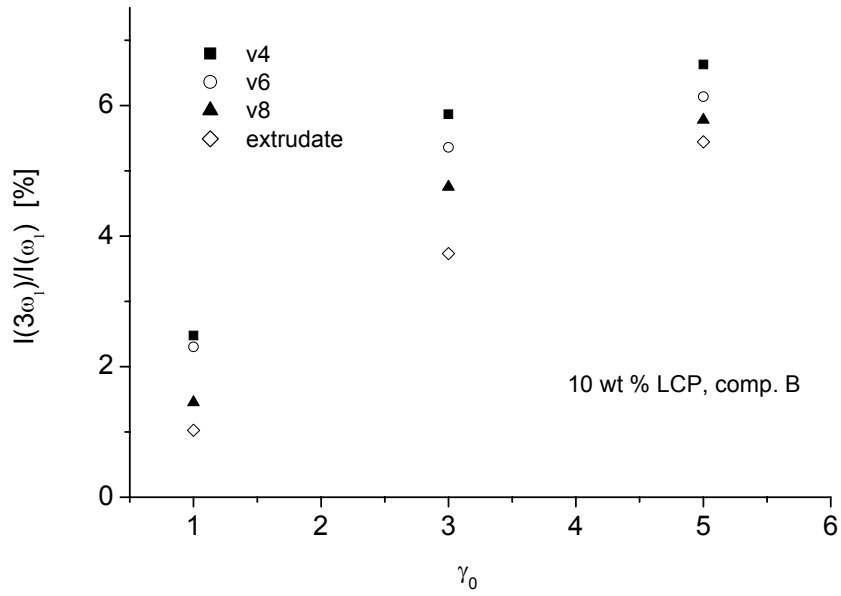


Figure 5.15 - Increase of $I(3\omega_1)/I(\omega_1)$ with the applied strain amplitude for the different samples collected along the extruder length (blend with compatibiliser B, at $T=170^\circ\text{C}$, $\omega_1/2\pi = 1$ Hz).

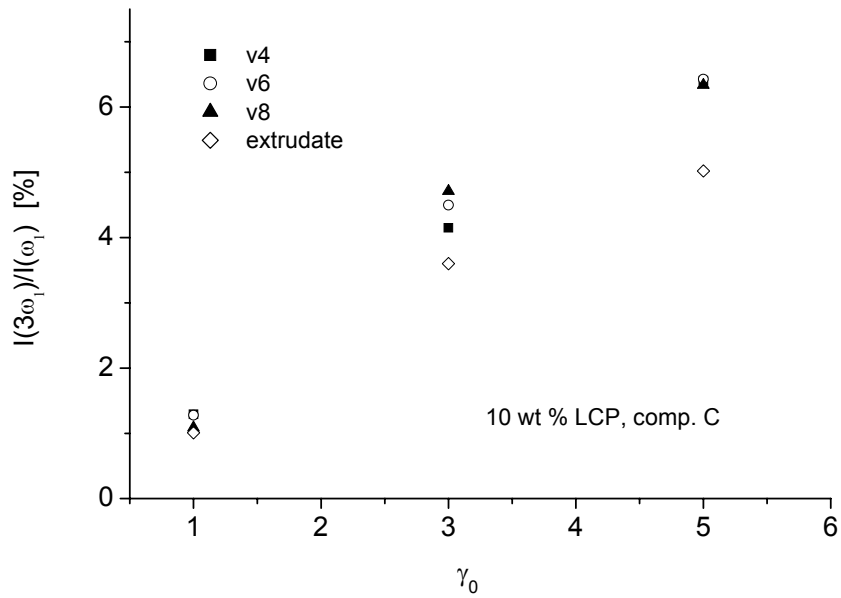


Figure 5.16 - Increase of $I(3\omega_1)/I(\omega_1)$ with the applied strain amplitude for the different samples collected along the extruder length (blend with compatibiliser C, at $T=170^\circ\text{C}$, $\omega_1/2\pi = 1$ Hz).

The blend with compatibiliser C, on the other hand, is the one in which the smallest differences were verified between samples collected at different valves (figure 5.16), which is an indication of a more homogeneous structure and is also compatible with the improved mechanical properties that this blends possesses. Again, a decrease of $I(3\omega_1)/I(\omega_1)$ occurred for the final extrudates, comparing with those of the samples collected at the valves.

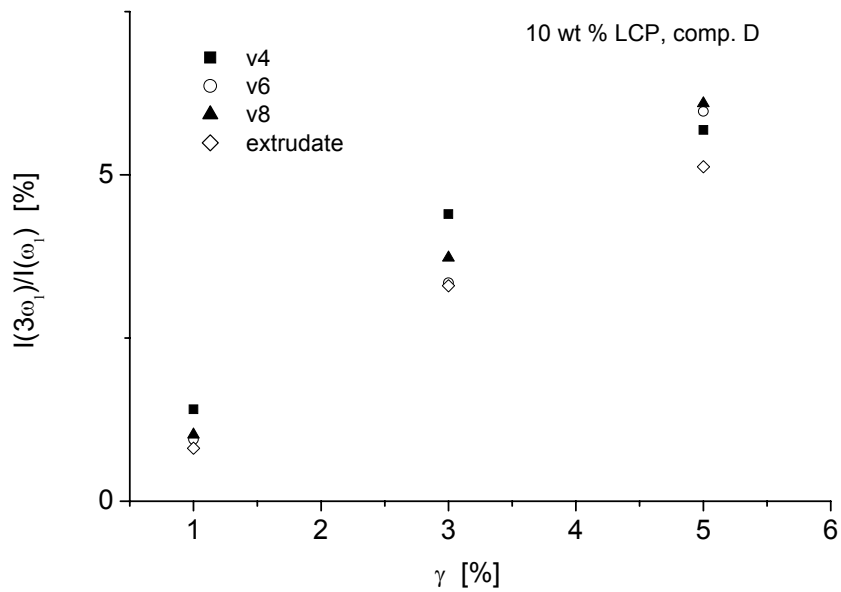


Figure 5.17 Increase of $I(3\omega_1)/I(\omega_1)$ with the applied strain amplitude for the different samples collected along the extruder length (blend with compatibiliser D, at $T=170\text{ }^\circ\text{C}$, $\omega_1/2\pi = 1\text{ Hz}$).

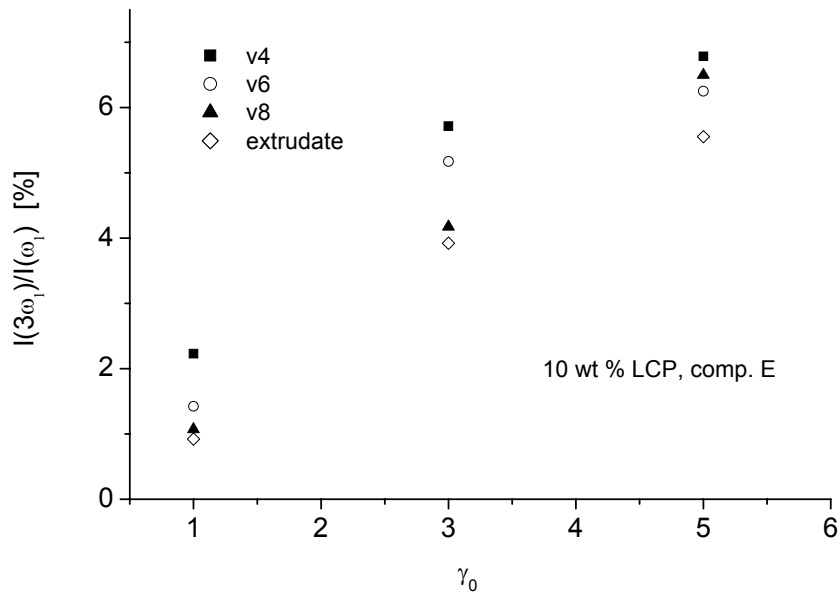


Figure 5.18 - Increase of $I(3\omega_1)/I(\omega_1)$ with the applied strain amplitude for the different samples collected along the extruder length (blend with compatibiliser E, at $T=170\text{ }^\circ\text{C}$, $\omega_1/2\pi = 1\text{ Hz}$).

In terms of final extrudates, it can be considered that the addition of compatibiliser leads to a decrease of the non-linear character for all the compatibilised blends, except for the blend with compatibiliser A, for which considerable higher non-linearities were observed.

In conclusion, LAOS is a very powerful tool in the indirect analysis of the evolution of the morphology of these blends along the extruder, being sensitive not only to the type of structure present, but also to the average dispersed phase dimensions.

CONCLUSIONS

Most of the fundamental research on the mixing of immiscible polymers has been focused on ideal systems, with typical Newtonian behaviours and well defined flow conditions. The study of the mixing processes that occur during the extrusion of liquid crystalline polymer and thermoplastic blends clearly involves a much higher degree of complexity, thus requiring an improved knowledge and an intense study, using several complementary methods.

To take advantage of the high mechanical strength of liquid crystalline polymers, the use of compatibilisers is required for preparation of LCP/TP blends. According to the chemical structure of the later, a different degree of compatibilisation may occur, which basically means that a different morphology will be obtained during the extrusion process. Taking the present work as a basis, it can be stated that the way how the morphology evolves along the extruder length differs according to the compatibiliser used, since different compatibiliser molecular structures induce different degrees of efficiency of both distributive and dispersive mixing. Additionally, the decrease of the LCP structures diameters occurs faster and the LCP fibrils of the final extrudate will become thinner and longer for the blends in which the compatibiliser acted more efficiently.

From the rheological point of view, the use of linear oscillatory shear was useful to distinguish between the types of microstructure present, but was not sensitive enough to study in depth the evolution along the extruder length. In order to do so, large amplitude oscillatory shear, LAOS, and FT-Rheology analysis were used. This analysis established that the degree of non-linearity decreases clearly along the extruder as a result of the progressive decrease of the LCP structures diameters, thus, the results show that the non-linear character seems to be strongly correlated with the efficiency of the compatibiliser. For example, the use of the least effective compatibiliser (compatibiliser A) led to an increase of the non-linear character, in contrast with what was verified for the blends in which compatibilisation was effective (compatibilisers B, C, D and E).

5.2 STUDY OF THE INFLUENCE OF DIFFERENT COMPATIBILISERS ON THE FINAL MORPHOLOGICAL, RHEOLOGICAL AND MECHANICAL PROPERTIES*

INTRODUCTION

In order to clarify the role of compatibilisers with different chemical natures on the mechanical performance of injection moulding specimens, namely in terms of their tensile and impact strengths, Rodrun LC3000/PP blends were compatibilised through the addition of five different compatibilisers. Three of these were custom-synthesized and are mostly linear structures, part of the backbone being compatible with the polyolefin (matrix) and the other part with a liquid crystal compatible polyester structure (see figure 3.2, chapter 3). By varying the size and composition of these two segments, it was possible to vary the compatibility with each one of the components of the blend and establish the influence of the size and composition of both segments on the mechanical performance of the blends (see figure 3.3, chapter 3). The remaining two compatibilisers were commercial ones, one of a thermoplastic nature and the other with an elastomeric nature, in both cases grafted with maleic anhydride (see figure 3.3, chapter 3).

From the rheological point of view, the emphasis of the previous studies on compatibilised liquid crystalline polymer and thermoplastic blends has been on the evaluation of their fundamental properties under stationary conditions [Liang 2002, Tjong 2003, Bualek-Limcharoen 1999, Brostow 1996, Magagnini 1998, O'Donnell 1995, Lee 2003] and not under transient ones which are, in fact, those most relevant to processing sequences. One of the few exceptions is the work of Lazkano *et al.*, where the authors studied the transient response of two LCP non-compatibilised blends of Rodrun LC5000/PP with 30 wt % LCP [Lazkano 2002].

* adapted from S. Filipe, J. M. Maia, A. Duarte, C. R. Leal, M. T. Cidade, *Influence of type of compatibiliser on the rheological and mechanical behaviour of blends under different stationary and non-stationary shear conditions*, submitted to J. Appl. Polym. Sci. (June 2004)

In order to help fill some of the gaps in knowledge identified above, the main aims of this chapter are: a) to determine which rheometrical technique(s), oscillatory shear, FT-Rheology or transient shear is/are more sensitive to the variations in blend morphology and under which conditions, b) with this information, assess the influence that different compatibilisers have in the rheological and mechanical behaviour of injection moulded samples of Rodrun LC3000/PP blends and c) to evaluate the influence of different compatibilisers on the elongational flow behaviour of LCP/TP blends.

RESULTS AND DISCUSSION

MORPHOLOGICAL PROPERTIES

In order to analyse the morphology of the different blends, scanning electron microscopy was performed for the extrudates. In addition to the typical transversal cuts, longitudinal cryogenic fracture was performed, in order to better clarify the formation of LCP fibrils.

The first observation that can be made is that the addition of compatibilisers leads to the formation of thinner and longer fibrils, with a more homogeneous distribution than that observed for the non-compatibilised blends. From the analysis performed for the longitudinal cuts (figure 5.19) it can be concluded that the addition of compatibilisers B, C, D and E leads to the formation of LCP fibrillar structures with a good dispersion along the thermoplastic matrix. This is not as obvious for the blend with compatibiliser A, a fact that will be of great relevance to the tensile properties (see below). The morphology obtained for these compatibilised blends, reveals that the aspect ratio of the LCP fibrils seems to be higher and the distribution of the dispersed phase is more uniform for the blends with compatibilisers B, C and E, than for the blend with compatibiliser D. In principle, this behaviour is related to the rheological properties of the different compatibilised blends as will be discussed later.

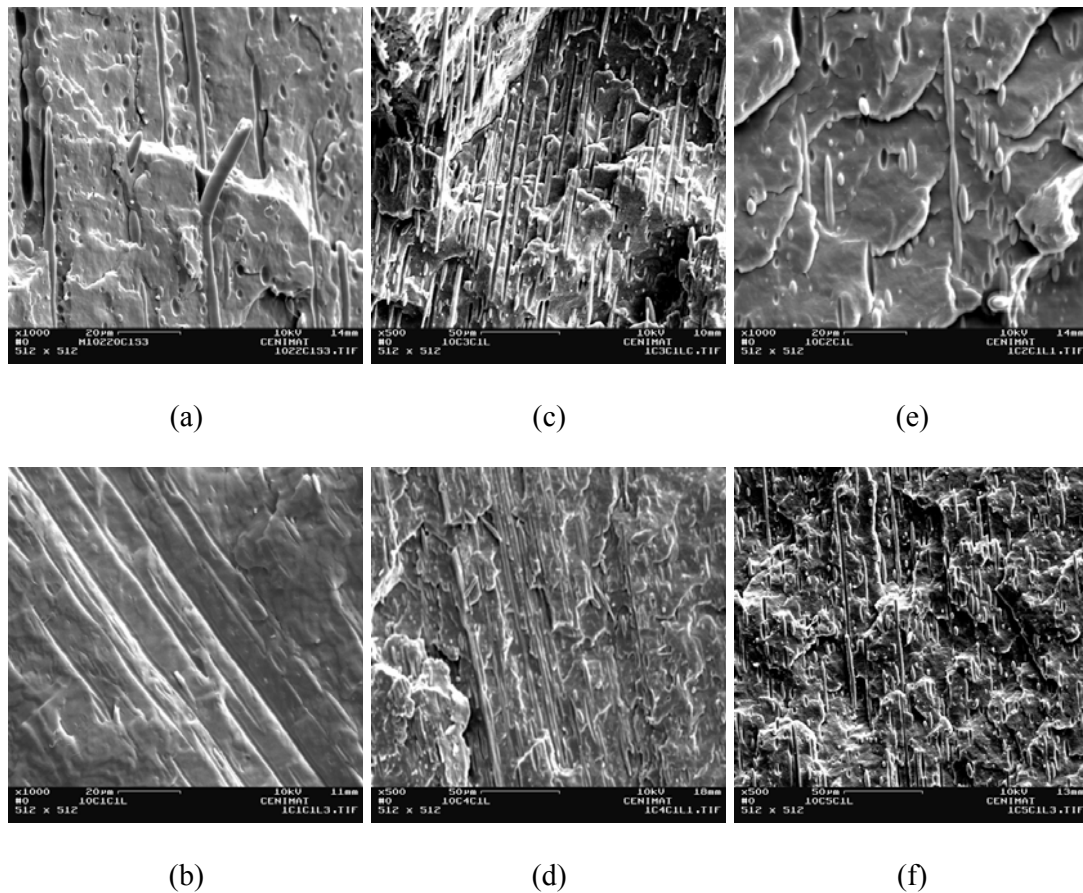


Figure 5.19 - SEM images for the longitudinal cuts performed to the final extrudates of blends with 10 wt % LCP- (a) without compatibiliser; (b) with compatibiliser A; (c) with compatibiliser B; (d) with compatibiliser C; (e) with compatibiliser D; (f) with compatibiliser E (figures *a*, *b* and *e* with magnification of x1000, and figures *c*, *d* and *f* with magnification of x500).

The observation of the transversal cuts (figure 5.20) showed that the addition of these compatibilisers is not enough to avoid the pullout of the LCP fibrils from the matrix that usually occurs during the cryogenic fracture and is due to the lack of adhesion between the dispersed and the continuous phases. In this case, there were no significant differences between the different blends and, therefore, a similar behaviour for the impact properties is to be expected.

In conclusion, the addition of 2 wt % compatibiliser to the blend with 10 wt % LCP leads to an enhancement of the fibrillar formation in the extrusion direction and to an improvement of fibril dispersion.

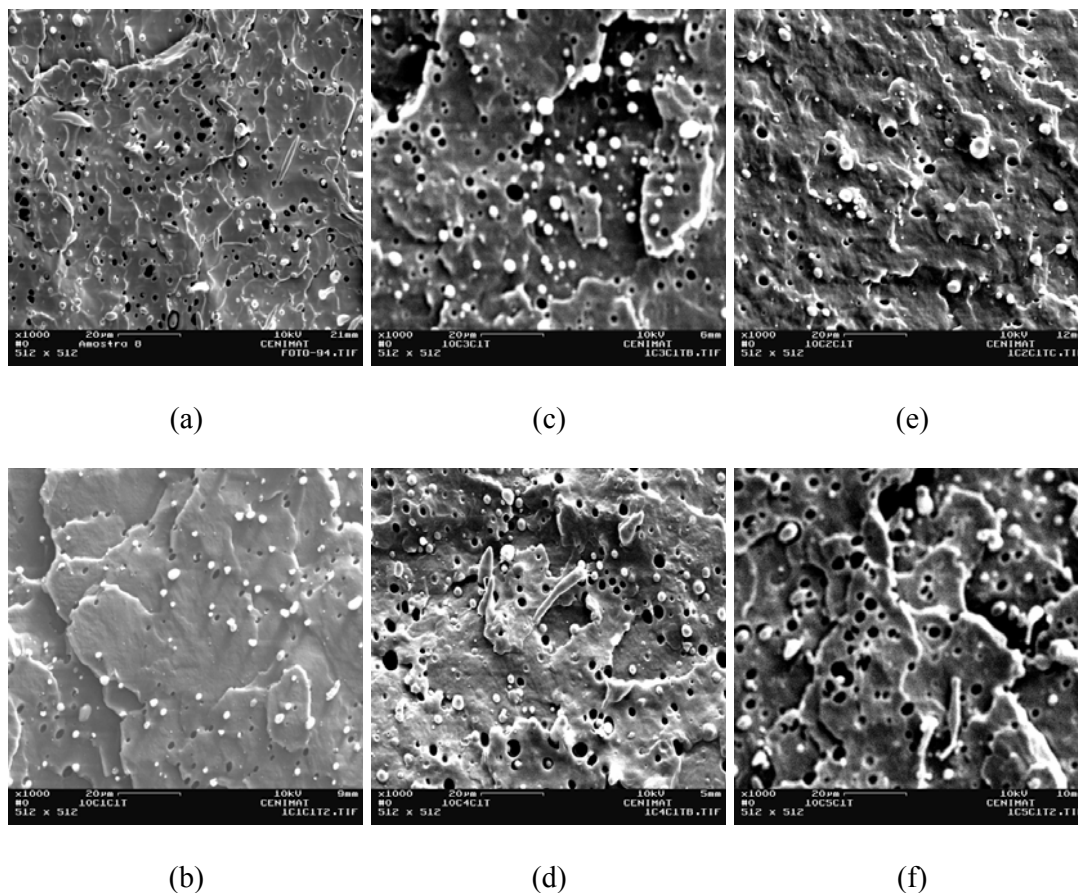


Figure 5.20 - SEM images for the transversal cuts performed to the final extrudates of blends with 10 wt % LCP - (a) without compatibiliser; (b) with compatibiliser A; (c) with compatibiliser B; (d) with compatibiliser C; (e) with compatibiliser D; (f) with compatibiliser E (magnification of x1000 for all the figures).

RHEOLOGICAL PROPERTIES

The rheological measurements performed in oscillatory shear revealed that there are no significant differences between the different compatibilised blends, as can be seen in figures 5.21, 5.22 and 5.23, with the possible exception of the blend with compatibiliser E, which shows slightly higher complex viscosity and storage modulus than the remainder. These results are somewhat unexpected, especially for the non-compatibilised blend and that with compatibiliser A since these showed larger morphological differences. This is a clear indication that linear oscillatory shear is not sensitive enough to the changes in morphology induced by the presence of the compatibilisers.

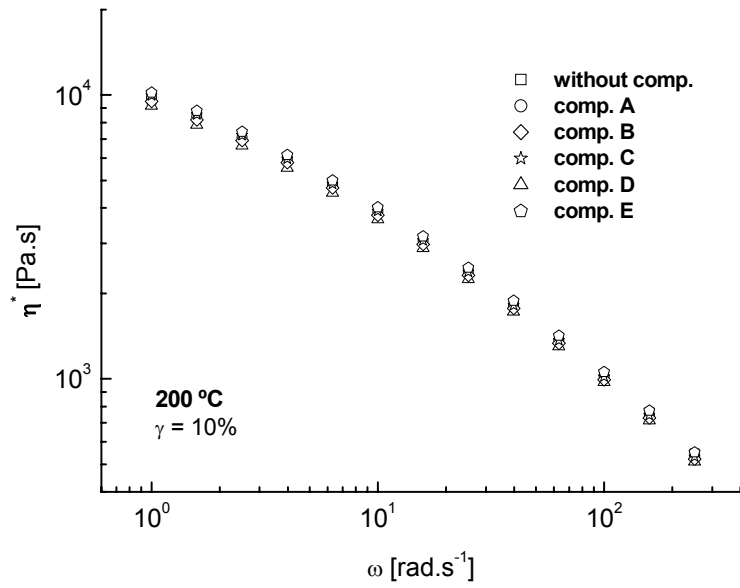


Figure 5.21 - Influence of the compatibiliser type on the complex viscosity of 10 wt % LCP blends at 200 °C, $\gamma_0 = 0.1$.

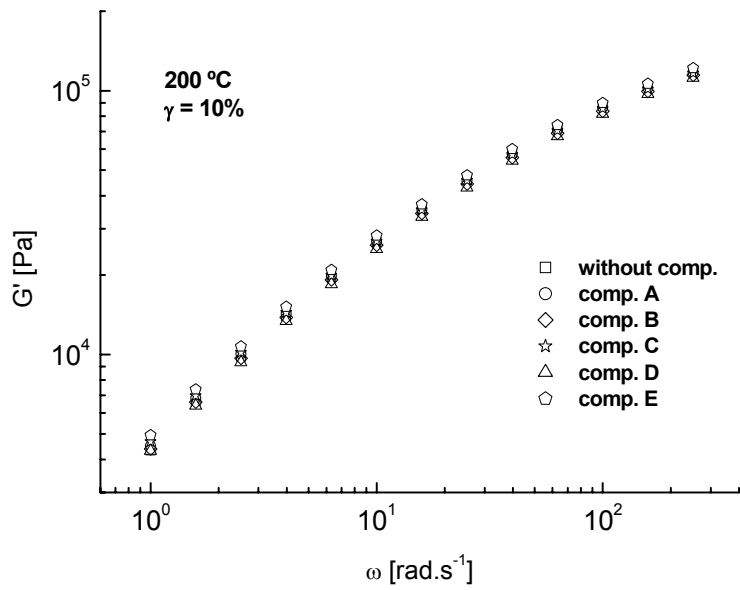


Figure 5.22 - Influence of the compatibiliser type on the storage modulus of 10 wt % LCP blends at 200 °C, $\gamma_0 = 0.1$.

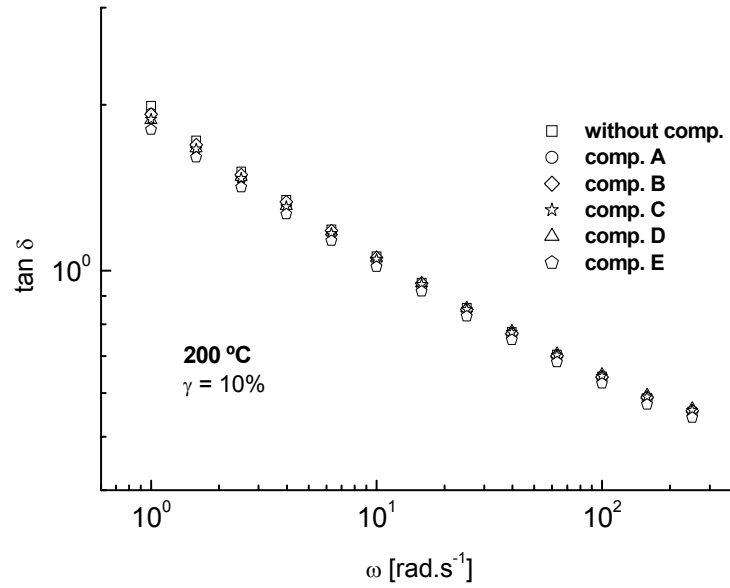


Figure 5.23 - Influence of the compatibiliser type on the loss tangent of 10 wt % LCP blends at 200 °C, $\gamma_0 = 0.1$.

In order to do so, one must resort to Large Amplitude Oscillatory Shear, LAOS, as shown in Figure 5.24.

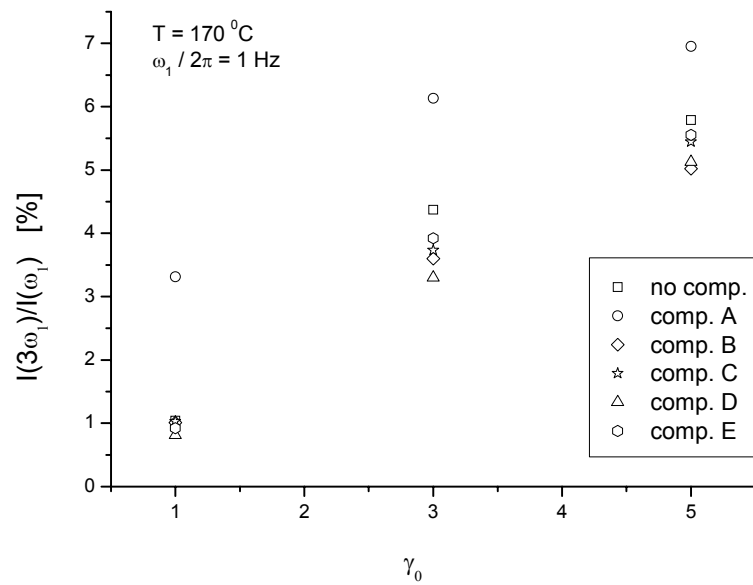


Figure 5.24 - Influence of the compatibiliser type on the evolution of $I(3\omega_1)/I(\omega_1)$ with applied strain at 170 °C.

By this technique it was possible to observe a decrease of the non-linear character of all the blends in which the compatibilisation was more effective (B, C, D and E) and an increase for the blend with compatibiliser A relatively to that of the non-compatibilised blend, as was expected from the observed differences in fibrillar structure. Thus, it seems that there is a relationship between the effectiveness of the compatibiliser, via the observed fibrillar structure, and the non-linear character, expressed by means of $I(3\omega_1)/I(\omega_1)$. Despite that, the use of FT rheology is not still sensitive enough to clearly distinguish between blends in which the compatibilisation was more successful (blends with comp. B, C, D and E). In order to do so, another technique is needed to evaluate distinct interfacial effects that arise from the addition of different compatibilisers.

Considering this need, transient shear measurements were performed at a shear rate of 1 s^{-1} during 600 s and after application of pre-shear of 0.3 s^{-1} for 600 s. The evolution of the transient stress as a function of the strain for the blends with compatibilisers A to E and also for the non-compatibilised blend is presented in figure 5.25.

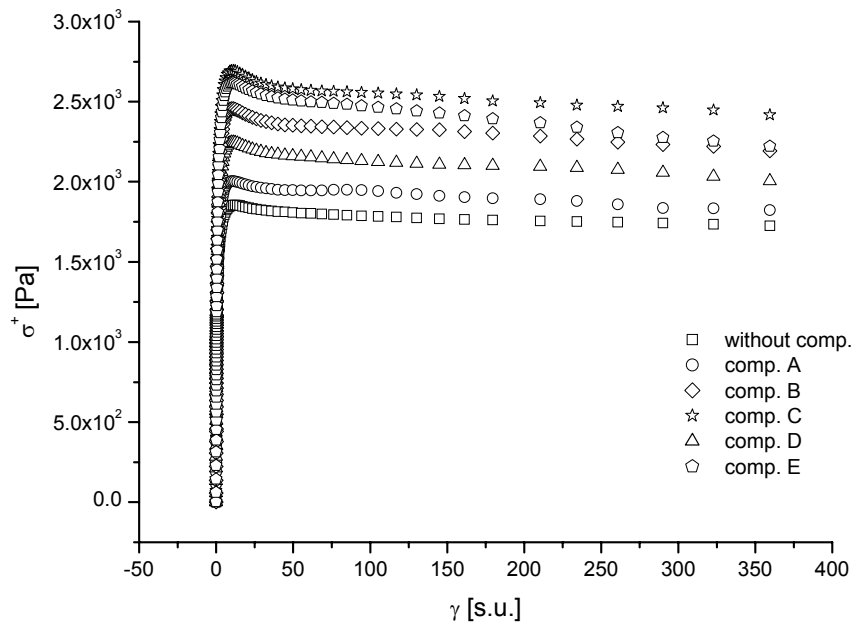


Figure 5.25 - Transient Stress (σ^+) for 10 wt % LCP blends with and without compatibiliser (Start-up at 1 s^{-1} , $T = 200 \text{ }^\circ\text{C}$).

The addition of the compatibiliser leads in all the cases (for a similar strain of 11.1 strain units) to an increase of the transient stress, which is probably related to the interfacial modifications that occur by the addition of the compatibiliser. The overshoot here described is usually observed in liquid crystalline polymer and thermoplastic blends and is associated to the rotation of the director of the LCP into the flow direction (see subchapter 4.2). The magnitude of this overshoot is different according to the compatibiliser used, being higher for the blends with compatibiliser C and E and lower for the non-compatibilised blend and that with compatibiliser A. After a strain of 11.1 strain units a decay of the transient stress is observed for all the blends, until plateau values are reached.

Thus, the indications are that while LAOS experiments are essentially sensitive to the fibrillar structure, transient measurements are more so to interfacial interactions between the two phases.

In the transient first normal stress difference, N_1^+ , despite a larger experimental scatter, differences for the different compatibilised blends were also observed (see figure 5.26).

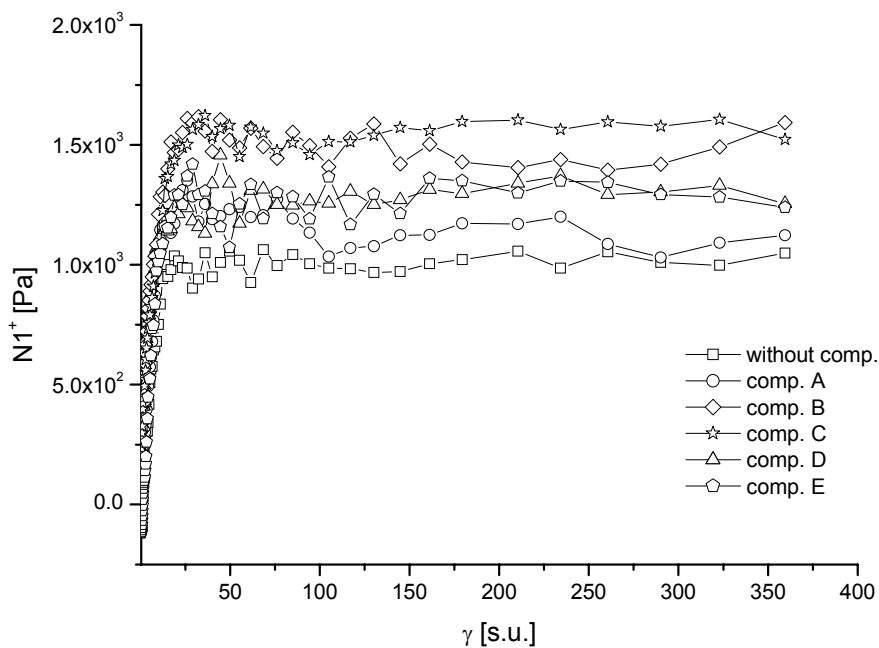


Figure 5.26 - Transient First Normal Stress Difference (N_1^+) for 10 wt % LCP blends with and without compatibiliser (Start-up at 1 s^{-1} , $T = 200 \text{ }^\circ\text{C}$).

Similarly to the transient stress, an increase of the transient first normal stress difference was observed for the compatibilised blends, which must be once more attributed to changes in the interfacial tension between the LCP and thermoplastic. For the higher strains, the highest values of N_1^+ were observed for the blend with compatibiliser C. Despite this, these differences were not as pronounced as those observed for the transient stress. For example, the blends with compatibiliser C and B show very similar values of N_1^+ for low strains. It should be pointed out, however, that the chemical structure of these two compatibilisers is quite similar, the most important difference being the length of the aliphatic chain that is longer in

compatibiliser B. Additionally, it can be stated that compatibilisers D and E (with the same maleic anhydride content) present a similar behaviour for the evolution of N_1^+ with the strain.

Contrary to what happened with the Lazkano *et al.* work [Lazkano 2002], no shear stress undershoot was observed. However, the blends under study possess a much lower LCP content (10 wt %) when compared with 30 wt % LCP of their blends. This means that in this case the droplets must be comparatively smaller, which may prevent the appearance of the shear stress undershoot.

As previously mentioned the effectiveness of the mechanical enhancement in liquid crystalline polymer and thermoplastic systems often requires the addition of compatibilisers, as reported by Datta and Baird, Miller *et al.* and Bualek Limcharoen *et al.*, among others [Datta 1995, Miller 1995, Bualek-Limcharoen 1999].

It is important to analyse properly the influence of the addition of different compatibilisers on the behaviour under extensional flow, since this is the one with the highest importance (when compared with shear flow) on the formation of the LCP fibrils during processing.

For this reason, the transient uniaxial extensional viscosity was measured for the different compatibilised blends (figures 5.27 to 5.31) and compared with the non-compatibilised blend containing the same LCP content (figure 5.32 and figure 5.33).

The results obtained showed that all the compatibilised blends present a strain hardening behaviour, for the lower and for the higher strain rates, as seen in figures 5.27 to 5.31.

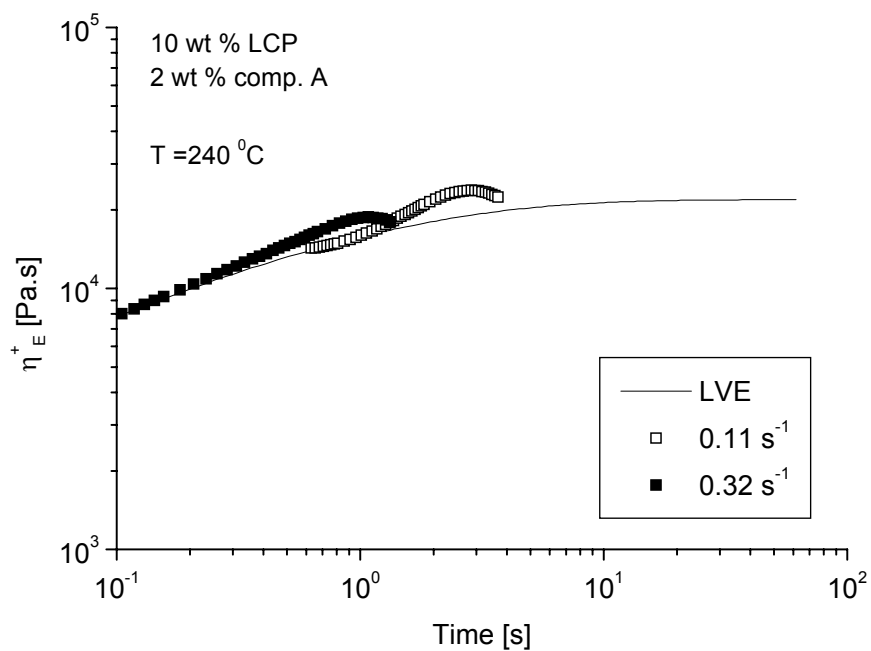


Figure 5.27 - Transient uniaxial extensional viscosity at 240 °C for compatibilised blend with 10 wt % LCP and 2 wt % compatibiliser A.

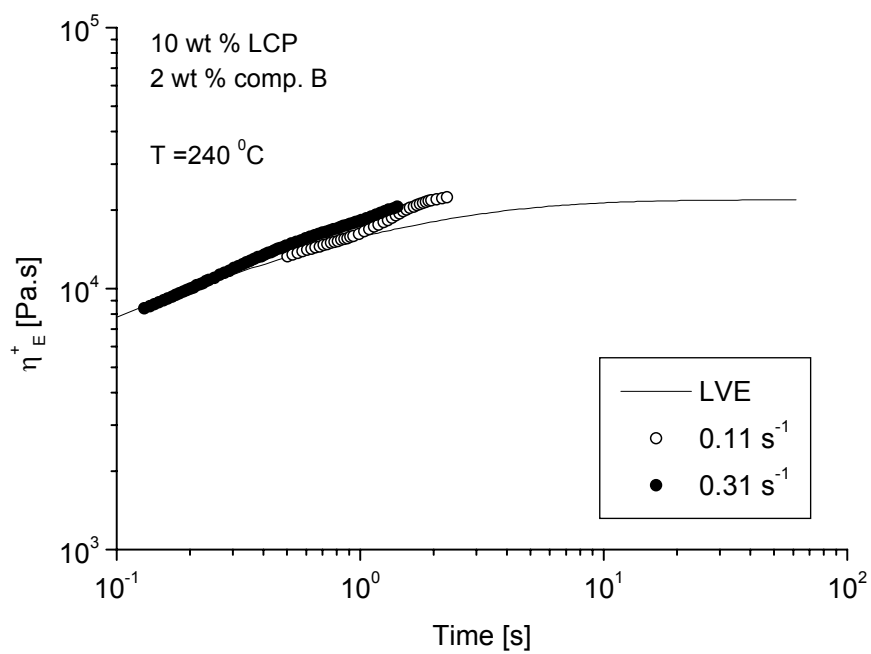


Figure 5.28 - Transient uniaxial extensional viscosity at 240 °C for compatibilised blend with 10 wt % LCP and 2 wt % compatibiliser B.

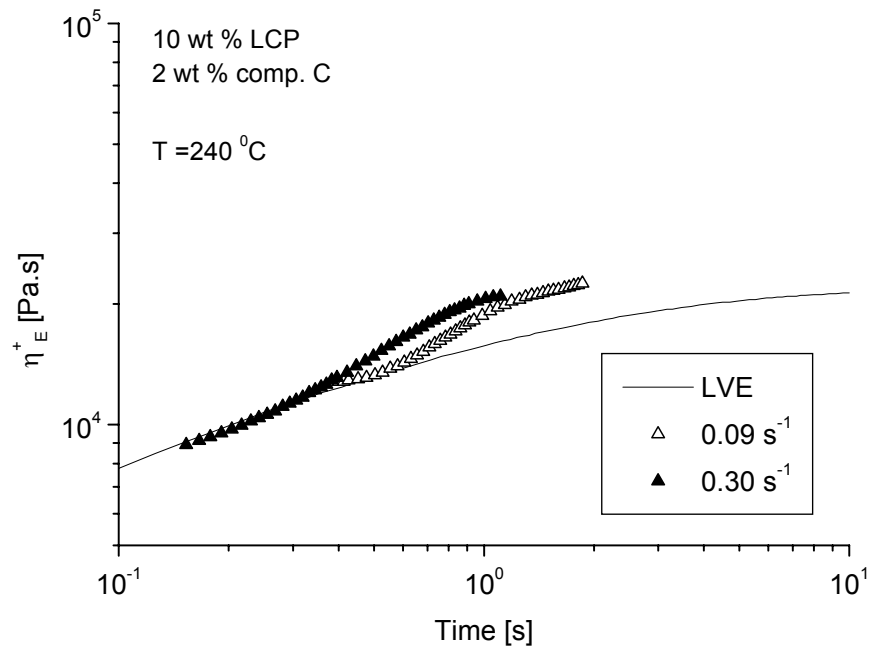


Figure 5.29 - Transient uniaxial extensional viscosity at 240 °C for compatibilised blend with 10 wt % LCP and 2 wt % compatibiliser C.

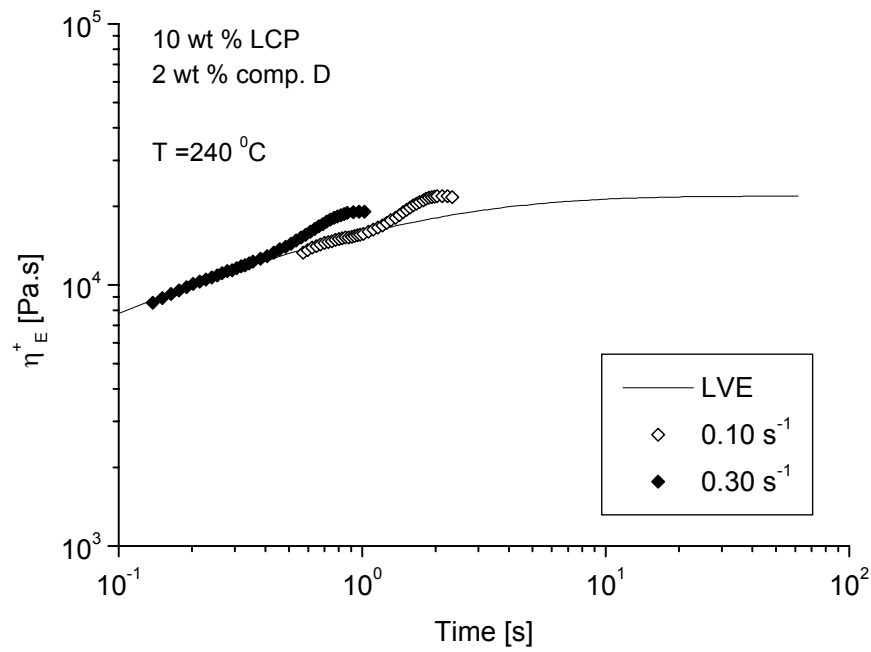


Figure 5.30 - Transient uniaxial extensional viscosity at 240 °C for compatibilised blend with 10 wt % LCP and 2 wt % compatibiliser D.

Comparing the compatibilised blends with the non-compatibilised blend, it can be stated that the addition of compatibiliser leads always to an increase of the deviation from the LVE, for all the strain rates studied (see figures 5.32 and 5.33).

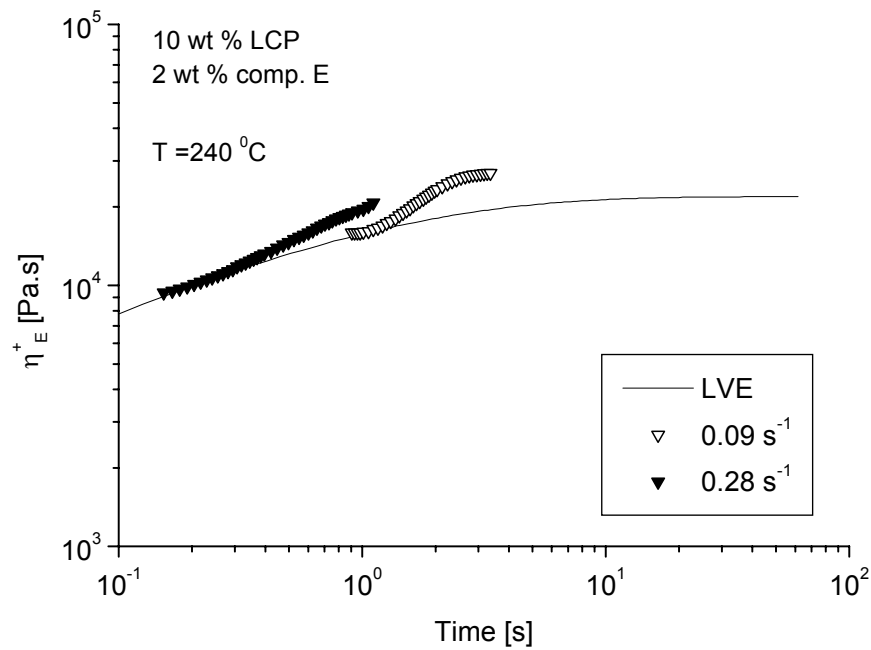


Figure 5.31 - Transient uniaxial extensional viscosity at 240 °C for compatibilised blend with 10 wt % LCP and 2 wt % compatibiliser E.

The distinction between the several blends is easier for the lower than for the higher strain rates, which was predictable, since these are in fact those conditions that are expected to be more sensitive to morphological differences. For the lower strain rates, it looks like the deviation from the LVE is related with the chemical structure of the compatibiliser used (see figure 5.32).

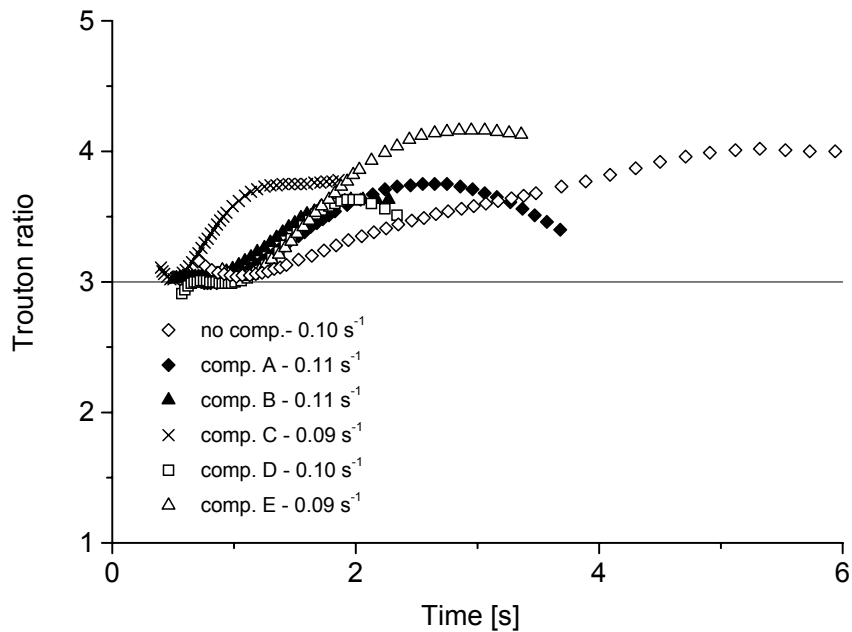


Figure 5.32 - Influence of the compatibiliser on the Trouton ratio of blends with 10 wt % LCP, at 240 °C (strain rates around 0.09-0.11 s⁻¹).

Considering the blends with commercial compatibilisers (compatibiliser D and compatibiliser E) it is possible to state that the addition of an ethylene-propylene grafted with anhydride maleic (comp. E), which possess an elastomeric nature, leads to a higher Trouton ratio (around 4.2) than that of the blend with compatibiliser D (which is a polypropylene grafted with similar amount of anhydride maleic, but with a thermoplastic nature). This is in accordance with the results obtained in steady and oscillatory shear, previously shown.

In the case of the blends in which synthesised compatibilisers were used (comp. A, B and C), no significant differences can be made between the blends with compatibiliser A and B (for the lower times, the Trouton ratio is slightly higher for the blend with compatibiliser B than for the one with compatibiliser A). For the lower times (lower than 2 s), the Trouton ratio of the blend with compatibiliser C is higher than that of blends with compatibiliser A and B.

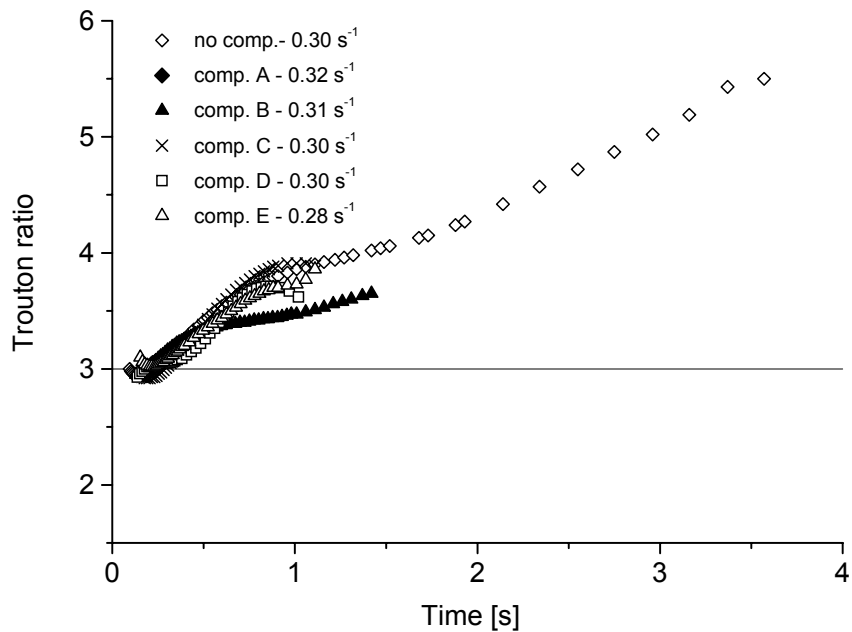


Figure 5.33 - Influence of the compatibiliser on the Trouton ratio of blends with 10 wt % LCP, at 240 °C (strain rates around 0. 28-0.32 s⁻¹).

As already stated, no clear distinction can be made between the different compatibilised blends (A to E), when higher strain rates are applied, as seen in figure 5.33.

Quite surprisingly, it was not possible to establish correlations between the transient uniaxial extensional flow behaviour and the mechanical properties, namely the Young's modulus (see below).

Interestingly, in all the cases, the durability of the compatibilised blends is smaller than that of the non-compatibilised one, which can be explained by the increased interactions between the two phases that prevents the PP from continuing its extension.

MECHANICAL PROPERTIES

In order to understand the influence of the addition of different compatibilisers on the mechanical properties of liquid crystalline polymer and thermoplastic blends, five blends with

10 wt % LCP and 2 wt % compatibiliser A to E were produced by extrusion followed by injection moulding (preparation of the specimens). Specimens of these blends were tested and compared with injection-moulded specimens of blends with the same LCP content, without compatibiliser.

The tensile measurements revealed an improvement of the tensile properties for all the compatibilised blends when compared with the non-compatibilised one, as shown in figure 5.34, with the exception of the blend with compatibiliser A. In this case, it must be assumed that there is no influence, since the experimental error is larger than the observed differences in average Young's modulus. The reason for this behaviour is probably related to the fact that compatibiliser A is highly compatible with one of the components of the blend (matrix) and tends to act as a plasticizer. For the blend with compatibiliser B an improvement of 15 % for the Young's modulus was obtained, which can be explained by its chemical structure. The LCP is a copolymer of PET with HBA and, thus, PET present in compatibiliser B is expected to be more compatible with it than the oligomeric polyester (TerolTM) used in compatibiliser A.

Analysing the tensile properties shown for the blend with compatibiliser C, it can be concluded that this polymer is the more suitable among all the compatibilisers with a thermoplastic nature (from A to D) for the compatibilisation of PP and Rodrun LC3000. The Young's modulus increased 27 % against no increase, 15 % and 17 % obtained for compatibilisers A, B and D, respectively. It must be noted that compatibiliser B differs from compatibiliser C in the length of the aliphatic chain, that is much higher for compatibiliser B (C50) than for compatibiliser C (C20). Therefore, the reduction of the interfacial tension that is usually responsible by an increase of the tensile strength is not only dependent on the functional groups of the compatibiliser, but also on the length of the aliphatic chain. In the present case, it seems that the longer alkyl chains in compatibiliser B, cause a decrease in the

electronic interactions at the interface due to the increase in the free volume. As far as the compatibiliser with an elastomeric nature is concerned, the results are similar to those of compatibiliser D.

Compatibiliser C was the only one that presented a Young's modulus with a positive deviation from the rule of mixtures (see figure 5.34).

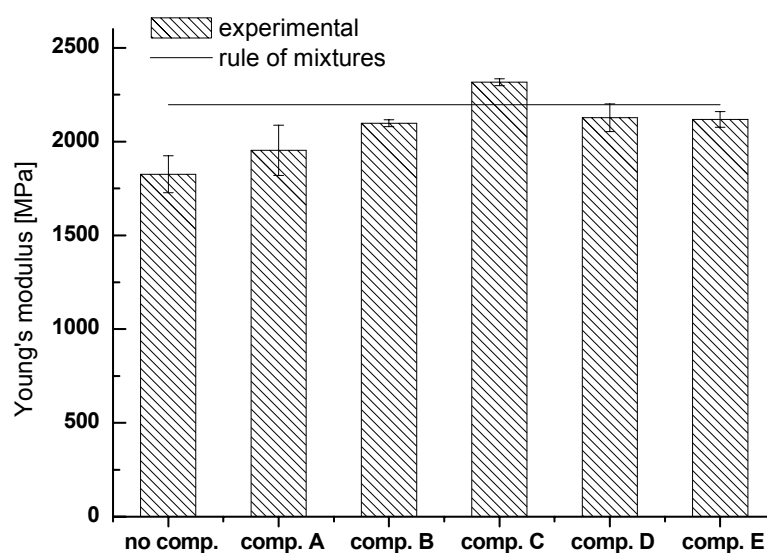


Figure 5.34 - Effect of the compatibiliser type on the Young's modulus for blends 10 wt % LCP.

Contrary to what was verified in the work of Datta and Baird [Datta 1995], the addition of PP grafted with anhydride maleic (compatibiliser D) did not show a positive deviation from the rule of mixtures (the value presented was 3.3 % smaller than the one expected). In their work, however, they used a higher LCP content (20, 50 and 80 wt %) and observed that the improvement of the mechanical properties obtained by the addition of PP grafted with anhydride maleic is higher for blends with higher LCP content [Datta 1995]. The processing conditions used for the preparation of their blends were also quite different from those used in this work. Additionally, the amount of polypropylene grafted with maleic

anhydride (MA-g-PP) used in their study was 10 wt % (with respect to the polypropylene matrix) while in our case was only 2 wt %. All these facts may be the explanation for the different results obtained in this work, comparing with those obtained by Datta and Baird [Datta 1995].

In terms of elongation at break, on the other hand, the elastomeric nature of the EP-g-MA compatibiliser (E) allows a significant increase of the elongation at break relatively to the blends with compatibilisers having a thermoplastic nature (A to D), as would be expected. In fact, the elongation at break obtained for the blend compatibilised with EP-g-MA (165 %) was closer to that of the non-compatibilised blend (192 %) than those obtained for the blends with compatibilisers A, B, C and D (77, 46, 30 and 88 %, respectively), as can be observed in figure 5.35.

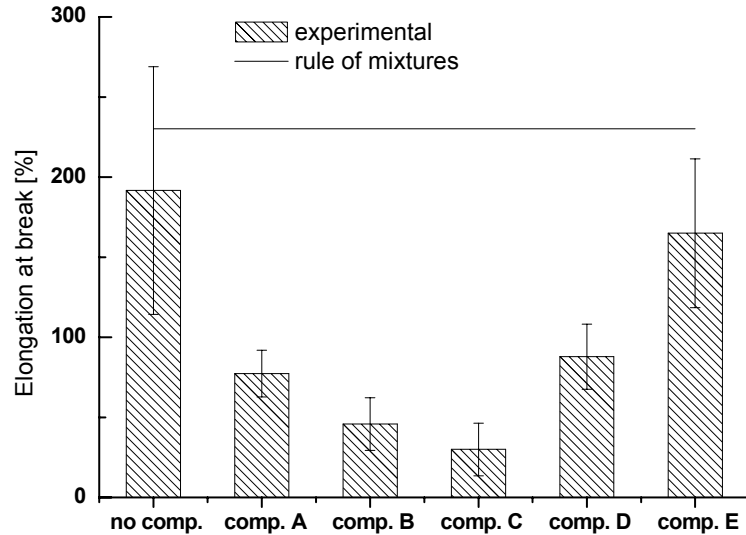


Figure 5.35 - Effect of the compatibiliser type on the elongation at break for blends with 10 wt % LCP.

In terms of the impact measurements, the energy absorption during the impact load is usually higher for blends with compatibilisers with an elastomeric nature, as shown in figure 5.36.

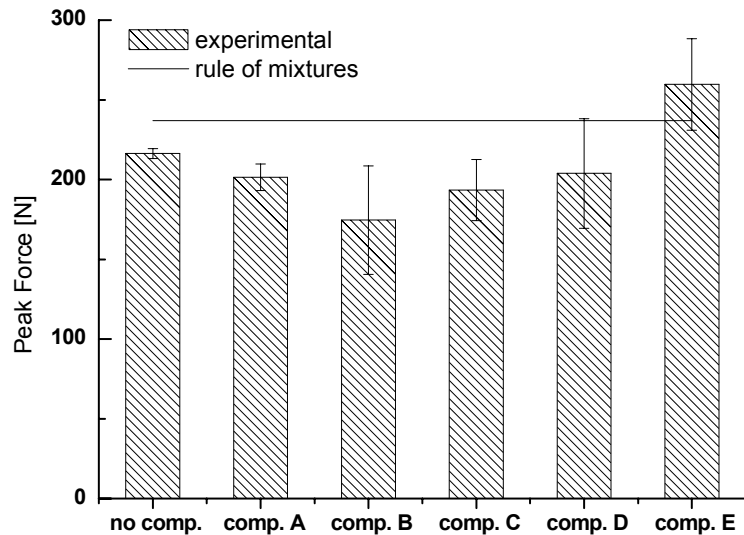


Figure 5.36 - Effect of the compatibiliser type on the impact force for blends with 10 wt % LCP.

The highest impact strength was obtained for the blend with compatibiliser E (in fact, this was the only blend for which an improvement of the impact strength was obtained, within experimental error, relatively to that observed for the non-compatibilised blend). The peak force presented by the blend with compatibiliser E is above the predicted by the rule of mixtures, and in line with the findings of Bualek-Limcharoen *et al.* for composite films containing PP and Rodrun LC3000 [Bualek-Limcharoen 1999]. In fact, EP-g-MA acts as impact modifier for the liquid crystalline polymer and thermoplastic blend, improving the impact strength.

As expected, the values of the flexural modulus in the direction longitudinal to the flow were higher than those in the transversal direction, as is shown in figure 5.37, since the fibrils formed during injection moulding are oriented in the direction of the flow. This behaviour was verified for all the blends with and without compatibiliser. The only relatively

unexpected finding is that the blend with the elastomeric compatibiliser (E) did not show a significant increase in flexural modulus relatively to the others, as would be expected from its nature and the peak force results.

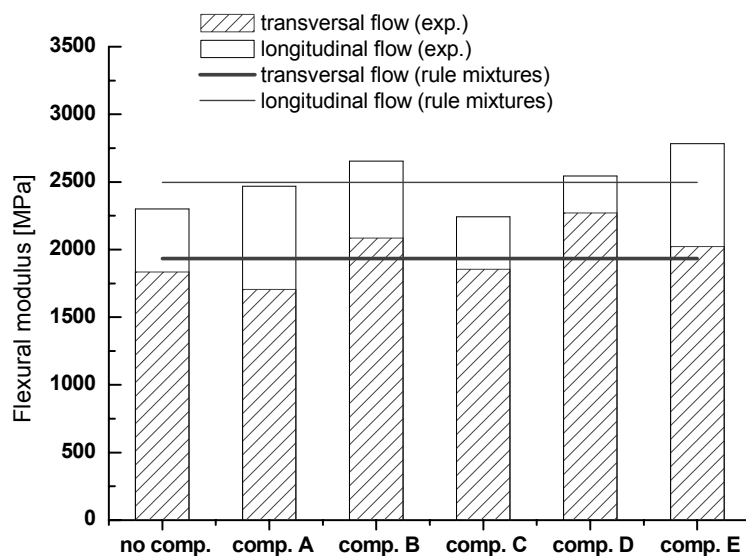


Figure 5.37 - Effect of the compatibiliser type on the flexural modulus for blends with 10 wt % LCP.

CONCLUSIONS

During the last few years, significant attention was focused on the mechanical improvement of LCP/TP blends by the addition of compatibilisers. However, the compatibilisation often results in the improvement of tensile modulus at the expense of tensile elongation and toughness. In line with this need, five different compatibilisers, differing in terms of chemical structure and nature were used in order to obtain the best mechanical enhancement in both strength and toughness.

The results of the present work indicate that if this is to be accomplished, then compatibilisers with an elastomeric nature must be used. For example, in our case, this compatibiliser was the only one that was able to yield an improvement in both tensile modulus and impact resistance, which can be attributed to the increase in energy absorption during

impact, when compared with the other blends where compatibilisers with a thermoplastic nature were used, without a significant decrease in elongation at break. This result is essential for applications where both high tensile strength and high elongation at break are needed. Thus, the blend compatibilised with EP-g-MA (compatibiliser E) is the one that can be used for a wider range of applications. However, for applications where the tensile strength is the determinant factor (like in cables, for instance), compatibiliser C is the one that leads to better properties, due to the higher values of tensile modulus.

In terms of the morphology/rheology/properties relationships, the indications are that LAOS experiments are mostly sensitive to the existence (or otherwise) of the desired fibrillar structure present under processing, while transient measurements are more so to interfacial interactions between the two phases. The results also seem to indicate that transient shear stress growth is the type of rheological experiment that correlates better with final blend properties, since the blends that show better mechanical properties are also those that show higher initial stress overshoots and equilibrium values.

References

- [Boersma 1999] A. Boersma and J. Van Turnhout *Polym.* **40**, 5023 (1999)
- [Bordereau 1992] V. Bordereau, Z. H. Shi, L.A. Utracki, P. Sammut and M. Carrega *Polym. Eng. Sci.* **32**, 1846 (1992)
- [Brostow 1996] W. Brostow, T. Sterzynski and S. Triouleyre *Polym.* **37**, 1561 (1996)
- [Bualek-Limcharoen 1999] S. Bualek-Limcharoen, J. Samran and T. Amornsakchai, W. Meesiri *Polym. Eng. Sci.* **39**, 312 (1999)
- [Datta 1995] A. Datta and D. G. Baird *Polym.* **36**, 505 (1995)
- [Filipe 2004a] S. Filipe, M. T. Cidade, M. Wilhelm and J M. Maia *Polym.* **45**, 2367 (2004)
- [Filipe 2004b] S. Filipe, J. M. Maia and M. T. Cidade *Adv. Mat. Forum* **456**, 476 (2004)
- [Filipe 2004d] S. Filipe, J. M. Maia, A. Duarte, C. R. Leal and M. T. Cidade, *J. Appl. Polym. Sci.*, submitted (June 2004)

- [Guerrica-Echevarria 2000] G. Guerrica-Echevarria, J. I. Eguiazabal, J. Nazabal *Polym. Comp.* **21**, 864-871 (2000)
- [Lee 2003] M. W. Lee, X. Hu, C. Y. Yue, L. Li and K. C. Tam *Comp. Sci. Tech.* **63**, 339 (2003)
- [Liang 2002] Y. C. Liang and A. I. Isayev *Polym. Eng. Sci.* **42**, 994-(2002)
- [Magagnini 1998] P. L. Magagnini, M. Pracella, L. I. Minkova, T. S. Miteva, D. Sek, J. Grobelny, F. P. La Mantia and R. Scaffaro *J. Appl. Polym. Sci.* **69**, 391 (1998)
- [Miller 1995] M. M. Miller, J. M. G. Cowie, J. G. Tait, D. L. Brydon and R. R. Mather *Polym.* **36**, 3107 (1995)
- [Miller 1997] M. M. Miller, J. M. G. Cowie, D. L. Brydon and R. R. Mather *Polym.* **38**, 1565 (1997)
- [O'Donnel 1995] H. G. O'Donnel and D. G. Baird *Polym.* **36**, 3113 (1995)
- [Potente 2000] H. Potente, M. Bastian, A. Gehring, M. Stephan and P. Potschke *J. Appl. Polym. Sci.* **76**, 708 (2000)
- [Tjong 2003] S. C. Tjong *Mat. Sci. Eng.* **R41**, 1 (2003)
- [Wanno 2000] B. Wanno, J. Samran and S. Bualek-Limcharoen *Rheol. Acta* **39**, 311 (2000)
- [Wilhelm 2002] M. Wilhelm *Macromol. Mat. Eng.* **287**, 83 (2002)
- [Wilhelm 1998] M. Wilhelm, D. Maring and H. W. Spiess *Rheol. Acta* **37**, 399 (1998)

6 OPTIMISATION OF LCP AND COMPATIBILISER CONTENTS ON COMPATIBILISED LIQUID CRYSTALLINE POLYMER AND THERMOPLASTIC BLENDS*

INTRODUCTION

In the present chapter attention will be devoted to the study of compatibilised blends containing different compatibiliser and LCP contents. In chapter 5 the best compatibilisers were determined, *i.e.*, those that provided the best mechanical enhancement, from a range of five different compatibilisers, differing in terms of their chemical structure. The main task of this part of the thesis is to evaluate for compatibiliser C and E (which were defined as the best compatibilisers) the optimum amount to be used as well as the combination LCP content and compatibiliser content that result in the optimum ratio mechanical performance/cost.

The great majority of the work concerning compatibilised and non-compatibilised LCP/TP blends is devoted to their final rheological, morphological and mechanical properties. In this chapter the study performed in the above mentioned studies will be extended to the evolution of the morphology and rheology along the extruder length (see sub-chapters 4.2 and 5.2).

Improved knowledge of the rheological behaviour under non-linear conditions is critical, since these are the dominant conditions during processing. Several studies were already performed in order to quantify the influence of the LCP content and type of compatibiliser, but none of these studies focused its attention on the non-linear properties [Kwon 1995, Tjong 1998, Tjong 1997, Kozlowski 1997, Limcharoen 1999, Zeng 2003, Choi 2002, Bafna 1995].

The study of the mixing processes and the evaluation of the effectiveness of the compatibilisation for LCP/TP blends were subject of study in previous works [Filipe 2004d-e,

* adapted from S. Filipe, J. M. Maia, C. R. Leal, M. T. Cidade, *Optimisation of Rodrun LC3000/PP compatibilised blends: Influence of the compatibiliser and LCP contents on the rheological, morphological and mechanical properties*, submitted to J. Polym. Eng. (November 2004)

Tjong 2003, Liang 2002, Wanno 2000, Mandal 2003, Farasoglou 2000, Sukananta 2003, Lee 2003 a-b]. Quite a few studies were focused on the evolution of the morphological and rheological properties of LCP/TP blends during the processing itself, but there is some similar work on other non-compatibilised immiscible blends, like PP/PA and PS/HPDE [Potente 2000, Bordereau 1992]. Improved knowledge about the phenomena that occur along the different stages of the extrusion process is a main task to control and predict the final properties. None of these requirements was accomplished by previous studies and thus, there is a need to explore these phenomena. Dielectric spectroscopy was used to study the evolution of the morphology during extrusion [Boersma 1999], but this study did not cover the influence of the LCP content or the influence of different compatibilisers and compatibiliser contents.

An additional objective of this part of the thesis, is to try to explain the obtained optimised compatibiliser contents, by evaluating the evolution of both rheological and morphological properties along the extruder length (for the two compatibilisers and different compatibiliser contents), and to correlate it with the effectiveness of compatibilisation and thus, with their mechanical performance. The first part of the work (optimisation of the compatibiliser content) was only performed for blends containing a lower LCP content (10 wt %), since these are those for which *a priori* a better mechanical performance/cost ratio is expected and, therefore, are those that will have more interest in industrial applications. In the second part of the work the optimised contents of both compatibilisers were used to study the influence of the LCP content on the morphological, rheological and mechanical properties of the extrudates obtained.

RESULTS

INFLUENCE OF THE COMPATIBILISER CONTENT

As is already known, in order to attain a better adhesion between the two components, and consequently a better mechanical performance, the use of LCP/TP blends requires the addition of compatibilisers. It is also recognized that, as much as their chemical nature, the amount of compatibiliser will markedly influence the final morphology and thus the final mechanical properties. The use of these materials must be however clearly understood, since for example, the application of a high amount of compatibiliser may be detrimental for the formation of the fibrillar structures that are behind the typical mechanical enhancement of LCP/TP blends [Datta 1995].

Due to the fact that the final morphology depends strongly on the way how the morphology evolves along the extruder length, it is of primary interest to attain an improved knowledge on this process. Basically, one might be able to optimise the final morphology (and thus the final mechanical properties) by monitoring (and controlling) the kinetic of mixture processes along the extruder length, *i.e.*, at the valves. One of the tasks of this work is thus to monitor the influence of the compatibiliser content on the morphological evolution along the extruder length.

Additionally, the attention was focused on the influence of the compatibiliser content on the morphological and rheological properties and their correlation with the mechanical properties for the final extrudates of compatibilised Rodrun LC3000/PP blends. The main aim of this analysis was to determine the optimum compatibiliser content for two different kinds of compatibilisation, with compatibiliser C (of a thermoplastic nature) and compatibiliser E (of an elastomeric nature).

MORPHOLOGICAL CHARACTERISATION

Extrudates

For compatibiliser C, the main feature worth noticing is the fact that the fibrillar structures that are formed have a very high aspect ratio and show a very homogeneous distribution along the matrix for 2 wt %, which becomes progressively less homogeneous and with shorter aspect ratios as the compatibiliser content is increased, as can be seen in figure 6.1 (extrudates). In fact, for 2 % compatibiliser, the droplet like-structures present in the beginning of the extruder, turn into fibrillar structures under the action of the extensional and shear forces which are developed in the extruder, whereas for the blends with higher compatibiliser content (4 and 8 wt %), several of them remain in a droplet-like structure, more or less elongated, even though others also evolve into fibrils which are thicker than the ones observed for the 2 wt % compatibiliser.

An important observation that must be made with respect to the final extrudates, is that of an increase in temperature with compatibiliser content (table 6.1). As already known, a higher temperature leads to a lower viscosity ratio, which is detrimental for the deformation and elongation of the LCP droplets and which, in fact, may lead to some intensification of the coalescence [Filipe 2004a]. This was already demonstrated in chapter 4.

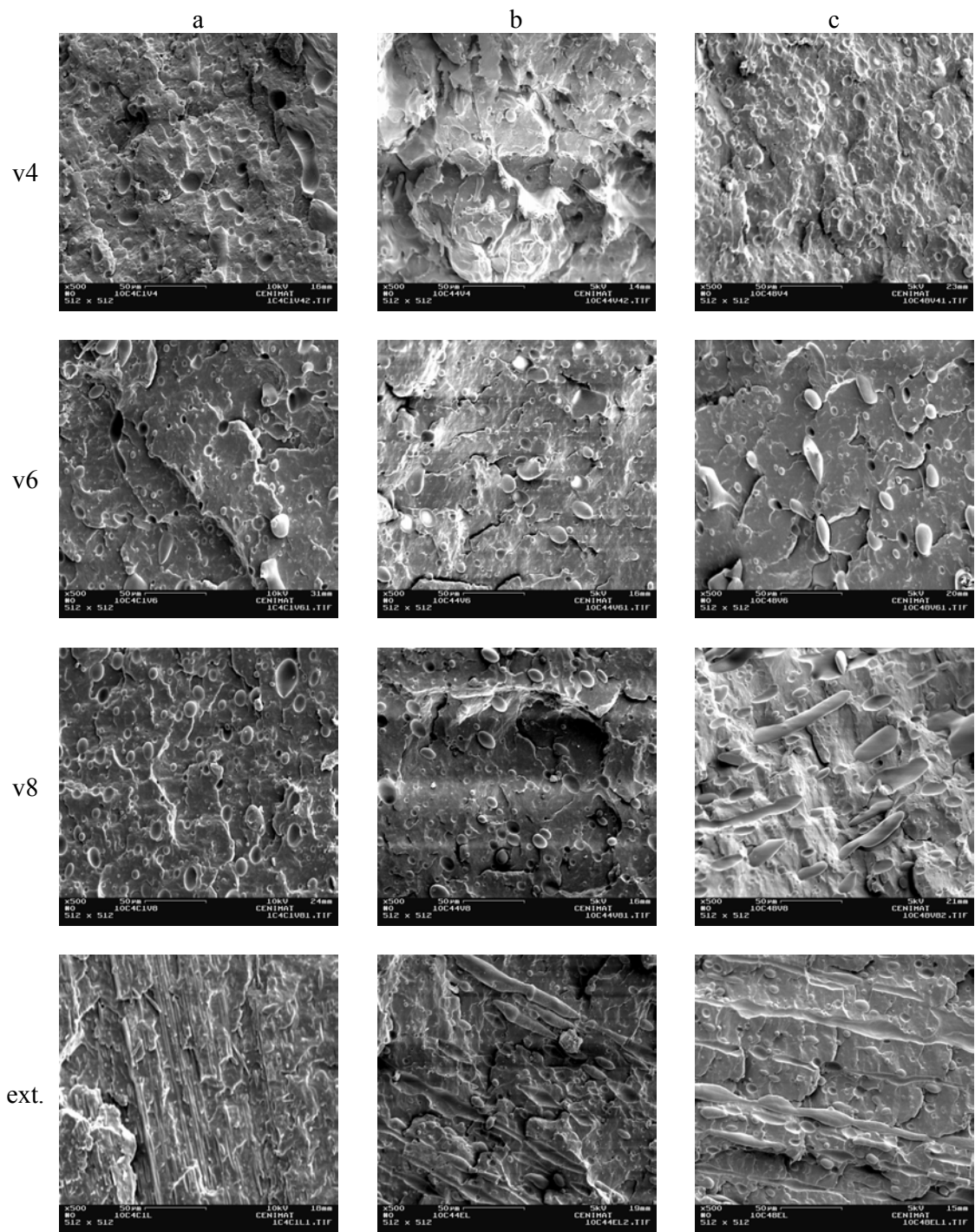


Figure 6.1 - SEM microphotographs for the blends with 10 wt % LCP and 2 (a), 4 (b) and 8 (c) % of compatibiliser C. Magnification of x500 for all the images.

Table 6.1-Temperature profiles along the extruder length for comp. C and comp. E-influence of compatibiliser content.

Blends		Position in the extruder			
		v4	v6	v8	extrudate
10 wt % LCP Compatibiliser C (wt %)	2	227.2	230.1	231.4	237.1
	4	230.1	231.2	236.7	239.2
	8	233.4	234.1	237.9	239.4
10 wt % LCP Compatibiliser E (wt %)	2	234.5	230.7	235.9	236.7
	4	230.1	231.8	236.3	237.2
	8	232.1	234.5	235.8	238.9

Considering the above findings and the fact that the lowest temperature at the die was found for the blend with the lowest compatibiliser content, it is not unexpected to find that the highest fibrillar formation and the best distribution were obtained for this blend (figure 6.1, extrudates). It is worthwhile to point out that temperature is the parameter that seems to control the degree of deformation at the valves (as will be seen later) and, also, the formation of fibrillar structures at the die.

Concerning the final extrudates of the blends with compatibiliser E, the increase in content from 2 to 4 wt % seems to improve the fibrillar morphology (figure 6.2, extrudates). Actually, while for the 2 wt % some elongated structures are still present, for the blend with 4 wt % compatibiliser only fibrils are observed. The increase of compatibiliser from 4 to 8 wt %, makes the distinction between the two phases more difficult with the number of fibrils *per* volume decreasing, even though the fibrils that remain seem to be thinner than the ones presented with the blends with lower compatibiliser content.

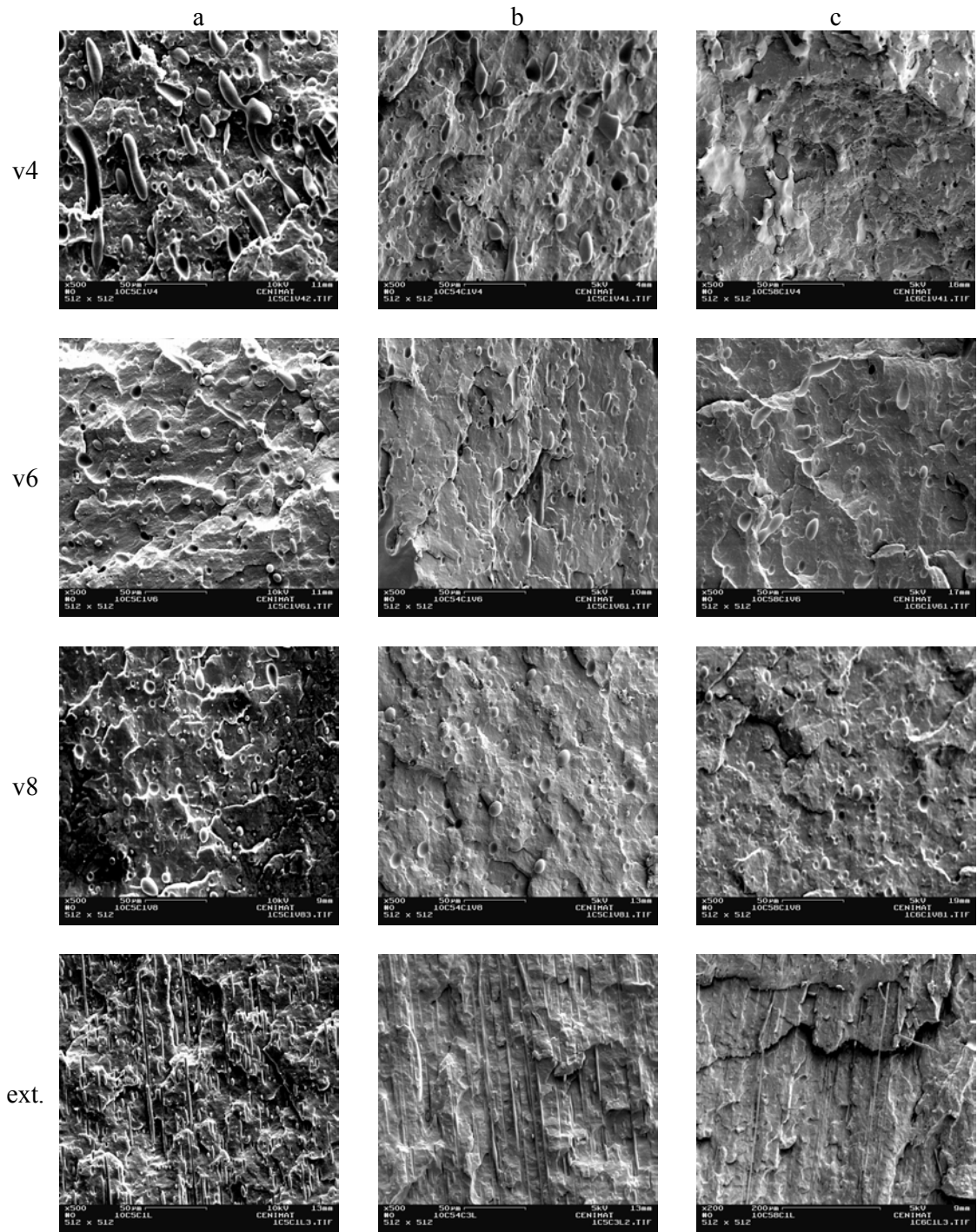


Figure 6.2 - SEM microphotographs for the blends with 10 wt % LCP and 2 (a), 4 (b) and 8 (c) % of compatibiliser E. Magnification of x500 for (a), (b) and (c) except for final extrudates of (c) (x200).

Evolution along the extruder length

In the study devoted to the evolution along the extruder length of non-compatibilised blends (chapter 5.2) a progressive elongation of the initial LCP droplet-like structures was observed from valve 4 to valve 6 and from this to valve 8, which was in accordance with a progressively decrease of the rheological parameters (η^* and G') from valve 4 to valve 8.

With the compatibilised blends such an evolution is not observed, at least for most of the compatibiliser contents studied. For all the blends with compatibiliser E and for those with 2 wt % and 4 wt % of compatibiliser C (see figures 6.1 and 6.2), the droplet-like structures observed at valve 4 seem to remain at valves 6 and 8, although their average size decreases slightly, as would be expected since the main role of the compatibiliser is to avoid the coalescence of the dispersed phase (the LCP), keeping the morphology as the material progress in the extruder.

It should be considered that the addition of compatibiliser leads to a clear decrease of the average droplet diameters, in comparison with those of non-compatibilised systems. In the presence of a suitable compatibiliser the break-up of the LCP droplets seems to occur at the beginning of the extrusion process, while for non-compatibilised systems (as well as blends in which the compatibilisation is not effective), it occurs in a more progressive way, *i.e.*, elongation and deformation, followed by break-up. In any of these cases (with or without compatibiliser), it is known that after a critical average diameter, these droplets can no longer be deformed (according to the Capillary number, the deformation and break-up is very difficult for droplets with low average diameters). In the presence of a suitable compatibiliser, the morphology formed (almost at the beginning of the process) is retained (as seen above), since the coalescence processes are prevented as the material progresses in the extruder length and only after the die these structures are converted into fibrils, as a result of the increased shear and elongational forces experienced at this point. This is in accordance with the behaviour

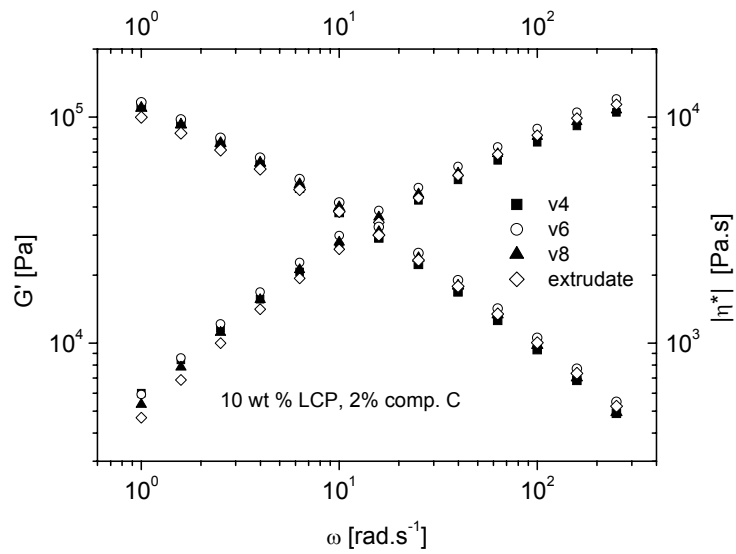
observed for the blend with 8 wt % compatibiliser (figure 6.1 (c)), for which a progressive elongation of the initial droplet-like structures along the extruder length occurred, in opposition with what happened for the lower compatibiliser contents.

RHEOLOGICAL CHARACTERISATION

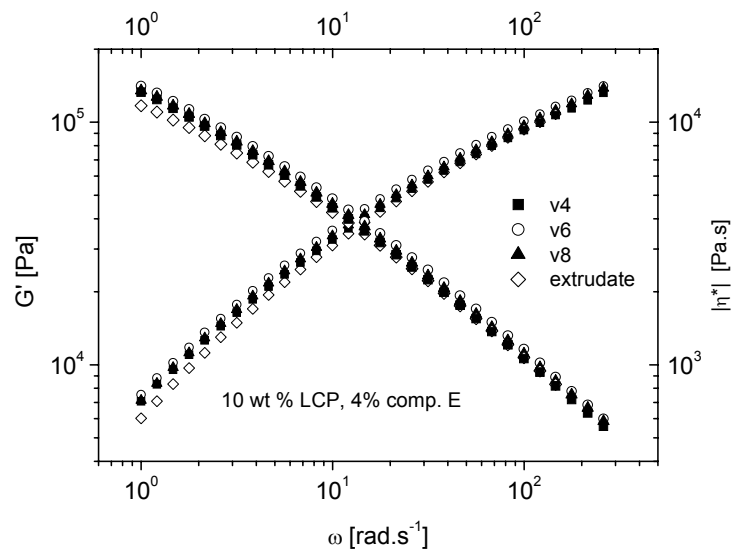
Linear regime

Surprisingly, the increase of the compatibiliser content does not have a significant effect on the linear viscoelastic behaviour of the blends (figure 6.3 (a) and 6.3 (b), which correspond to the blends with comp. C and comp. E, respectively). It seems, however, that, in general, the extrudates are the ones that present the lowest complex viscosity and storage modulus, for the lower and intermediate frequencies, followed by the values of valve 8. For the higher frequencies, even less significant differences can be observed between the samples collected in the valves and the extrudates.

Due to these facts, there is a clear need to perform other types of experiments that may replicate better the behaviour of the materials upon processing. For this purpose Large Amplitude Oscillatory Shear (LAOS) and Fourier Transform Rheology were used with considerable success in previous related works [Filipe 2004a, Filipe 2004e], as seen in chapter 4 and 5. Thus, this technique was also used in this part of the work.



a



b

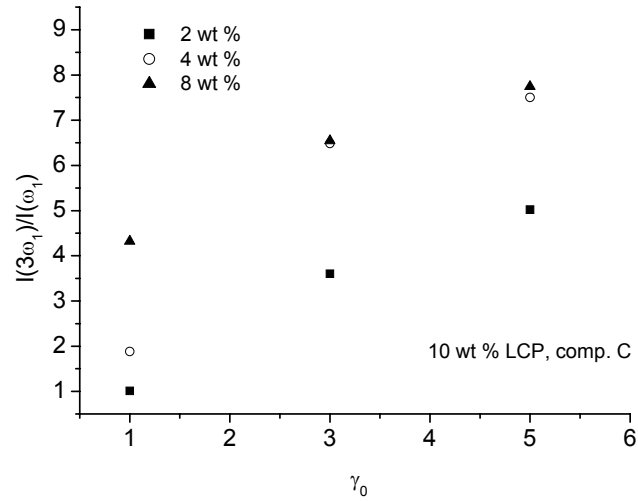
Figure 6.3 - Influence of compatibiliser content on the storage modulus and complex viscosity of blends with 10 wt % LCP for compatibiliser C (a) and E (b), $T = 200$ °C, $\gamma_0 = 0.1$.

Non-Linear regime

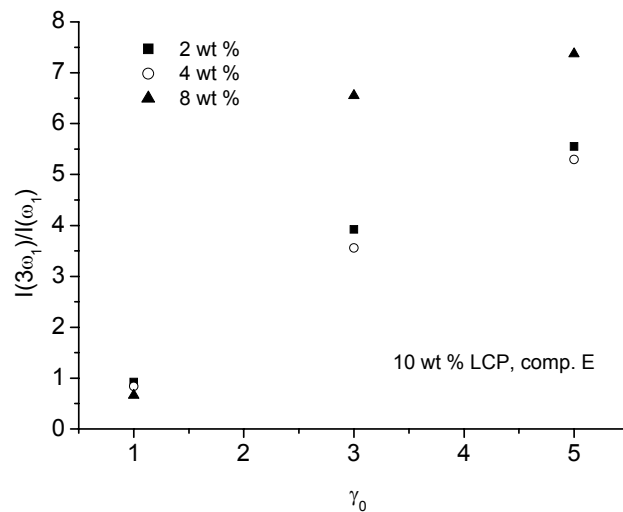
EXTRUDATES

Depending on the compatibiliser used, the increase of the compatibiliser content has different repercussions on the non-linear character, expressed by means of the normalised quantity $I(3\omega_1)/I(\omega_1)$: a) for the extrudates with compatibiliser C, an increase in $I(3\omega_1)/I(\omega_1)$ occurs with compatibiliser content (figure 6.4 (a)), while in the case of the extrudates with comp. E, one observed that the blend with 4 wt % comp. E is the one with the lowest non-linear character (figure 6.4 (b)) (with the exception for $\gamma_0 = 1$). Considering that the blends with 2 wt % comp. C and 4 wt % comp. E are those for which one has obtained the highest fibrillar formation and the highest Young's modulus (as will be seen later), it can be stated that the non-linear character seems to be related with the morphology presented and consequently with the mechanical performance.

Therefore, the relevance of the study of LCP/TP compatibilised systems by the use of LAOS is confirmed; this technique is very important to understand the behaviour of these blends under non-linear conditions, being much more sensitive to different morphologies and mechanical properties than other techniques (like oscillatory shear under linear conditions or steady shear).



a

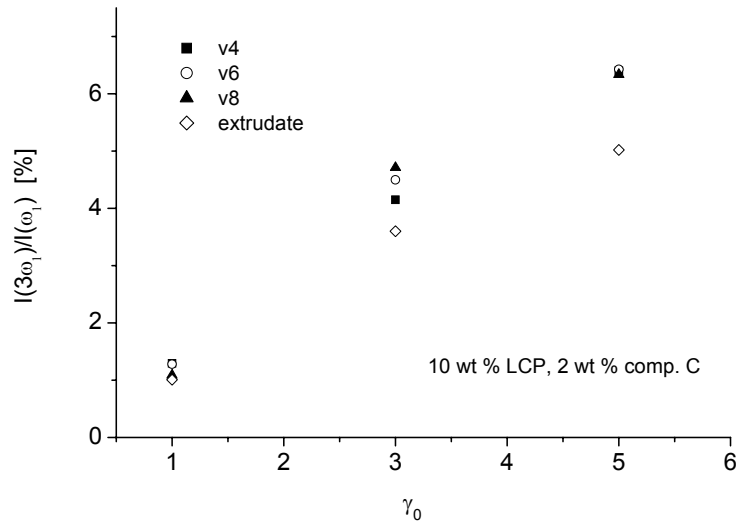


b

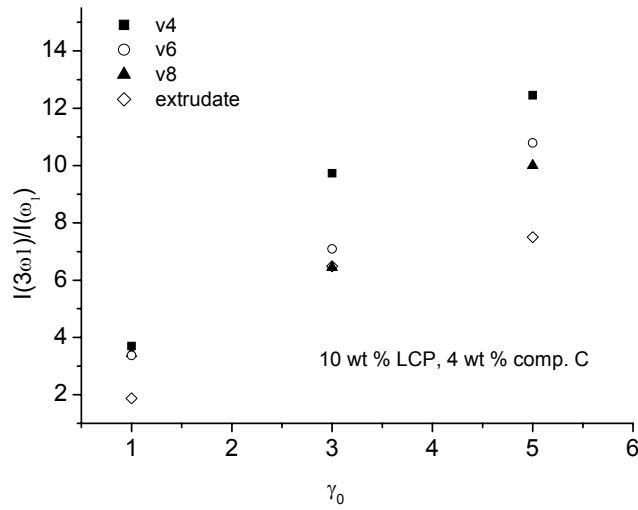
Figure 6.4 - Influence of compatibiliser content on the non-linear character for blends with 10 wt % LCP, compatibilisers C (a) and E (b) at $T=170\text{ }^\circ\text{C}$, $\omega_1/2\pi = 1\text{ Hz}$.

EVOLUTION ALONG THE EXTRUDER

The analysis of these results will be performed essentially in terms of the difference between the non-linear character in the beginning of the process (samples collected in valve 4) and at the end, after the die (the extrudates).



a



b

Figure 6.5 (a, b) - Evolution of the non-linear character along extruder length for the blend with 10 wt % LCP and with 2, a) and 4 b) compatibiliser C at $T=170\text{ }^\circ\text{C}$, $\omega_1/2\pi = 1\text{ Hz}$.

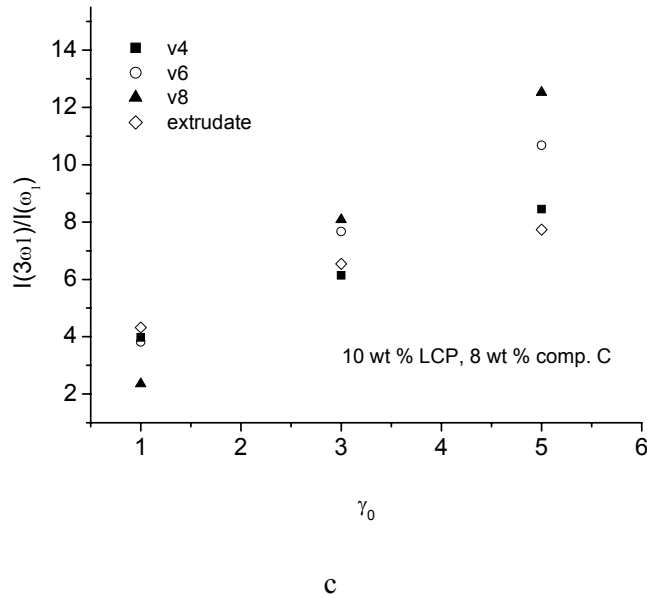
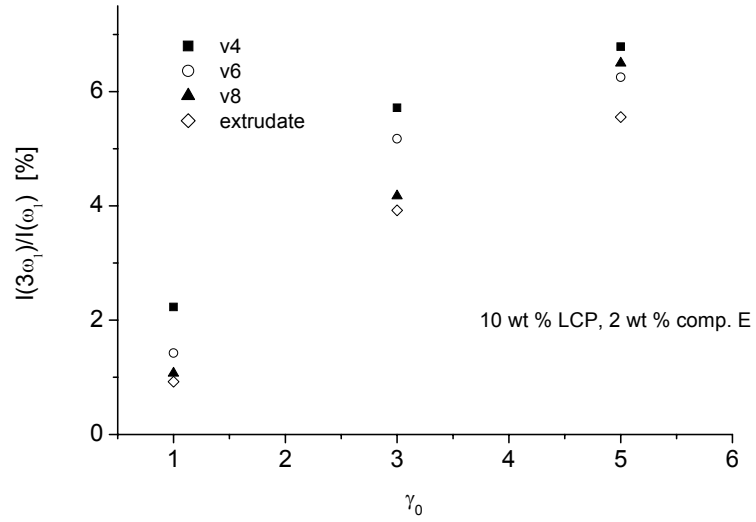


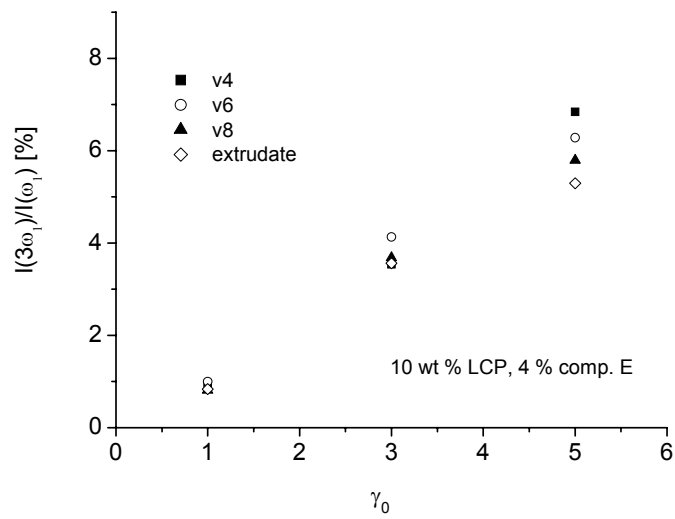
Figure 6.5 (c) - Evolution of the non-linear character along extruder length for the blend with 10 wt % LCP and with 8 wt %, c) compatibiliser C at $T=170\text{ }^\circ\text{C}$, $\omega_1/2\pi = 1\text{ Hz}$.

The main conclusions for compatibiliser C are (figure 6.5): (i) there is always an increase of the non-linear character with the increase of γ_0 , for all the samples; (ii) an increase in γ_0 always leads to an increase in the difference between the non-linear character for valve 4 and the extrudate; (iii) the extrudates always present the lowest non-linear character, relatively to the material inside the extruder.

For compatibiliser E (figure 6.6) it seems that it acts in a more effective way than compatibiliser C, making the distinction between the two pure components more difficult. However, the results are broadly in line with the latter since there is an increase of the non-linear character for all samples with an increase in γ_0 and, in general (the few exceptions may be due to experimental errors), the non-linear character is also always lower in the case of the extrudates.



a



b

Figure 6.6 (a,b) - Evolution of the non-linear character along extruder length for the blend with 10 wt % LCP and with 2, a), and 4, b) wt % compatibiliser E at $T=170\text{ }^\circ\text{C}$, $\omega_1/2\pi = 1\text{ Hz}$.

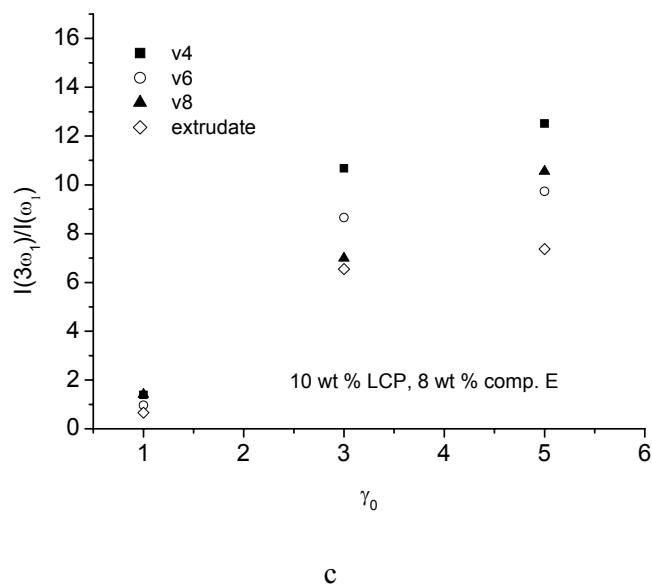


Figure 6.6 (c) - Evolution of the non-linear character along extruder length for the blend with 10 wt % LCP and with 8 wt %, c) compatibiliser E at $T=170$ °C, $\omega_1/2\pi = 1$ Hz.

Additionally, it should be pointed out that, for compatibiliser C, the blend in which compatibilisation was most effective (2 wt % compatibiliser) was the one for which one observed lower non-linear characters (for both valves and extrudates). In the case of the blends with compatibiliser E, similar observation can be made. The blend containing 8 wt % compatibiliser E (for which the compatibilisation was not effective) showed much higher non-linear character than the blend with 4 wt % compatibiliser. Considering that in some cases the morphology presented at the valves does not vary significantly according to the compatibiliser content, one may assume that the non-linear character is not only sensitive to different morphologies, but also to what happens at the interface, being thus its use essential to evaluate the compatibiliser activity.

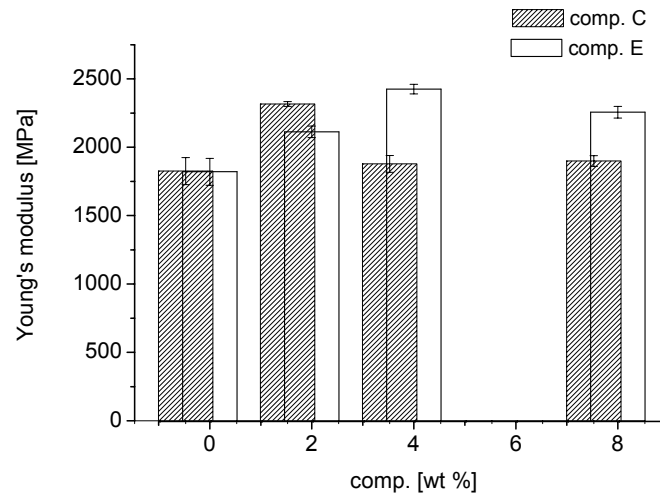
Therefore, it can be once more reaffirmed that LAOS is a much better technique to distinguish between different morphologies (comparing with the traditional oscillatory and steady shear measurements) and that is highly sensitive to the effectiveness of the

compatibiliser (the higher the efficiency of the compatibiliser, the lower the non-linear character at both valves and extrudates).

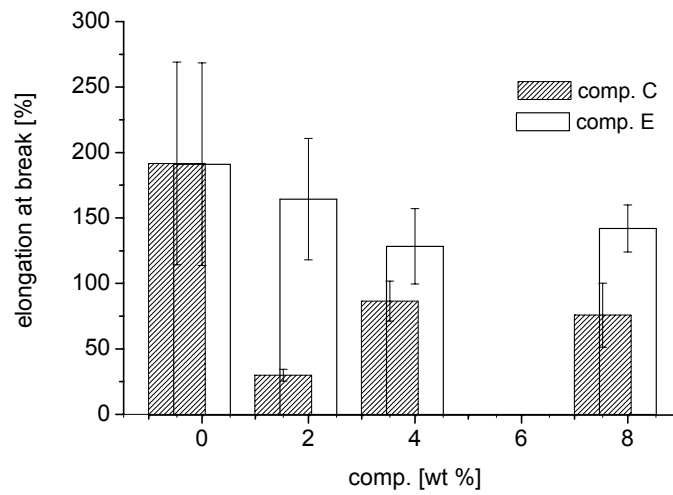
MECHANICAL CHARACTERISATION

For the blends with compatibiliser C, one can conclude that the increase of the compatibiliser content from 2 to 4 wt % leads to a pronounced decrease of the Young's modulus, as seen in figure 6.7(a), which certainly arises from a lower degree of fibrillation. Increasing the compatibiliser content from 4 to 8 wt % does not have a significant effect, the Young's modulus remaining almost the same for the two compositions.

On the other hand, for the blends containing compatibiliser E, the optimum compatibiliser content, *i.e.*, the one that yielded the highest Young's modulus, was obtained for the blend containing 4 wt % compatibiliser. This fact is in agreement with the results obtained in the morphological analysis, for which the maximum fibrillar formation was for this compatibiliser content (4 wt %). As expected, the improvement in terms of Young's modulus was gained at the expense of a decrease of elongation at break, as depicted in figure 6.7(b). Furthermore, it should be pointed out that the use of compatibiliser E leads to an increase of the Young's modulus relatively to that of the blend with compatibiliser C (when comparing the optimum content of each of the compatibilisers). It should be considered that this increase occurs with much lower decrease of the elongation at break than the one observed for comp. C (when comparing each of them with that of the pure matrix, that is around 247 %), which is basically due to its elastomeric nature. As expected, the use of both compatibilisers, C and E, always leads (independently of the compatibiliser content used) to an improvement of the Young's modulus with respect to the pure matrix (1704 MPa).



a



b

Figure 6.7 - Influence of compatibiliser content on the Young's Modulus (a) and elongation at break (b) of blends with compatibiliser C and E and with 10 wt % LCP.

Not surprisingly, the minimum at the elongation at break occurs with the content of compatibiliser that leads to the highest Young's modulus.

Influence of the LCP content

In this part of chapter 6, attention will be focused on the influence of the LCP content, for compatibilised blends containing 2wt % compatibiliser C and 4 wt % compatibiliser E, which were those for which the best mechanical properties were obtained. In fact, adding higher amounts of liquid crystalline polymer to a LCP/TP blend will presumably increase the number and dimensions of fibrils and, therefore, improve the mechanical properties of the material.

MORPHOLOGICAL CHARACTERISATION

Independently of the LCP content and compatibiliser used, it can be seen from the morphological analysis that the LCP structures have the form of highly oriented fibrillar structures after crossing the die, as can be seen on figures 6.8 and 6.9.

For the blends with compatibiliser C, a significant distinction in terms of density of fibrils, can be made between the blend with 10 wt % LCP and the blends containing 20 and 30 wt % LCP, as depicted in figure 6.8.

In the case of the blends containing compatibiliser E it can be noticed that fibrils and droplets are present for the lower LCP contents (10 and 20 wt %), whereas for the blend with 30 wt % LCP, only fibrils are observed (figure 6.9).

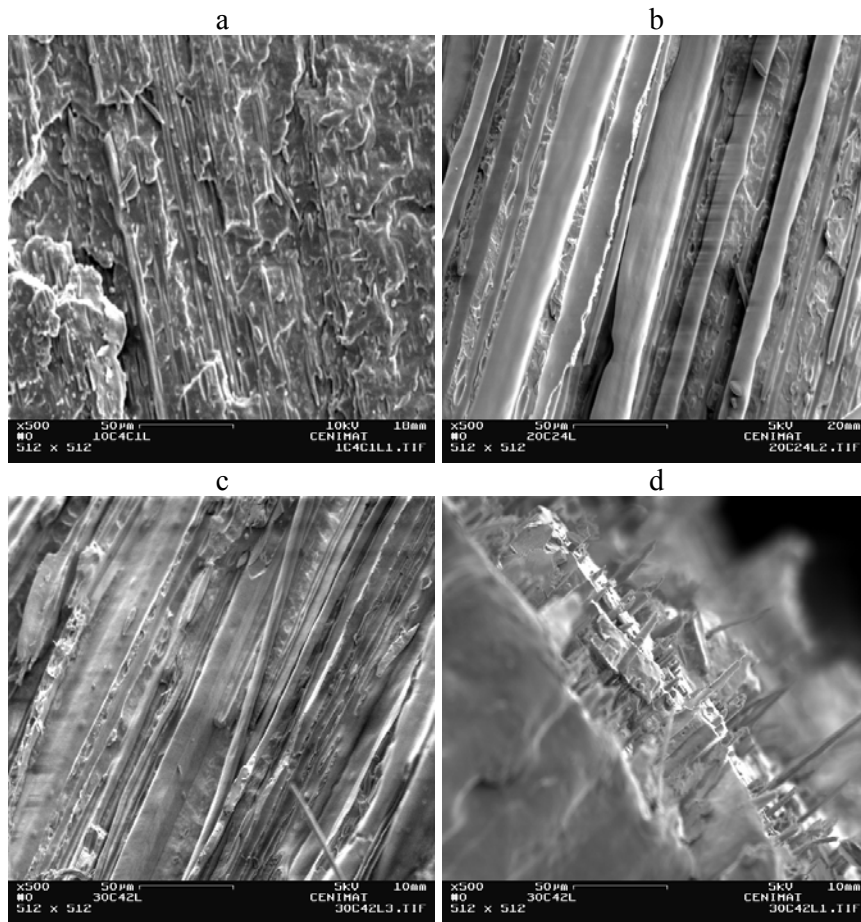


Figure 6.8 -SEM microphotographs for the blends with 10 (a), 20 (b) and 30 (c) and (d) wt % LCP and 2 wt % of compatibiliser C. Magnification of x500 for all the images.

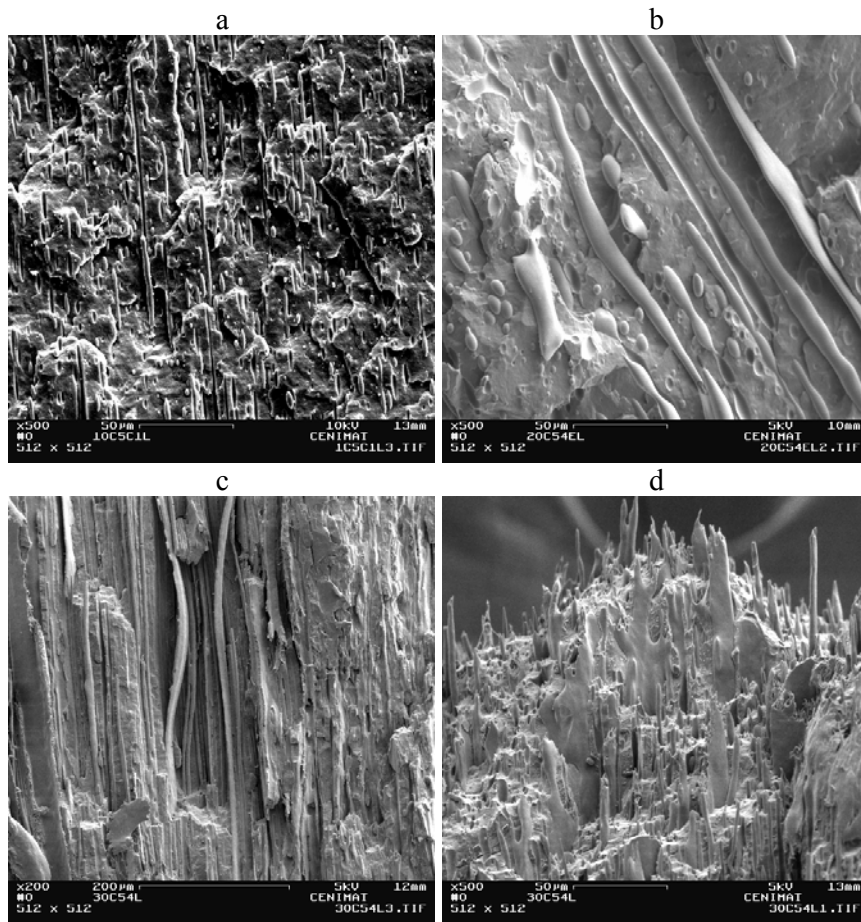


Figure 6.9 - SEM microphotographs for the blends with 10 (a), 20 (b) and 30 (c) and (d) wt % LCP and 4 % of compatibiliser E. Magnification of x500 for (a), (b) and (d) and x200 for (c).

RHEOLOGICAL CHARACTERISATION

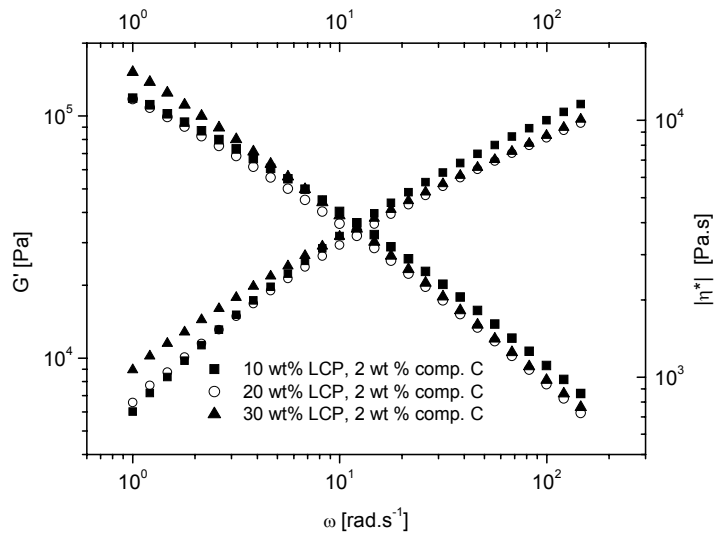
Linear regime

The increase of the LCP content has two distinct consequences on the storage and complex viscosity of the blends. In the case where compatibiliser C was used, two behaviours are observed. For the lower frequencies the blends containing lower LCP contents behave alike and the blend with 30 wt % LCP is the one presenting the highest complex viscosity and storage modulus. For the higher frequencies, the blend with the lowest LCP content (10 wt %)

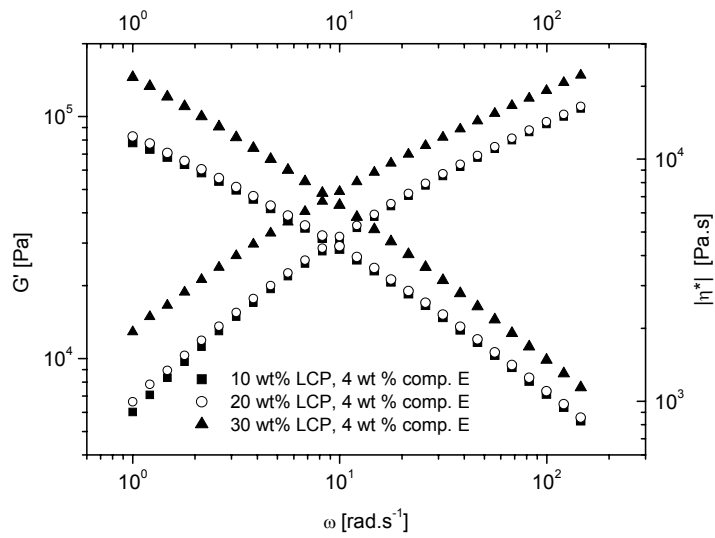
presents the highest elasticity and complex viscosity, while the blends with 20 and 30 wt % behave alike (figure 6.10 (a)).

This might be attributed to the fact that the addition of different LCP contents leads to different degrees of shear-thinning behaviour, *i.e.*, the increase of the LCP content often results in an increase of the shear-thinning character. This phenomenon is well-known and arises from the progressive orientation of the LCP domains, by action of shear, the intensity of which increases with increasing LCP content. This orientation of the LCP domains is, however, only possible when the matrix itself is oriented by the flow, which explains the crossover observed after a certain critical shear rate; below that, the orientation of the LCP domains are restricted by the matrix. Similar trend was verified for non-compatible blends, as shown in chapter 4.

For the blends with compatibiliser E, however, the addition of LCP leads to a large increase of the elasticity and complex viscosity, over the entire frequency range studied for the blend with 30 wt % LCP (figure 6.10(b)) the crossover not being observed. The reasons for this effect are not known at the moment, a tentative explanation being that at 30 wt % LCP the blend may be nearing its phase inversion threshold due to the presence of the compatibiliser. However, further work is necessary to solve this question.



a



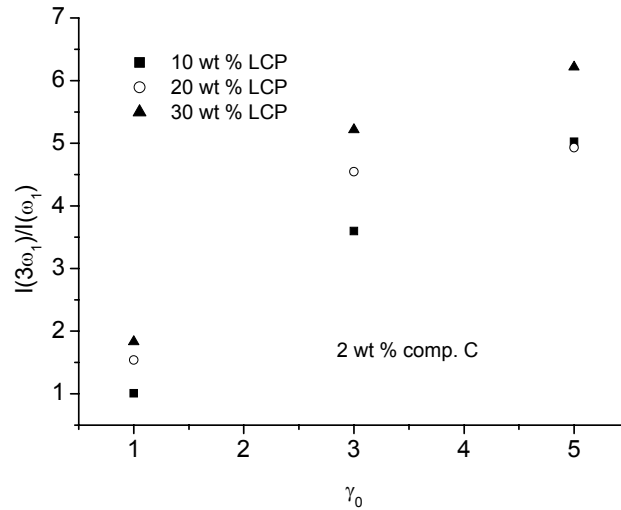
b

Figure 6.10 - Influence of LCP content on the storage modulus and complex viscosity of blends with 2 wt % compatibiliser C (a) and 4 wt % compatibiliser E (b), $T = 200$ °C, $\gamma_0 = 0.1$.

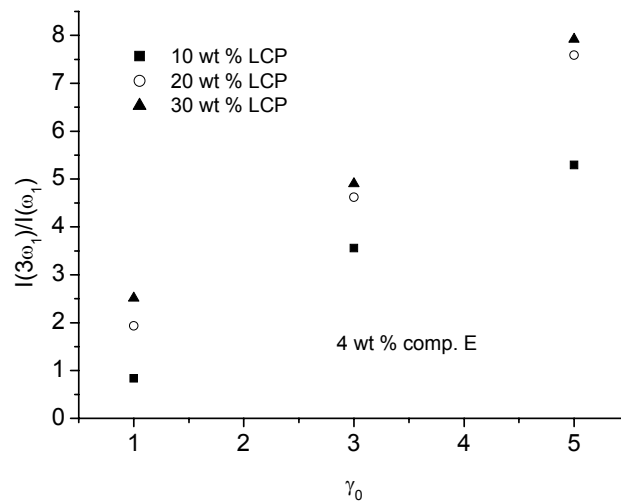
Non-linear regime

The main conclusions in this case are that, again, the technique is very sensitive to different morphologies, with the increase of the LCP content leading to the increase of the non-

linear character (figure 6.11), independently of the compatibiliser used and similarly to what was seen for non-compatibilised blends (see chapter 4). This is associated with the fact that blends containing higher LCP contents are also those for which one observes LCP structures with higher diameters, which can be more easily deformed.



a



b

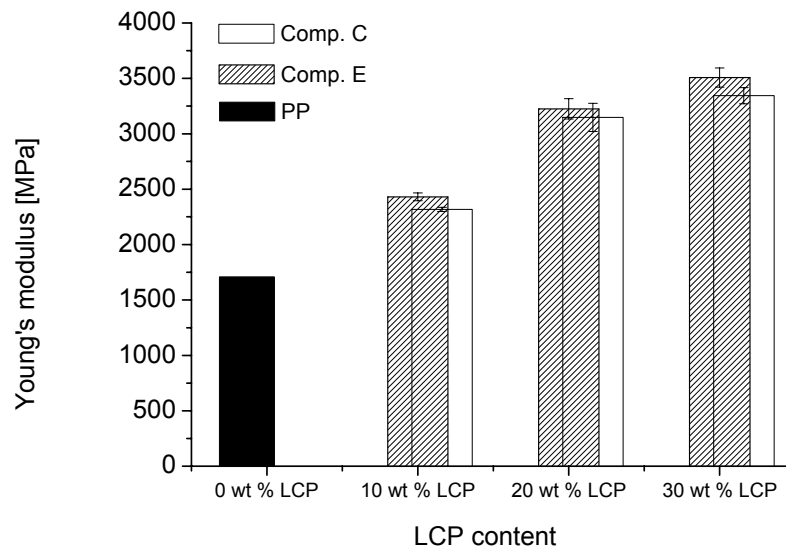
Figure 6.11 - Influence of LCP content on the non-linear character for blends with 2 wt % compatibiliser C (a) and 4 wt % compatibiliser E (b) at $T=170\text{ }^\circ\text{C}$, $\omega_1/2\pi = 1\text{ Hz}$.

MECHANICAL CHARACTERISATION

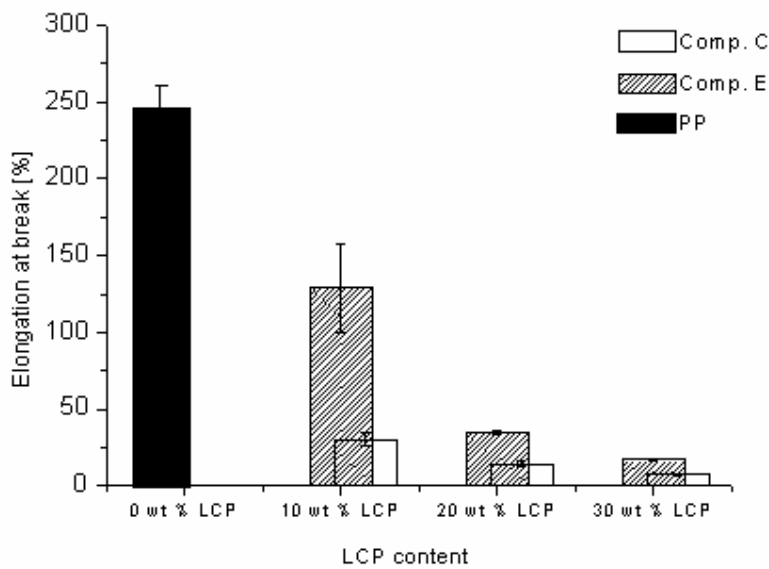
The tensile measurements carried out for the different compatibilised blends revealed that, as expected, there is an improvement of the strength with the increase of the LCP content, which results in an increase of the Young's modulus, arising from the higher content and diameter of LCP fibrils for the blends containing higher amounts of LCP. In all the cases the Young's modulus was higher than that observed for the pure matrix, which is around 1704 MPa. This observation is valid for both kinds of compatibilised blends, as depicted in figure 6.12(a). Nevertheless, the improvement in terms of tensile strength and Young's modulus, as usual, results in a drastic decrease of the elongation at break, as seen in figure 6.12(b).

Furthermore, two different kinds of fracture are observed, according to the LCP content; for the lower LCP contents (10 wt % LCP) a ductile fracture occurs (similarly to that of pure polypropylene, but with lower elongation at break), while for the higher LCP contents (20 and 30 wt % LCP) a fragile fracture is observed (similarly to that presented by the pure LCP, but with higher elongation at break).

It should be pointed out, however, that a lower decrease of the elongation at break occurs for those blends in which the compatibilisation is carried out by the use of an elastomeric compatibiliser (compatibiliser E), especially when small contents of LCP are used. Comparing the elongation at break of the pure matrix (247%) [Filipe 2004b] with that obtained for the compatibilised blends with 10 wt % LCP, one can state that there is a decrease of about 47 % of the elongation at break for the blend with compatibiliser E, against a much higher decrease, around 88 %, for the blend with compatibiliser C.



a



b

Figure 6.12 - Influence of LCP content on the Young's modulus (a) and elongation at break (b) of blends with compatibilisers C (2 wt %) and E (4 wt %).

For the compatibilised blends with 20 wt % LCP the decrease of the elongation at break, relatively to that of pure polypropylene was around 94 % and 86 %, for blends with compatibilisers C and E, respectively. Finally, when the amount of LCP is 30 wt %, a decrease

of 97 % (compatibiliser C) and 93 % (compatibiliser E) of the elongation at break were observed comparatively with that of the matrix. In conclusion, it is possible to state that an increase in LCP content leads to an increase of the tensile strength but to a decrease in the toughness, except for small contents of LCP, when a compatibiliser with an elastomeric nature is used.

CONCLUSIONS

The optimisation of the LCP and compatibiliser content was performed for Rodrun LC3000 and polypropylene blends and the main findings are that the use of non-linear oscillatory shear is highly sensitive to the effectiveness of compatibilisers, lower non-linear characters were observed for those blends in which the maximum fibrillar formation, and those for which the maximum mechanical improvement was achieved; in contrast, no significant differences were found under linear oscillatory shear.

As a result of the improvement in terms of both distributive and dispersive mixing, the rheological and morphological differences between samples collected along the extruder are less pronounced for those blends in which the compatibilisation was more effective. This may indicate that an improvement of the adhesion might lead to a morphology that is more homogeneous along the extruder length.

The increase of the LCP content in compatibilised LCP/TP systems leads to an increase of the non-linear character which is basically related with the increase of the dimensions of the LCP droplets, in the beginning of the extrusion process, and thus, their easier deformation. The increase of the LCP content leads to an increase of the mechanical strength, as expected.

The non-linear character increases with the increase of the strain amplitude, for all the samples (independently of their LCP and compatibiliser contents), as expected.

In compatibilised blends containing the same LCP content (like those studied in the first part of this chapter, with 10 wt % LCP), the lowest non-linear characters were obtained for the blends with the lowest average diameters and consequently those that originated best fibrillation (which were those for which one have obtained the best mechanical performance). For those systems in which one has varied the LCP content (keeping the same compatibiliser and compatibiliser content), like those studied in the second part of this chapter (containing 10, 20 and 30 wt % LCP), the highest non-linear character was obtained for the blends with the highest LCP content, which are actually those, that present the LCP structures with the highest average diameters and the highest mechanical properties. This may be, apparently, a contradiction, however it should be kept in mind that two different phenomena are involved, one is related with the quality of the fibrillation, while the other concerns the number and size of the fibrils (that are already well defined for all the LCP content).

Having in mind that the main aim of this study is to optimise the amount of both LCP and compatibiliser, one must evaluate the best combination mechanical performance/cost. Considering polypropylene as the matrix, the mechanical improvement obtained for the blends with higher LCP contents was higher than for those with lower LCP contents, as expected. Nevertheless, if one considers the high cost that is associated to the pure liquid crystalline polymer, on one hand, and the increase of the viscosity (particularly for the blend with compatibiliser E at high LCP contents), on the other hand, then one should be cautious about the choice of the LCP content to be used. Only an economical evaluation, at each time, and for each application, can give such an answer. This conclusion is valid for both compatibilised systems.

In applications with polypropylene as matrix in which the major need is essentially in terms of tensile strength (and for which a high elongation at break is not absolutely required), the best choice may be compatibiliser C. In fact, although the blends with compatibiliser E

show a slightly higher Young's modulus than those with compatibiliser C, it should be considered that the amount of compatibiliser needed to achieve the maximum fibrillar formation and thus, the maximum mechanical performance is, in this case, twice that of the blends with compatibiliser C. Once again an economical evaluation is needed to help in the choice of the best compatibiliser. In applications in which both tensile strength and toughness are important the best combination will be the use of a small amount of LCP (about 10 %) and 4 wt % of compatibiliser E.

References

- [Bafna 1995] S. S. Bafna, T. Sun, J. D. De Souza and D. G. Baird *Polym.* **36**, 259 (1995)
- [Boersma 1999] A. Boersma and J. Van Turnhout *Polym.* **40**, 5023 (1999)
- [Bordereau 1992] V. Bordereau V, Z. H. Shi, L. A. Utracki, P. Sammut and M. Carrega *Polym. Eng. Sci.* **32**, 1846 (1992)
- [Choi 2002] N. S. Choi, N. Cho, K. Takahashi and M. Kurokawa, *Mater. Sci. Eng. A* **323**, 467 (2002)
- [Datta 1995] A. Datta and D. G. Baird *Polym.* **36**, 505 (1995)
- [Farasoglou 2000] P. Farasoglou, E. Kontou, G. Spathis, J. L. Gomez Ribelles and G. Gallego Ferrer *Polym. Composite* **21**, 84 (2000)
- [Filipe 2004a] S. Filipe, M. T. Cidade, M. Wilhelm and J M. Maia *Polym.* **45**, 2367 (2004)
- [Filipe 2004b] S. Filipe, J. M. Maia and M. T. Cidade *Adv. Mat. Forum* **456**, 476 (2004)
- [Filipe 2004d] S. Filipe, J. M. Maia, A. Duarte, C. R. Leal and M. T. Cidade *J. Appl. Polym. Sci.*, submitted (June 2003)
- [Filipe 2004e] S. Filipe, M. T. Cidade, M. Wilhelm and J. M Maia *J. Appl. Polym. Sci.*, submitted (August 2003)
- [Kozlowski 1997] M. Kozlowski and F. P. La Mantia *J. Appl. Polym. Sci.* **66**, 969 (1997)
- [Kwon 1995] S. K. Kwon and I. J. Chung *Polym. Eng. Sci.* **35**, 1137 (1995)
- [Lee 2003] M. W. Lee, X. Hu, C. Y. Yue, L. Li and K. C. Tam *Comp. Sci. Tech.* **63**, 339 (2003)

- [Lee 2003] M. W. Lee, X. Hu, L. Lin, C. Y. Yue, K. C. Tam and L. Y. Cheong *Comp. Sci. Tech.* **63**, 1921 (2003)
- [Liang 2002] Y. C. Liang and A. I. Isayev *Polym. Eng. Sci.* **42**, 994 (2002)
- [Limcharoen 1999] S. B. Limcharoen, J. Samram, T. Amornsakchai and W. Meesiri *Polym. Eng. Sci.* **39**, 312 (1999)
- [Mandal 2003] P. K. Mandal, D. Bandyopadhyay and D. Chakrabarty *J. Appl. Polym. Sci.* **88**, 767 (2003)
- [Potente 2000] H. Potente, M. Bastian, A. Gehring, M. Stephan and P. Potschke *J. Appl. Polym. Sci.* **76**, 708 (2000).
- [Sukananta 2003] P. Sukananta and S. Bualek-Limcharoen *J. Appl. Polym. Sci.* **90**, 1337 (2003)
- [Tjong 1998] S. C. Tjong, R. K. Y. Li and Y. Z. Meng *J. Appl. Polym. Sci.* **67**, 521 (1998)
- [Tjong 1997] S. C. Tjong and Y. Z. Meng, *Polym. Inter.* **42**, 209 (1997)
- [Tjong 2003] S. C. Tjong *Mat. Sci. Eng.* **R41**, 1 (2003)
- [Wanno 2000] B. Wanno, J. Samran and S. Bualek-Limcharoen *Rheol. Acta* **39**, 311 (2000)
- [Zeng 2003] X. Zeng, J. Zhang and J. He *J. Appl. Polym. Sci.* **87**, 1452 (2003)

7 OPTIMISATION OF PROCESSING CONDITIONS FOR COMPATIBILISED LCP/TP BLENDS*

INTRODUCTION

Polymer blends allow the combination of the individual properties of pure components, and may actually result in the production of new materials, which possess improved characteristics and, in some cases, new properties.

The importance of co-rotating twin-screw extruders in blending processes is clearly recognized, considerable consensus existing about their efficiency in terms of both distributive and dispersive mixing [Utracki 1991]. In intermeshing co-rotating twin-screw extruders a relatively uniform shear rate distribution is provided along the conveying screw sections. Additionally mixing and shear rate capabilities can be provided by the use of kneading blocks and reverse-conveying elements [Utracki 1991]. In this kind of equipment it is possible to change the geometrical characteristics of both barrel and screw (the so-called, modular construction), as well as the processing conditions, in accordance with the required needs [Todd 1998, Rauwendaal 1990]. The deliberate optimisation of the material properties, by means of monitoring the physico-chemical phenomena developed along the extruder axis is needed, since these processes are directly related with the final characteristics of the material and therefore, with its ultimate mechanical performance [Potente 2000, Bordereau 1992, Boersma 1999, Chin 1979, Wu 1987, Han 1981, Serpe 1990]. Several studies were performed in order to quantify the degree of break-up, coalescence and deformation of dispersed phase particles at the different stages of the extrusion process [Potente 2000, Bordereau 1992, Boersma 1999, Sundaraj 1995, Filipe 2004a, Filipe 2004c-d]. This work was in its majority performed for non-compatibilised systems but there are some exceptions, like the work of

* adapted from S. Filipe, M. T. Cidade, C. R. Leal, J. M. Maia, *Optimization of the Processing Conditions for Compatibilised Rodrun LC3000/PP blends*, submitted to *Polym. Eng. Sci.* (December 2004)

Majumdar *et al.* and Nishio *et al.* (and our own work), in which the attention was focused on compatibilised systems [Majumdar 1997, Nishio 1991, Filipe 2004a, d].

In this part of the work, some important issues on the influence of different processing conditions on the deformation, break-up and coalescence processes of compatibilised liquid crystalline polymer and thermoplastic blends will be addressed. The study of compatibilised systems is essential, especially if one considers the implications that are related with the use of a compatibiliser. The reduction in the interfacial tension is essential for the decrease of the dispersed phase diameters but also, and perhaps more important, is crucial in the stabilization against coalescence, during the extrusion process. In chapter 5 and 6 the influence of different compatibilisers and different LCP contents on the competition between break-up and coalescence along the extruder length and on its influence on the final mechanical properties was studied. In this chapter, the main purpose is to understand and attain improved knowledge on the processing conditions that lead to the creation of a suitable phase morphology, by monitoring the break-up and coalescence processes for distinct processing conditions. Since the above-mentioned phenomena are essentially dynamic processes, which change progressively according to the region of the extruder, it is of primary interest to study their evolution along the extruder length. There is a need to understand the applicability of the knowledge described above on the control of the morphology development during compounding in a twin-screw extruder, having in mind the optimisation of the mechanical performance. A home-built collecting device system (described in chapter 3) [Covas 2001] was used in this study, to monitor, morphology, rheology and temperature as the melt proceeds downstream in the extruder axis. Some work was already performed on non-compatibilised LCP/TP systems, concerning the influence of both processing conditions and type of blending equipment on the final morphology [Heino 1994]. However this study was only focused on the final extrudates and not on the morphology development during the extrusion process.

Unlikely, in the work of Boersma and Van Turhnout, the attention was focused on the monitoring of the evolution of the morphology by means of dielectric spectroscopy [Boersma 1999]. Unfortunately, and similarly to Heino *et al.*, they only studied non-compatibilised systems [Heino 1994]. As is already known, the application of LCP/TP blends on industrial applications requires the use of compatibilisers, and therefore, one should enlarge this kind of studies to compatibilised systems. Chapter 5 and 6 included the study of the influence of different compatibilisers and different compatibiliser contents [Filipe 2004d], as well as different LCP contents, on the morphological and rheological evolution along the extruder length. However, some important unanswered questions still remained, namely, what is the influence of the processing conditions on the kinetic of mixture for compatibilised systems and how does it affect the final morphology and the final mechanical properties. The main objective of this part of the work is thus, not only to answer to the questions previously described, but also to determine the processing conditions, namely, screw speed, output, and temperature, that lead to the best mechanical enhancement for compatibilised liquid crystalline polymer and thermoplastic blends.

EXPERIMENTAL

MATERIALS AND PROCESSING CONDITIONS

The blends which were chosen for this part of the work were those that presented the highest mechanical performance/cost ratio, *i.e.*, 2 wt % compatibiliser C and 4 wt % compatibiliser E, containing 10 wt % LCP (see chapters 5 and 6). The blends were produced by extrusion using the screw and cylinder configuration defined as configuration 1, in chapter 3 (figure 3.4). The optimisation of the processing conditions was performed by changing several process parameters, namely, temperature, screw speed and output. The processing conditions used are depicted in table 7.1.

Table 7.1- Processing conditions employed in the optimisation process.

Processing conditions	Condition 1	Condition 2	Condition 3	Condition 4	Condition 5	Condition 6
Temperature (°C)	220	240	220	220	220	220
Screw Speed (rpm)	150	150	100	200	150	150
Output (kg/h)	4	4	4	4	2	8

MORPHOLOGICAL CHARACTERISATION AND IMAGE ANALYSIS

SEM measurements were performed for both final extrudates and for the samples collected along the extruder length (by means of the collecting device system described in chapter 3). For the analysis of the SEM images, namely, for the determination of the particle size distribution and average diameters UTHSCSA Image Tool was used. The area was determined by the use of ellipses and was used afterwards to determine the equivalent diameter, by using the following equation:

$$d = \sqrt{\frac{4}{\pi} \cdot A}$$

For a number of particles, n , the average diameter was calculated by using:

$$d_a = \frac{\sum d_i}{n}$$

RESULTS

MORPHOLOGICAL CHARACTERISATION ALONG THE EXTRUDER LENGTH

It is already known that in intermeshing twin screw extruders, the majority of the mixing takes place in the mixing elements, since this is the place where the highest shear and elongational forces are present. During extrusion several processes occur; deformation, break-up and coalescence take place in a different range depending on several parameters, namely, extruder location, temperature, screw speed, output, shear rate, residence time, and so on. The above mentioned processes are mainly governed by the capillary number (see equation 2.1, chapter 2) and by the viscosity ratio of the blend components, which depend markedly on the temperature. The former parameter decreases continuously along the extruder due to a decrease of the size of the dispersed phase structures. At the beginning of the process the dispersed phase is formed by droplets with a more or less elongated form that might be described by a length and a diameter (see schematic representation on figure 7.1).

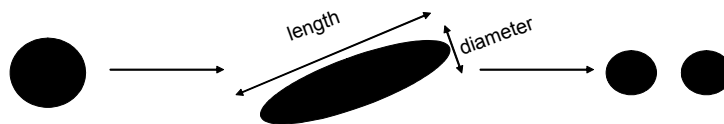


Figure 7.1 - Schematic representation of deformation and break-up of dispersed phase.

Due to stretching of the dispersed phase structures, arising from the fact that $Ca \gg Ca_{critical}$, the diameters of these elongated droplets will decrease and their length will increase as proceeding downstream in the extruder. This process will give rise to the formation of droplets, which arise from the break-up of the elongated droplets. In case the residence time is shorter than the time needed for break-up, the LCP droplets previously formed will relax to their initial shape. In more dramatic cases, like for example in non-compatibilised systems,

coalescence might take place, giving rise to an increase of the average diameters. Therefore, in order to quantify the break-up and coalescence processes one should be aware of the residence time, of the time needed for break-up, as well of the total applied strain, temperature and viscosity ratio.

According to the theory [Shi 1992], the total strain (elongation and shear) applied to the dispersed phase in an extruder can be expressed by:

$$\gamma = \left(\dot{\gamma}_f \cdot t_f + \dot{\gamma}_c \cdot t_c \right) \cdot \frac{2t_r N}{60} \quad 7.1$$

where,

γ is the total strain

$\dot{\gamma}_f$ is the strain rate at the flight

$\dot{\gamma}_c$ represents the strain rate at the channel

t_f is the time at the flight

t_c is the time at the channel

t_r is the residence time at a given output

and

N is the screw speed

As seen above the total applied strain increases with the increase of the screw speed and with the increase of the residence time.

On the other hand the mean residence time is given by:

$$\bar{t}_r = \frac{\pi D H L}{Q} \quad 7.2$$

where

D is the diameter of the screw

H is the mean channel depth

L is the screw length

Q the volumetric output

Therefore, by increasing the output, a decrease of the residence time occurs. The time for break-up is another important parameter to consider in order to evaluate whether coalescence or break-up occurs. The time for break-up usually decreases along the axial position in the extruder, due to the decrease of the diameters of the dispersed phase. Additionally the time needed for break-up generally decreases with increasing rotation speed, because, in principle, the diameter of the dispersed phase structures should decrease with the increase of the screw speed. In any case, one should be aware of two points: higher screw speeds generate higher shear rates, which will lead to an increase of the temperature. Additionally, the residence time decreases with the increase of the screw speed.

All the above considerations will be taken into account during the discussion.

Blends with 10 wt % LCP and 2 wt % compatibiliser C

INFLUENCE OF PROCESSING TEMPERATURE

The study of influence of the processing temperature on the morphological evolution by SEM for the blend with compatibiliser C showed that an increase of the droplet's diameters occurs by the increase of the temperature, independently of the location in the extruder (figure 7.2).

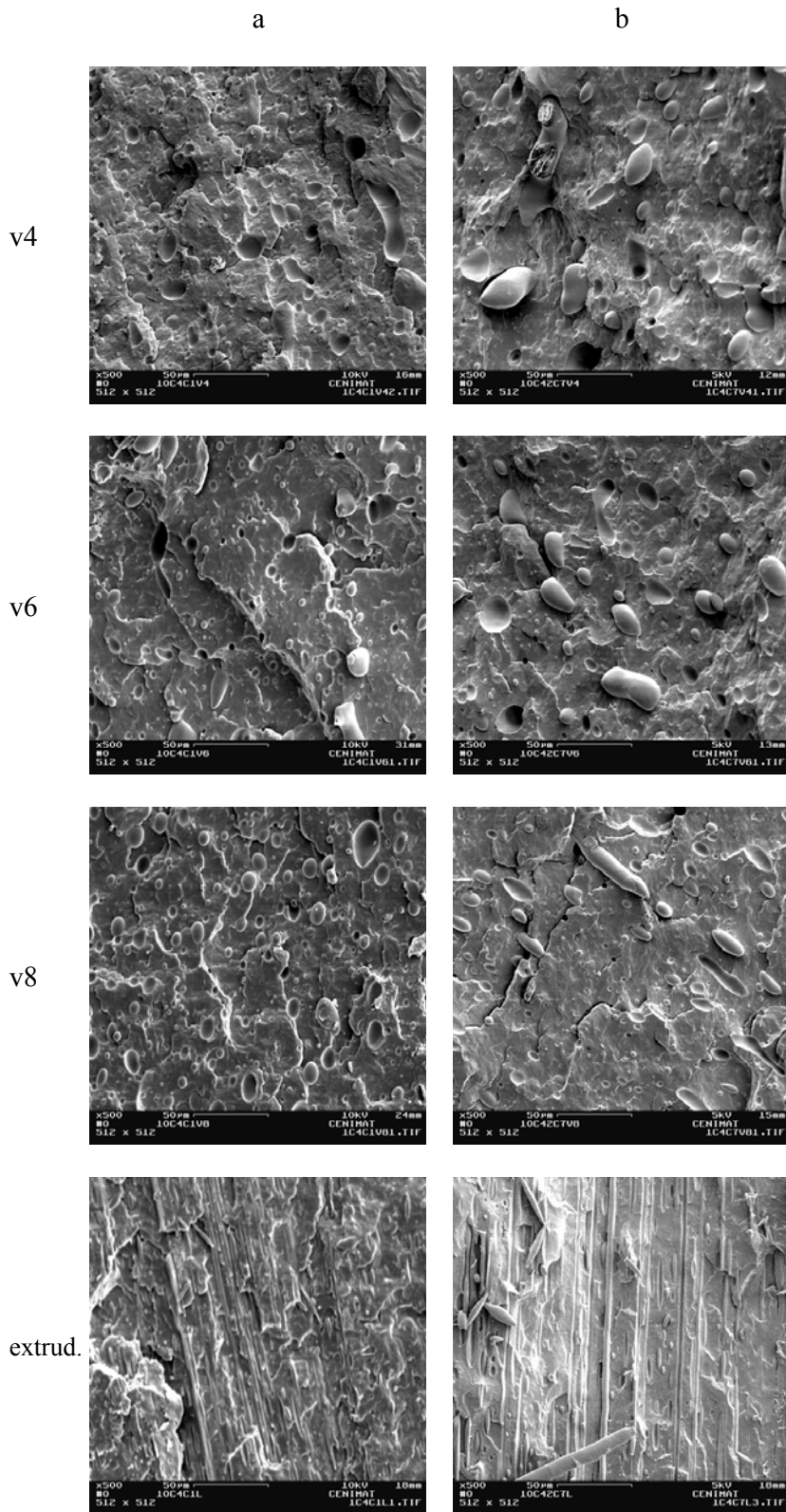


Figure 7.2 - SEM images for blends with 10 wt % LCP and 2 wt % compatibiliser C, processed at 220 °C (a) and 240 °C (b)- Magnification of x500, for all images.

The degree of dispersive and distributive mixing was clearly enhanced for the lower processing temperature, which was expected and is in agreement with previous preliminary results (see chapter 4) since higher temperatures usually lead to a decrease of the viscosity of the pure components and thus to an improvement of the coalescence processes (figure 7.2). The diameters distribution for both blends shows that the average diameters are clearly lower for the blend processed at a lower processing temperature, as seen in figure 7.3. For valve 6 the average diameter is 5.87 μm for the lower temperature and 8.57 μm for the higher temperature, similar trend being observed for valves 4 and 8.

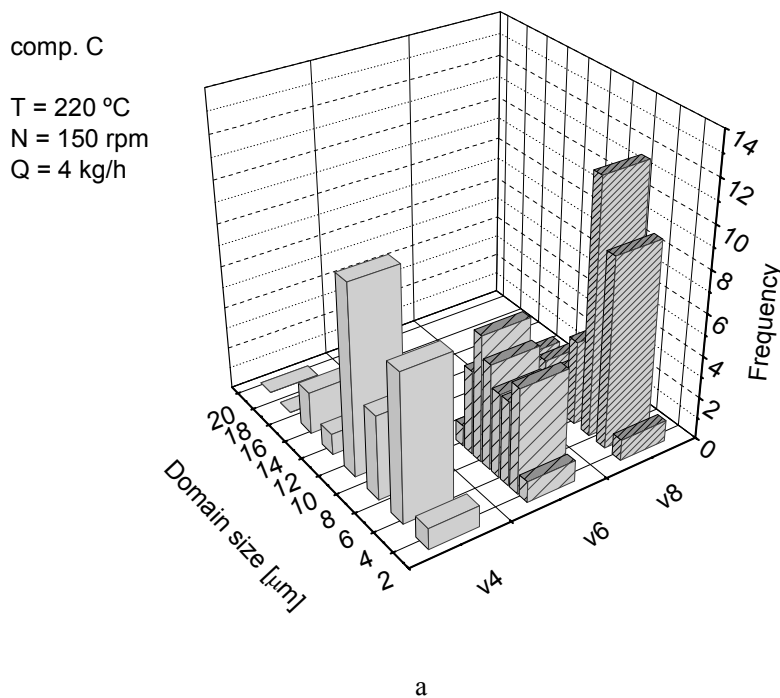


Figure 7.3 (a) - Particle size distribution along the extruder length for blends with 10 wt % LCP and 2 wt % compatibiliser C, processed at 220 °C (a). *original data in appendix III

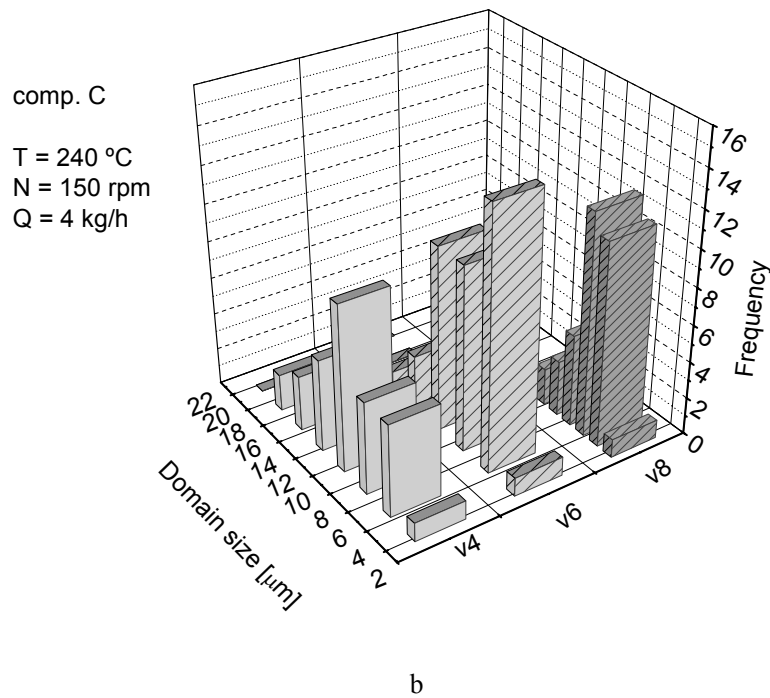


Figure 7.3 (b) - Particle size distribution along the extruder length for blends with 10 wt % LCP and 2 wt % compatibiliser C, processed at 240 °C (b). *original data in appendix III

INFLUENCE OF SCREW SPEED

In what regards the blend containing compatibiliser C, it must be pointed out that lower screw speeds (100 rpm) seem to result in a lower degree of mixing in the beginning of the extrusion process, more precisely, in the conveying elements region (valve 4), as depicted in figure 7.4 (a). For the lower screw speeds and at this point, the LCP remains in the form of big aggregates, a co-continuous morphology is present (figure 7.4 (a)), while for the higher screw speeds (150 and 200 rpm, figures 7.4 (b) and 7.4 (c), respectively) they are essentially constituted by droplets, dispersed along the thermoplastic matrix (note that figure 7.4 (b) is the same as figure 7.2 (a), however, for an easier comparison to the reader it was decided to include these results in this figure too). This was the expected behaviour, since the higher the screw speed, the higher the shear rate, and thus, the higher the degree of mixing.

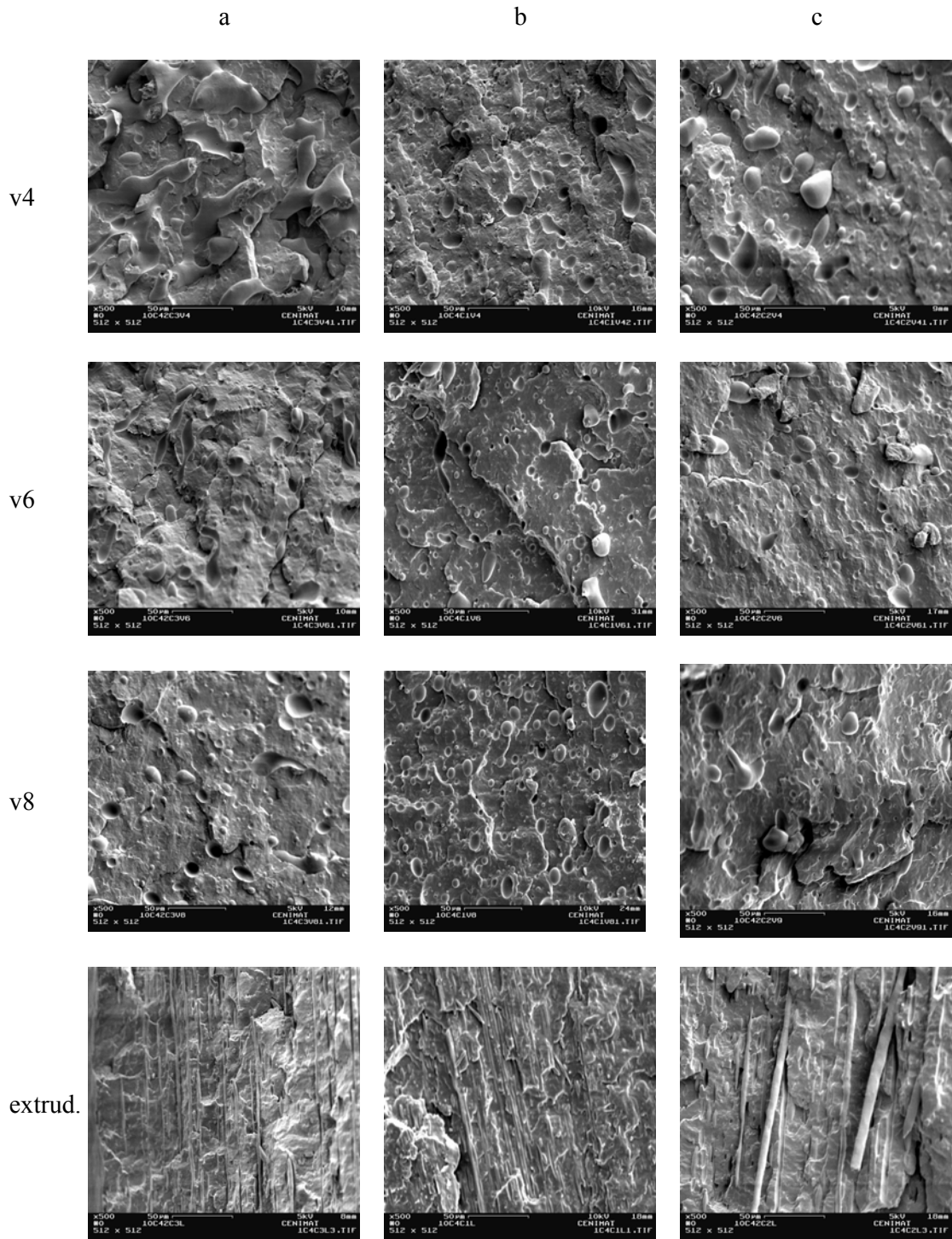


Figure 7.4 - SEM images for blends with 10 wt % LCP and 2 wt % compatibiliser C, processed at 100 rpm (a), 150 rpm (b) and 200 rpm (c) - Magnification of x500, for all images.

At this point it is clear that an increase of the screw speed leads to an improvement of the degree of mixing, since for the lower screw speed one observed a co-continuous

morphology, whereas a droplet-like morphology was seen for the higher outputs, 150 and 200 rpm. However, and contrary to our expectations it seems that the application of higher screw speeds does not lead to a decrease of the LCP droplets, especially in the beginning of the process, valve 4 (figure 7.4).

As the process continues, an increase of the temperature with the increase of the screw speed occurs, and, as will be shown, this will affect the morphology development. For example, at the beginning of the kneading blocks region (valve 6) it looks like the application of lower screw speeds (100 and 150 rpm) results in a higher degree of deformation and break-up than for 200 rpm. At this point (valve 6), the dispersed phase of the blends processed at 100 and 150 rpm is essentially constituted by elongated-like and droplet-like structures. At valve 6 there are no significant differences in terms of both dispersive and distributive mixing between the different screw speeds. Despite the fact that for lower screw speeds one expects lower shear rates (and thus, lower shear stresses), one should be aware that under these conditions higher residence times and lower temperatures are anticipated (see table 7.2).

Table 7.2- Temperatures measured along the extruder length for different processing conditions (Blend with 10 wt % LCP, 2 wt % comp. C).

Processing conditions		Position in the extruder			
		v4	v6	v8	extrudate
Q (kg/h) (T = 220 °C, N = 150 rpm)	2	232.1	233.3	235.4	237.3
	4	227.2	230.1	231.4	237.1
	8	226.1	227.4	228.2	227.7
N (rpm) (T = 220 °C, Q = 4 kg/h)	100	226.4	226.7	231.0	233.9
	150	227.2	230.1	231.4	237.1
	200	227.5	234.7	235.4	238.2
T (° C) (Q = 4 kg/h, N = 150 rpm)	220	227.2	230.1	231.4	237.1
	240	244.1	245.9	246.2	248.1

Therefore, it can be expected that lower screw speeds will result in a finer morphology at the last valves (since the temperature is lower for this conditions). This

behaviour is in contradiction with the theory, which states that a higher decrease of the dispersed phase structures will occur by the use of higher screw speeds. However, and as already reported by other authors [Potente 2000, Luciani 1996, Majumdar 1997], in the presence of mixing elements, the use of higher screw speeds may increase the viscous dissipation, leading to a decrease of the viscosity of both matrix and dispersed phase. Consequently, the viscosity ratio will drop to lower values and the deformation and break-up of the dispersed structures will be more difficult, despite the higher shear rates anticipated for the higher screw speeds. Additionally, the residence time is lower for the higher screw speeds, which may also reduce the degree of break-up.

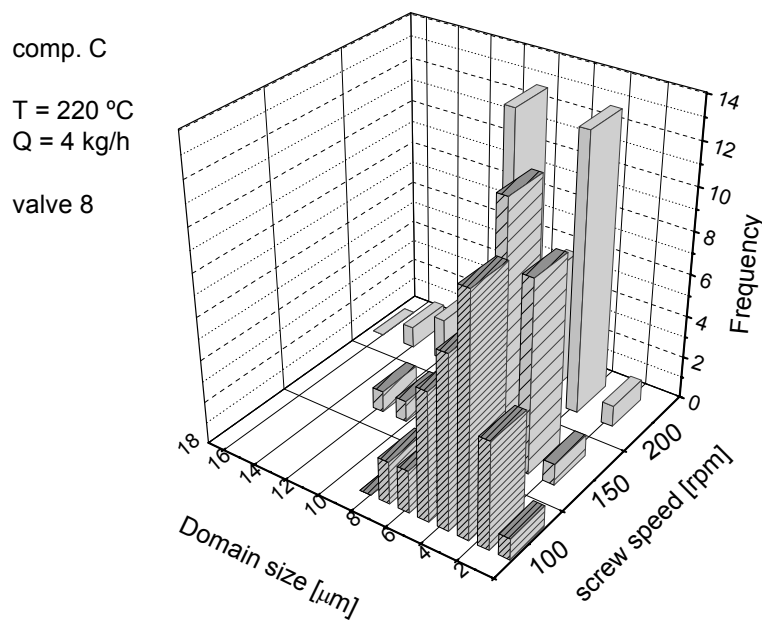


Figure 7.5 - Particle size distribution at valve 8, for blends with 10 wt % LCP and 2 wt % compatibiliser C, processed at 220 °C, using 100, 150 and 200 rpm. *original data in appendix III

When the screw speed is increased to 200 rpm an increase of the average diameters (figure 7.4 (c)) occurs at valve 8 (at the end of the kneading blocks region), the majority of the LCP droplets possess diameters between 5 and 9 µm (figure 7.5). The average diameters are at this point (valve 8) 4.53 µm for 100 rpm, 6.15 µm for 150 rpm and 7.7 µm for 200 rpm,

meaning that an increase of the average diameter occurs by the increase of the screw speed. Similar observation was made by Potente *et al.*, when they studied the influence of the rotational speed on the morphology along the extruder length, for PP/PA blends [Potente 2000]. This behavior was also seen in the work of Luciani *et al.* and Majumdar *et al.* [Luciani 1996, Majumdar 1997]. As in our case, they verified that for the higher screw speeds (100 min^{-1} , in their case), an increase of the average diameters of the dispersed phase occurs, immediately after the kneading-blocks. This behaviour is against the usually predicted by the theory, according which a lower average diameter is expected for the higher screw speeds. It looks like this phenomenon is related with the pronounced viscous dissipation effects that occur at the kneading blocks and which arise from the high shear rates developed in this part of the extruder. The increase of temperature will lead to a decrease of the viscosity of both matrix and dispersed phase, which will result in an improvement of the coalescence. This increase of the coalescence seems to occur for all the screw speeds, but it looks like its intensity is increased with the increase of the screw speed, probably because higher screw speeds generate higher temperatures (see table 7.2). Another point worth of remark is the fact that the increase of the temperature with the increase of the screw speed is more pronounced for valves 6 and 8 (located at the kneading blocks region) than for valve 4 (at the reverse-conveying elements). This is expected, since an higher degree of viscous dissipation can be anticipated for the regions in which a higher shear stress is applied, like that present at the mixing elements. The viscous dissipation is more pronounced for those conditions in which a higher shear rate is expected (200 rpm). As a result, a thickening of the LCP fibrils is anticipated for the higher screw speeds (200 rpm), which actually occurred (figure 7.4 (c)). For the higher screw speeds the shear stress that is provided is not by itself enough, to ensure efficient break-up of the droplets at the valves, since at the same time the residence time is clearly reduced (and is lower than the time needed for break-up). In conclusion, lower screw speeds usually lead to lower

temperatures (and higher residence times), while a higher screw speed usually implies a higher temperature (and a lower residence time). In fact, this was what one observed, as depicted in table 7.2. Therefore, it is not unexpected that the break-up of LCP droplets and formation of LCP fibrils is enhanced by the use of lower screw speeds in opposition to what happens for the higher screw speeds, for which a higher degree of coalescence occurs. Therefore, the screw speed that yielded the best fibrillar formation was the lowest screw speed, 100 rpm.

INFLUENCE OF OUTPUT

For compatibiliser C it looks like that an increase from 2 to 4 kg/h leads to a decrease of the average diameters (figures 7.6 (a) and 7.6 (b), respectively), at the beginning of the extrusion process (most precisely at valve 4). This behaviour is somehow unexpected, since according to the theory, the application of lower outputs should result in a higher shear rate and higher residence time (thus, higher deformation and break-up). However, and similarly to what happened with the higher outputs (200 rpm), one should be aware that higher shear rates also imply higher temperatures (see table 7.2). Even if higher residence times are associated with lower outputs, it looks like the temperature has a higher influence on the deformation and break-up of the LCP structures. Therefore, at least in which concerns the evolution along the extruder, before the die, it looks like the most important parameter controlling the morphology is, in this case, the viscosity ratio, which, dramatically changes with the temperature.

The increase of the output for even higher values (8 kg/h) results in a lower efficiency in terms of mixing at the beginning of the process (valve 4) which might arise from a lower temperature at this location, comparing with lower outputs (see table 7.2). This lower temperature will lead to a lower degree of melting of both dispersed and continuous phase; at valve 4, the majority of the LCP is still in the form of big aggregates, a co-continuous morphology is present, similarly to what was seen at the same location for the blend processed at 100 rpm (figure 7.4 (a)).

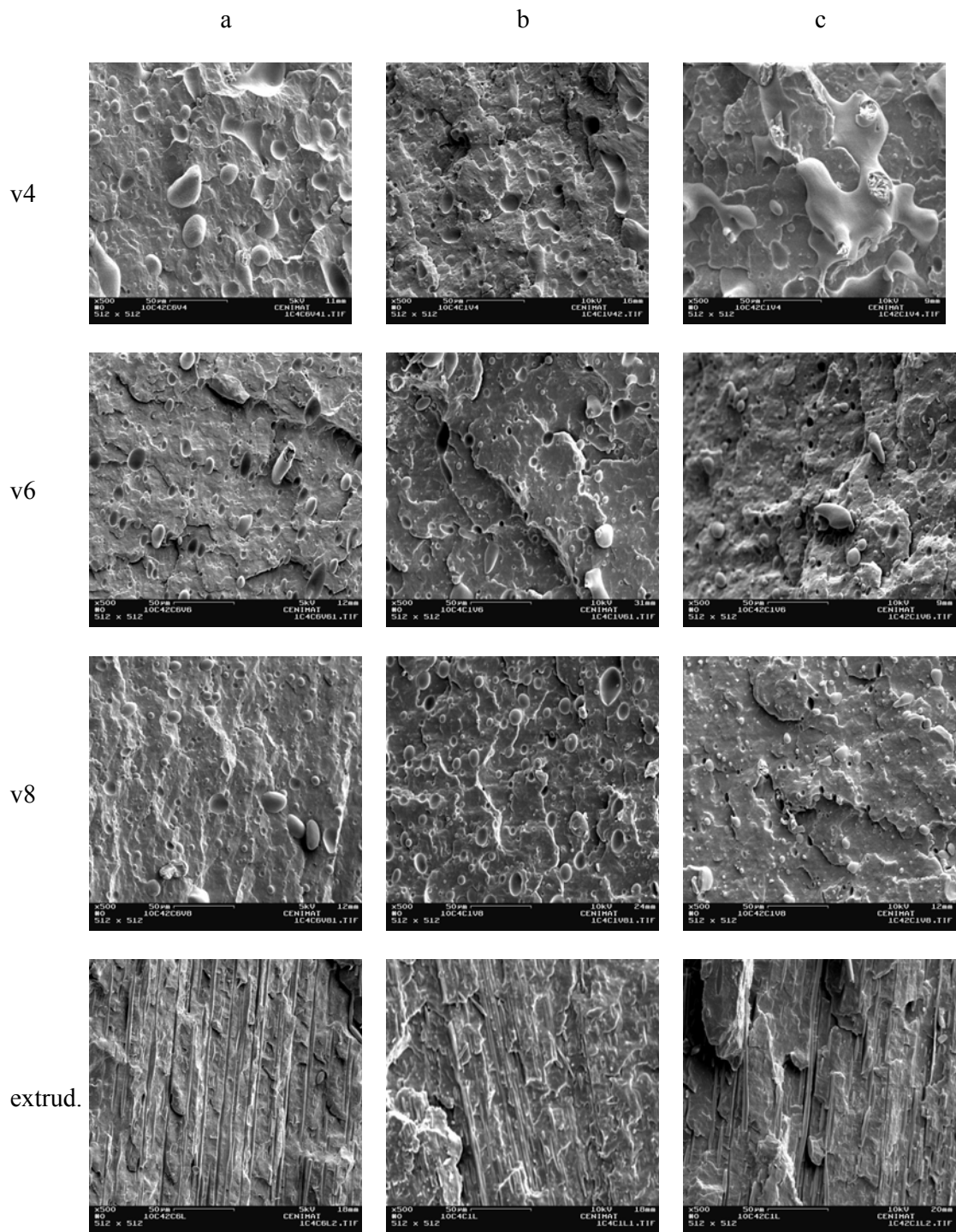


Figure 7.6 - SEM images for blends with 10 wt % LCP and 2 wt % compatibiliser C, processed at 2 kg/h (a), 4 kg/h (b) and 8 kg/h (c) - Magnification of x500, for all images.

After valve 4 the droplets are subjected to elongation and break-up, giving rise to the appearance of spherical structures at valves 6 and 8 (figure 7.6). Analysing the particle size

distribution at valve 8 (figure 7.7), one observed that for the higher outputs (8 kg/h) the LCP droplets possess smaller diameters than those observed for the lower outputs. Once more, this can be explained by a lower temperature at all the extruder locations, for the highest output (8 kg/h).

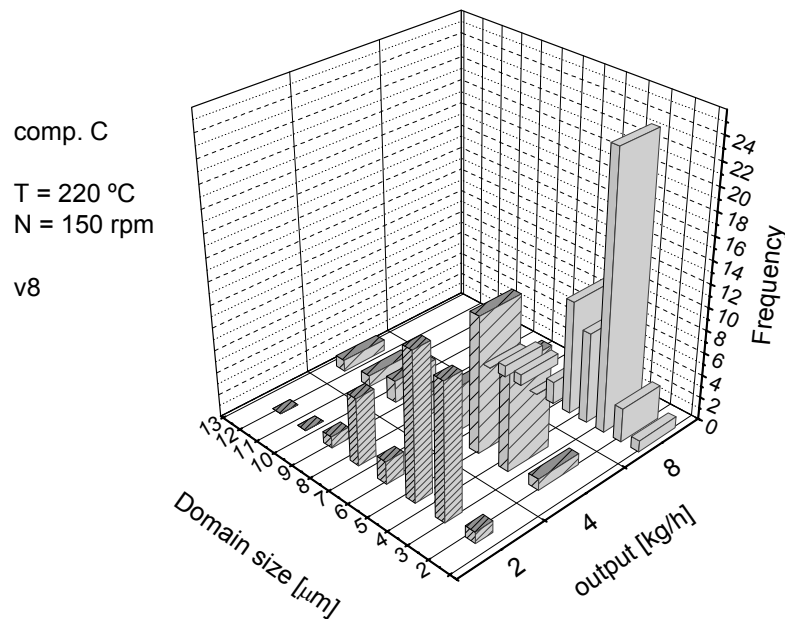


Figure 7.7 - Particle size distribution for blends with 10 wt % LCP and 2 wt % compatibiliser C, processed at 100, 150 and 200 rpm at valve 8. *original data in appendix III

Despite the fact that at valve 8, the average diameters of the LCP droplets for the blend processed at 8 kg/h are lower than those seen for lower outputs (3.84 µm for 8 kg/h against 5.27 and 6.15 µm, for 2 and 4 kg/h. respectively), the formation of fibrils was not enhanced for the higher outputs. About this, one can state that the application in excess of an intensive mixing, by the use of staggering kneading blocks, may actually be detrimental for the fibrillation process. This is due to the fact that the deformation is no longer possible (or is much more difficult) after the minimum particle size as been attained (which seemed to be the

case after valve 8, for the higher output (8 kg/h)). This may actually explain the occurrence of a lower fibrillation for the higher outputs (8 kg/h). Similar observation was done by Majumdar *et al.*, which stated that some conditions that intuitively are expected to improve the degree of mixing in non-compatibilised blends, may actually have the opposite effect in compatibilised systems, in which the dispersed phase is much more “finely dispersed” [Majumdar 1997].

In conclusion, the best fibrillar formation seems to occur for the intermediate outputs.

Blends with 10 wt % LCP and 4 wt % compatibiliser E

INFLUENCE OF PROCESSING TEMPERATURE

For the blend with compatibiliser E, the increase of the average diameters by the use of an higher processing temperature is not so obvious as the one observed for the blends with compatibiliser C (figures 7.8 (a) and 7.8 (b)).

In fact, at the beginning of the process (valve 4) the average diameters between the blends processed at 220 and 240 °C are almost indistinguishable. Another point of remark is that at valve 6 the average diameters are lower for 240 than for 220 °C (6.59 and 6.39 µm, for the lower and for the higher temperature, respectively) which is somewhat unexpected (figure 7.9 (a) and 7.9 (b)), since by the increase of the temperature one expected an increase of the average diameters.

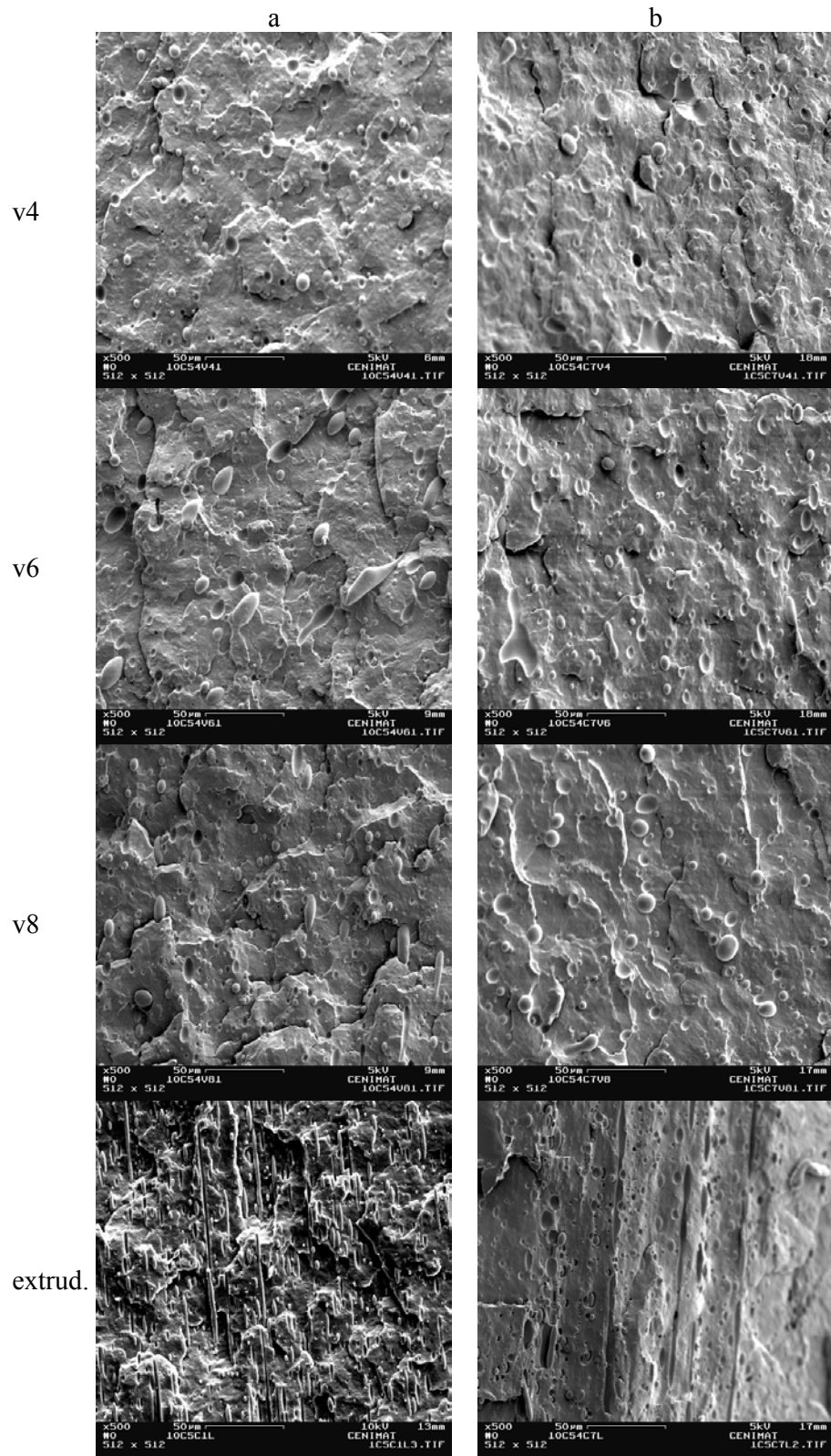
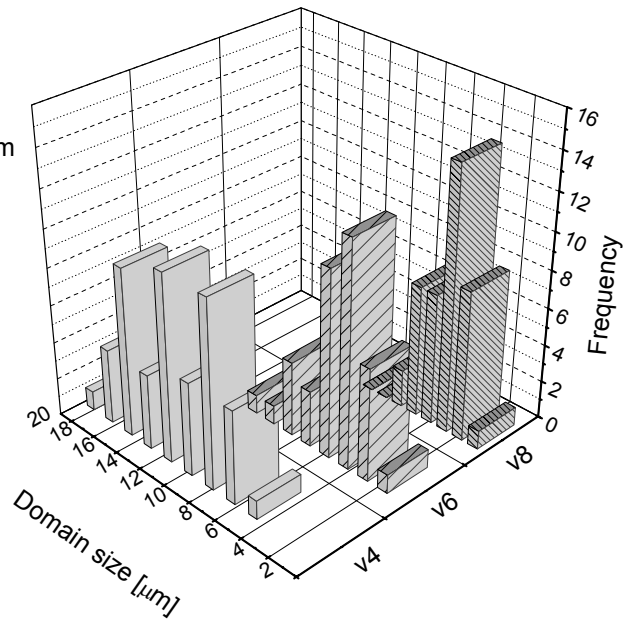


Figure 7.8 - SEM images for blends with 10 wt % LCP and 4 wt % compatibiliser E, processed at 220 °C (a) and 240 °C (b) - Magnification of x500, for all images.

comp. E

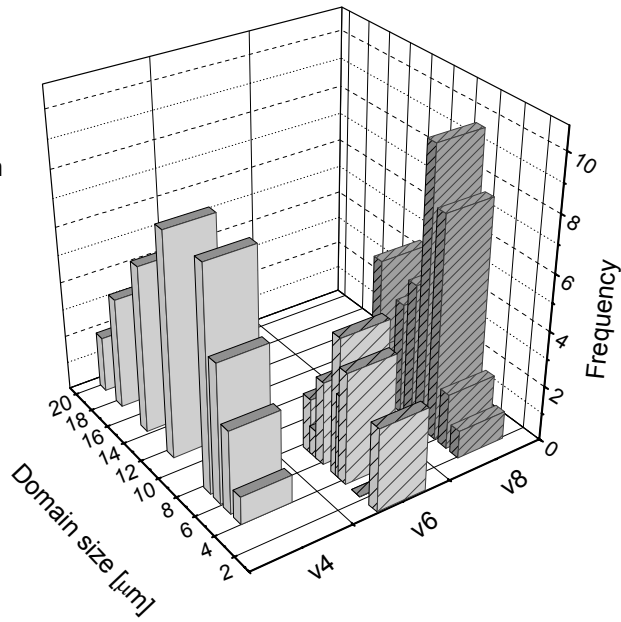
T = 220 °C
N = 150 rpm
Q = 4 kg/h



a

comp. E

T = 240 °C
N = 150 rpm
Q = 4 kg/h



b

Figure 7.9 - Particle size distribution along the extruder length for blends with 10 wt % LCP and 4 wt % compatibiliser E, processed at 220 °C (a) and 240 °C (b). *original data in appendix III

For 220 °C (see figure 7.9 (a)) a progressive elongation and break-up seems to occur as proceeding along the extruder length (the average diameters decrease progressively, 12.2 µm, 6.59 µm and 4.53 µm, for valves 4, 6 and 8), while for 240 °C (figure 7.9 (b)) there is a decrease of the average diameters from valve 4 to valve 6 (from 7.25 µm to 6.39 µm), followed by an increase from valve 6 to valve 8 (from 6.39 µm to 7.23 µm), arising maybe, from coalescence processes. Additionally, it is clear that for the blend with compatibiliser E a higher processing temperature (240 °C), results in a much lower degree of fibrillation when compared with the one observed for 220 °C (figure 7.8 (b)), the majority of the LCP structures remaining in the form of droplets. Higher temperatures result in lower viscosities for the pure components and thus into a lower intensity of the shear stress, which can explain the absence of fibrils for the blend with compatibiliser E processed at a higher temperature.

Table 7.3- Temperatures measured along the extruder length for different processing conditions (Blend with 10 wt % LCP, 4 wt % comp. E).

Processing conditions		Position in the extruder			
		v4	v6	v8	extrudate
Q (kg/h) (T = 220 °C, N = 150 rpm)	2	232.9	233.4	237.1	238.1
	4	230.1	231.8	236.3	237.2
	8	228.1	223.6	231.1	233.9
N (rpm) (T = 220 °C, Q = 4 kg/h)	100	228.5	229.1	233.4	235.1
	150	230.1	231.8	236.3	238.4
	200	232.4	229.4	237.1	240.2
T (° C) (Q = 4 kg/h, N = 150 rpm)	220	230.1	231.8	236.3	240.2
	240	245.4	247.1	248.4	248.8

INFLUENCE OF SCREW SPEED

For the blend with compatibiliser E it is not so clear, but it looks like a better dispersion and a higher fibrillar formation at the end of the process occurs for the lower screw speeds (figures 7.10).

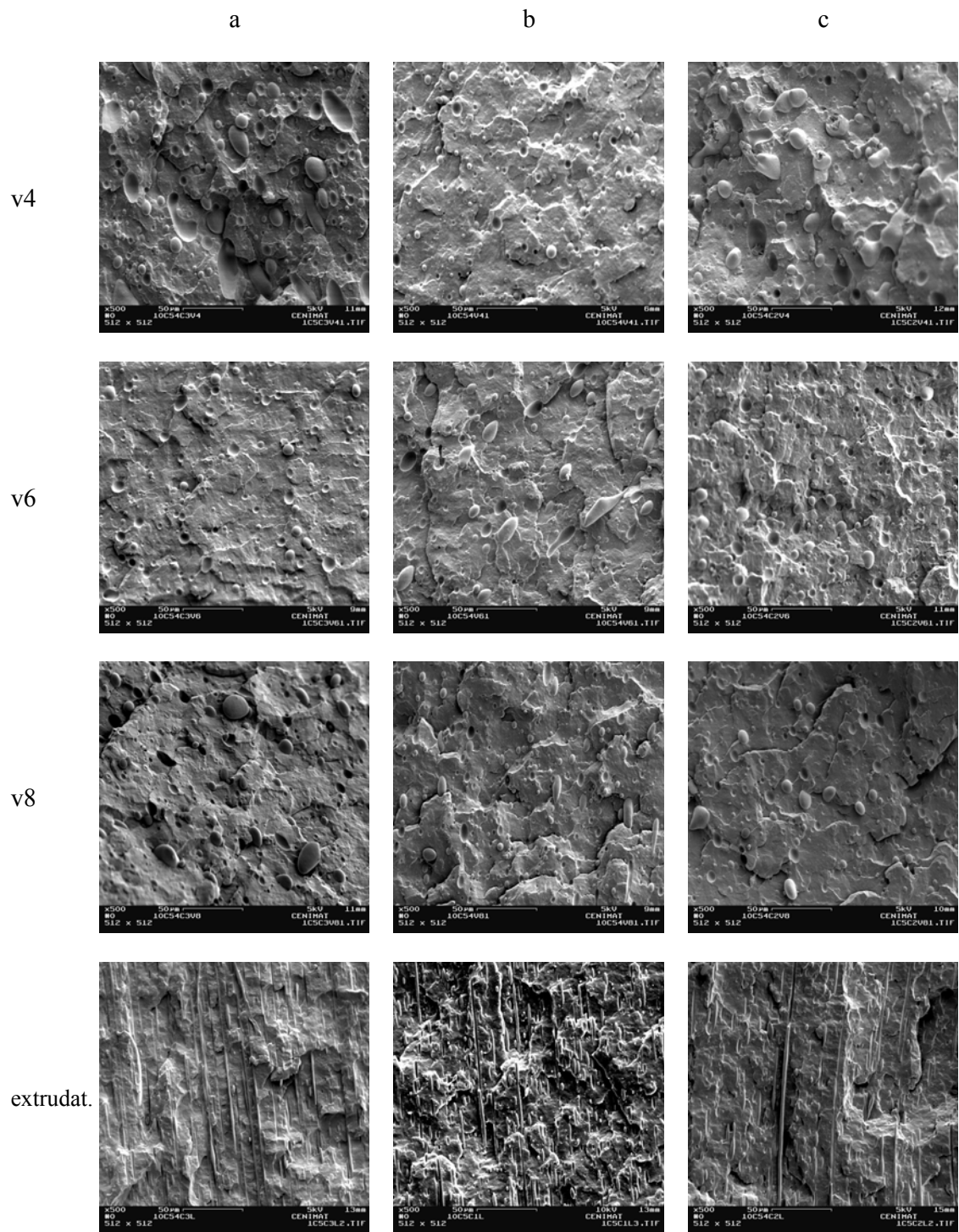


Figure 7.10 - SEM images for blends with 10 wt % LCP and 4 wt % compatibiliser E, processed at 100 rpm (a), 150 rpm (b) and 200 rpm(c) - Magnification of x500, for all images.

At valve 4 the main difference between the blends processed at 100 and 200 rpm is that in the former the average diameter of the droplets is lower than that of the later (8.0 μm

and 8.7 μm , for 100 and 200 rpm) . After this point (most precisely at the beginning of the kneading blocks, valve 6), the temperature inside the extruder was around 229.4 $^{\circ}\text{C}$ for a screw speed of 200 rpm (therefore, lower than previously, at valve 4, 232.4 $^{\circ}\text{C}$), which might have induced a slight increase of the viscosity. Under these conditions, an easier deformation and break-up of the LCP droplets would be expected for the higher screw speeds (comparing with 100 and 150 rpm, for which one observed an increase of the temperature between valve 4 and valve 6). Nevertheless, at valve 6 the average diameters are slightly higher for 200 than for 150, which, by its turn is higher than for 100 rpm (5.7, 6.6 and 6.8 μm for 100, 150 and 200 rpm, respectively).

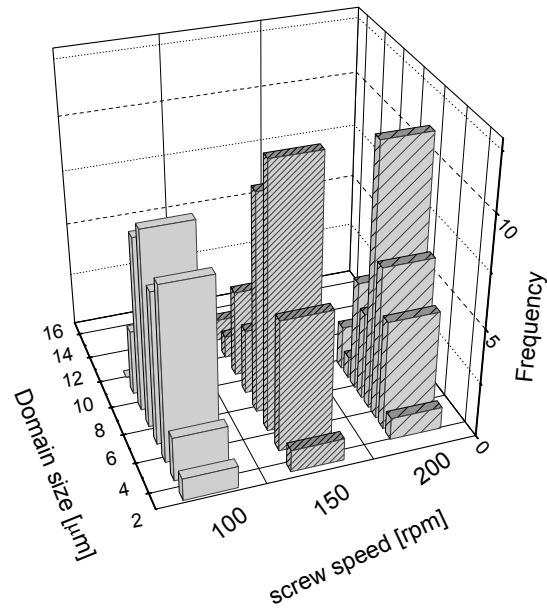
The question is now to determine differences between blends processed at 100 and 150 rpm (figure 7.11(a)). At valve 6, the diameter distributions for 100 rpm is slightly deviated to higher diameters relatively to that of 150 rpm. However, the average diameters are around 5.7 and 6.6 μm , to 100 and 150 rpm, respectively. At valve 8 the average diameter is higher for the blend processed at 100 than for 150 rpm (5.6 μm against 4.5 μm), however, for the former the majority of the LCP diameters are around 4.5 μm , while for the later the LCP diameters are distributed in a wider range, between 3 and 6 μm (figure 7.11 (b)). At the final extrudates for 150 rpm fibrils and droplet-like structures are present, while for 100 rpm, only fibrils exist.

comp. E

T = 220 °C

Q = 4 kg/h

v6



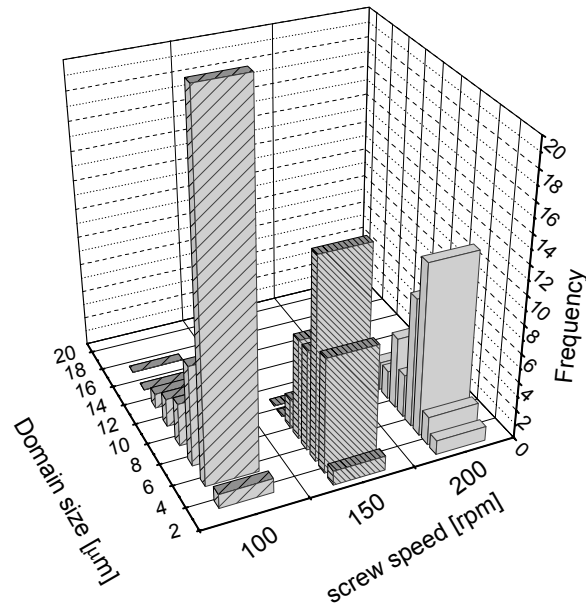
a

comp. E

T = 220 °C

Q = 4 kg/h

v8



b

Figure 7.11 - Particle size distribution for blends with 10 wt % LCP and 4 wt % compatibiliser E, processed at 100, 150 and 200 rpm at valve 6(a) and at valve 8(b). *original data in appendix III

Additionally, for 100 rpm one expects a more homogeneous morphology, since the fibrils were the result of the deformation of a range of droplets with a much narrower distribution of diameters, than that observed for 150 rpm.

Furthermore, it should be mentioned, that a temperature increase occurs from valve 6 to valve 8, the intensity of which is much higher for the higher screw speeds, as seen in table 7.3 (4.3, 4.5 and 7.7 °C for 100, 150 and 200 rpm, respectively). Therefore, and as a result of the temperature increase promoted by the higher shear rates and shear stresses, together with a decrease of the residence time with the increase of the screw speed (that, as already pointed out, promote coalescence and difficult break-up), an increase of the LCP diameters might occur downstream in the extruder (figure 7.11 (b)) and after the kneading blocks (after valve 8), leading to the formation of thicker fibrils for the higher screw speeds.

Similarly to what was seen for the blends with compatibiliser C, the fibrillar formation seems to be enhanced by the use of lower screw speeds, *i.e.*, 100 rpm.

INFLUENCE OF OUTPUT

For compatibiliser E the formation of fibrillar structures is enhanced for the intermediate outputs (4 kg/h); for the lower outputs (2 kg/h), a higher temperature (see table 7.3) and possibly, decrease of the viscosity, lead to an improvement of the coalescence processes, as seen in figure 7.12.

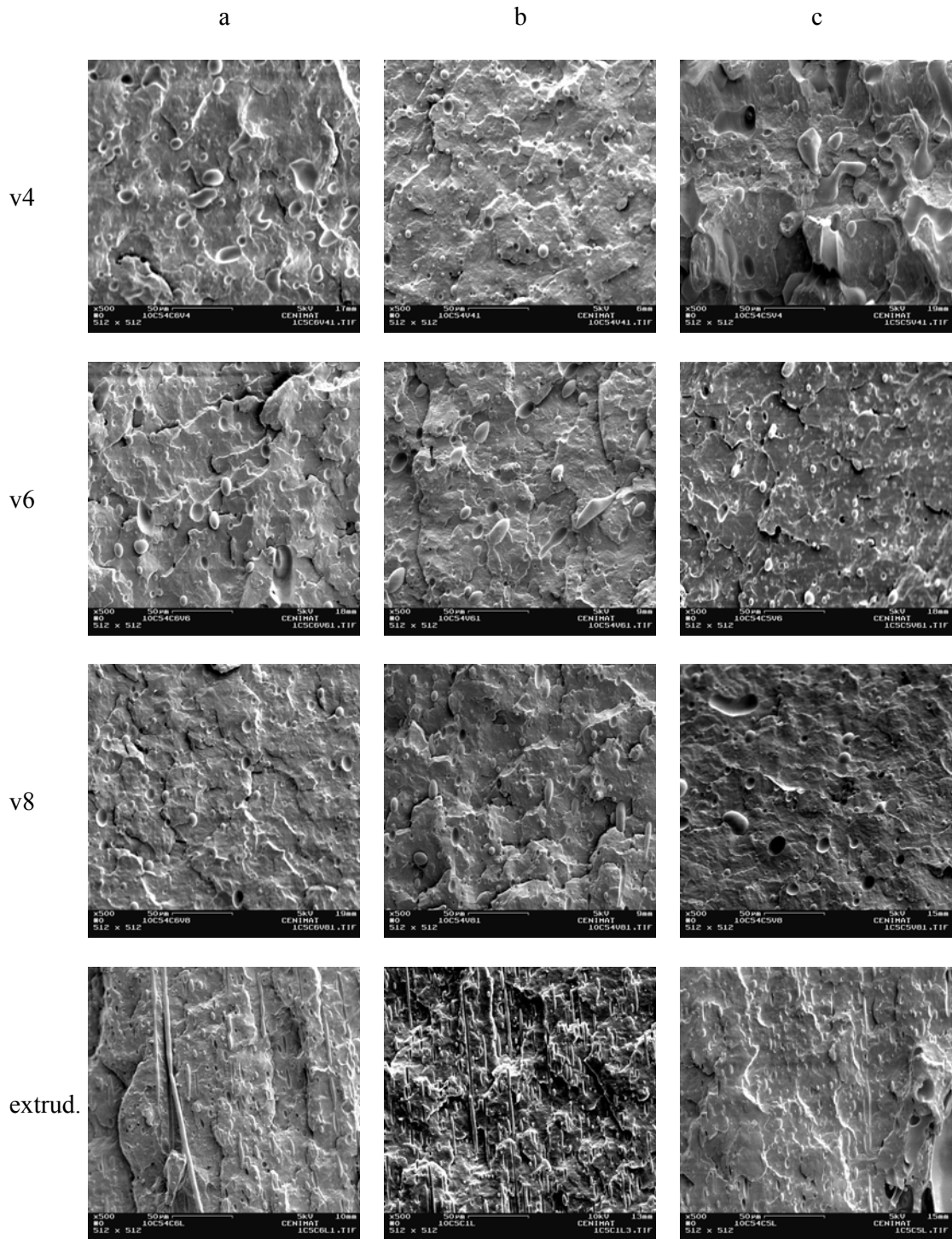


Figure 7.12 - SEM images for blends with 10 wt % LCP and 4 wt % compatibiliser E, processed at 2 kg/h (a), 4 kg/h (b) and 8 kg/h (c) - Magnification of x500, for all images.

Increasing the output usually leads to a decrease of both temperature and residence time (see table 7.3). The effects of increasing output on the dispersed phase diameters are

usually opposite to those observed for higher screw speeds. According to theoretical and experimental studies [Majumdar 1997, Utracki 1991], the use of higher outputs gives origin to a decrease of the “length” of the dispersed phase, which will result in an increase of their diameter. Since the time needed for break-up depends on the latter parameter, it can be stated that increasing the output should result in an increase of the time needed for break-up, and thus on a dispersed phase with higher diameters. However, and contrary to our expectations, the increase of the output to 8 kg/h had an important repercussion on the dispersive mixing at the beginning of the region of higher shear rates and deformations (at valve 6, more precisely). At this point (beginning of the kneading-blocks region, valve 6) a clear decrease of the LCP droplets occurred (figure 7.13), resulting in a coarsening of the morphology and in an improvement of the distribution of the dispersed phase structures, comparing with those observed for the lower outputs (2 and 4 kg/h). One possible explanation for this behaviour is the fact that at this point a decrease of the temperature (see table 7.3) occurred in comparison with that of valve 4, contrary to what was observed for the lower outputs, for which an increase of the temperature between valve 4 and valve 6 occurred. The decrease of temperature from valve 4 to valve 6, for the higher outputs, might result in a slight increase of the viscosity, and thus an improvement of the dispersive mixing.

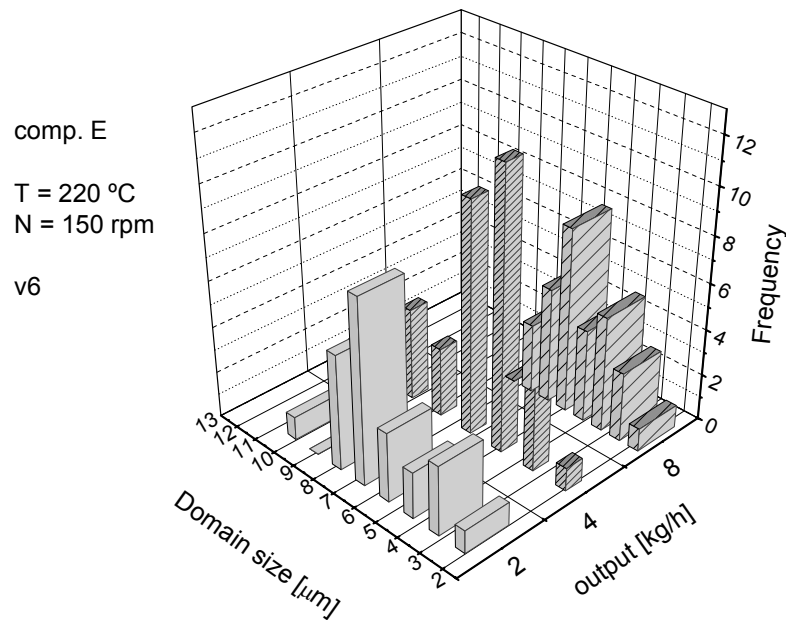
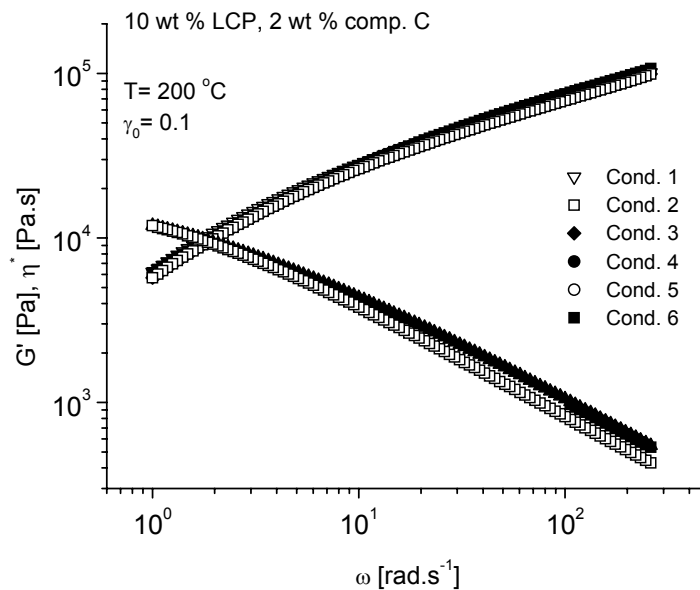


Figure 7.13 - Particle size distribution for blends with 10 wt % LCP and 4 wt % compatibiliser E, processed at 2, 4 and 8 kg/h at valve 6. *original data in appendix III

Nevertheless, after the kneading blocks region, the average diameters of the dispersed phase are higher than those observed for the lower outputs (at valve 8 the average diameters are 5.53, 4.53 and 6.96 µm, for 2, 4 and 8 kg/h, respectively). If one considers that for higher outputs, the residence time is lower and that the time needed for break-up is higher than for lower outputs, than it can be anticipated an increase of the dispersed phase diameters. Adding this to the fact that an increase of the temperature occurs from valve 6 to valve 8, the intensity of which is highest for the higher outputs (an increase of about 8 °C occurs for 8 kg/h, against 4 and 5 °C for 2 and 4 kg/h), a higher increase of the droplets diameters as a result of the coalescence at the kneading blocks region, is anticipated for the higher outputs (8 kg/h), as seen in figure 7.12. Using a higher output (8 kg/h) results in the absence of significant number of fibrils in the final extrudates, the majority of the LCP structures, remaining in the form of droplets (figure 7.12). The use of intermediate outputs seems to be the condition that favours the fibrillar formation.

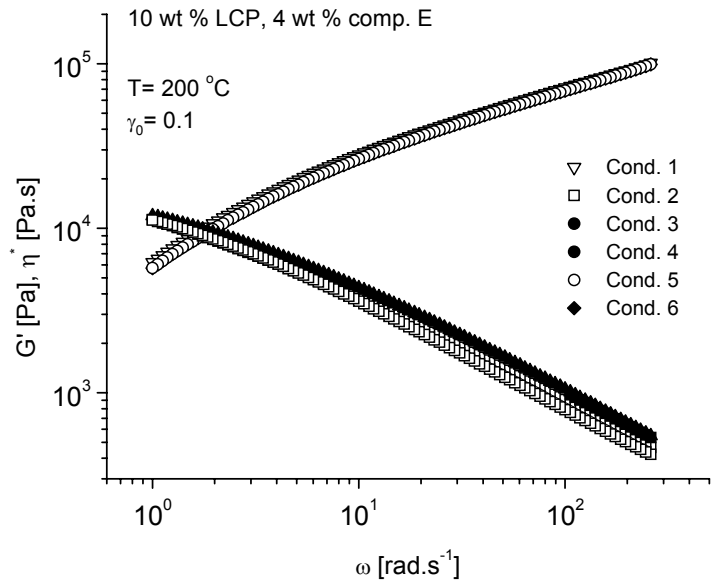
RHEOLOGICAL CHARACTERISATION

As already seen in sub-chapter 4.2, the increase of the temperature for non-compatible systems leads to very slight differences in terms of shear viscosity of the final extrudates (see figure 4.39 to 4.41). The use of FT-Rheology was in that case, useful to distinguish between blends (extrudates) processed at 220 and 240 °C (figure 4.42 to 4.44). In this case, however, and unexpectedly, none of the available rheological techniques (steady and transient shear, oscillatory shear, LAOS) allowed to distinguish between blends processed at different processing temperatures, as seen in figures 7.14 and 7.15.



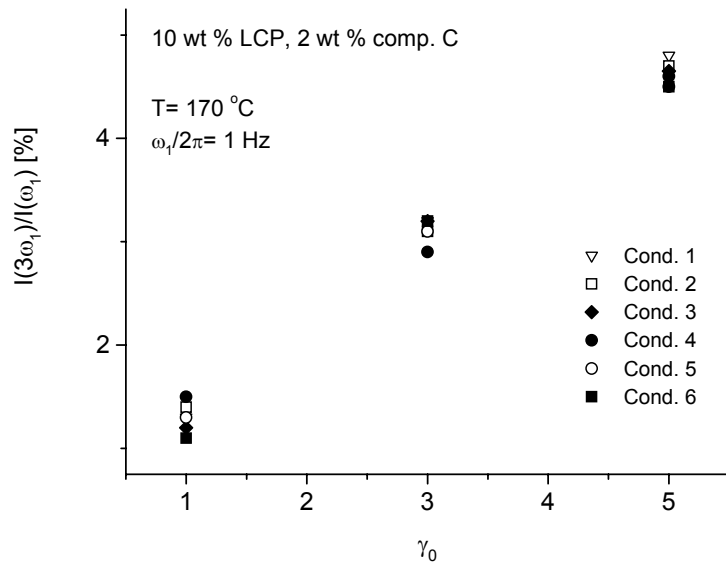
a

Figure 7.14 (a) –Complex viscosity and storage modulus for different processing conditions for the blend with 2 wt % compatibiliser C (a) at 200 °C.



b

Figure 7.14 (b) –Complex viscosity and storage modulus for different processing conditions for the blend with 4 wt % compatibiliser E (b) at 200 °C.



a

Figure 7.15 (a) – Non-linear character for different processing conditions for the blend with 2 wt % compatibiliser C (a) at 170 °C.

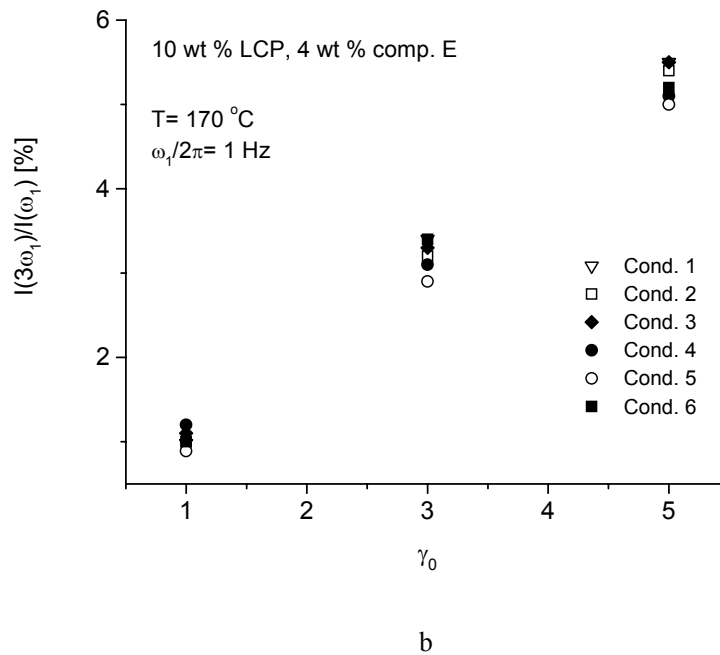


Figure 7.15 (b) – Non-linear character for different processing conditions for the blend with 4 wt % compatibiliser E (b) at 170 °C.

In any case it should be considered that the increase of the temperature often results in a decrease of the viscosity ratio, which will be disadvantageous for the deformation of LCP droplets and subsequent formation of fibrillar structures after crossing the die. As expected, the increase of the temperature from 220 to 240 °C resulted in a clear decrease of the viscosity ratio (figure 7.16), which might explain the differences in terms of morphology seen between the two processing temperatures.

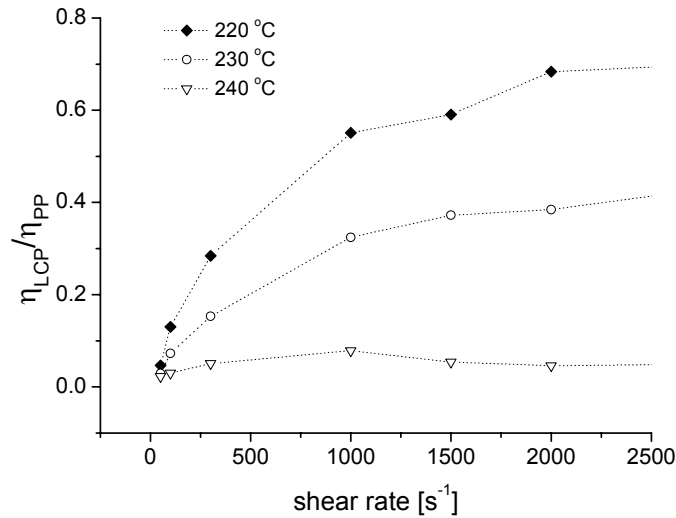


Figure 7.16 - Viscosity ratio between matrix and dispersed phase at 220, 230 and 240 °C. Lines are guides to the eyes.

Therefore, an enhancement of the fibrillar formation was observed (as seen in figures 7.2 and 7.8 (a) and (b)) and thus a higher mechanical improvement for the blends processed at a lower temperature is expected.

In terms of the influence of the screw speed employed on the rheological properties of the final extrudates, and similarly to the previous case (different processing temperatures), one could not make any clear distinction in terms of rheological properties of the extrudates, resulting from a processing done at 100, 150 and 200 rpm (conditions 3, 1 and 4 in figure 7.14 and 7.15). Nevertheless and taking into account that the increase of the screw speed leads to an increase of the shear rate, one can attribute the differences in terms of morphology with differences in the viscosity ratio, arising from different temperatures for the different screw speeds (see tables 7.2 and 7.3).

Therefore, if one has the objective of study the influence of the use of different screw speeds on the final properties of the blends, one should thus be aware of the real temperature that is inside each location in the extruder (as seen in table 7.2). The monitoring of the temperature allowed to establish that, independently of the screw speed, the temperature

increases as proceeding along the extruder (with some exceptions, as seen in tables 7.2 and 7.3), the lowest temperatures being observed for the lowest screw speeds (for all the valves and for the extrudates). This is very important, since for lower temperatures higher viscosity ratios and thus an easier deformation of the LCP droplets are expected. These observations are valid for both kinds of compatibilised systems.

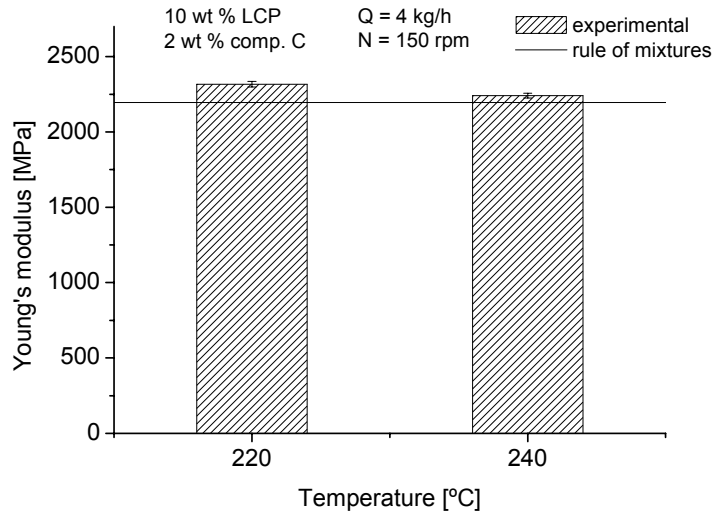
Finally, and as seen for different processing temperatures and different screw speeds, no rheological differences were seen between blends processed at different outputs (2, 4 and 8 kg/h, conditions 5, 1 and 6, in figures 7.14 and 7.15).

MECHANICAL CHARACTERISATION

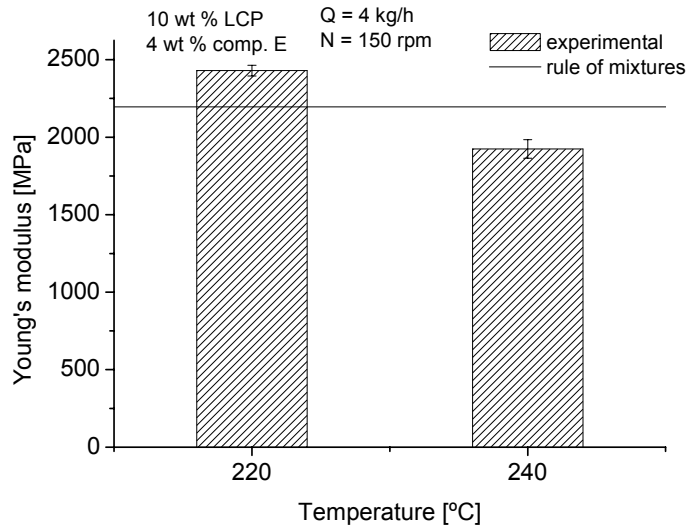
Before starting the analysis it is appropriate to keep in mind that the injection moulding process (from which one obtained the tensile specimens used for the mechanical analysis) induces an extra thermo-mechanical history, which is supposed to alter the morphology with respect to the one previously obtained for the final extrudates. Nevertheless, the influence of the processing conditions during extrusion on the morphological properties, can still be correlated with the mechanical properties here described since, independently of the material, all the injection moulded specimens were produced by applying the same processing conditions.

INFLUENCE OF PROCESSING TEMPERATURE

As already expected the processing temperature has a significant effect on the mechanical properties of compatibilised LCP/TP blends. The use of higher processing temperatures is detrimental for the formation of fibrillar structures, since these conditions lead to a decrease of the viscosity that favours the coalescence processes. As a consequence, the mechanical enhancement is higher for the blends processed at 220 °C than for those processed at an higher temperature (240 °C), as depicted in figure 7.17.



a



b

Figure 7.17 - Young's modulus for blends processed at 220 and 240 °C, with 10 wt % LCP and 2 wt % compatibiliser C (a) and 4 wt % compatibiliser E (b).

This was already verified for non-compatibilised blends, previously studied (chapter 4). Another point of remark, is that the Young's modulus is above the predicted by the rule of the mixtures for the blends processed at 220 °C, in opposition to the observed for the higher temperatures (except for compatibiliser C, for which the Young's modulus is above the rule of mixtures, independently of the processing temperature). The influence of the processing

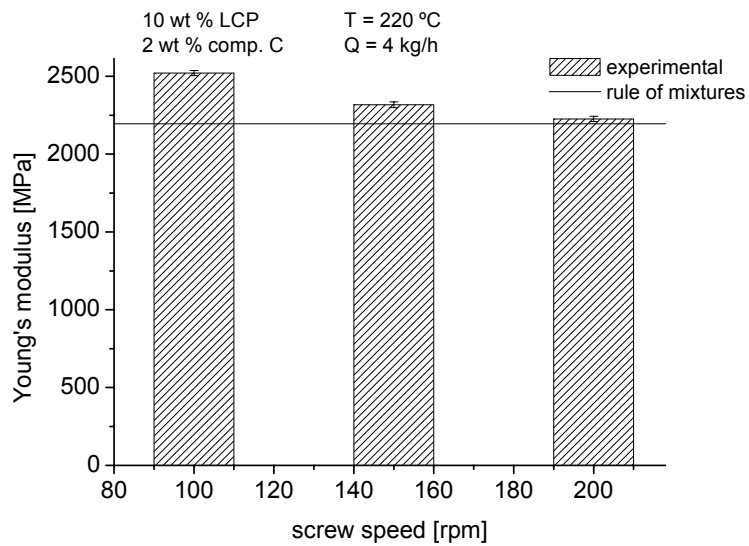
temperature on the tensile strength was more severe for the blends containing compatibiliser E than for the blends containing compatibiliser C. In the former case, the fibrillar formation did not occur at all for the higher processing temperature (figure 7.12 (a), 7.12 (b)), while for the later thicker fibrils were formed in comparison with those obtained for the blends processed at 220 °C (figures 7.2 (a) and 7.2 (b)). Considering these results one should keep in mind that a special care must be taken on the choice of the processing temperature, since this might influence significantly the final morphology, and, thus the desired mechanical performance.

INFLUENCE OF SCREW SPEED

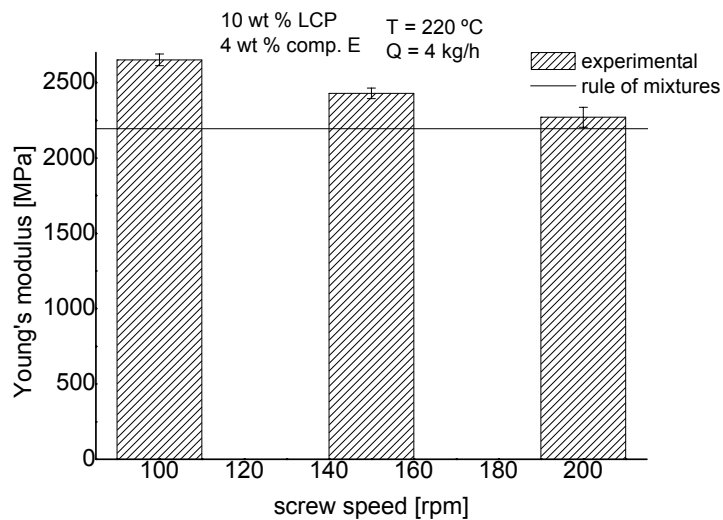
From the mechanical analysis it is clear that the best mechanical properties were obtained for those blends processed at a lower screw speed (figure 7.18). As already pointed out, a lower screw speed leads to lower shear rates, and a lower deformation would be expected under these conditions.

However, the residence time is increased and the shear stress provided is enough to ensure the deformation of the LCP structures, *i.e.*, basically the lower shear rates are fairly compensated by the increase of the time available for deformation and thus a higher fibrillar formation is obtained. Additionally the temperatures involved under lower screw speeds are normally lower than those of higher screw speeds, which will additionally lead to a decrease of the viscosity ratio and thus an improvement of the fibrillation.

Another point worth of remark, is that the Young's modulus is above the predicted by the rule of mixtures in all the cases, independently of the screw speed employed, as depicted in figure 7.18. These observations are valid for both blends, with compatibiliser C and with compatibiliser E.



a



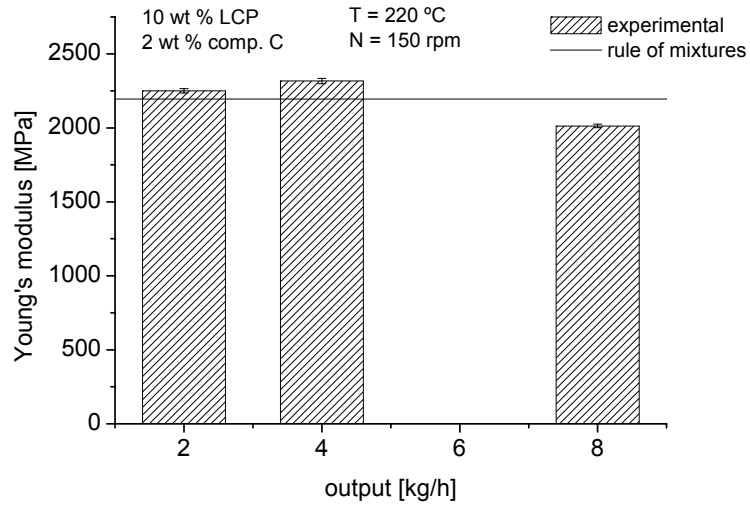
b

Figure 7.18 - Young's modulus for blends processed at 100, 150 and 200 rpm, with 10 wt % LCP and 2 wt % compatibiliser C (a) and 4 wt % compatibiliser E (b).

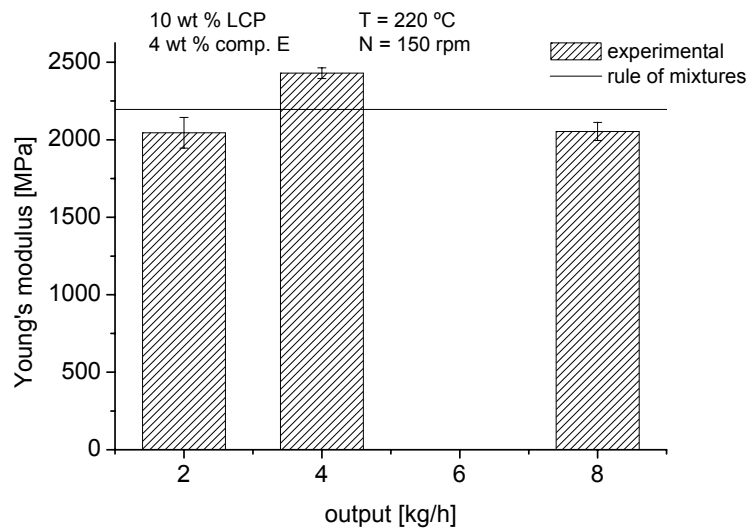
INFLUENCE OF OUTPUT

The mechanical analysis revealed that the higher Young's modulus was observed for those blends processed at an output of 4 kg/h, as depicted in figure 7.19. This was verified for both blends and seems therefore to be independent of the compatibiliser used. A lower output (2 kg/h) leads to a higher shear stress, thus higher temperature, which will give rise to an

improvement of the coalescence and to a broadening of the morphology that will result in a lower fibrillar formation.



a



b

Figure 7.19 - Young's modulus for blends processed at 2, 4 and 8 kg/h, with 10 wt % LCP and 2 wt % compatibiliser C (a) and 4 wt % compatibiliser E (b).

CONCLUSIONS

The formation of fibrillar structures and thus, the mechanical enhancement provided in the direction of the flow are largely dependent on the processing conditions employed,

namely screw speed, output and temperature. Therefore, if one has as main task the optimisation of LCP/TP blends, one should understand the influence of each parameter on the final properties, and if possible, correlate it with the kinetic of mixture in each step of the extrusion process. The control of the processing parameters here studied revealed to be crucial for the optimisation of LCP/TP blends. The main findings were that:

(i) lower temperatures provide higher shear stresses and give rise to a lower viscosity ratio, thus improving the deformation of the LCP structures and the formation of fibrils. Therefore, blends processed at 220 °C possess better mechanical properties than those processed at 240 °C

(ii) lower screw speeds result in lower shear rates (which will intuitively be disadvantageous for the break-up), lower temperatures (and thus, higher viscosity ratios) along with higher residence times (in principle, the two later parameters, favour the break-up processes). Considering the results of this work, one may state that the parameters that seem to control in this case, are the residence time and the temperature, since even for lower shear stresses, one observes an improvement of the deformation and break-up for the lower screw speeds and a better fibrillation, with consequent mechanical improvement.

(iii) intermediate outputs are required in order to achieve a considerable fibrillar formation. Both, higher and lower outputs lead to a much lower degree of mechanical enhancement.

According to the previous considerations and considering the mechanical measurements it can be concluded that the best mechanical properties were obtained for the following processing conditions: 220 °C, 100 rpm and 4 kg/h. This was verified for both kinds of blends, with compatibiliser C and with compatibiliser E.

It is clear from the present study that some factors, namely higher screw speeds, which are intuitively believed to improve the degree of dispersive and distributive mixing, may actually have an opposite effect in compatibilised systems, like those studied in this work. Indeed, the application of an intensive mixing (by the increase of the screw speed or by the addition of mixing elements), may induce an increase of the temperature, which can promote coalescence and lead to the formation of significantly larger particles. Thus, in addition to shear, one should provide a higher degree of elongational forces and at the same time, an increase of the residence time. Both cases seem to be a good strategy to achieve a well-fibrillated blend morphology and a significant mechanical enhancement.

References

- [Boersma] A. Boersma and J. Van Turnhout *Polym.* **40**, 5023 (1999)
- [Bordereau 1992] V. Bordereau, Z. H. Shi, L.A. Utracki, P. Sammut and M. Carrega *Polym. Eng. Sci.* **32**, 1846 (1992)
- [Chin 1979] H. B. Chin and C. D. Han *J. Rheol.* **29**, 557 (1979)
- [Covas 2001] J. A. Covas, O. S. Carneiro and J. M. Maia *Intern. J. Polym. Mat.* **50**(3-4): 445 (2001)
- [Duarte 2004] A. Duarte, M. T. Cidade, S. Filipe, C. B. Correia, J. Clarke and J. C. M. Bordado, *to be published*
- [Filipe 2004a] S. Filipe, M. T. Cidade, M. Wilhelm and J. M. Maia *Polym.* **45**, 2367 (2004)
- [Filipe 2004c] S. Filipe, J. M. Maia, A. R. Menon, A. Duarte, C. R. Leal and M. T. Cidade, *J. Polymer Engineering*, *submitted* (November 2004)
- [Filipe 2004d] S. Filipe, M. T. Cidade, M. Wilhelm and J. M. Maia, *J. Appl. Polym. Sci.*, *submitted* (August 2004)
- [Han 1981] C. Han, *Multiphase Flow in Polymer Processing*, Academic Press, New York, (1981)
- [Heino 1994] M. T. Heino, P. T. Hietaoja and T. P. Vainio, J. V. Seppälä *J. Appl. Polym. Sci.* **51**, 259 (1994)

- [Luciani 1996] A. Luciani, M. F. Champagne and L. A. Utracki, *Polym. Netw. Blend.* **6**(1), 41 (1996)
- [Majundar 1997] B. Majundar, D. R. Paul and A. J. Oshinski, *Polym.* **38**, 1787 (1997)
- [Nishio 1991] T. Nishio, Y. Suzuki, K. Kojima and M. Kakugo, *J. Polym. Eng* **10**, 123 (1991)
- [Potente 2000] H. Potente, M. Bastian, A. Gehring, M. Stephan and P. Potschke *J. Appl. Polym. Sci.* **76**, 708 (2000)
- [Rauwendaal 1990] C. Rauwendaal, *Polymer Extrusion*, Hanser Publishers, Munich, Germany (1990)
- [Serpe 1990] G. Serpe, J. Jarrin and F. Dawnas, *Polym. Eng. Sci.* **30**, 553 (1990)
- [Shi 1992] Z. H. Shi and L. A. Utracki, *Polym. Eng. Sci.* **32**, 1834 (1992)
- [Sundaraj 1995] U. Sundaraj and C. W. Macosko *Macromol.* **28**, 2647 (1995)
- [Utracki 1991] L. A. Utracki, Ed., *Progress in Polymer Science, Two-Phase Polymer Systems*, Hanser Publishers, Munich, Germany (1991)
- [Todd 1998] D. B. Todd, Ed., *Plastics Compounding*, Hanser Publishers, Munich, Germany (1998)
- [Wu 1987] S. Wu *Polym. Eng. Sci.* **27**, 335 (1987)

8 GENERAL CONCLUSIONS

In this thesis a set of experiments was set up in order to analyse the final microstructure and its development along the extruder length, of compatibilised and non-compatibilised blends of a liquid crystalline polymer, Rodrun LC3000 and a thermoplastic, Polypropylene. The experiments described above included rheological measurements (under oscillatory, steady and transient shear and large amplitude oscillatory shear), morphological measurements, performed by means of Scanning Electron Microscopy (to samples collected at different locations along the extruder length and to the final extrudates) and mechanical measurements that included impact, tensile and flexural experiments.

Based on the experiments mentioned above some correlations were established between the morphological properties (as developed along the extruder length and at a final stage, at the extrudates) and the rheological and mechanical properties of compatibilised and non-compatibilised LCP/TP systems. The investigations described above led to a more in deep knowledge about these systems. The main conclusions are described in this chapter.

The first two main objectives of this thesis were the preparation of LCP/TP systems and their characterisation in terms of the kinetic of mixture processes, by resorting to new and more insightful techniques, than those used in the past to analyse this kind of systems. The most important conclusions arising from this analysis are described bellow.

In compatibilised and non-compatibilised systems, such as those in study, there is a straight relationship between the way how the morphology evolves as they are being processed by extrusion, and their final morphology, which will directly define their mechanical performance. In line with this statement, powerful and sensitive techniques need to be employed, in order to understand the influence of several parameters, such as material's properties, type of compatibiliser and processing conditions on the morphological development along the extruder length. The analysis was performed resorting to SEM measurements as well

as ordinary oscillatory rheology in order to monitor the evolution process. The later technique was quite effective for the analysis of non-compatibilised systems, for which both rheological and morphological evolution along the extruder axis occurred in a progressive way (chapter 4, sub-chapter 4.1). Nevertheless, in compatibilised systems the use of oscillatory shear under linear conditions revealed to be less sensitive and not efficient to distinguish between very similar microstructures (chapter 5, sub-chapter 5.1). Large Amplitude Oscillatory Shear revealed to be a powerful and extremely sensitive technique for the analysis of the extrusion of all the LCP/TP systems (compatibilised and non-compatibilised) at the different stages of the process (chapter 4 and chapter 5, sub-chapters 4.1 and 5.1).

In terms of the final extrudates the attention was essentially focused on the behaviour under non-stationary conditions (transient shear and non-linear oscillatory shear), which has not been suitably studied before. These kind of measurements assessed successfully to changes in the processing conditions (chapter 4 and chapter 5, sub-chapters 4.2 and 5.2) as well, changes in blend's composition namely, the type of compatibiliser and the LCP content, and were much more insightful than experiments performed under stationary conditions (chapter 4 and chapter 5, sub-chapters 4.2 and 5.2).

The results performed under transient shear revealed to be sensitive to the effectiveness of the compatibiliser- those blends for which one observed higher mechanical performance, were those for which one obtained higher initial stress overshoots and higher equilibrium values (chapter 4 and chapter 5, sub-chapters 4.2 and sub-chapter 5.2). The use of LAOS revealed to be sensitive to the compatibilisation process, higher values of the non-linear character being observed for those blends in which the compatibilisation was less effective, like for example, the blend with compatibiliser A and blends with low or excessive amount of compatibiliser (chapter 5, sub-chapter 5.2).

From this study it was possible to conclude that rheological experiments performed under non-stationary conditions, such as those performed by FT-Rheology, are much more sensitive to the changes in morphology that occur when the processing temperature is changed than rheological experiments under stationary conditions (chapter 4, sub-chapter 4.2).

Another important point to remark, is the influence of the screw and cylinder profiles on the final microstructure and thus, on the mechanical performance of LCP/TP systems. Quite unexpected was the final morphology and mechanical properties obtained by the use of a configuration with an increased number of mixing elements, distributed along the extruder length (configuration 2, chapter 4, sub-chapter 4.3). In fact, one would intuitively anticipate an improvement of the degree of mixing and an enhancement of the fibrillar formation (most precisely, the formation of fibrils with higher L/D ratio, which would lead to an increase of the mechanical performance). However, for non-compatibilised systems, such as those investigated in this part of the work, the utilization of this kind of screw configuration, with a high number of mixing elements (kneading blocks) revealed to be disadvantageous. By the use of this type of configuration the decrease of the LCP diameters occurs at an earlier stage in the extrusion process, while for other screw configurations, with lower number of mixing elements, such as configuration 1, a progressive elongation and break-up occurs. After a minimum average diameter is reached, the droplets can no longer be deformed. In the absence of compatibiliser it is difficult to keep this microstructure (formed at the beginning of the process) until the die exit, the coalescence is not prevented and an increase of the average diameters occurs progressively, as proceeding along the extruder length. When a lower degree of mixing elements is used (like in configuration 1), the elongation and break-up occurred in a much more progressive way, which somehow helped to prevent the coalescence of the LCP droplets, in the later stages of the extrusion and until the die exit. Additionally, the use of a screw configuration with a higher number of mixing elements also led to an increase of the

viscous dissipation, leading to a decrease of the viscosity ratio, and thus to a more difficult deformation and break-up of the LCP structures (chapter 4, sub-chapter 4.3). As a result, the fibrils formed by the use of configuration 1, with a lower number of mixing elements, showed higher aspect ratios than those of blends processed with configuration 2 (chapter 4, sub-chapter 4.3).

Due to the great importance of extensional flow in industrial processes transient uniaxial extensional flow measurements were additionally performed. The main conclusions were that the extensional flow behaviour of LCP/TP blends is dependent on the applied strain rate: for the lower strain rates the increase of the LCP content leads to an increase of the deviation from the LVE (until 20 wt % LCP), while for the higher strain rates the opposite occurs. However, the behaviour of the blend with the highest LCP content (40 wt % LCP) is extremely different from the one observed for the blends with lower LCP contents. Independently of the strain rate employed, this material presents an extremely high strain hardening behaviour, possibly attributed to the presence of some residual crystallinity. Quite unexpectedly, it was not possible to establish relationships between the uniaxial transient extensional flow behaviour of compatibilised systems and their mechanical properties, the blends behaving similarly for different kinds of compatibilisation.

Another important task of this work was to increase the interest of the use of LCP/TP systems in industrial applications. The compatibilisation of LCP/TP blends often results in the improvement of tensile modulus at the expense of tensile elongation and toughness. One way to accomplish this objective was to find out a strategy to improve both strength and toughness in such systems. As a result of the research developed during this work, it was possible to conclude that in order to yield an improvement in tensile modulus and impact resistance, a compatibiliser with an elastomeric nature, such as compatibiliser E, should be employed.

The last part of this thesis was devoted to the optimisation of compatibilised LCP/TP systems, by changing the processing conditions during extrusion.

As already mentioned, the final morphology and thus, the final mechanical performance of LCP/TP systems are directly related with the way how the morphology evolves along the extruder length. It is also clear, that the later process is intimately related with the processing conditions employed, such as temperature, screw speed and output.

The control of the above mentioned processing parameters was performed and the main conclusions were that the use of lower processing temperatures leads to an increase of the applied shear stresses, and a higher viscosity ratio presented (chapter 7). Under these conditions an improvement of both deformation and break-up of the LCP structures is anticipated and a higher fibrillar formation is expected. Therefore, blends processed at 220 °C possess better mechanical properties than those processed at 240 °C

The use of such conditions which intuitively will allow a better degree of dispersive and distributive mixing, such as higher screw speeds, must be studied carefully. Considering the results of the present work, one should be aware that under the given conditions, the use of higher screw speeds are detrimental for the degree of mixing and for the break-up processes. In regions where a high number of mixing elements is present, the use of higher screw speeds may lead to an increase of the viscous dissipation, which will result in a decrease of the viscosity ratio (that is detrimental for the deformation and break-up in LCP/TP systems). Additionally, lower residence times are predicted for the higher screw speeds, meaning that the use of higher screw speeds is disadvantageous for the fibrillation in LCP/TP systems. In such blends it can be said that the residence time and the temperature are the most important parameters, since they are the ones that seem to control the morphological evolution (Chapter 7). The application of an intensive mixing (by the increase of the screw speed or by the addition of mixing elements), after the minimum particle size has been attained, can be disadvantageous for the

fibrillation process, since it might promote the coalescence and lead to the formation of significantly larger particles (which is due to the increase of the viscous dissipation by the increase of the screw speed at the kneading blocks region). It seems also that in compatibilised systems the main task is to achieve a considerable low average diameter at the beginning of the process. The second task is to keep this morphology until the die exit, so that at this point a significant fibrillar formation occurs, *via* the action of the intensive shear and elongational forces experienced at the die (chapter 7).

9 FUTURE WORK

The mechanical properties of the LCP/TP systems investigated in this study were analysed on specimens produced by an ordinary injection moulding technique. It should be pointed out that the mechanical enhancement was obtained in one direction (flow direction) at the expense of the other, due to the highly anisotropic character typical of liquid crystalline polymers. In order to overcome this drawback an advanced injection moulding technique must be employed, which takes advantage of the orientation of the LCP fibrils in both directions, in order that a mechanical improvement in both transversal and longitudinal direction is achieved.

The *off-line* rheological and morphological characterisation revealed to be highly insightful to the analysis of the kinetic of mixture in complex systems, such as LCP/TP blends. It is essential to extend this study to *on-line* measurements, exploiting the sensitivity of rheological techniques, namely oscillatory shear under linear and non-linear conditions (FT-Rheology) and extensional flow. By this analysis one expects not only to predict the final morphology, having by basis the morphological and rheological evolution, but also to control it, having as main task the optimisation of the mechanical performance.

From this work it was not possible to establish correlations between the transient uniaxial extensional flow behaviour and the mechanical properties, namely the Young's modulus. One possible alternative to better characterise the linear viscoelastic behaviour of these blends is resorting to stress relaxation measurements, after a step strain, which revealed in previous works to be quite successful in the characterisation of blends [Barroso 2003].

Further work should be done on the synthesis of graft and functionalised compatibilisers, which would improve even more the mechanical enhancement of these blends, increasing thus their industrial potential.

Finally, it is hoped that the analysis described above might be also appropriate to characterise and control in the future, other complex systems.

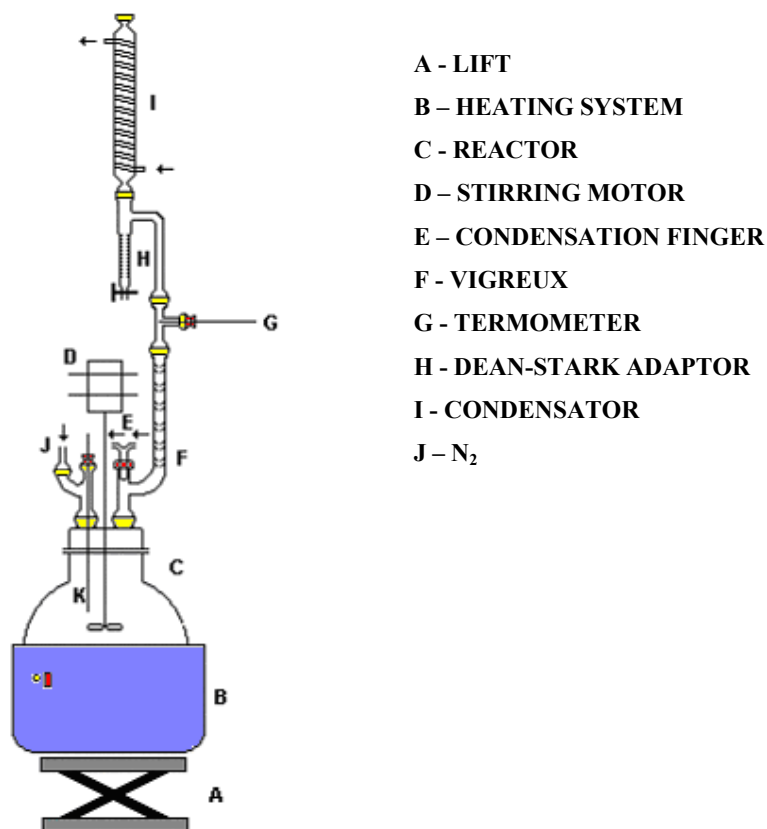
References

[Barroso 2003]

V. C. Barroso, Ph. D. Thesis, *Viscoelasticity of polymer melts in uniaxial extension flows* (2003)

APPENDIX I- SYNTHESIS OF COMPATIBILISERS A TO C

The chemical synthesis of compatibilisers A, B, C was performed using the same reactor, which is presented in figure A.I.1.



*cortesy of A.P. Duarte)

Figure A.I.1- Schematic representation of the reactor used for the synthesis of compatibilisers A, B and C.

The chemical synthesis of compatibiliser A was based on the following reactants: dodecanol, dimeric acid and an oligomeric polyester (with commercial name terolTM). The experimental procedure was performed as follows:

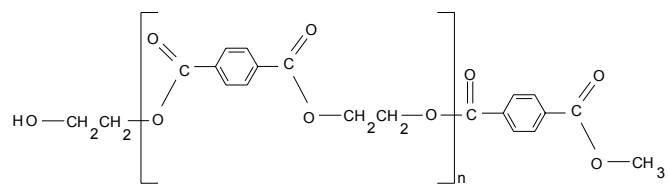
one mol of terolTM (A, in figure A.I.2) and one mol of dimeric acid (B in figure A.I.2) were placed together at 240 °C in a chemical reactor (2 dm³). The reaction was kept until the end of

formation of water, which took around 4 hours. After that, the temperature was lowered to 200 °C and after stabilisation of temperature, one mol of dodecanol (C in figure A.I.2) was added. After this step the temperature was again raised until 240 °C, and the reaction continued until the formation of a product (compatibiliser A, E in figure A.I.2) with a ph value lower than 1 (this part of the reaction took around 3 hours).

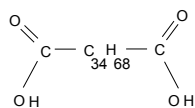
The reaction described above occurred according to the following reactional scheme:



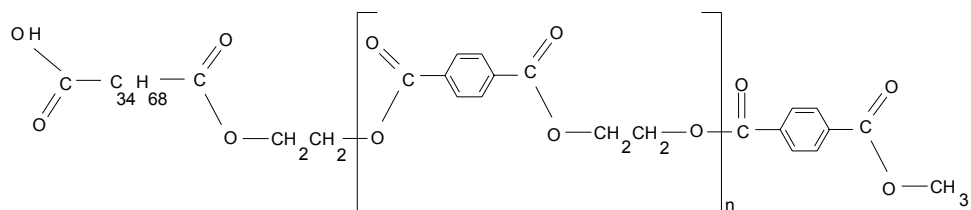
with A (oligomeric polyester, terolTM), B (dimeric acid) and C (intermediate product), D (dodecanol) and E (compatibiliser A). The chemical structures of A, B and C are described by the following chemical structures (figure A.I.2), while D and E are displayed in figure A.I.3.



A

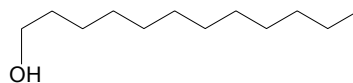


B

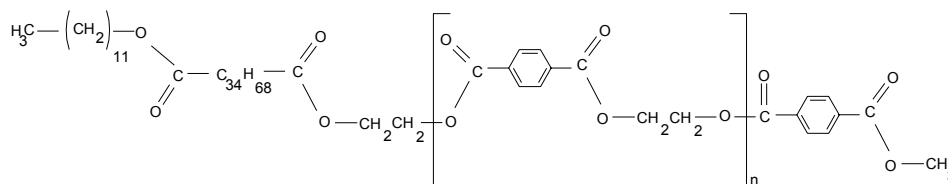


C

Figure A.I.2- Chemical structures of the oligomeric acid, terolTM (A), dimeric acid (B) and intermediate product (C).



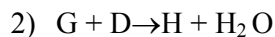
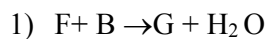
D



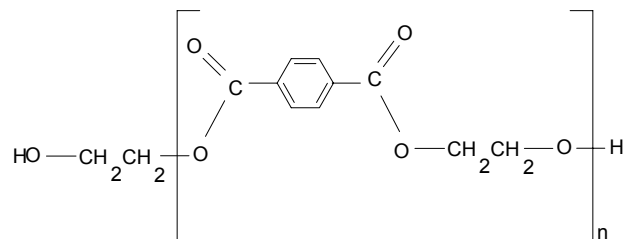
E

Figure A.I.3- Chemical structures of dodecanol (D) and compatibiliser A (E).

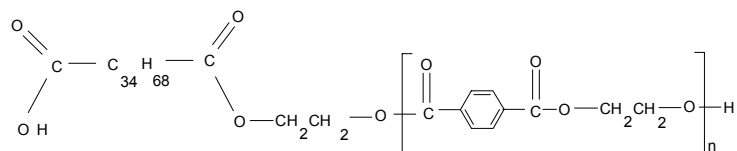
For the chemical synthesis of compatibiliser B, dodecanol, dimeric acid and polyethylene terephthalate (PET) were used. The reaction was carried out by mixing 0.04 mol of PET, 0.04 mol of dimeric acid and 50 ml of xylene. The mixture was kept in nitrogen atmosphere at 250 °C, until total removal of water. After this procedure 0.04 mol of dodecanol were added and the reaction proceeded at the same temperature. After complete elimination of water, the temperature was lowered until 200 °C and 0.05 % (with respect to the mass of dimeric acid) of a catalyst tetra-isopropyl ortho titanate were added to the resultant products and the reaction continued until achievement of a pH lower than 1. The reactional scheme for the preparation of compatibiliser B, can be described by:



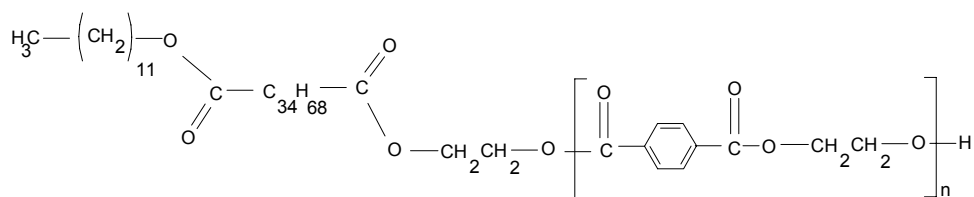
in which B and D are depicted in figures A.I.2 and A.I.3, respectively, whereas F (PET), G (intermediate product), and H (compatibiliser B) are depicted in figure A.I.4.



F



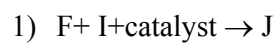
G



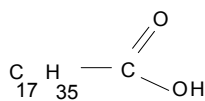
H

Figure A.I.4- Chemical structures of PET (F), intermediate product (G), and compatibiliser B (H).

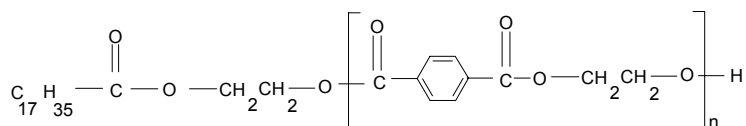
Compatibiliser C was prepared by mixing 0.04 mol of PET, 0.04 mol of TOFA (tall oil fatty acid) and 50 ml of xylene. This mixture reacted in nitrogen atmosphere at 250 °C until complete elimination of water. Afterwards 0.03 % of tetra isopropyl ortho titanate (catalyst) were added to the resultant products (the amount of catalyst was added with respect to the mass of TOFA). The reaction was finished after achievement of a ph lower than 1. The reactional scheme can be described as follows:



in which F (PET) is depicted in figure A.I.4, whereas I (TOFA), and J (compatibiliser C) are depicted in figure A.I.5.



I



J

Figure A.I.5- Chemical structures of TOFA (I) and compatibiliser C (J).

APPENDIX II- FOURIER TRANSFORM RHEOLOGY

The application of a single harmonic sinusoidal torque with a frequency ω_1 , the so-called fundamental frequency, can be described by the force balance of the kinematic, frictional and potential contributions, as well as the applied force or torque [Wilhelm 2000a]. The result can be expressed by a differential equation balance the force analogous to:

$$m\ddot{\gamma} + \eta\dot{\gamma} + k\gamma = A_0 \cdot \exp(i\omega_1 t) \quad (\text{II.1})$$

where

m	mass of the sample
η	viscosity (constant)
k	elastic modulus (constant)

Considering steady state, the mathematical solution of equation (II.1) for the strain can be expressed as:

$$\gamma(t) = \gamma_0 \exp(i(\omega_1 t + \delta)) \quad (\text{II.2})$$

in which $\frac{\omega_1}{2\pi}$ is the excitation frequency of the stress and δ is the characteristic phase shift.

However it should be pointed out that this equation is only valid for the case in which both viscosity and spring constant, are invariable (not a function of the applied shear rate and shear amplitude, respectively).

As seen above, the applied torque and the strain response differ in terms of their amplitude, (A_0 for the applied torque and γ_0 for the strain response). The phase of the strain response is shifted from that of the applied torque by an offset of δ (phase lag).

In case of a purely viscous material, the shear stress can be expressed as function of the shear rate, as follows:

$$\sigma = \eta \cdot \dot{\gamma} \quad (\text{II.3})$$

Assuming steady shear the viscosity depends only on the absolute shear rate, *i.e.*:

$$\eta = \eta(\dot{\gamma}) = \eta(-\dot{\gamma}) = \eta(|\dot{\gamma}|) \quad (\text{II.4})$$

In the presence of non-linearity the viscosity becomes, in general, a function of both shear rate and time, *i.e.*, $\eta(\dot{\gamma}, t)$.

Considering steady shear or instantaneous adjustment of the viscosity towards the applied shear rates, the viscosity can be described as Taylor expansion, such as that described in equation (II.5).

$$\eta = \eta_0 + a|\dot{\gamma}| + b|\dot{\gamma}|^2 + c|\dot{\gamma}|^3 + \dots \quad (\text{II.5})$$

In the case where a controlled rate is applied, the strain can be described as follows:

$$\gamma = \gamma_0 \sin \omega_1 t \quad (\text{II.6})$$

Consequently the time dependent strain rate is given by:

$$|\dot{\gamma}| = \omega_1 \gamma_0 |\cos \omega_1 t| \quad (\text{II.7})$$

The application of Fourier Transform analysis to the absolute shear rate results in a sum of different harmonic contributions [Ramirez 1985, Bracewell 1986], from equation (II.7):

$$|\dot{\gamma}| = \omega_1 \gamma_0 \left[\frac{2}{\pi} + \left[\frac{4 \cos 2\omega_1 t}{\pi \cdot 1 \cdot 3} - \frac{\cos 4\omega_1 t}{3 \cdot 5} + \frac{\cos 6\omega_1 t}{5 \cdot 7} + \dots \right] \right] \quad (\text{II.8})$$

or in a reduced way

$$|\dot{\gamma}| \propto a' + b' \cos 2\omega_1 t + c' \cos 4\omega_1 t + \dots \quad (\text{II.9})$$

The expression of the stress will be than described as:

$$\sigma \propto \left(\eta_0 + a |\dot{\gamma}| + b |\dot{\gamma}|^2 + \dots \right) \cos \omega_1 t \quad (\text{II.10})$$

considering equation (II.9)

$$\sigma \propto \left(\eta_0 + a (a' + b' \cos 2\omega_1 t + c' \cos 4\omega_1 t + \dots) + b (a' + b' \cos 2\omega_1 t + c' \cos 4\omega_1 t + \dots)^2 + \dots \right) \cos(\omega_1 t) \quad (\text{II.11})$$

rearranging:

$$\sigma \propto (a'' + b'' \cos 2\omega_1 t + c'' \cos 4\omega_1 t + \dots) \cos \omega_1 t \quad (\text{II.12})$$

The final equation that defines the stress for a purely non-Newtonian viscosity is given by:

$$\sigma \propto A \cos \omega_1 t + B \cos 3\omega_1 t + C \cos 5\omega_1 t + \dots \quad (\text{II.13})$$

The application of Large Amplitude Oscillatory Shear (LAOS) for a non-linear response material generates higher harmonics. When a sinusoidal strain is applied, for a given frequency ($\omega_1/2\pi$) the resultant torque response can be Fourier transformed, generating a complex Fourier spectra [Wilhelm 2000]. The Fourier Transformation of any real or complex

time signal, $s(t)$ and its frequency dependent spectrum, $S(\omega)$ can be described in the following way:

$$s(t) = \frac{1}{2\pi} \int_{-\infty}^{+\infty} S(\omega) e^{+i\omega t} d\omega \quad (\text{II.14})$$

$$S(\omega) = \int_{-\infty}^{+\infty} s(t) e^{-i\omega t} dt \quad (\text{II.15})$$

The complex spectra which results from the Fourier transformation consists of several peaks, located at $3 \omega_1$, $5 \omega_1$, $7 \omega_1$, etc., and also at the fundamental frequency at $(\omega_1/ 2\pi)$. Each one of these peaks is described by means of an amplitude (a_n) and a phase (ϕ_n), where n is the multiple of the fundamental frequency. One possibility to quantify the non-linear character is obtained from the relative intensity between the third harmonic ($3 \omega_1/ 2\pi$) and the fundamental frequency ($\omega_1/ 2\pi$) and is represented by the normalized quantity $I(3 \omega_1/ 2\pi)/ I(\omega_1/ 2\pi) : = I_{3/1}$. Higher values of $I_{3/1}$ are related to a higher non-linear the response. The use of this normalized quantity is useful because it increases reproducibility, since it prevents possible experimental variations, arising for example, from differences in terms of sample preparation. A typical time signal and the respective spectrum obtained by Fourier analysis is shown in figure II.16.

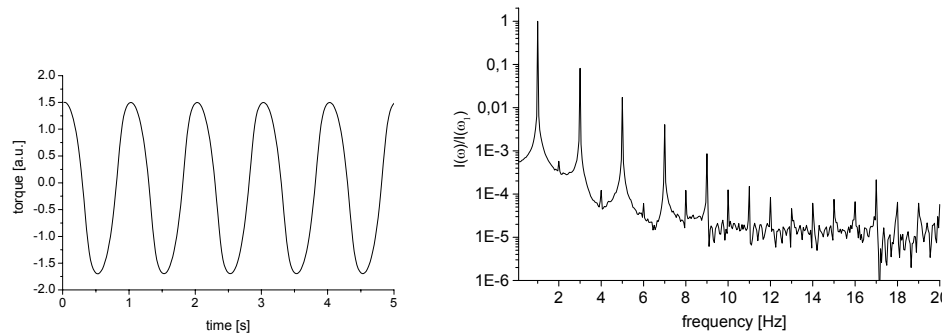


Figure II.16- Time and frequency data set for polyvinyl alcohol solution at 298 K, 1 Hz and for a strain amplitude of 20.

Finally, it should be mentioned that the implemented FT-Rheology software is extremely sensitive and different from other experimental realizations previously used [Davis 1978, Dodge 1971, Krieger 1973, Giacomini 1993, Reimers 1996, Tarique 1998, among others], which is basically due to the fact that a specific FT-algorithm (not the simple butterfly FFT) is applied [Wilhelm 1999, Van Dusschoten 2001]. This modification, combined with oversampling [Van Dusschoten 2001] leads to a significant improvement of about 2-3 decades in the signal to noise ratio. There are other methods, namely Lissajous figures that are able to predict the non-linear character. Nevertheless, these methods do not take into consideration the periodic excitation, contrary to the method described above [Wilhelm 2000a] and are unable to quantify the non-linearity.

References

- [Bracewell 1986] R. N. Bracewell, *The Fourier Transformation and its Applications*, New York, McGraw-Hill (1986)
- [Davis 1978] W. M. Davis, C. W. Macosko, *J. Rheol.* **22**, 53 (1978)
- [Dodge 1971] S. Dodge, I. M. Krieger, *Trans. Soc. Rheol.* **15**, 589 (1971)
- [Giacomin 1993] A. J. Giacomini, J. M. Dealy, *Large-amplitude oscillatory shear*, in Collyer A. A. (ed.), *Techniques in Rheological Measurements*, London, Chapman and Hall (1993)
- [Krieger 1973] I. M. Krieger, T. F. Niu, *Rheol. Acta* **12**, 567 (1973)
- [Ramirez 1995] R. W. Ramirez, *The FFT fundamentals and Concepts*, Prentice-Hall, Engelwood Cliffs (1995)
- [Van Dusschoten 2001] D. Van Dusschoten, M. Wilhelm, *Rheol. Acta* **40**, 395 (2001)
- [Wilhelm 1998] M. Wilhelm, D. Maring, H. W. Spiess *Rheol. Acta* **37**, 399 (1998)
- [Wilhelm 1999] M. Wilhelm, P. Reinheimer, M. Ortseifer *Rheol. Acta* **38**, 349 (1999)
- [Wilhelm 2000] M. Wilhelm, P. Reinheimer, M. Ortseifer, T. Neidhofer, H. W. Spiess *Rheol. Acta* **39**, 241 (2000)
- [Wilhelm 2000a] M. Wilhelm *Fourier Transform Rheology* Thesis for German Habilitation, Mainz, Germany (2000)

APPENDIX III-DISTRIBUTION OF THE LCP DIAMETERS FOR DIFFERENT PROCESSING CONDITIONS

comp. C 220 100 rpm v4	
C3	
Domain size (μm)	Frequency
-	-
-	-
-	-
-	-
-	-
-	-
-	-
-	-
-	-

comp. C 220 100 rpm v6	
C3	
Domain size (μm)	Frequency
2.68	1
3.58	5
4.49	4
5.39	4
6.30	5
7.20	6
8.10	4
9.01	1

comp. C 220 100 rpm v8	
C3	
Domain size (μm)	Frequency
1.41	1
2.54	5
3.66	11
4.79	8
5.92	6
7.04	2
8.17	2
9.29	0

comp. C 220 150 rpm v4	
C1	
Domain size (μm)	Frequency
2.74	1
5.28	7
7.83	4
10.37	9
12.92	1
15.46	2
18.00	0
20.55	0

comp. C 220 150 rpm v6	
C1	
Domain size (μm)	Frequency
3.87	1
6.03	15
8.18	6
10.34	5
12.49	4
14.65	3
16.80	2
18.96	0

comp. C 220 150 rpm v8	
C1	
Domain size (μm)	Frequency
2.68	1
4.14	9
5.61	12
7.07	4
8.53	2
9.99	2
11.46	1
12.92	1

comp. C 220 200 rpm v4	
C4	
Domain size (μm)	Frequency
2.68	1
4.27	2
5.86	3
7.45	7
9.05	10
10.64	2
12.23	5
13.82	0

comp. C 220 200 rpm v6	
C4	
Domain size (μm)	Frequency
2.76	1
4.64	10
6.26	4
10.03	10
12.60	5
13.77	3
16.24	4
18.44	0

comp. C 220 200 rpm v8	
C4	
Domain size (μm)	Frequency
2.82	1
4.89	13
6.96	6
9.03	13
11.10	3
13.17	2
15.24	1
17.31	0

comp. C 220 2 kg/h v4	
C5	
Domain size (μm)	Frequency
2.21	1
4.56	8
6.90	14
9.25	6
11.59	3
13.94	1
16.28	5
18.63	1

comp. C 220 2 kg/h v6	
C5	
Domain size (μm)	Frequency
2.26	1
3.67	3
5.08	12
6.49	8
7.90	5
9.31	5
10.72	3
12.13	2

comp. C 220 2 kg/h v8	
C5	
Domain size (μm)	Frequency
2.23	1
3.69	12
5.15	13
6.61	2
8.07	6
9.52	1
10.98	0
12.44	0

comp. C 220 8 kg/h v4	
C6	
Domain size (μm)	Frequency
-	-
-	-
-	-
-	-
-	-
-	-
-	-
-	-
-	-

comp. C 220 8 kg/h v6	
C6	
Domain size (μm)	Frequency
2.23	1
3.86	19
5.49	12
7.11	8
8.74	4
10.37	1
11.99	2
13.62	1
15.25	0

comp. C 220 8 kg/h v8	
C6	
Domain size (μm)	Frequency
1.61	1
2.44	3
3.27	24
4.10	8
4.93	10
5.76	2
6.59	0
7.42	1
8.25	1

comp. C 240 v4	
C2	
Domain size (μm)	Frequency
3.08	2
6.84	10
9.34	8
11.23	10
12.41	3
15.12	1
17.65	0
18.33	0

comp. C 240 v6	
C2	
Domain size (μm)	Frequency
3.19	1
5.78	14
8.38	10
10.97	10
13.56	3
16.15	1
18.75	0
21.34	0

comp. C 240 v8	
C2	
Domain size (μm)	Frequency
2.86	1
4.18	11
5.49	12
6.81	5
8.13	3
9.44	2
10.76	0
12.07	0

comp E 220 100 rpm v4	
C3	
Domain size (μm)	Frequency
2.94	2
4.64	5
6.34	7
8.04	12
9.75	6
11.45	5
13.15	1
14.85	1

comp. E 220 100 rpm v6	
C3	
Domain size (μm)	Frequency
3.22	1
4.00	5
4.78	7
5.56	12
6.34	4
7.12	5
7.90	1
8.68	2

comp. E 220 100 rpm v8	
C3	
Domain size (μm)	Frequency
2.58	1
4.53	25
6.49	7
8.44	3
10.40	2
12.35	1
14.30	0
16.26	0

comp. E 220 150 rpm v4	
C1	
Domain size (μm)	Frequency
5.83	1
7.52	5
9.20	10
10.89	5
12.57	10
14.26	4
15.94	9
17.63	4
19.31	1

comp. E 220 150 rpm v6	
C1	
Domain size (μm)	Frequency
2.63	1
4.06	6
5.50	12
6.93	10
8.37	3
9.80	4
11.23	1
12.67	1

comp. E 220 150 rpm v8	
C1	
Domain size (μm)	Frequency
1.79	1
2.92	8
4.04	14
5.17	7
6.30	7
7.42	2
8.55	0
9.67	0

comp. E 220 200 rpm v4	
C4	
Domain size (μm)	Frequency
2.82	1
4.89	13
6.96	6
9.03	13
11.10	3
13.17	2
15.24	1
17.31	0

comp. E 220 200 rpm v6	
C4	
Domain size (μm)	Frequency
2.4	1
3.66	2
4.91	8
6.17	7
7.43	9
8.68	8
9.94	3
11.19	0

comp. E 220 200 rpm v8	
C4	
Domain size (μm)	Frequency
1.82	1
2.79	2
3.75	12
4.72	9
5.69	3
6.65	5
7.62	2
8.58	2

comp. E 220 2 kg/h v4	
C5	
Domain size (μm)	Frequency
2.63	1
3.36	0
4.08	3
4.81	2
5.53	1
6.26	2
6.98	0
7.71	1

comp. E 220 2 kg/h v6	
C5	
Domain size (μm)	Frequency
2.73	1
3.88	3
5.02	2
6.17	3
7.32	8
8.46	5
9.61	0
10.75	1

comp. E 220 2 kg/h v8	
C5	
Domain size (μm)	Frequency
3.15	1
4.11	11
5.07	10
6.02	7
6.98	4
7.94	2
8.90	0
9.85	2

comp. E 220 8 kg/h v4	
C6	
Domain size (μm)	Frequency
2.7	1
4.20	4
5.71	8
7.21	5
8.72	6
10.21	4
11.72	2
13.23	1

comp. E 220 8 kg/h v6	
C6	
Domain size (μm)	Frequency
2.36	1
3.17	3
3.98	5
4.78	4
5.59	8
6.40	5
7.21	3
8.01	0

comp. E 220 8 kg/h v8	
C6	
Domain size (μm)	Frequency
3.57	2
4.97	10
6.37	9
7.77	3
9.18	3
10.58	0
11.98	2
13.38	2

comp. E 240 v4	
C2	
Domain size (μm)	Frequency
3.37	1
4.42	3
5.47	5
6.52	8
7.57	8
8.61	6
9.66	4
10.71	2

comp. E 240 v6	
C2	
Domain size (μm)	Frequency
4.05	1
4.68	0
5.30	4
5.93	3
6.55	5
7.18	3
7.80	8
8.42	2

comp. E 240 v8	
C2	
Domain size (μm)	Frequency
3.28	1
4.37	2
5.47	8
6.56	10
7.65	5
8.74	4
9.84	2
10.93	5